
Electronic Thesis and Dissertation Repository

8-15-2012 12:00 AM


Human Equilibrative Nucleoside Transporter Subtype 1: Structure-Function Analysis Using Cysteine Mutagenesis and Thiol Modifying Techniques

Jamie Park
The University of Western Ontario

Supervisor
Dr. James R. Hammond
The University of Western Ontario

Graduate Program in Pharmacology and Toxicology
A thesis submitted in partial fulfillment of the requirements for the degree in Doctor of Philosophy
© Jamie Park 2012

Follow this and additional works at: <https://ir.lib.uwo.ca/etd>

 Part of the [Biochemistry Commons](#), [Laboratory and Basic Science Research Commons](#), [Molecular Biology Commons](#), [Other Biochemistry, Biophysics, and Structural Biology Commons](#), and the [Pharmacology Commons](#)

Recommended Citation

Park, Jamie, "Human Equilibrative Nucleoside Transporter Subtype 1: Structure-Function Analysis Using Cysteine Mutagenesis and Thiol Modifying Techniques" (2012). *Electronic Thesis and Dissertation Repository*. 758.
<https://ir.lib.uwo.ca/etd/758>

This Dissertation/Thesis is brought to you for free and open access by Scholarship@Western. It has been accepted for inclusion in Electronic Thesis and Dissertation Repository by an authorized administrator of Scholarship@Western. For more information, please contact wlsadmin@uwo.ca.

Human Equilibrative Nucleoside Transporter Subtype 1: Structure-Function Analysis
using Cysteine Mutagenesis and Thiol Modifying Techniques

(Spine Title: Cysteine directed structure-function analysis of hENT1)

(Thesis Format: Monograph)

by

Jamie Park

Graduate Program of Pharmacology and Toxicology

A thesis submitted in partial fulfillment

of the requirements for the degree of

Doctor of Philosophy

The School of Graduate and Postdoctoral Studies

The University of Western Ontario

London, Ontario, Canada

© Jamie S. Park 2012

THE UNIVERSITY OF WESTERN ONTARIO
SCHOOL OF GRADUATE AND POSTDOCTORAL STUDIES

Certificate of Examination

Supervisor

Dr. James R. Hammond

Supervisory Committee

Dr. Rommel Tirona

Dr. Jane Rylett

Dr. Brian Shilton

Examiners

Dr. Susan Cole

Dr. Lina Dagnino

Dr. Jeff Dixon

Dr. David Heinrichs

The thesis by

Jamie S. Park

entitled:

**Human Equilibrative Nucleoside Transporter Subtype 1: Structure - Function
Analysis**

Using Cysteine Mutagenesis and Thiol Modifying Techniques

is accepted in partial fulfillment of the
requirements for the degree of
Doctor of Philosophy

Date _____

Chair of the Thesis Examination Board

Abstract

Human equilibrative nucleoside transporter 1 (hENT1) is the main mediator of bi-directional nucleoside flux into and out of cells and is found ubiquitously in all tissues. Inhibitor and substrate interactions with ENT1 are known to be affected by cysteine-modifying reagents. Our aim was to investigate the importance of cysteine residues in hENT1 function and identify which residues were sensitive to thiol modification for further application of cysteine scanning mutagenesis on extracellular loop 5. Transporter function was assessed by the binding of [³H] nitrobenzylmercaptapurine riboside (NBMPR) and the cellular uptake of [³H]2-chloroadenosine. Treatment of hENT1 with the neutral sulfhydryl-modifier methyl methanethiosulfonate (MMTS) enhanced [³H]NBMPR binding but decreased [³H]2-chloroadenosine uptake. The membrane impermeable positively charged reagent [2-(trimethylammonium)ethyl] methane-thiosulfonate (MTSET), but not the negatively charged reagent sodium-(2-sulfonatoethyl)-methanethiosulfonate (MTSES), inhibited [³H]NBMPR binding and enhanced [³H]2-chloroadenosine uptake. Furthermore, all three sulfhydryl modifiers decreased [³H]NBMPR binding when allowed cytoplasmic access. Site-directed mutagenesis on Cys222 eliminated the effect of MMTS on NBMPR binding. Mutation of Cys378 abolished the effect of MTSET on NMBPR binding and indicated that Cys378 is an extracellularly-located residue. Mutation of Cys414 led to an enhancement of the ability of MTSET to inhibit NBMPR binding and this effect was eliminated by co-mutation of Cys378. Mutation of Cys416 abolished the effect of charged sulfhydryl reagents to inhibit NBMPR binding in isolated membranes. Additionally, Cys416 to serine also eliminated transport function supporting a conformational linkage between the fifth intracellular loop and the NBMPR binding domain, and implicates this region in the translocation function of hENT1. To further confirm the importance of this region, extracellular loop 5 (EL5) was examined by cysteine scanning mutagenesis as residues in EL5 were individually mutated to cysteines. Mutation of N379, F390, E391, H392, and D393 to cysteine abolished uptake of [³H]2-chloroadenosine indicating their role in the transport mechanism of hENT1. Treatment of EL5 mutants with MTSET inhibited NBMPR binding

in all but the V389C mutant. Co-incubation of NBMPR with MTSET was able to protect N379C from thiol modification while co-incubation of adenosine with MTSET protected R384C, Y385C, and L386C from MTSET effects. Our results indicate that adenosine may bind in close vicinity or in direct contact to these residues to prevent MTSET to attain access.

Key Words: Equilibrative nucleoside transport, methanethiosulfonate, cysteine mutagenesis, structure-function

Acknowledgements

Thank you to Dr. Hammond for allowing me to pursue my graduate studies in his laboratory, for all his help, and pints of Guinness at the Grad Club. Thank you to Catherine for those warm welcomes and words of encouragements in the end. I would also like to acknowledge my advisory committee members for their input and suggestions throughout this project. To Dr. Chidiac and Dr. DiGuglielmo, thank you for being so generous in both lab supplies and in counselling. I am extremely grateful for all the members of the Hammond Lab for their endless assistance and help they provided. Sumeeta, Milica, and Arielle the girls of my twilight years, thank you for keeping the lab busy and alive with your scientific queries and upbeat natures. Diana, I am enormously grateful for all your wit and humour, kind words of wisdom, and of course your amazing technical skills. Scott and Frances, thank you for all the happy memories blaring bad music in the lab, walk dancing to Einsteins, cracking off beat jokes, and basically being amazing lab mates. To Mistre, Jeff, Ciric, Eddie, Adrian, Boun, and Sarah, I am indebted to you for keeping me sane and laughing. Your friendships, positivity, and advice have meant the world to me. To my parents, Jess and Thomas; thank you for all your love and support, for constantly asking when I will graduate, and finally encouraging me to do so. Finally, to Remi, I am truly thankful for your love and patience throughout this time in my life. Thank you for everything.

Co-authorship

A portion of the results from this thesis presented in Chapter 4 have been previously published in the peer-reviewed journal of *Molecular Pharmacology*.

Park J.S., Hughes S.J., Cunningham F.K.M., Hammond J.R. (2011). Identification of Cysteines Involved in the Effects of Methanethiosulfonate Reagents on Human Equilibrative Nucleoside Transporter 1. *Molecular Pharmacology*. 80(4):735-746.

Park J.S and Hammond J.R. (2012) Cysteine residues in the TM9-TM11 region of the human equilibrative nucleoside transporter subtype 1 play an important role in inhibitor binding and translocation function. *Molecular Pharmacology*. Epub ahead of print July 26, 2012 as doi:10.1124/mol.112.079616.

The remaining results from this thesis presented in Chapter 4 are in a manuscript in progress.

J. Park contributed to experimental design, manuscript preparations, and performed experiments for Figures 4.1-4.9, 4.11-4.56.

J.R. Hammond contributed to experimental design, manuscript preparation, and performed experiments for Figure 4.10.

F. Cunningham (MSc.) contributed to experiments performed in Figures 4.14-4.16.

S. Hughes (4th year honors student, MSc.) contributed to experiments performed in Figures 4.17-4.19.

L. Frieburger (4th year honors student) contributed to experiments performed in Figures 4.39 and 4.40.

All experiments performed by F. Cunningham, S. Hughes, and L. Frieburger were repeated by J. Park. All experiments were conducted in the laboratory of Dr. James R.

Hammond in the Department of Physiology and Pharmacology at the University of Western Ontario.

Table of Contents

Certificate of Examination	ii
Abstract.....	iii
Acknowledgements	v
Co-authorship	vi
Table of Contents.....	viii
List of Tables	xii
List of Figures	xiii
List of Appendices.....	xvii
List of Abbreviations	xviii
Chapter 1: Introduction	1
1.1 Nucleosides	1
1.2 Nucleoside analogues	4
1.3 Nucleoside transporters.....	5
1.4 ENT1 subtype	9
1.4.1 Characterization of ENT1.....	13
1.4.2 Homologues of ENT1	15
1.5 Clinical relevance of hENT1.....	19
1.5.1 Inhibitors: NBMPR and the vasodilators	19
1.5.2 Substrates: Cytotoxic nucleoside analogues	19
1.6 Molecular characteristics of hENT1	21
1.6.1 Membrane topology and protein structure determinants	21
1.6.2 Pharmacophore modeling	24
1.6.3 Mechanism of translocation function	26
1.6.4 Predicted 3-D topology of ENT1	28
1.6.5 Thiol modifications	32
1.7 Substituted cysteine accessibility method.....	35
Chapter 2: Rationale	37
2.1 Hypothesis #1:.....	37
2.2 Hypothesis #2:.....	39

2.3 Hypothesis #3:.....	39
2.4 Specific Aims:	40
Chapter 3: Materials and Methods.....	43
3.1 Materials:	43
3.2 Plasmid generation:	44
3.3 Single amino acid mutagenesis.....	44
3.4 Stable cell line generation:.....	45
3.5 Transient transfections:	47
3.6 Crude Cell Membrane Preparations:	48
3.7 Treatment with MTS reagents:	48
3.8 [³ H]NBMPR binding assay:	49
3.9 5'-S-[2-(1-[(fluorescein-5-yl) thioureido] hexanoamido) ethyl]-6-N (2-nitrobenzyl) -5'-thio adenosine (FTH-SAENTA) Inhibition Assay:.....	49
3.10 [³ H]2-chloroadenosine uptake assay:.....	49
3.11 Inhibition studies:	50
3.12 Cell Surface Biotinylation:	51
3.13 Western Blot Analysis:	51
3.14 Data analysis and statistics:	52
Chapter 4: Results.....	53
4.1 Validation that hENT1-p3XFlag functions in PK15-NTD cells:.....	53
4.2 Optimization of MTS reagents	58
4.3 Effects of MTS reagents on hENT1 function and ligand binding:	58
4.3.1 Effects of MMTS on NBMPR Binding: the NBMPR binding site is sensitive to neutral thiol modification.....	60
4.3.2 Effects of MMTS on 2-chloroadenosine uptake: substrate transport by hENT1 is sensitive to neutral thiol modification.....	65
4.3.3 Protection of hENT1 from the effects of MMTS	67
4.3.4 Effects of MTSES on NBMPR binding and on 2-chloroadenosine uptake: the NBMPR binding pocket is sensitive to negatively charged thiol modification of cytoplasmic cysteines.	67

4.3.5 Effects of MTSET on NBMPR binding and 2-chloroadenosine uptake: the NBMPR binding pocket and substrate translocation site are sensitive to a thiol modifier with a positive charge	71
4.4 Summary of MTS effects	71
4.5 Mutation of 10 endogenous cysteines	73
4.5.1 Mutation of C87 to serine	75
4.5.2 Mutation of C193 to serine	75
4.5.3 Mutation of C213 to serine	81
4.5.4 Mutation of C222 to serine	87
4.5.5 Mutation of C297 to serine:	93
4.5.6 Mutation of C333 to serine:	98
4.5.7 Mutation of C378 to serine:	98
4.5.8 Mutation of C414 to serine:	103
4.5.9 Mutation of C416 and C439 to serines and alanines:	109
4.7 SCAM analysis of Extracellular loop 5	124
4.7.1 Assessment of [³ H]NBMPR binding for EL5 mutants	125
4.7.2 Assessment of [³ H]2-chloroadenosine uptake for EL5 mutants	125
4.7.3 Effects of MTSET on extracellular loop five mutants	129
4.8 Summary of EL5 mutants	133
Chapter 5: Discussion.....	135
5.1 Wild-type hENT1 is sensitive to neutral and positively charged thiol modification	137
5.2 Assessment of single cysteine to serine mutants	140
5.2.1 Mutation of C416 to alanine alters the transport mechanism	143
5.2.2 Cysteine 222 is responsible for MMTS effects	146
5.2.3 Cysteine 378 is responsible for MTSET effects.....	149
5.2.4 Cysteine 416 is responsible for MTSES effects in membrane preparations ...	153
5.3 Role of residues in EL5	154
5.3.1 N379C, F390C, E391C, H392C, and D393C are critical in transporter function	155
5.3.2 MTSET effects on EL5 mutants.....	156

5.4 General conclusions	157
Chapter 6: References	159
Appendices.....	171
Curriculum Vitae	177

List of Tables

Table	Title	Page
1.1	Characteristics of the Equilibrative Nucleoside Transporter (ENT) Family members	10
3.1	List of the PCR primers used for single site-directed mutagenesis	46
4.1	Summary of the effects of MTS reagents on [³ H]NBMPR binding and [³ H]2-chloroadenosine uptake by hENT1	74
4.2	Effect of cysteine mutations on the binding of [³ H]NBMPR and the uptake of [³ H]2-chloroadenosine by hENT1	77
4.3	Effects of MTS reagents on [³ H]NBMPR binding by cell membranes transfected with hENT1 and with C416A or C439A cysteine mutants	122

List of Figures

Figure	Title	Page
1.1	Chemical structures of physiological nucleosides	2
1.2	Schematic pathways of adenosine breakdown and formation	3
1.3	Chemical structures of anti-cancer cytotoxic nucleoside analogues	6
1.4	Chemical structures of antiviral cytotoxic nucleoside analogues	7
1.5	Chemical structures of ENT inhibitors	16
1.6	The Equilibrative Nucleoside Transporter family rootless phylogenetic tree	18
1.7	Predicted 2-D topology of hENT1 created in TMPPres2D	22
1.8	Topology model of hENT1 with amino acid residues that have been identified as structurally or functionally important determinants	25
1.9	Generated pharmacophore model aligned against NBMPR obtained from PHASE	27
1.10	Schematic depicting the alternating access model for ENT1	29
1.11	Structural models of LdNT1.1 based on <i>ab initio</i> analysis	31
1.12	Chemical structures of methanethiosulfonate reagents	34
2.1	Predicted 2-D topology of hENT1 with location of 10 endogenous cysteine residues	41
4.1	Characterization of PK15-hENT1	55
4.2	Inhibitor profile for PK15-hENT1	56
4.3	Effect of DTT on PK15-hENT1 activity	57
4.4	Varying incubation times with MTS reagents to PK15-hENT1 cells	59
4.5	Treatment of hENT1 with MMTS	61
4.6	Effects of isolating membranes to the treatment of hENT1 with MMTS	62
4.7	MMTS effects are dependent on pH	63
4.8	Effects of the treatment of hENT1 with MMTS to inhibitor binding	64
4.9	NBMPR binding to hENT1 is sensitive to pH	66

Figure	Title	Page
4.10	Effects of the treatment of hENT1 with MMTS on inhibition of substrate uptake	68
4.11	NBMPR and adenosine are unable to protect against MMTS effects	69
4.12	Treatment of hENT1 with MTSES	70
4.13	Treatment of hENT1 with MTSET	72
4.14	Characterization of PK15-C87S	76
4.15	Treatment of C87S with MMTS	78
4.16	Treatment of C87S with MTSET and MTSES	79
4.17	Characterization of PK15-C193S	80
4.18	Treatment of C193S with MMTS	82
4.19	Treatment of C193S with MTSET and MTSES	83
4.20	Characterization of PK15-C213S	84
4.21	Treatment of C213S with MMTS	85
4.22	Treatment of C213S with MTSET and MTSES	86
4.23	Characterization of PK15-C222S	88
4.24	Treatment of C222S with MMTS: NBMPR binding to C222S is insensitive to MMTS	89
4.25	Treatment of C222S with MTSET and MTSES	90
4.26	Cell membrane treatment of C222S with MMTS	91
4.27	Cell membrane treatment of C222S with MTSET	92
4.28	NBMPR binding to C222S is insensitive to pH	94
4.29	Characterization of PK15-C297S	95
4.30	Treatment of C297S with MMTS	96
4.31	Treatment of C297S with MTSET and MTSES	97
4.32	Characterization of PK15-C333S	99
4.33	Treatment of C333S with MMTS	100
4.34	Treatment of C333S with MTSET and MTSES	101

Figure	Title	Page
4.35	Characterization of PK15-C378S	102
4.36	Treatment of C378S with MMTS	104
4.37	Treatment of C378S with MTSET and MTSES: NBMPR binding to C378S is insensitive to MTSET	105
4.38	Characterization of PK15-C414S	106
4.39	Treatment of C414S with MMTS and MTSES	107
4.40	Treatment of C414S with MTSET: enhanced inhibition of NBMPR binding	108
4.41	Characterization of PK15-C378-C414S	110
4.42	Treatment of C378-414S with MMTS and MTSES	111
4.43	Treatment of C378-414S with MTSET: NBMPR binding to C378-414S is insensitive to MTSET	112
4.44	Treatment of PK15-hENT1 with 2-Br	114
4.45	Characteristics of PK15-C416A and PK15-C439A: PK15-416A does not transport 2-chloroadenosine	115
4.46	Analysis of the plasma membrane expression of PK15-hENT1 and PK15-C416A via biotinylation and FTH-SAENTA competition assays	117
4.47	2-chloroadenosine can effectively block NBMPR binding to C416A	118
4.48	Cell membrane treatment of C439A with MTSET and MTSES	120
4.49	Treatment of C416A with MMTS, MTSET, MTSES: NBMPR binding to C416A is insensitive to MTS reagents	121
4.50	NBMPR and adenosine are unable to protect against MTSES effects in membranes	123
4.51	EL5 mutants bind NBMPR with high affinities	126
4.52	N379C, F390C, E391C, H392C, and D393C show no measurable uptake of 2-chloroadenosine	127
4.53	Quantification of cell-surface hENT1 by competitive inhibition assay of NBMPR and FTH-SAENTA of N379C, F390C, E391C, H392C, or D393C	128

Figure	Title	Page
4.54	2-chloroadenosine can effectively block NBMPR binding to N379C, F390C, E391C, H392C, or D393C	130
4.55	NBMPR binding of all EL5 mutants except V389C are sensitive to MTSET	131
4.56	NBMPR is able to protect N379C against MTSET effects in cells	132
4.57	Adenosine is able to protect R384C, Y385C, and L386C against MTSET effects in cells	134
5.1	Predicted topology of hENT1 with C378 highlighted in grey as the target residue for positively charged thiol modification with MTSET	141
5.2	Simulated topologies of hENT1 based on the <i>ab initio</i> model of LdNT1.1.	145
5.3	Predicted topology of hENT1 with C222 highlighted in grey as the target residue for neutral thiol modification with MMTS	147
5.4	Simulated topology of hENT1 based on the <i>ab initio</i> model of LdNT1.1. highlighting extracellular negatively charged amino acids	152

List of Appendices

Title	Page
Permission to reprint Figures from J.Park <i>et al.</i> (2011) <i>Molecular Pharmacology</i> . 80(4):735-746	207
Permission to reprint Figures from J.Park and J.R. Hammond (2012) <i>Molecular Pharmacology</i> . mol.112.079616. published ahead of print July 26, 2012	208
Permission to reprint Figure 1.6	209
Permission to reprint Figure 1.9	210
Permission to reprint Figure 1.11	212

List of Abbreviations

2-Br	2-Bromohexadecanoic acid
3TC	(-)- β -L-2',3'-dideoxy-3'-thiacytidine
A1, 2a, 2b, 3	Adenosine receptor subtype 1, 2a, 2b, 3
AP	Alkaline phosphatases
Ara-C	Arabinofuranosyl Cytidine
AZT	3'-azido-3'-deoxythymidine
B _{max}	Maximum number of binding sites
cAMP	Cyclic adenosine monophosphate
CD73	Ecto-5' nucleotidase
CeENT1-2	Caenorhabditis elegans equilibrative nucleoside transporter subtype1, 2
cGMP	Cyclic guanosine monophosphate
CK2	Casein kinase II
CNS	Central nervous system
CNT	Concentrative nucleoside transporters
ddI	2',3'-dideoxyinosine
DMSO	Dimethyl sulfoxide
DNA	Deoxyribonucleic acid
dNTP	Deoxynucleoside triphosphate
DTT	Dithiothreitol
EL5	Extracellular loop 5
E-NPP	pyrophosphatase/phosphodiesterases
ENT	equilibrative nucleoside transporters
ENT1-4	Equilibrative nucleoside transporter subtype 1, 2, 3, 4
ENT1-KO	Equilibrative nucleoside transporter subtype 1 knock out mouse
E-NTPDase	Triphosphate diphosphohydrolases
FLAG	N-DYKDDDDK-C peptide tag
FTH-SAENTA	5'-S-[2-(1-[(fluorescein-5-yl)thioureido]hexanoamido)

	ethyl]-6-N(2-nitrobenzyl) -5'-thio adenosine
G1	Gap 1 phase
G2	Gap 2 phase
G418	Geneticin
GFP	Green fluorescent protein
GlpT	Glycerol-3-phosphate transporter
GltT	Glutamate transporter
Glut1	Glucose transporter
Gly	Glycine
GTP	Guanosine triphosphate
hENT1	Human equilibrative nucleoside transporter subtype 1
HIF-1	Hypoxia inducible factor 1
HMEC-1	Human microvascular endothelial cells
hOCT2	Human organic cationic transporter subtype 2
HUVEC	Human umbilical vein endothelial cells
IC ₅₀	Half maximal inhibitory concentration
kDa	Kilodalton
K _i	Inhibition constant
K _m	Substrate affinity
LacY	Lactose permease
LdNT1.1.-2	Leishmania donovani nucleoside transporter subtype 1.1 and 2
L-FTC	(-)-β-L-2',3'-dideoxy-3'-thia-5-fluoro-cytidine
MAP kinase	Mitogen activated protein kinase
MAZ	Myc-associated zinc finger protein
MCF-7 cells	Michigan Cancer Foundation – 7 breast cancer cell
MDCK	Madin-Darby Canine Kidney Cells
MEM	Modified Eagle`s Medium
mENT1	Mouse equilibrative nucleoside transporter subtype 1
mENT1Δ11	Mouse equilibrative nucleoside transporter delta 11 subtype

MFS	Major Facilitator Superfamily
MMTS	Methyl methanethiosulfonate
MPP+	1-methyl-4-phenylpyridinium
MTS	methanethiosulfonate
MTSES	sodium (2-sulfonatoethyl)methanethiosulfonate
MTSET	2-(trimethylammonium)ethyl]methanethiosulfonate bromide
NBMPR	6-S-[(4-Nitrophenyl)methyl]-6-thioinosine
NBTGR	Nitrobenzylthioguanosine
NEM	N-ethyl maleimide
NHE1	Na ⁺ /H ⁺ exchanger
NMG	N-methyl-D-glucamine
NTP	Nucleoside triphosphate
P1	Purinoceptor subtype 1
P1 and P2	Typanosoma brucei nucleoside transporter subtype 1 and 2
PBS	Phosphate-buffered saline
pCMBS	P-chloromercuribenzenesulfonate
pCREB	cAMP response element binding protein
PfENT1-4	Plasmodium falciparum equilibrative nucleoside transporter subtype
PK15-NTD	Pig kidney nucleoside transporter-deficient cells
PKC	Protein kinase C
PMAT	Plasma membrane monoamine transporter
QSAR	Quantitative structure-activity relationships
RNA	Ribonucleic acid
SCAM	Substituted cysteine accessibility method
SDS-Page	Sodium dodecyl sulfate-polyacrylamide gel electrophoresis
SLC28	Solute carrier gene for concentrative nucleoside transporter
SLC29	Solute carrier gene for equilibrative nucleoside transporter
TM	Transmembrane
V _{max}	Maximum transport rate

Chapter 1: Introduction

1.1 Nucleosides

Nucleosides are endogenous purine and pyrimidine heterocyclic nitrogenous bases attached to a ribose or 2-deoxyribose sugar. The main naturally occurring nucleosides include adenosine, guanosine and inosine (purines) and thymidine, uridine, and cytidine (pyrimidines) (Figure 1.1) [1, 2]. The primary functions of nucleosides are to form the base structural unit of nucleotides and nucleic acids. Once formed, nucleotides are then involved in multiple events such as DNA/RNA formation (NTP, dNTP), energy supply (ATP/GTP), and signaling pathways (cAMP, cGMP). The main source of nucleoside formation is through a series of resourceful enzymatic cascades involving the breakdown of nucleotides. These pathways are performed by 5' nucleotidases found intracellularly and by ectonucleotide hydrolyzing enzymes such as triphosphate diphosphohydrolases (E-NTPDase), pyrophosphatase/phosphodiesterases (E-NPP), ecto-5' nucleotidase (CD73) and alkaline phosphatases (AP) located extracellularly on plasma membranes [3-7] (Figure 1.2). In this cyclical manner, there is a continuous supply of nucleosides and nucleotides under basal conditions. The generation of these nucleoside pools can have an important impact on their secondary function as signaling molecules, specifically as purinergic agonists. For example, adenosine is a ubiquitous signaling molecule in purinergic pathways by binding to its purinergic receptors (P1) also known as adenosine receptors that are widely distributed throughout the body [8-10]. These P1 receptors are a class of G protein-coupled receptors further divided into 4 subtypes (A1, A2a, A2b, and A3) [11]. The four adenosine receptors subtypes differ in their molecular structure, tissue distribution, and pharmacological profile and mediate diverse biological effects [12-16].

For instance, the A1 receptor subtype is found largely in the central nervous system (CNS) particularly in the cerebral cortex, hippocampus, cerebellum, and spinal cord. When adenosine binds to pre and postsynaptic A1 receptors, it inhibits

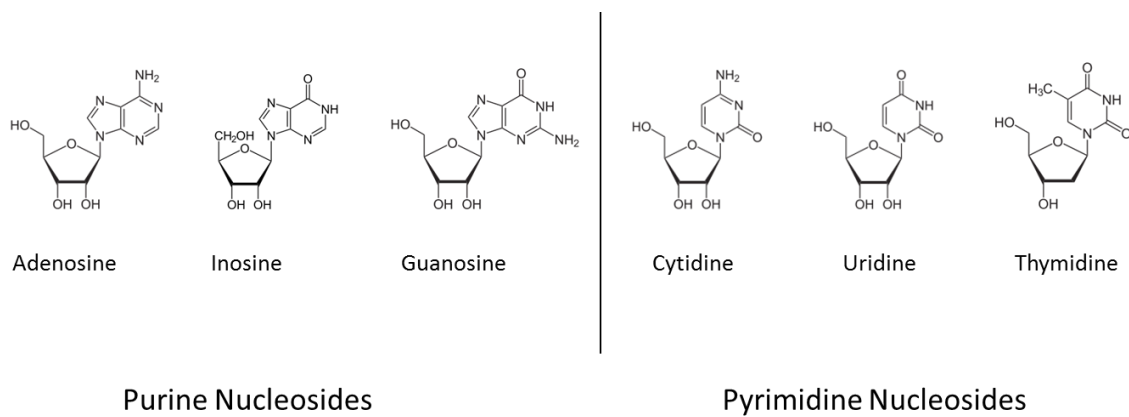


Figure 1.1. Chemical structures of physiological nucleosides

Adenosine, inosine and guanosine are purine nucleosides while cytidine, uridine, and thymidine are pyrimidine nucleosides.

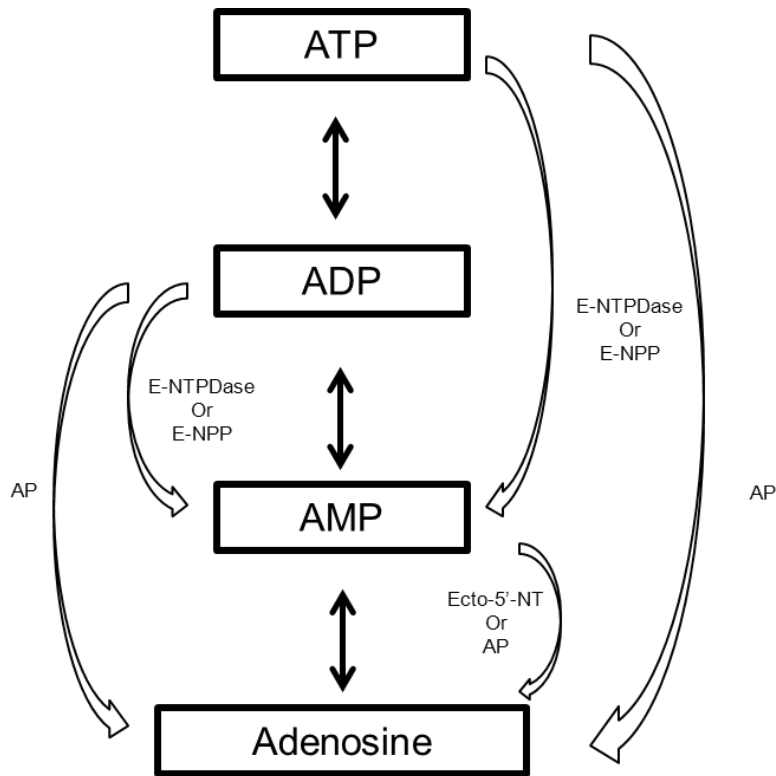


Figure 1.2. Schematic pathways of adenosine breakdown and formation

Adenosine is formed from the breakdown of adenosine triphosphate (ATP), adenosine diphosphate (ADP), and adenosine monophosphate (AMP) by enzymatic activity of alkaline phosphatase (AP), ecto 5' nucleotidase (Ecto-5'-NT), ecto-nucleoside triphosphate diphosphohydrolase (E-NTPDase), or ecto-nucleotide pyrophosphatase/ phosphodiesterase (E-NPP).

neurotransmitter release to cause a depression of neuronal activity. This is especially important in times of hypoxia and ischemia because adenosine which is released in high doses during times of stress can act as a neuroprotective agent to reduce neuronal activity and oxygen consumption [17-19]. Adenosine receptors expressed in the cardiovascular system can also elicit responses such as cardiac depression and vasodilation when activated by adenosine. A1 receptor activation in the sinoatrial and atrioventricular nodes can result in bradycardia and heart block to slow down the heart rate; this event has been applied to treat supraventricular tachycardia. Alternatively, adenosine binding to the A2a receptor subtype located on vascular smooth muscles of coronary arteries can elicit a relaxation response by activation of adenylate cyclase [9, 20]. Thus it is clear that endogenous adenosine plays an important role in human physiology and can impact a wide variety of processes including cardiovascular function, neurotransmission, inflammatory reactions, and immune responses.

1.2 Nucleoside analogues

Given the importance of nucleosides as metabolic precursors to biologically important molecules, their properties have been capitalized upon for the treatment of many diseases by the design of nucleoside analogues. Cytotoxic nucleoside analogues are used as antimetabolites that interfere with the synthesis of nucleic acids. These agents can exert cytotoxicity either by being incorporated into and altering the DNA and RNA macromolecules themselves, or by interfering with various enzymes involved in synthesis of nucleic acids, or even by modifying the metabolism of physiological nucleosides [21-26]. In this manner, nucleoside analogues can be used as antiviral, chemotherapeutic, and immunosuppressive agents. Currently there are several analogues that are clinically used for their anticancer properties (Figure 1.3). Specifically, cladribine and fludarabine are two purine analogues used for their treatment of low-grade malignant disorders of the blood [27, 28]. Pyrimidine analogues, such as cytarabine and gemcitabine, are extensively used in the treatment of acute leukaemia; various solid tumours and some hematological malignant diseases [29-33]. Additionally,

the fluoropyrimidines 5-fluorouracil and capecitabine have shown to have activity against colorectal and breast cancers [34-37].

Cytotoxic nucleosides are also used in anti-viral therapy against various highly active viral diseases such as acquired immunodeficiency syndrome (AIDS) and diseases caused by the herpes simplex virus (HSV). Anti-viral nucleoside analogues include 2', 3'-dideoxyinosine (ddI, didanosine), 3'-azido-3'-deoxythymidine (AZT, zidovudine, Retrovir), (-)- β -L-2', 3'-dideoxy-3'-thiacytidine (3TC, lamivudine), and (-)- β -L-2', 3'-dideoxy-3'-thia-5-fluoro-cytidine (L-FTC, emtricitabine) (Figure 1.4). Once again, they produce their therapeutic effects by becoming phosphorylated intracellularly and inhibiting viral DNA synthesis or by involving mitochondrial toxicity. However, all of these anti-viral agents and the anti-cancer agents described above utilize membrane transporters to gain access to target cells for further activation by intracellular kinases and cytosolic metabolic reactions in forming their active phosphate derivatives.

1.3 Nucleoside transporters

Given the importance of nucleosides and their analogues in their roles in extracellular signaling and intracellular nucleotide generation, the ability of cells to effectively accumulate these molecules relies on their efficient movement across membranes. Nucleosides and their analogues are hydrophilic due to the hydrogen bonding nature of the hydroxyl groups found on the sugar moiety and consequently, the presence of specialized transporters are necessary to effectively facilitate their import. Additionally, cells that lack *de novo* nucleoside synthesis capabilities such as enterocytes, bone marrow cells, and certain brain cells, rely heavily on these nucleoside transporters to salvage nucleosides from the extracellular milieu [38-40]. Nucleoside transporters are characterized into two separate gene families that differ in their structure and transport mechanism, and are termed concentrative nucleoside transporters (CNT) and equilibrative nucleoside transporters (ENT) [41-43].

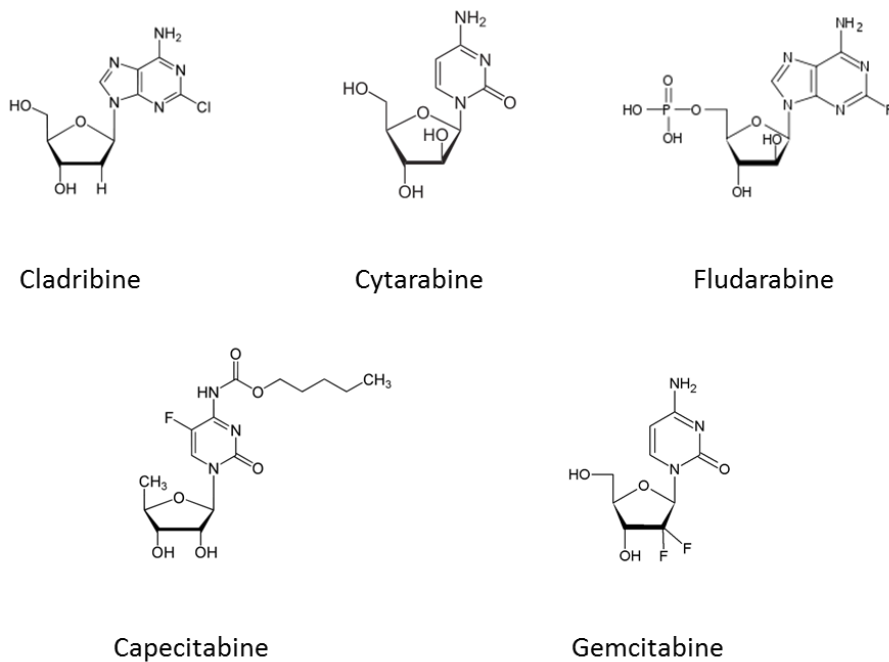


Figure 1.3. Chemical structures of anti-cancer cytotoxic nucleoside analogues

Cladribine, cytarabine, fludarabine, capecitabine, and gemcitabine are nucleoside analogues used in the treatment of certain cancers.

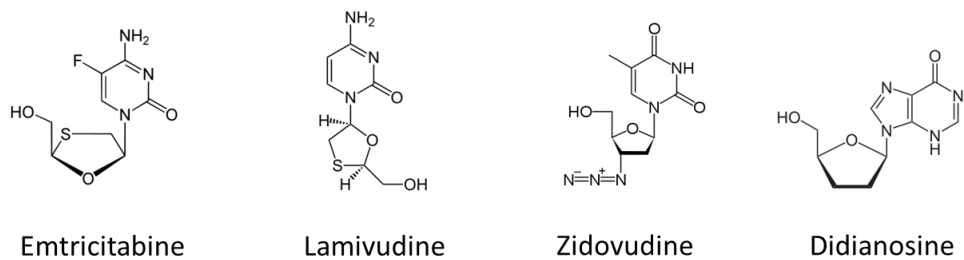


Figure 1.4. Chemical structures of antiviral cytotoxic nucleoside analogues

Emtricitabine, lamivudine, zidovudine, and didanosine are nucleoside analogues used in the treatment of multiple viral infections.

The concentrative nucleoside transporters (gene *SLC28*) are sodium-dependent symporters that move nucleosides unidirectionally into cells in an active energy-costly process [44, 45]. CNTs are generally found in apical membranes of specialized epithelial cells of the intestine and kidney and can play a major role in active absorption or reabsorption processes. There are three sub-families of CNTs that have been cloned, CNT1, CNT2 and CNT3, that differ in their substrate selectivity and sodium:nucleoside stoichiometry [46, 47]. CNT1 selectively transports pyrimidine nucleosides and adenosine while CNT2 transports purines and uridine. CNT3 transports both purine and pyrimidine nucleosides and functions by translocating two sodium molecules per nucleoside. These three concentrative nucleoside transporters are plasma membrane transporters and share a general topology based on 13 putative transmembrane domains, a long intracellular N-terminus, and an extracellular C-terminus [48].

The equilibrative nucleoside transporters (gene *SLC29*) are sodium-independent facilitated diffusers that have been confirmed to transport nucleosides bi-directionally down concentration gradients [49]. These transporters are found in most if not all cell types, and can transport a wide variety of purines and pyrimidines and in some cases nucleobases. There are four subtypes of ENTs (ENT1-4) that have been cloned to date and differ in their substrate selectivities and inhibitor sensitivities [43, 50] (Table 1.1). ENT1 and ENT2 were the first transporters to be characterized by their differential inhibition by nitrobenzylthioinosine (NBMPR), ENT1 being sensitive to NBMPR at a nM range [51]. ENT2, insensitive to NBMPR, transports nucleosides as well as nucleobases such as hypoxanthine and is found predominantly in skeletal muscle, although its expression has been detected in brain, heart, placenta, and kidney. ENT3 and ENT4 have recently been characterized as members of the ENT family of transporters that are active in acidic pH. ENT3 is found intracellularly and contains an endosomal/lysosomal targeting motif and is shown to have elevated expression in human placenta [52, 53]. ENT4 found abundantly in heart and brain is also termed plasma membrane monoamine transporter (PMAT) because it efficiently transports serotonin and MPP⁺ at neutral pH

while only transporting adenosine at acidic pH [54]. All four equilibrative nucleoside transporters transport adenosine and therefore can influence the many physiological processes described above such as cardiovascular tone and neurotransmission.

1.4 ENT1 subtype

The ENT1 subtype has been suggested to be the main mediator of adenosine flux and cytotoxic accumulation of nucleoside analogues, as inhibition of ENT1 has been proven to increase adenosine levels and adenosine signaling in cardiovascular tissues, CNS, and kidney [55-57]. Since the ENT1 subtype is highly and widely expressed and mediates the entry of cytotoxic nucleoside analogues, it is not surprising that the loss of ENT1 expression has been correlated to drug resistance in *in vitro* models of malignant cancer cells. Additionally, studies with the ENT1-knock out mouse (ENT1-KO) have found higher levels of circulating adenosine and ribavirin (a nucleoside drug) compared to their wild-type counterparts suggesting that ENT1 is a major contributor to extracellular adenosine concentrations and uptake of nucleoside drugs [58, 59]. The ENT1 knock-out mouse was first created by Choi *et al.* (2004) through deletion at exons 2-4 of the protein-coding region of the ENT1 gene. The ENT1 knock-out mice in those studies that were less than 4 months of age, reproduced normally, were viable, showed apparent normal mortality rates, and had normal brain anatomy [60]. However, these mice had a lower body weight (8.7% less than wild-type littermates), and were found to show a slower rate of intoxication and increased preference for ethanol consumption. This enhancement for ethanol consumption was associated with increased levels of cAMP response element binding protein (pCREB) in the striatum through an increase in glutamate signaling. Furthermore, when examining the behaviour of the ENT1-KO mice, it was shown that they showed less of an anxiety phenotype when compared to their wild-type counterparts. They also showed a lowered natural aversion to the centre of an open field indicating that they showed less anxiety; however, the locomotor activity was similar to that of wild-type [61]. When wild-type mice were injected with NBMPR

Table 1.1. Characteristics of the Equilibrative Nucleoside Transporter (ENT) Family members

	ENT1 family member	Permeant Selectivity	Tissue Distribution
	hENT1	Purine and pyrimidines	Ubiquitous
scale	hENT2	Purine, pyrimidines and nucleobases	Ubiquitous, abundant in skeletal muscle
	hENT3	Purine, pyrimidine, adenine at pH 5.5	Ubiquitous, localized intracellularly
	hENT4/PMAT	Adenosine at pH 5.5 and organic cations	Brain, Heart, Liver

(specific ENT1 inhibitor) in the amygdala, they also showed reduced anxiety indicating that the behavioural effects in the ENT1-KO mice were due to a loss of ENT1 and not through developmental changes. Additionally, phenotypic changes have been recently identified in older ENT1-KO mice (12 months of age) in our lab. Current studies from our lab (unpublished work from Bone and Warraich *et al.*) have found ENT1-null mice acquired spinal stiffness, hind limb dysfunction and eventual paralysis by 12 months of age. Upon further examination, it was found that the mice showed signs of ectopic mineralization of paraspinal tissues in the cervical-thoracic region (as early as 2 months of age) forming lesions that contained high amounts of calcium and phosphorus. These unpublished studies by Bone and Warraich *et al.*, are the first to identify ENT1 as playing a role in regulating the calcification of soft tissues.

The cardiovascular system has also been studied in the ENT1-null mouse, as its substrate adenosine is a significant contributor to vascular tone and heart function. Initial examination of the ENT1-null mouse found it to be cardioprotected such that myocardial infarcts were significantly smaller after subjected to ischemia (coronary occlusion for 30 min and reperfusion for 2h) [55]. Cardiomyocytes isolated from these mice showed no significant differences in gene expression profiles of the other ENT subtypes or adenosine receptors indicating that there was no compensation of the loss of ENT1 in these cells [58]. However, when examining isolated microvascular endothelial cells from the ENT1-KO mice, there was a 2 fold increase in expression of the A2a receptor and adenosine deaminase enzyme was observed [62]. Given that there is an increase in circulating adenosine in KO mice, increased expression of these genes may reflect compensatory mechanisms in the animal to handle the excess adenosine.

The expression of ENT1 itself is still under investigation with a large body of evidence obtained from studies using cultured human cells indicating that hENT1 expression was coordinated with the cell cycle [63-66]. Expression of hENT1 showed a doubling between the G1 and G2-M phases indicating that cellular deoxynucleotide levels could play a role in cell cycle regulation by coordinating transporter expression. Additionally, studies in HeLa and MCF-7 cells showed that ENT1 expression responded to

phorbol ester treatment by activation of protein kinase C (PKC) isoforms [67-70]. The specific targets on mouse ENT1 (mENT1) for PKC-mediated phosphorylation have been shown to involve serines 279 and 286 and threonine 274 located in the large intracellular loop between transmembrane 6 and 7 [71]. Alternatively, hENT1 also contains casein kinase II (CK2) consensus sites which are known to play a role in regulating proliferation [72, 73]. Inhibition of CK2 phosphorylation was shown to increase hENT1 activity and NBMPR binding in human osteosarcoma cells [74]. Our own lab has demonstrated that the expression of a catalytically inactive CKII subunit which inhibits endogenous CKII activity caused an enhancement in hENT1-specific NBMPR binding and transport of the substrate 2-chloroadenosine in U2OS cells [75]. Taken together, these data have demonstrated that ENT1 is a phosphoprotein that can be directly phosphorylated at several sites which shows that it is involved in a complex array of pathways in its regulation.

Besides post-translational regulation by phosphorylation, pre-transcriptional events also regulate hENT1 expression. The promoter sequence of hENT1 (involving one transcriptional initiation site 58 base pairs downstream of the TATA box) has been shown to contain consensus sites for ERE, MAZ, Sp1, AP-2, and CREB transcription factors [76]. Studies investigating hENT1 expression and activity have shown that human umbilical vein endothelial cells (HUVEC) isolated from gestational diabetic pregnancies showed a decrease in hENT1 expression [77]. A second study found hENT1 expression was reduced in HUVECs when exposed to hyperglycemic conditions by the engagement of nitric oxide, MAP kinase, and PKC. Incubation with N(G)-nitro-L-arginine methyl ester (L-NAME, nitric oxide synthase inhibitor), PD-98059 (MEK1/2 inhibitor), or calphostin C (PKC inhibitor) prevented hENT1 downregulation in the hyperglycemic environment [78]. Additionally, when measuring Sp1 protein levels, they found Sp1 expression increased when hENT1 promoter activity decreased, suggesting that Sp1 may be a negative transcriptional factor for hENT1 [79]. These studies link the importance of hENT1 regulation in certain pathologies such as gestational diabetes where the

adenosine-modulated placenta to fetus blood flux is damaged and loss of hENT1 causes a loss of the endothelium ability to remove adenosine from the extracellular space.

Furthermore, ENTs are also predominantly expressed in endothelial cells of the cardiovascular system with minimal contribution from the CNTs [80]. In human microvascular endothelial cells (HMEC-1), it was found that, under hypoxic conditions, ENT1 expression was downregulated in a HIF-1 (hypoxia inducible factor 1)-dependent manner [81]. These findings indicate that an innate protective mechanism is present that serves to enhance adenosine signaling in times of cellular stress by decreasing uptake of nucleosides into cells by ENT1.

1.4.1 Characterization of ENT1

The NBMPR-sensitive transporter ENT1 was first purified from human erythrocytes which allowed for the cloning of hENT1 from human placental cDNA [82]. Previous studies examining cells that transported nucleosides relied on the use of radioligand binding and uptake assays. These initial studies on ENT1 activity found that nitrobenzylthioinosine bound to high-affinity sites on human and sheep erythrocyte membranes and on rat, mouse, guinea pig, and dog cortical membranes in a saturable manner ($K_d \sim 0.1-1$ nM) [83-88]. Binding data from these studies indicated that NBMPR had a specific interaction with functional nucleoside-transport sites that could be inhibited by nitrobenzylthioguanosine (NBTGR), dipyridamole (a vasodilator), and uridine (substrate). Additionally, transport processes examined in human and sheep erythrocytes showed [3 H]NBMPR inhibition of [14 C]uridine influx, consistent with a simple competitive inhibition model (apparent $K_i = 1$ nM). Binding of inhibitor to these sites was competitively blocked by uridine, a well characterized substrate for the nucleoside transporter (apparent $K_i = 1.25$ and 0.9 mM, respectively). These apparent K_i values were found to be close to the apparent K_m for uridine equilibrium exchange in human erythrocytes, indicating that NBMPR competes directly with nucleosides for the permeation site of the nucleoside transporter, and that the inhibitor binds preferentially to the external membrane surface [85].

Human ENT1 is 456 amino acids and is 78% identical in sequence to rat ENT1 and 79% identical to mouse ENT1 [82, 89, 90]. Splice variants of hENT1 are not reported, however, there are multiple variants found in mouse shown to possess different functional characteristics [75, 91]. One functional splice variant mENT1.2 altered at the end of exon 7, lacks a potential casein kinase II phosphorylation site and has shown to be widely expressed with mENT1.1. This mouse variant, mENT1.2, was also found to have an altered affinity for the prototypical ENT1 inhibitor NBMPR. Another splice variant of mouse ENT1 involving the exclusion of exon 11 during pre-RNA processing is widely distributed in multiple tissues. This functional variant termed mENT1 Δ 11 bound inhibitors and transported substrates with high affinities and was predicted to possess nine TM domains and cytoplasmic COOH and NH₂ termini. Additionally, rat ENT1 is found to be inhibited by NBMPR but is resistant to inhibition by the vasodilator compounds dilazep, draflazine and dipyridamole [82] (Figure 1.5).

Human, mouse and rat ENT1, transport a wide range of purine and pyrimidine nucleosides with affinities ranging from 0.05 mM for adenosine to 0.6 mM for cytidine. However ENT1 subtypes are unable to transport the pyrimidine base uracil. Human and rat ENT1 also poorly transport the antiviral nucleosides ddC, ddi and AZT (compared to the anti-neoplastic analogues). These anti-viral drugs are pyrimidine nucleoside analogues that lack the C³-hydroxyl group, revealing the importance of the hydroxyl group for permeant recognition by ENT1 [92]. In contrast, the anticancer analogues such as gemcitabine and fludarabine are transported readily and efficiently by the ENT1 subtype [93].

ENT1 is expressed ubiquitously in all tissues but at differing levels. For example, hENT1 is found in brain tissue with higher expression in the frontal and parietal lobes of the cortex [94]. In the rat kidney cortex, rENT1 is found on the basolateral surface of the tubular epithelial cells similarly seen in hENT1-GFP tagged proteins in MDCK cells in vitro [45]. Additionally, rENT1 found in high abundance in the sinoatrial node of the heart is suggested to play a role in modulating the chronotropic effects of adenosine [95]. Therefore though ENT1 is found throughout the body, its abundance can vary depending

on tissue and cell location. Furthermore, though ENT1 is primarily expressed as a plasma membrane transporter, there are also studies that suggest it can also be detected in nuclear membranes and endoplasmic reticulum [96]. Functional human ENT1 is also found in the mitochondria where it has been suggested to play a part in the mitochondrial toxicity effects of the antiviral agents [97]. This feature seems to be specific for the human homologue, as rat and mouse ENT1 lack the mitochondrial-targeting motif (PEXN). These subpopulations of intracellular ENT transporters are thought to contribute to the nucleoside passage between the cytosol and lumen of cellular compartments and could also correspond to a pool of intracellular transporters available for membrane recruitment at crucial time points.

1.4.2 Homologues of ENT1

Following the initial cloning of hENT1, homologues of mammalian ENTs have been detected in protozoa, fungi, plants, nematodes, and insects due to their sequence similarity to mammalian ENTs [50, 98] (Figure 1.6). Within the nematode *Caenorhabditis elegans* genome, there are five genes encoding equilibrative nucleoside transporters, two of which (CeENT1 and Ce ENT2) are closely related with 94% sequence similarity. The substrate specificities of the CeENTs closely resemble those of hENT1 and hENT2. However, their sequence similarities to hENT1 and hENT2 are between 15-24% and they both differ from the mammalian transporters in that they are not sensitive to NBMPR, dilazep, or draflazine. Dipyridamole, on the other hand, does show moderate inhibition of CeENT1 and Ce ENT2 at an IC_{50} 300 nM, indicating that inhibitors with different structures interact with the protein at different residues. The CeENTs also are capable of transporting the cytotoxic dideoxynucleosides (ddl, ddC, AZT) with high efficiency [99, 100].

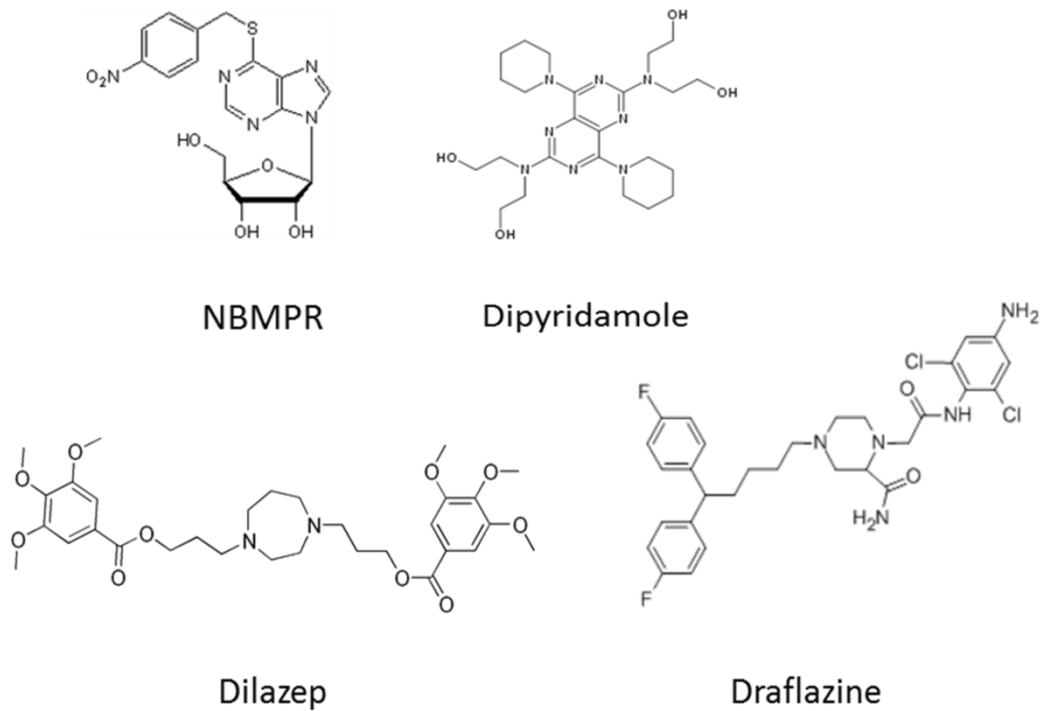


Figure 1.5. Chemical structures of ENT inhibitors

Nitrobenzylmercaptapurine riboside (NBMPR), dipyridamole, dilazep, and draflazine are potent inhibitors of hENT1.

The parasite *Plasmodium falciparum*, which is the causative microbe in malaria, also possess ENT family members that have been designated as PfENT1-4 [40, 101, 102]. The PfENTs have broad substrate specificity and have 18% sequence identity to hENT1 and hENT2. Similar to the CeENTs, PfENTs are not proton dependent and have conserved sequence motifs in the region of the transmembrane spanning segments confirming that they are members of the ENT protein family. The majority of transporter expression has been detected during the erythrocytic stages of the parasite which are known to be responsible for the clinical pathogenesis of the disease. PfENTs are efficient in transporting natural nucleosides with apparent affinities (K_m) of 320 μM similarly reported for mammalian ENTs. However, PfENTs are not sensitive to NBMPR or the inhibitory vasodilators up to the mM concentrations.

Mammalian ENTs are also homologous to the active, proton-linked transporters in kinetoplastid protozoa in *Leishmania* and *Trypanosoma* [103-105]. Transporters in the *Trypanosoma brucei*, include two high affinity transporters (P1 and P2) that differ in their substrate selectivity [106-108]. The P1 transporters mediate the movement of adenosine and inosine with higher affinity (low K_m) than the PfENTs. P2 transporters passage adenosine and the nucleobase adenine and was initially identified through its sequence similarity from the *Leishmania donovani* nucleoside transporter LdNT1.1.

In *Leishmania donovani*, there are also two nucleoside transport processes, one selective for adenosine and pyrimidine nucleosides (LdNT1.1 and LdNT1.2) and the other for inosine and guanosine (LdNT2) [109-111]. Comparing LdNT1.1 and LdNT1.2, they have almost identical sequences and transport adenosine at high affinities of $K_m < 1 \mu\text{M}$ however uridine is also transported at a much lower affinity. The LdNT2 transporter selectively carries inosine with a high affinity (K_m 0.3 μM) as well as guanosine (K_m 1.7 μM). Despite the functional difference from mammalian transporters in the fact that they are proton linked and therefore not equilibrative diffusers, they are confirmed to belong to the ENT family due to their amino acid sequences and membrane topologies.

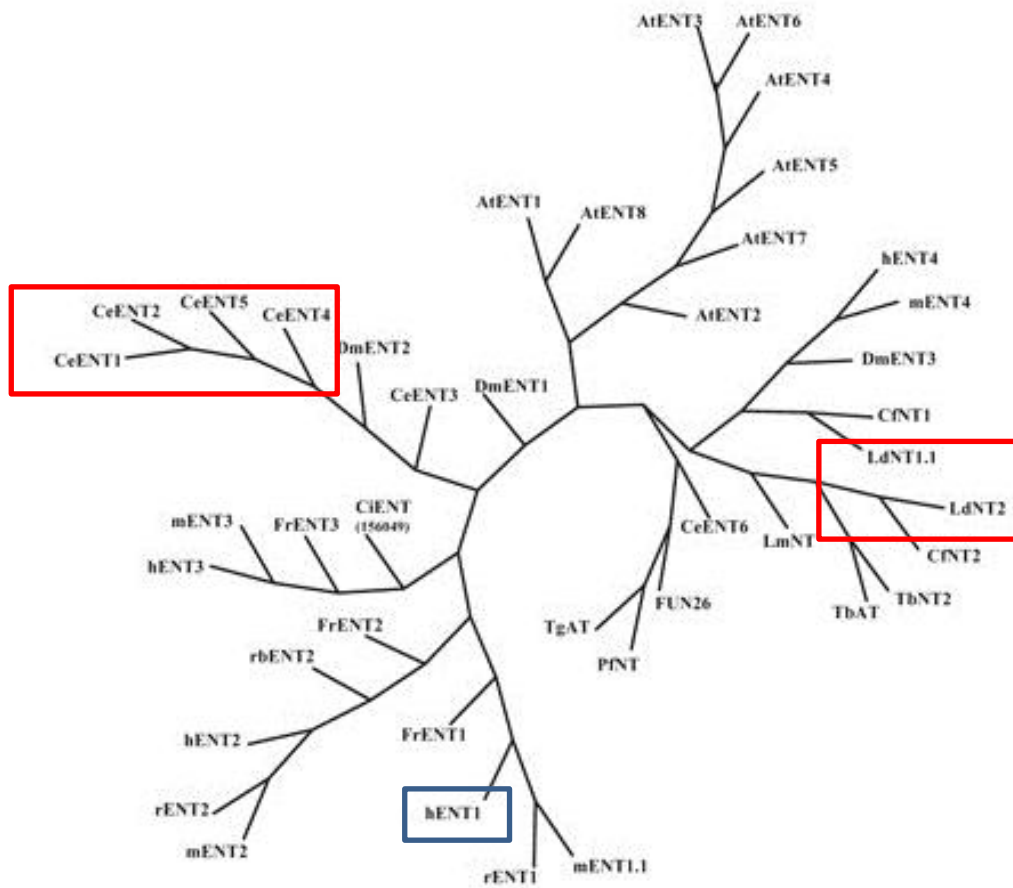


Figure 1.6. The Equilibrative Nucleoside Transporter family rootless phylogenetic tree.

The blue box highlights hENT1 and the red boxes highlight homologs of hENT1 described in Section 1.4.1

Permission to use copyrighted material : adapted from Acimovic and Coe, 2002 [112]

1.5 Clinical relevance of hENT1

1.5.1 Inhibitors: NBMPR and the vasodilators

The influence of ENT1 on the extracellular levels of adenosine, a nucleoside with physiological activity, indicates that it is a viable target for drug therapy in multiple pathologies. Inhibition of hENT1 is of particular importance because it is the main contributor of adenosine uptake and clearance from the extracellular space [49, 98]. By blocking the removal of adenosine, there is enhancement of adenosine signaling through adenosine receptors which can impact the neurological, cardiovascular, and immunological systems [113]. NBMPR and the coronary vasodilators such as dipyridamole, dilazep, and draflazine (Figure 1.5) inhibit ENT1 leading to enhanced extracellular concentrations of adenosine [114-117]. Studies in murine cardiomyocytes show that adenosine uptake is sodium independent, saturable, and inhibited by NBMPR, dilazep, and dipyridamole [118]. In endothelial cells, the inhibition of hENT1 by draflazine provided increased A1/A3 signaling shown to be beneficial in the ischemic/reperfused myocardium [119, 120]. Additionally, administration of dipyridamole during percutaneous transluminal coronary angioplasty in humans also reduced the incidence of abrupt vessel closure by inhibition of ENTs [121]. The ENT1-KO mice also been have shown to have a cardioprotected phenotype especially during times of ischemia/reperfusion by having enhanced circulating adenosine levels compared to wildtype [55].

In addition to blocking adenosine reuptake, hENT1 inhibitors have shown to be useful in anti-cancer therapy as well. For example, the cytotoxic effect of cladribine uptake by nucleoside transporters is complemented with co-treatment of NBMPR to prevent drug efflux [122]. Therefore selective inhibition of ENTs may be useful in combined drug therapy in the treatment of many cancers to improve drug efficacy.

1.5.2 Substrates: Cytotoxic nucleoside analogues

A frequent avenue in drug therapy for cancer and viral diseases utilizes cytotoxic nucleoside analogues. The ENTs play an important part for entry of these drugs inside

the target cells. Specifically, human ENT1 has been shown to enhance the transport of chemotherapeutic agents such as cladribine, cytarabine, fludarabine, gemcitabine, and capecitabine (Figure 1.3) [93, 123, 124]. These nucleoside analogues function in a variety of ways: by incorporation into nucleic acids, through interfering with the nucleic acids synthesis, and by modifying the metabolism of endogenous nucleosides. By depleting the endogenous pools of nucleosides, the cytotoxic nucleosides increase their chances for incorporation into newly forming DNA and RNA. Expression of hENT1 in highly proliferating cells such as the malignant cancerous cells contributes to the selectivity for nucleoside analogues since they require higher transport of nucleosides for their replication [125]. For example, in acute lymphoblastic leukaemia cells, hENT1 expression was correlated to increased sensitivity to cladribine [126]. In accord with this evidence, the downregulation of hENT1 was also suggested to contribute to clinical resistance of cytarabine and gemcitabine given that ENT1 is the major route of entry for these drugs [127]. Specifically, leukemic cells resistant to Ara-C treatment showed a downregulation in hENT1 gene expression [128]. Moreover, hENT1 is now known as a positive predictive marker of patients receiving gemcitabine treatments for pancreatic cancer and metastatic lung disease [127, 129].

Recent studies highlight the importance in measuring hENT1 levels as a predictive tool for better drug therapy protocols that are specific to individual patients as levels of hENT1 in patients with different breast cancers, Hodgkin's disease, and pancreas adenocarcinoma have shown a significant range of distribution. Additionally, the expression of hENT1 has been shown to be positively correlated with a three-fold increase in the survival of patients receiving gemcitabine treatment [130]. Imaging analogues of NBMPR for specific binding to hENT1 have proven useful in determining the abundance of transporter expression at the plasma membrane to guide drug treatment protocols [131]. Given that cancer cells have a higher demand for extracellular nucleosides to maintain their increased proliferation rates, nucleoside analogues are relatively specific for target cells. With higher levels of hENT1 being a

predictive marker in pancreatic cancer and non-small cell lung cancer, it is of significant importance to improve the selectivity and specificity of drugs for cancer cells to help decrease normal cell toxicity and death.

1.6 Molecular characteristics of hENT1

1.6.1 Membrane topology and protein structure determinants

The original hydropathy plot of hENT1 indicated a 2-D topology of an intracellular N-terminus, 11 transmembrane domains (TM), an extracellular C-terminus, and a large intracellular loop linking TM6 and 7 (Figure 1.7) [90]. This generated figure was then confirmed and supported using biochemical studies using antibodies as topological probes in combination with glycosylation scanning mutagenesis [132]. Additionally, hENT1 is shown to have a glycosylation site in the extracellular loop 1 at residue Asn48, however, this modification does not seem to have an essential role in either activity or expression at the plasma membrane [133]. Given that rat ENT1 had a different inhibitor profile sensitivity to vasodilator compounds [134], studies based on human and rat chimeras identified regions containing TM 3-6 to have a significant role in hENT1 functionality in both inhibitor binding and substrate interactions [135]. This region is thought to form the major site of interaction with NBMPR and substrates as multiple studies have shown their ability to competitively inhibit each other [86, 136]. Mutational analyses within this region have also validated the importance of this domain. For example, mutations of Gly154 and Ser160 in TM4 affected permeant translocation and NBMPR binding, indicating that they possessed dual roles recognizing inhibitors and substrates [137, 138].

Mutation of Gly154 to serine caused a loss of NBMPR binding and decreased affinities of hENT1 for adenosine and cytidine. The important roles of glycine residues have also been implicated in hENT1 structure as mutations at the conserved Gly179 and Gly184 residues altered hENT1 activity and reduced plasma membrane expression respectively [139]. Although TM3 is crucial for ENT1 function, characterization of other point mutations throughout the transporter has also revealed important

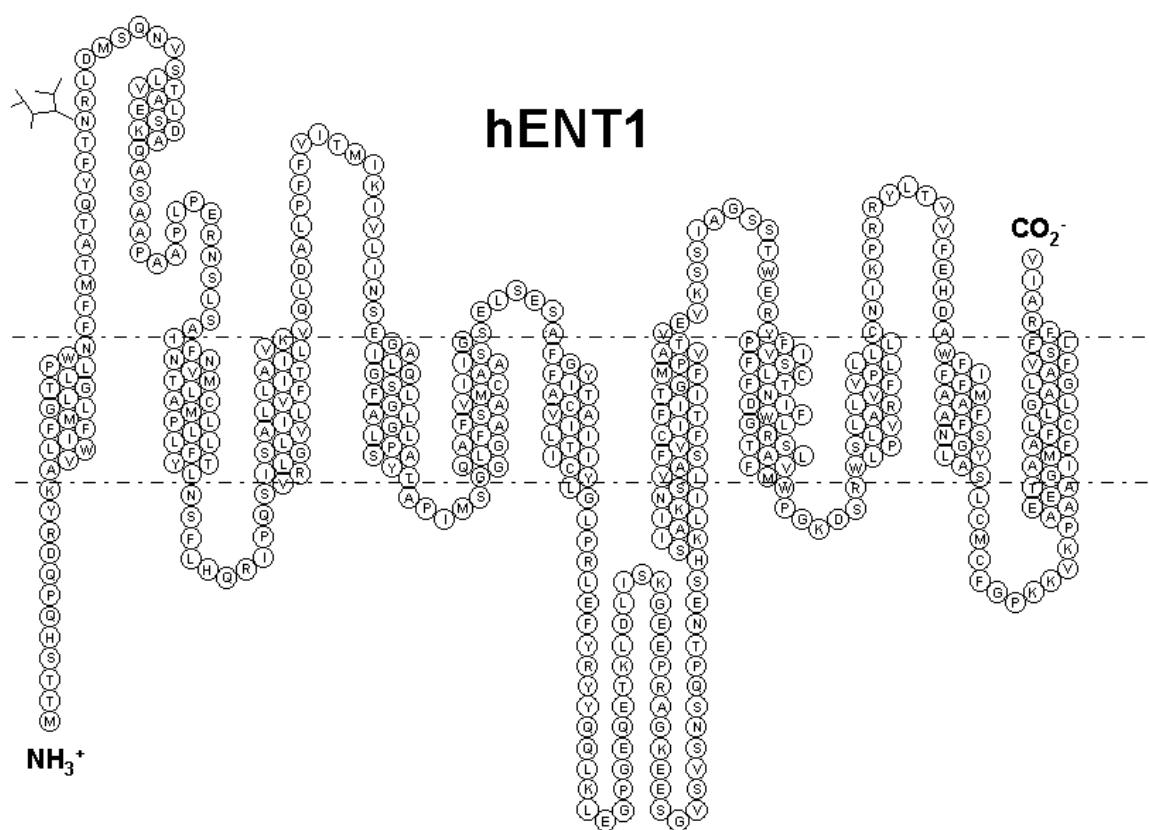


Figure 1.7. Predicted 2-D topology of hENT1 created in TMPPres2D [140]

The primary amino acid sequence of hENT1 was inserted into the TMPPres 2D program and predicted the membrane-spanning regions and their orientation.

structural/functional roles for other regions of hENT1. In particular, mutations of Met89 and Leu92 in TM2 produced changes in transporter affinities for adenosine, guanosine, NBMPR and dipyridamole [138, 141]. Additionally, Leu442 in TM11 was found to be involved in dipyridamole sensitivity when Met33 in TM1 was first mutated to isoleucine [100]. This study indicated a functional interaction between TM1 and TM11, regions outside the predicted crucial domain (TM3-6) and implicated Met33 in dipyridamole and NBMPR binding interactions. Additionally, the highly conserved residue Trp29 was found to have a selective role in pyrimidine transport activity (uridine and cytidine) [142]. Mutation of Trp29 also decreased the ability of the inhibitors to interact with hENT1. A helical wheel projection of this transmembrane helix (TM1) suggested that Trp29 and Met33 were in close proximity and therefore validates the importance of this region in hENT1 activity.

Further evidence for the involvement of the terminal domains was revealed by mutations at Phe334 and Asp338 in TM8 altered the ability of hENT1 to be inhibited by the coronary vasodilators [143]. Specifically, Phe334 (TM8) mutated to tyrosine increased the rate of transport of 2-chloroadenosine suggesting an altered conformation state of hENT1 to accept the substrate. Mutational analysis of the LdNT2 transporter has also implicated a role for TM8 in ENT functions, where hydrophilic residues Asp341 and Arg345 (corresponding to Phe334 and Asp338 in hENT1) are essential for expression and function of the transporter [110]. As a result of these studies (summarized in Figure 1.8), it is suggested that though there is one overlapping recognition site for inhibitors and substrates, there are multiple regions that contribute to ENT1 function. In effect, each individual mutation that was examined did not alter all interactions with different inhibitors or substrates which indicates that each ligand has its own individual points of contact with hENT1. As hENT1 is shown to have therapeutic potential through its inhibition as well as its cytotoxic nucleoside translocation, development of specific drugs to recognize and preferentially select for hENT1 may prove helpful. Understanding the structure and mechanism of action of hENT1 in terms of where the permeants bind and

how they interact with the protein can help in the design of such drugs. However, there are no 3-D models of hENT1 given its unyielding nature for biophysical techniques such as x-ray crystallography, therefore the advancement of such rational drug design has been slow moving.

1.6.2 Pharmacophore modeling

One way to gain an understanding of the binding determinants of nucleosides and inhibitors to their transporters is to use a computational approach to model *in vitro* affinity data. *In silico* studies can be used as a tool to direct the exploration of new ligand to nucleoside transporters. Given that the structure of ENTs have not yet been elucidated, studies predicting ligand interactions have employed the use of ligand-based quantitative structure-activity relationships (QSAR). Current biological tested models of inhibitor and substrate interactions have found that on NBMPR, the nitrobenzyl moiety is critical for high-affinity binding to the transporter. Specifically, electron-withdrawing substituents at the 6-position benzyl substituent have been indicated to contribute to high affinity binding of the transporter [144, 145]. Addition of a nitro group at that position enhanced affinity by 50-fold compared to NBMPR itself. A specific feature of the nitro group was its electron-withdrawing capabilities as well as its negative charge, suggesting that negative charges interact with positively charged moieties in the binding site of the transporter.

Given the size of the nitrobenzyl moiety and the enhanced interaction with the nitro group, these data suggest that the area where NBMPR binds is in a large pocket that is able to accommodate its chemical structure containing an area of positively charged residues. A separate study analyzing the ability of C²-purine position-substituted analogs of NBMPR to inhibit ENT1 has identified that substitutions at the C² lead to a general decrease in the ability of the analogues to inhibit hENT1 activity compared to NBMPR [146]. These data suggest that C² interacts with the transporter in a very specific manner and any addition to that area via steric bulk sizes or charges impacts on the

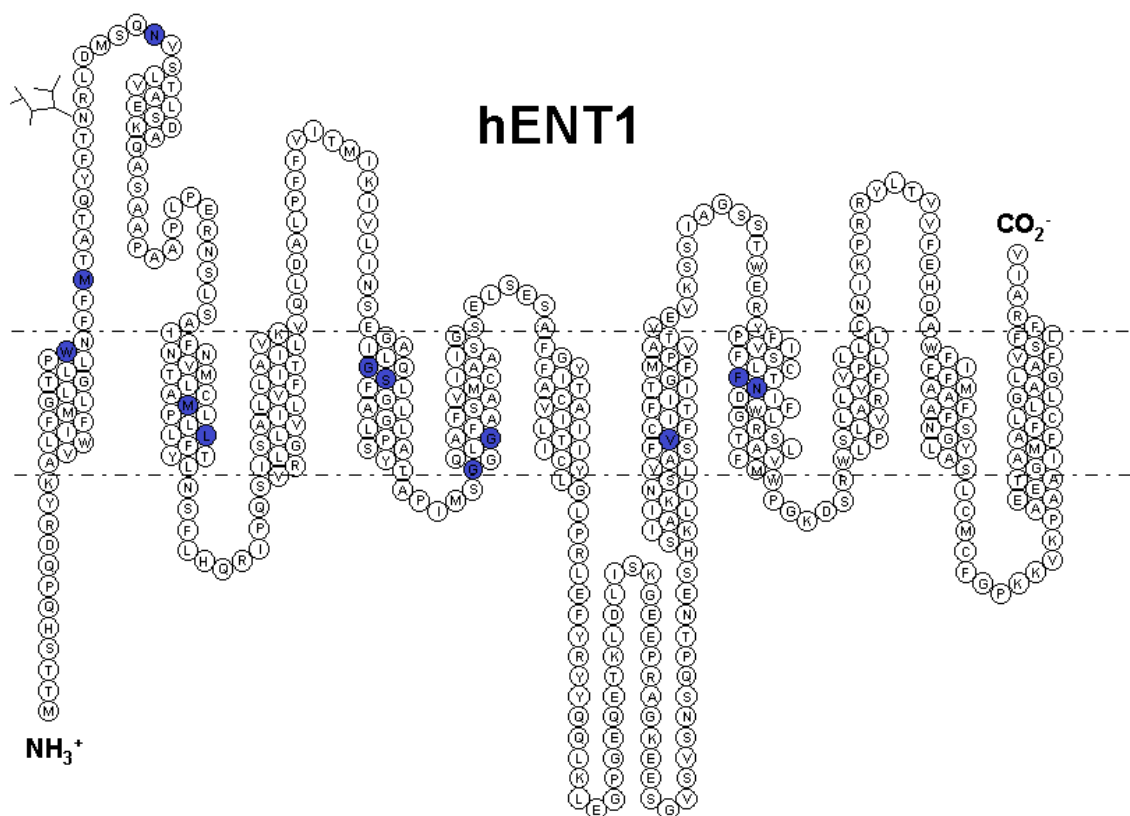


Figure 1.8. Topology model of hENT1 with amino acid residues that have been identified as structurally or functionally important determinants.

The 2-D topology of hENT1 is shown with residues identified to be important for ENT activity indicated by the blue filled circles.

ability of the purine portion of NBMPR to bind with hENT1. Additionally, examination on the structure-activity relationship of ENTs to substrates found the requirement of sugar moiety for transporter interaction specifically with the presence of the C³ hydroxyl [92]. Selective structural determinant for ENT1 also include C² and C⁵ in comparison to ENT2 requiring only the C⁵ interaction [147, 148]. Further investigations using bioinformatics found incorporation of electrostatic and steric features at the C³ position and a negative charge at the 2,7 position of the purine (3,5-position pyrimidine) to contribute to enhanced affinity to hENT1, validating again a positively charged region within the ligand binding pocket [149, 150]. These 3-D QSAR models are based on correlations between ligand affinities and variations on their structural features and validated the importance of the substrates C³ position and the pentose ring structure for hydrogen bond formation (Figure 1.9). As mentioned previously, these models should assist the design of high-affinity nucleoside transporter inhibitors and substrates; however, caution should be taken when interpreting these data before assessment in biological models.

1.6.3 Mechanism of translocation function

It is believed that nucleoside transporters share a common evolutionary origin with the MFS (Major Facilitator Superfamily) of transporters of which the majority function as monomers, transporting substrates in an “alternating access mechanism” [85, 151, 152]. In this manner, ENT1 is also predicted to have an extracellular and intracellular substrate site that when bound, produces a conformational change in the transporter to reorient itself and release the substrate on the opposite side of the membrane (Figure 1.10). In this case, there would be two primary conformations for ENT1 that alternated regardless of substrate binding, one inward facing and one outward facing. However, only one site would be accessible at any time. NBMPR binds specifically to the extracellular site of the protein and would potentially lock it into this conformation in this model [46, 153]. Additionally, depending on the permeant bound, hENT1 may be able to alter the rate at which the conformation would change. For example, hENT1 expressed in human

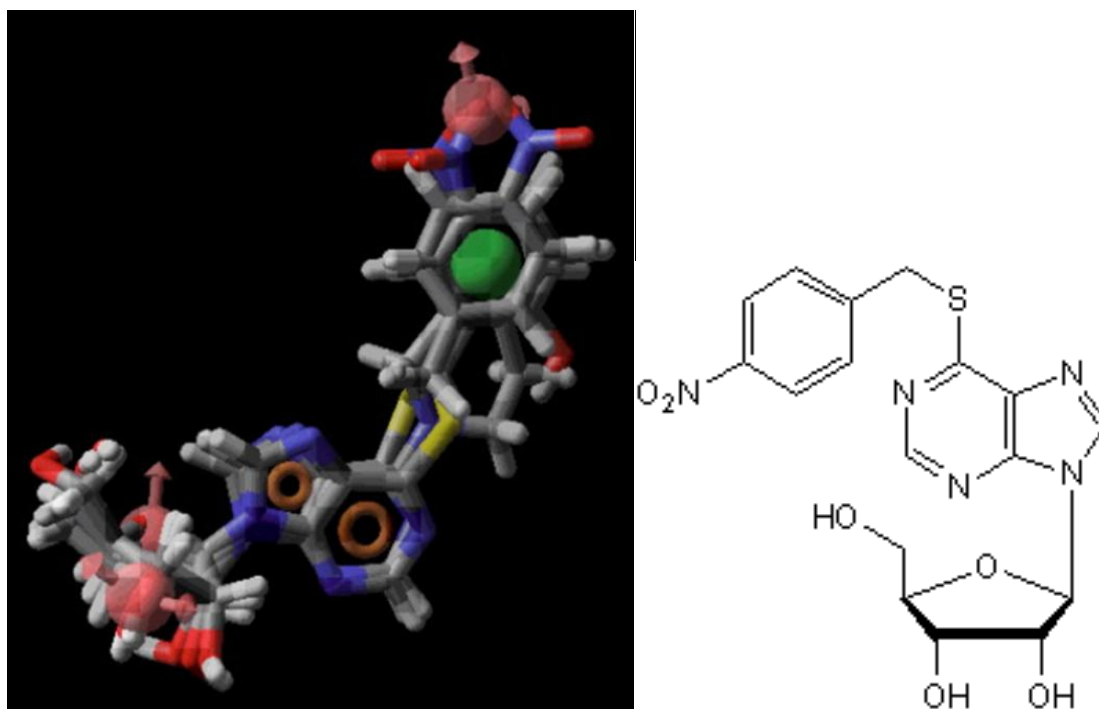


Figure 1.9. Generated pharmacophore model aligned against NBMPR obtained from PHASE.

Chemical structure of NBMPR shown on the right beside the Pharmacophore model. Red points indicating hydrogen-bond acceptors (oxygen), orange points for aromatic groups, green indicated for hydrophobic regions, blue points indicate nitrogen, yellow points showing sulfur, gray is showing carbon and white highlights hydrogen.

Permission to use copyrighted material : adapted from Zhu and Buolamwini, 2008. [149]

erythrocytes showed a rapid conformation change with pyrimidine nucleosides and a slower change with 2-chloroadenosine [51]. However, there are other complex models of hENT1 that have been proposed where the transporter may exist as an oligomer with allosteric sites. Several studies have found the presence of higher molecular weight bands on immunoblots probing for ENT1 in multiple tissues in rats. From our own lab, photoaffinity labelling of mouse ENT1 with [³H]NBMPR found that mENT1 was present at a higher molecular weight band at approximately 100 kDa, or twice the size of the ENT1 monomer. Additionally, unpublished data from Cunningham F. *et al.*, found hENT1 at a higher molecular mass complex (147-180 kDa) compared to its monomer size (55 kDa) under native conditions using the blue native gel electrophoresis technique. It has been previously suggested that there are two permeant recognition sites for hENT1, one that is a high affinity site for NBMPR and substrates and a second lower affinity site which may allosterically modulate the higher affinity site. Data from [³H]NBMPR inhibition studies using dipyridamole and the lidoflazine analogues as competitive inhibitors found them to have pseudo-Hill coefficients that were not equal to unity indicating the presence of co-operativity or multiple sites. Additionally, studies examining the rates of dissociation of [³H]NBMPR binding found nucleosides to enhance dissociation rates versus inhibitors such as dipyridamole and dilazep decreased dissociation rates. This suggests the presence of a second site that can influence the first high affinity site which could indicate either multiple sites or co-operativity. However, there is still not enough evidence to distinguish between the two possibilities and mechanisms.

1.6.4 Predicted 3-D topology of ENT1

Clearly, understanding the structure, function, and mechanism of hENT1 would be of considerable value in drug discovery. Current homology and comparative modeling of ENT1 have generated several putative configurations of the transporter since the primary sequences have been validated and secondary structures have been proposed.

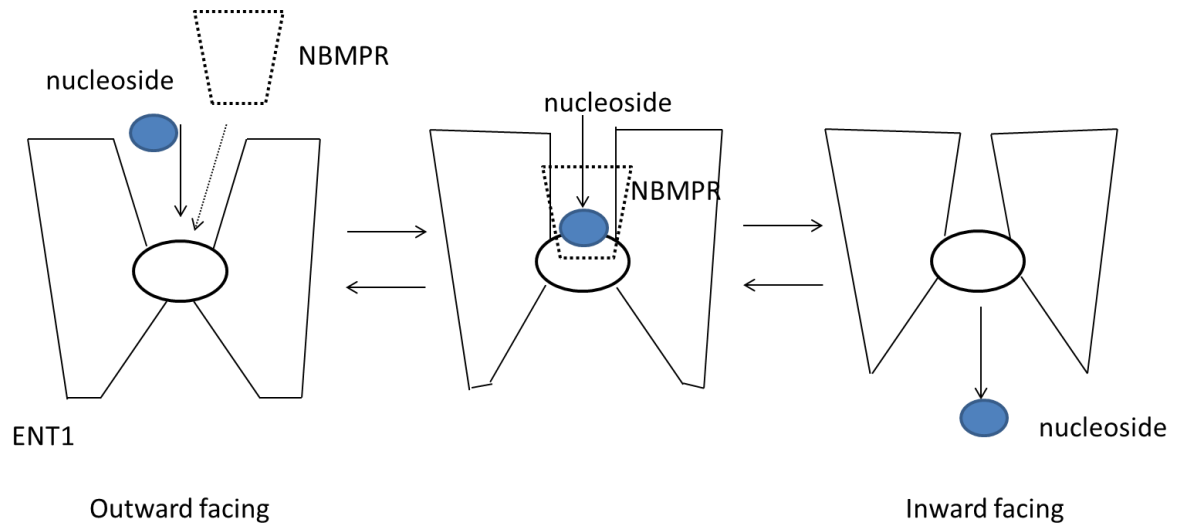


Figure 1.10. Schematic depicting the alternating access model for ENT1.

The substrate/nucleoside binding site will be alternately exposed from the extracellular milieu (outward facing) to the cytoplasm (inward facing). NBMPR shown in dashed lines would only access ENT1 from the extracellular side and lock it in the outward facing conformation.

Recent high resolution crystal structures of the prokaryotic transporters lactose permease LacY and the glycerol-3-phosphate transporter GlpT [154, 155] have identified important structural and molecular mechanisms of membrane proteins. Surprisingly both transporters show similar folding patterns though they are functionally different. Therefore, new investigations using comparative modeling of unknown transporter structures revolve around the premise that all MFS transporters share a similar folding pattern. Analysis of the primary and secondary sequences of nucleoside transporters have led to the generation of putative models of ENTs that are based on the known 3-D models of proteins in the MFS superfamily.

One model from Baldwin *et al.* compared PfENT1, a Plasmodium falciparum ENT against the template of the bacterial GlpT [40]. This model suggested that TMs 1, 2, 4, 5, 8 and 11 are surrounding the solvent-accessible permeant binding site which has also been shown for the LacY transporter. An alternative modeling approach utilized the template-independent *ab initio* technique. In this manner, the ENT model would be based solely on its primary sequence and a combination of different algorithms and modeling techniques. The proposed *ab initio* model of the LdNT1.1 transporter also found TM domains 1, 2, 4, 5, 7, 8, 10 and 11 to surround the general hydrophilic crevice further validating the previous model on PfENT1 (Figure 1.11) [156]. However, this study also suggested that TM1, 10, and 11 directly line the substrate translocation pathway. Our lab has identified a functional splice variant of mouse ENT1 where the last three TM helices and associated loops were missing [157]. This splice variant (mENT1 Δ 11) was able to both bind NBMPR and translocate 2-chloroadenosine which is contradictory to the proposed 3-D model. Therefore though the models are good foundations to build future studies upon, caution needs to be taken when interpreting these generated models to different species of ENT1 and there is need for them to be experimentally tested.

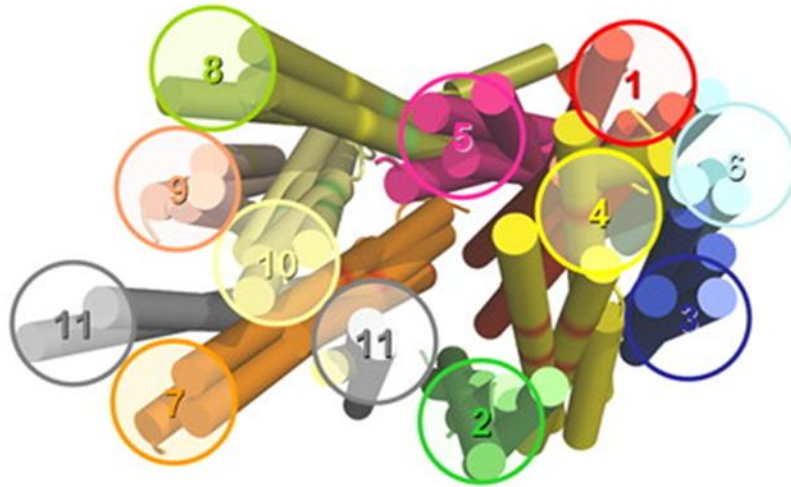


Figure 1.11. Structural model of LdNT1.1 based on *ab initio* analysis.

Transmembrane helices are indicated by rigid cylinders and are numbered 1–11 shown from the cytoplasmic side. Three hypothetical *ab initio* models for LdNT1.1 derived from Rosetta modeling are presented and compared with a model obtained by threading analysis upon the template of the 3-glycerol-phosphate transporter of *E. coli*.

Permission to use copyrighted material: from Valdes *et al.*, 2009 [156]

1.6.5 Thiol modifications

Generally, interactions and orientations comprising the translocation domains are not well defined as there is limited information on the 3-D structure of ENT1. Therefore, useful ways to determine important residues in hENT1 structure and function include mutational techniques and chemical modifying reagents. Chemically modifying a particular amino acid can identify if it is or is not an important residue in the binding of ligands or function of the protein. Since cysteines contain sulfhydryl groups which may form important disulfide bonds in protein folding they are an amino acid of interest. The sulfhydryl moiety of a Cys residue may be located in one or more possible regions: a water accessible region on the extracellular surface; a hydrophobic region of the transmembrane domains; or the cytoplasmic region of the cell's interior. Depending on its location, a cysteine residue will react differently to sulfhydryl compounds of with various physicochemical properties. For example, a cysteine residue located extracellularly in a negatively charged environment may be more accessible to a thiol modifying reagent that is positively charged versus a cysteine located in the lipophilic transmembrane domain which would be more readily accessed by a neutral thiol modifying reagent. Additionally, mutation or modification of endogenous cysteine residues that could interact directly with substrates and inhibitors will alter transporter function and/or inhibitor binding. By determining whether the endogenous Cys residue can be protected from the effects of thiol modification with co-incubation with either substrate or inhibitor, information regarding whether they are located within or close to the permeation site will be provided. Since inhibitors and substrates of hENT1 competitively inhibit each other and therefore are predicted to interact with the transporter in one site but with a separate set of determinants, it will be conducive in finding their separate points of contact.

A previous study of rat ENT2 found an exofacial Cys involved in the functionality of the transporter [158]. Chemical modification of rENT2 with p-chloromercuribenzylosulfonate (pCMBS) (a membrane impermeable sulfhydryl-specific reagent) inhibited rENT2 activity via interaction of pCMBS with Cys140 in TM4.

Additionally, uridine at high concentrations was able to block these effects indicating that Cys140 was located at the exofacial, solvent accessible side of TM4 (given that pCBMS is negatively charged and unable to cross membranes) and was either directly involved in the substrate translocation pathway or in close proximity. The corresponding residue in hENT1 is Gly154 in TM4 which, when mutated to serine, caused a decrease in affinity for the inhibitors NBMPR, dilazep, and dipyridamole in addition to a decrease in affinity for adenosine and cytidine [137]. This suggested that Gly154 was in an important region of the permeant binding site. Not surprisingly, this region of TM 3-6 has already been implicated in both inhibitor and nucleoside binding in hENT1 [134]. Within this region, there are three cysteine residues (Cys 193 in TM5, Cys213 in TM6, and Cys 222 in TM6) that could also potentially contribute to the active site.

The localization of functionally important sulfhydryl groups within membrane proteins has also been achieved through the comparison of the reaction with membrane-permeant and membrane-impermeant sulfhydryl-reactive derivatives [159-161]. Specific reagents used in this thesis include the MTS reagents that all contain a methanethiosulfonate (MTS) moiety attached to a neutral methyl (MMTS) group or various charged groups: ethyltrimethylammonio (MTSET) or ethylsulfonate (MTSES) (Figure 1.12). These reagents add a positive or negative charge at the position of a previously neutral Cys residue, and could cause structural changes in the transporter that can be measured by functional assays. The selectivity and reactivity of these reagents compared to their less reactive counterparts (NEM and pCBMS) is highly desirable for cysteine modifying studies. Additionally, as they come in a variety of sizes and charges, their properties can be exploited to determine if affected residues are in an aqueous or lipid phase of the membrane. These reagents have been exploited in many studies to assess various features of the structure of channel proteins. Recently, they have been used to assess the transmembrane topology of the pore-forming regions of K^+ channels and their relatives, the cyclic nucleotide-gated channels [162-166].

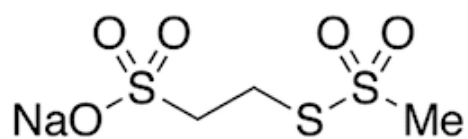
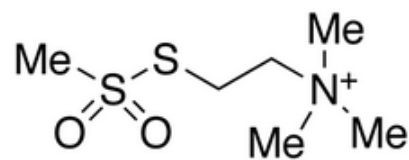
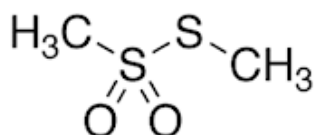
**MTSES (-)****MTSET (+)****MMTS (neutral)**

Figure 1.12. Chemical structures of methanethiosulfonate reagents (MTS): MTSES, MMTS, and MTSET

MTS reagents are thiol modifying reagents that react rapidly and specifically with cysteine groups.

1.7 Substituted cysteine accessibility method

Substituted cysteine accessibility method (SCAM) is a method that has been proven helpful in examining membrane topology and structure of membrane-bound transporters [162, 167]. This technique utilizes site-directed mutagenesis in combination with specific chemical modifying reagents that react with cysteine sulfhydryls. Mutation of a residue to a cysteine can first identify if the loss of the mutated residue was critical for expression and/or function and if the introduced cysteine at that location alters function. Secondly, after the residue is mutated to a cysteine, the protein can be treated with a multitude of thiol modifiers with different characteristics (sizes, charges, membrane permeabilities) to assess if modification alters protein function. If the data shows that the cysteine mutant protein was sensitive to different thiol modifiers compared to the wild-type protein, it may provide evidence as to the location and type of environment of where the introduced cysteine lies. In this manner, if the sequential mutations are carried out on specific domains of a protein (whole transmembrane domains), the resulting data can provide evidence as to which parts of the protein are exposed to the extracellular side as well as determine which residues line the pore or are involved in substrate binding.

By using this technique, information on transmembrane configurations can be elucidated for integral membrane proteins. Such studies have been applied to an array of mammalian transporters such as the glucose transporter (Glut1), glutamate transporter (GltT), and the Na^+/H^+ exchanger 1 (NHE1) [168-170]. However, in order to use cysteine scanning mutagenesis, there is a necessity of having a membrane protein that lacks any endogenous sulfhydryl groups or one that is insensitive to sulfhydryl modification. Most studies employ the use of molecular mutational techniques to remove existing cysteines in order to acquire a cysteine-less construct. This cysteine-less construct must still have wild-type functional characteristics in order to obtain biological meaningful data.

Results of the investigations in determining the role of cysteine functional groups within ENT1 have proven to be variable, apparently due to the use of different species and cell types [171-173]. The outcomes of these studies prove to be debatable as one study using murine myeloma cells found the affinity of NBMPR to ENT1 to be lowered by NEM treatment but had no effect on B_{max} . Alternatively, in other models, NEM had complex effects on the transporter, where it inhibited function or ligand binding at low concentrations but enhanced function/binding at higher concentrations; this once again could be attributed to differences in cell lines and treatment conditions. In our own lab, a previous study has implicated cysteines to be of importance in the binding of NBMPR to ENT1. In mouse ENT1, N-ethylmaleimide (NEM) (a membrane permeable thiol modifying reagent) produced a concentration-dependent biphasic effect on NBMPR binding affinity (K_d) as well as binding sites (B_{max}) in intact cells [174]. As NEM is targeted to block free sulfhydryls by forming covalent thioether bonds at cysteine residues, the resulting loss of NBMPR binding is attributed to a loss of reactive cysteine residues. Additionally, NEM effects were lost when cells were co-incubated with NBMPR, adenosine, or uridine indicating that the sulfhydryls modified by NEM are located within the binding domains of these agents. This same study found p-chloromercuribenzylosulfonate (pCMBS), a membrane-impermeable negatively charged thiol modifying reagent, to cause no effect in intact cells but a decrease in B_{max} and K_d with broken cell preparations supporting a role for intracellular cysteines in ENT1-ligand interactions. A second study in our lab found that the functional truncated slice variant mENT1 Δ 11, missing the last three TM domains (TM9-11) and associated extracellular and intracellular loops 5, could not be photolabeled with [3 H] NBMPR and showed a decrease in NEM sensitivity on NBMPR binding and [3 H] 2-chloroadenosine uptake [156,[157] These data suggest that the loss of the last three TM domains and associated extracellular loop (EL5) leads to a change in reactive residues in the area of the NBMPR binding pocket. It is suggested that TM9-11 and EL5 must have a peripheral role in the NBMPR binding pocket crucial for photoaffinity labeling.

Chapter 2: Rationale

It is well established that nucleoside transporters modulate the flux of physiologically important nucleosides and cytotoxic nucleoside analogues into and out of cells [43, 93, 175]. As mentioned in Chapter 1, ENT1 is the main contributor to the regulation of extracellular concentrations of adenosine available to purinergic receptors and is therefore a viable therapeutic target for drug development [98, 114-117]. Additionally, the successful delivery of nucleoside-based drugs into their intracellular sites of action is dependent on functional nucleoside transporters at the plasma membrane, highlighting the role that nucleoside transporters play in targeted chemotherapies [123, 124, 176, 177]. However, the current understanding of ENT1 structures is limited to predicted topologies and low resolution homology modeling. The generation of specific drugs that can target hENT1 will be greatly assisted if the structure and mechanism of how ENTs function is elucidated. Identifying the specific regions and residues that contribute to the inhibitor binding pocket and substrate translocation site will be important to further refine the current structural model of ENT1. Since integral membrane proteins like hENT1 are not readily amenable to crystallization procedures, alternative techniques such as cysteine scanning mutagenesis are required to access information on its structure.

As mentioned previously, results from previous studies attempting to identify the importance of cysteine residues in ENT1 function are variable given the use of different models, species of ENT1, reagents and treatment conditions. However, the general findings from these studies suggest that modification of cysteine residues alters the function of ENT1. This thesis further probes the general finding by utilizing site-directed mutagenesis techniques and specific sulfhydryl reagent treatments to attempt a systematic analysis of the ligand binding site of hENT1 to better understand the molecular mechanisms of nucleoside transport and its structure.

2.1 Hypothesis #1:

There is a cysteine in a hydrophobic environment that, when modified, affects NBMPR binding.

Rationale #1:

A previous study by Vyas *et al.*, examined a range of group-specific amino acid modifiers for their effects on NBMPR binding and found that treatment with phenylglyoxal (targets arginines), diethylpyrocarbonate (targets histidines), acetic anhydride, succinic anhydride, or ethyl acetimidate (targets lysines) had no effect on NBMPR binding [174]. However, treatment with trinitrobenzylsulfonic acid (TNBS) inhibited NBMPR binding. Since TNBS reacts with lysine (amino groups) and cysteines (sulfhydryl groups), and ethyl acetimidate produced no effect on NBMPR binding, the effect of TNBS was suggested to be due to cysteine groups. This suggestion was further confirmed using the sulfhydryl modifiers NEM and pCMBS which are more selective for sulfhydryl groups on cysteines. Treatment with NEM (a neutral membrane permeable thiol modifier) produced an irreversible biphasic inhibition on cells and cell membrane preparations and a decrease in NBMPR binding affinity (K_d) as well as binding sites (B_{max}) in intact Ehrlich cells. In contrast, the membrane-impermeable negatively charged reagent pCMBS had no effect on intact cells. As NEM is targeted to block or alkylate free sulfhydryls from cysteine residues, the resulting loss of NBMPR binding is attributed to a loss of reactive cysteine residues.

Additionally, NEM effects were lost when cells were co-incubated with NBMPR, adenosine, or uridine indicating that the sulfhydryls modified by NEM are located within the binding domains of these agents. Given that NEM but not pCMBS produced effects, we hypothesize that there is a cysteine residue that contributes to NBMPR binding located in a hydrophobic region of hENT1. Human ENT1 has 7 cysteine residues (C87, C193, C213, C222, C297, C333, and C439) predicted to be in TM helices and therefore may be located in potential hydrophobic regions (Figure 2.1). One or more of these residues may be accessible for neutral thiol modifiers and impact the functional site of hENT1. Additionally, another study examining mouse ENT1 found that NEM had no effect on NBMPR binding to mENT1 Δ 11, (a mouse ENT1 variant missing the last three transmembrane domains TM9-11) [157]. This indicated that cysteines residing in TM9-11

and interacting loops in ENT1 were responsible for NEM effects to full length mENT1. In human ENT1 there are four cysteines residues in that region (Cys378 in TM9, Cys 414 in IL5, Cys 416 in IL5, and Cys 439 in TM11) indicating that they could also be targeted for sulfhydryl modification to impact transporter function.

2.2 Hypothesis #2:

There is a cysteine residue in a cytoplasmic region of hENT1 that, when modified, affects NBMPR binding.

Rationale #2:

As previously mentioned, the study by Vyas *et al.* examined the effects of pCMBS (membrane impermeable thiol modifier) on mouse and human ENT1 function. In intact cells, pCMBS had no effect on NBMPR binding to mouse or human ENT1. However, when pCMBS was applied to broken cell preparations of Ehrlich cells and human erythrocyte membranes, NBMPR binding (B_{max} and K_d) decreased by 100%. Given that pCMBS cannot cross the cell membrane and had no effect to intact cells, this indicated that the inhibition to NBMPR binding to cell membranes was caused by modification of intracellular cysteine residues. We therefore hypothesize that intracellular cysteine residues impact the binding site of NBMPR. There are two likely cytoplasmic cysteines (Cys414 and Cys416) found in the C-proximal half of hENT1. It is possible that these residues contribute to the extracellular facing NBMPR binding site.

2.3 Hypothesis #3:

Residues in EL5 are involved in the NBMPR binding pocket and permeant recognition site.

Rationale #3:

The study by Robillard *et al.*, examining mENT1 Δ 11, (a mouse ENT1 variant lacking the last three TM domains TM9-11 and associated loops EL5 and IL5) found that the functional truncated splice variant could not be photolabeled with [³H]NBMPR compared to the full length wild-type variant mENT1. Therefore, this suggested that the loss of the C-terminal region of mENT1 causes either a loss of residues involved in

NBMPR cross-linking or a shift in ENT1 conformation which prevented the residues to become accessible for covalent attachment to NBMPR. Given that the region of ENT1 that is predicted to covalently attach with NBMPR after UV exposure is in the N-terminal half of the protein [178-180], these data suggested that the loss of the last three TM domains and associated extracellular loop (EL5) lead to a change in reactive residues in the area of the NBMPR binding pocket available for covalent modification. It was suggested that TM9-11 and EL5 must have a peripheral role in the NBMPR binding pocket crucial for photoaffinity labeling. Therefore we hypothesized that residues in the extracellular loop five are involved in the NBMPR binding pocket and permeant recognition site.

Experimental objectives:

The aim of this research project was to perform cysteine mutagenesis combined with thiol modifications on endogenous cysteine residues of hENT1 and on the residues of extracellular loop 5 to expand the current knowledge of hENT1 structure and to isolate the specific residues that are important in the functional characteristics of hENT1. Utilizing site-directed mutagenesis with the addition of sulfhydryl reagent treatments, this thesis attempted a systematic analysis of a portion of the extracellular binding pocket of hENT1 to better understand the molecular mechanisms of nucleoside transport and the structure of hENT1.

2.4 Specific Aims:

1. To determine the sensitivity and accessibility of endogenous cysteines in hENT1 with methanethiolsulfonate reagents of varying sizes and charges by:
 - a. Determining the cysteine residue(s) involved in MMTS effects (neutral membrane permeable thiol modifier)
 - b. Determining the cysteine residue(s) involved in MTSET effects (positively charged, membrane impermeable thiol modifier)

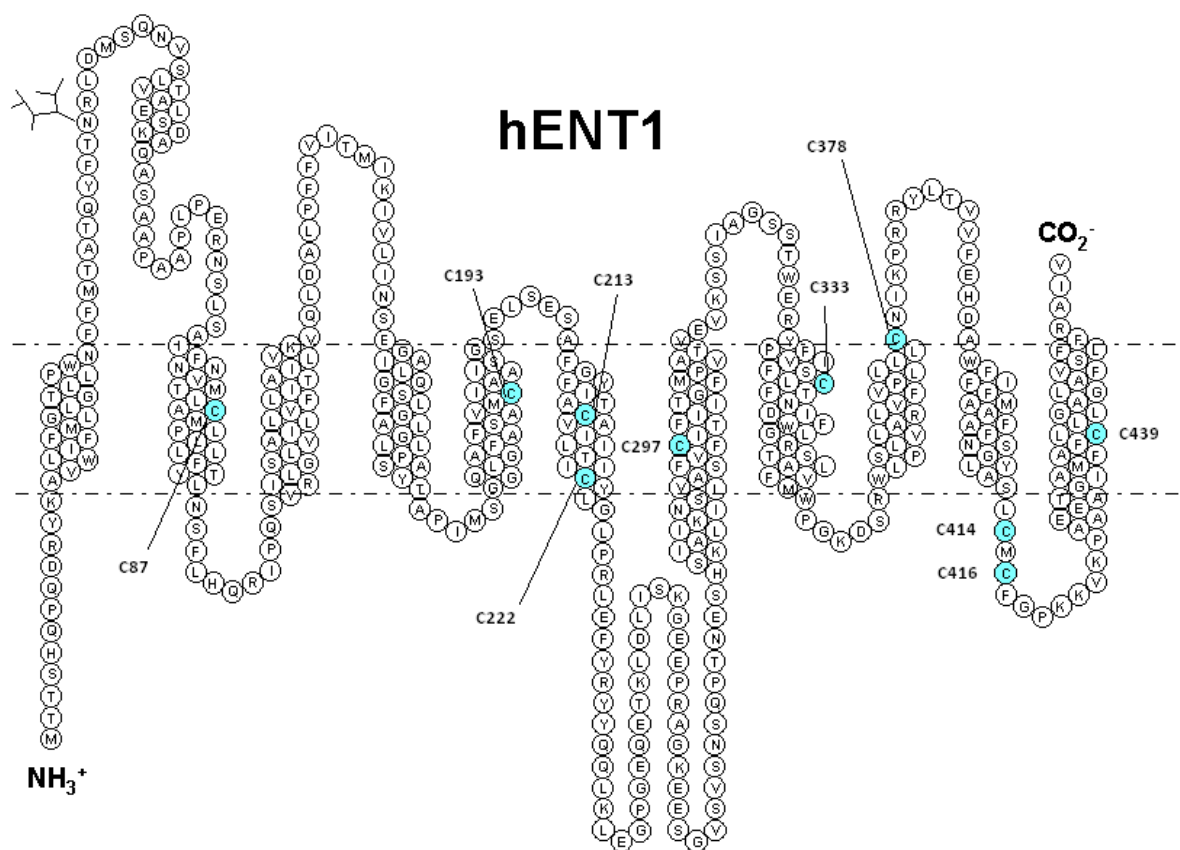


Figure 2.1. Predicted 2-D topology of hENT1 with location of 10 endogenous cysteine residues indicated in light blue circles.

- a. Determining the cysteine residue(s) involved in MTSES effects (negatively charged, membrane impermeable thiol modifier)
-
2. Create an extracellular-cysteine-less mutant for SCAM analysis of extracellular binding determinants of substrates and inhibitors
 3. To determine the effects of mutating residues in EL5 to cysteines on NBMPR binding and 2-chloroadenosine uptake
 4. To probe the accessibility of the introduced cysteines in EL5 to MTSET and determine if they are protected by hENT1 ligands

Chapter 3: Materials and Methods

3.1 Materials:

[³H]NBMPR (5.5-20.1 Ci/mmol), [³H]2-chloroadenosine (9.1 Ci/mmol), and [³H]-labeled water (1 mCi/g) were obtained from Moravek Biochemicals (Brea, CA). Methyl methanethiosulfonate (MMTS), [2-(trimethylammonium)ethyl]methanethiosulfonate bromide (MTSET), and sodium (2-sulfonatoethyl)methanethiosulfonate (MTSES) were acquired from Toronto Research Chemicals (Toronto, ON). Culture-grade phosphate-buffered saline (PBS), Modified Eagle's Medium (MEM), G418 (Geneticin), penicillin/streptomycin, trypsin/EDTA, sodium pyruvate, nonessential amino acids, and Lipofectamine LTX® and Lipofectamine 2000® were purchased from Invitrogen (Burlington, ON). Bovine growth serum (BGS) was supplied by ThermoScientific, Hyclone Laboratories (Utah, USA). T175 flasks, T75 flasks, T25 flasks, 12-well plates and 24-well plates were purchased from BD Biosciences (Bedford, MA). Cloning cylinders were supplied by Bel-Art Products (Pequannock, NJ). Oligonucleotide primers were obtained from Sigma-Genosys (Oakville, ON). NBMPR, 2-chloroadenosine, dipyrindamole, nitrobenzylthioguanosine riboside [NBTGR; S-(4-nitrobenzyl)-6-thioguanosine], and p3×FLAG-CMV10 vector were purchased from Sigma-Aldrich (Oakville, ON). The QIAprep Spin miniprep kit was provided by Qiagen (Mississauga, ON). TRIZOL® Reagent, Superscript™ First Strand Synthesis System for RT PCR, Platinum® Pfx DNA Polymerase, and the PureLink™ Quick Gel Extraction Kit were purchased from Invitrogen (Burlington, ON). Dilazep (N,N'-bis[3-(3,4,5-trimethoxybenzyloxy)propyl]-homo-piperazine) was provided by Asta Werke (Frankfurt, Germany) and draflazine [2-(aminocarbonyl)-4-amino-2,6-dichlorophenyl]-4-[5,5-bis(4-fluorophenyl) pentyl]-1-piperazine acetamide 2HCl] was acquired from Janssen Research Foundation (Beerse, Belgium). 2-Bromohexadecanoic acid (2-bromopalmitic acid [2-Br]) was purchased from Sigma Aldrich (Oakville, ON). The primary monoclonal mouse anti-FLAG Ab and secondary goat anti-mouse Ab were purchased from Sigma Aldrich (Oakville, ON). The primary monoclonal mouse anti-Na⁺, K⁺-ATPase Ab were purchased from AbNova (Cambridge, MA., USA). Cell lysis buffer (10X) and LumiGLO® chemiluminescent substrate were

purchased from Cell Signaling Technology (Danvers, MA). The mammalian protease inhibitor cocktail was purchased from Calbiochem (Billerica, MA). The Bradford colorimetric protein assay kit was purchased from Thermo Fisher Scientific (Waltham, MA). Pierce Cell Surface Protein Isolation Kit was purchased from ThermoScientific (Rockford, IL). PK15-NTD (Pig Kidney nucleoside transporter-deficient) cells and hENT1-pcDNA3.1 were generously provided by Dr. Ming Tse (Johns Hopkins University, Baltimore, MD). 5'-S-[2-(1-[(fluorescein-5-yl) thioureido]-hexanamido) ethyl]-6-N-(4-nitrobenzyl)-5'-thioadenosine (FTH-SAENTA) was generously donated by Dr. John K. Buolamwini (The University of Tennessee Health Science Centre, Memphis, TN).

3.2 Plasmid generation:

EcoRV and KpnI restriction sites were added, respectively, to the 5' and 3' ends of the cDNA encoding hENT1 (primers 5' EcoRV: 5`AGCGCGGATATCGATGACAACCACT3` and 3' Kpn I: 5`TAGCTAGGTACCTCACAC AATTGCCCG3`) (Sigma Aldrich), and the resulting construct was ligated into p3xFLAG-CMV-10 using standard techniques. Briefly, the p3xFLAG-CMV-10 expression vector was digested with KpnI and EcoRV restriction enzymes (Fermentas, Burlington, ON) at 37°C for 1 hr, after which the hENT1 cDNA was ligated into it with a femtomolar vector/insert ratio of 1:3, using a T4 DNA Ligase Kit (Invitrogen, Burlington, ON). The resulting expression plasmid, hENT1-p3xFLAG (N-terminal epitope tag-DYKYYYD), was amplified and purified using the QIAprep® Spin Miniprep Kit (Qiagen, Mississauga, ON). The sequence of the vector was confirmed by DNA sequencing at the Roberts Research Institute Sequencing Facility (London Regional Genomics Centre, London, ON).

3.3 Single amino acid mutagenesis

Single amino acid substitutions were introduced into the hENT1-p3xFLAG template using the Stratagene Quikchange mutagenesis kit (Stratagene, Mississauga, ON) following the manufacturer's instructions. Primers for all mutations are listed in Table 2. Briefly, 25 ng of hENT1-p3xFLAG template and 125 ng each of the respective forward (5') and reverse (3') primers were added to a PCR mixture containing 10X reaction buffer,

deoxyribonucleotide triphosphates (dNTPs), ddH₂O and *PfuUltra* High Fidelity DNA polymerase (2.5 U/μl). The reactions were overlaid with 30 μl of mineral oil and cycled in a Perkin-Elmer 480 thermal cycler using the following parameters: 95°C for 30 sec (1 cycle); 95°C for 30 sec, 55°C for 1 min and 68°C for 8 min (16 cycles). Completed reactions were placed on ice for 2 min and then incubated with 1 μl of *Dpn* I restriction enzyme (10 U/μl) at 37°C for 1 hr to digest parental dsDNA. Digested plasmid DNA was transformed into XL1-Blue supercompetent cells, plated onto LB-ampicillin agar plates containing 80 μg/ml X-gal and 20 mM IPTG and incubated overnight at 37°C. The next day, viable colonies were picked, shaken overnight (250 rpm, 37°C) in LB broth containing 0.1 mg/ml ampicillin, and plasmid DNA was extracted using the QIAprep® Spin Miniprep Kit (Qiagen, Mississauga, ON). The hENT1-p3xFLAG and hENT1-mutants-p3xFLAG were sequenced by DNA sequencing at Robarts Research Institute Sequencing Facility (London Regional Genomics Centre, London, ON). The resulting sequence was compared with the full published coding region of hENT1 (GenBank accession number: gi:1845345e).

3.4 Stable cell line generation:

The PK15 cells of pig kidney epithelial tissue were donated from Dr. Ming Tse (Johns Hopkins University, Baltimore, MD, USA) were initially made nucleoside transport deficient by treating them first to with ethylmethanesulfonate, a chemical mutagen, and secondly to the cytotoxic nucleosides cytarabine (AraC) and tubercidin. After a 3 week treatment period, viable cells that survived the cytotoxic nucleoside exposure were screened for [³H]uridine transport to determine whether or not resistance was due to the absence of nucleoside uptake [181]. After confirmation of nucleoside transport deficiency, the PK15-NTD cells were transfected with hENT1-p3xFLAG (wild-type) or Ser-substituted hENT1-mutations using Lipofectamine 2000®. Near (90%) confluent cells were incubated with 1.6 μg of plasmid, 4.8 μl of Lipofectamine® and 200 μl of OptiMEM®. After 24 hr incubation, transfected cells were placed under a three week

Table 3.1. List of the PCR primers used for single site-directed mutagenesis of cysteine residues to serine residues on the hENT1 template. Underlined base pairs indicate the mutation site.

Cysteine Mutation	Prime sequence (5' to 3')
C87S Forward	CAATGTCATGACCCTAT <u>CTG</u> CCATGCTGCCCTGC
C87S Reverse	GCAGGGGCAGCATGGC <u>AGAT</u> AGGGTCATGACATTG
C193S Forward	CCATGATCT <u>CCG</u> CTATTGCCAGTGGCTC
C193S Reverse	GAGCCACTGGCAATAGC <u>GG</u> AGATCATGG
C213S Forward	CGGCTACTTTATCACAGCCT <u>CTG</u> CTGTTATCATTGACC
C213S Reverse	GGTCAAAATGATAACAGC <u>AGAG</u> GCTGTGATAAAGTAGCCG
C222S Forward	GACCATCAT <u>CTC</u> TTACCTGGGCCTGCC
C222S Reverse	GGCAGGCCAGGTA <u>AGAG</u> ATGATGGTC
C297S Forward	GTCCTGGCTTTCTCTGT <u>CTC</u> CTTCATCTTCAC
C297S Reverse	GTGAAGATGA <u>AGGAG</u> ACAGAGAAAGCCAGGAC
C333S Forward	CGTTACTTCATTCTGTGT <u>CTC</u> TTCTTGACTTTC
C333S Reverse	GAAAGTCA <u>AGAA</u> AGAGGACACAGGAATGAAGTAACG
C378S Forward	CCACTGCTGCTGCTG <u>TCCA</u> ACATTAAGCCCCG
C378S Reverse	CGGGGCTTAATGTT <u>GGAC</u> AGCAGCAGCAGTGG
C414S Forward	GGCTACCTCGCCAGCCT <u>CTC</u> TATGTGCTTCGGGCCAAG
C414S Reverse	CTTGGGCCGAAGCACAT <u>AGAG</u> AGGCTGGCGAGGTAGCC
C416S Forward	CTCGCCAGCCTCTGCATG <u>TCT</u> TTCGGGCCCAAGAAAGTG
C416S Reverse	CACTTTCTGGGCCGAA <u>AGAC</u> ATGCAGAGGCTGGCGAG
C439S Forward	CATCATGGCCTTCTTCTGT <u>CTC</u> TGGGTCTGGCACTGGGG
C439S Reverse	CCCCAGTGCCAG <u>ACCC</u> AGAGACAGGAAGAAGGCCATGATG

selection period using 500 µg/ml G418 in modified Eagle's medium supplemented with 10% (v/v) bovine growth serum (BGS), 100 U of penicillin, 100 µg/ml of streptomycin, 0.1 mM nonessential amino acids, and 1 mM sodium pyruvate (Selection media). Individual cell colonies were selected and expanded in media containing 300 µg/ml G418 (Maintenance media) at 37°C in a 5% CO₂ humidified atmosphere. Each individual monoclonal population of cells were then checked for hENT1 transcript by collecting mRNA, performing reverse-transcription PCR, and sequencing. Briefly, total RNA was isolated using TRIZOL® reagent (Invitrogen, Burlington, ON) following the manufacturer's instruction. Isolated mRNA was then reverse transcribed to cDNA using a Superscript™ First Strand Synthesis kit and amplified using Platinum® Pfx DNA Polymerase. Primers for the hENT1 cDNA (forward primer: hENT1 5' – GACAACCAGTCACCAGCCTCAGGACAG; reverse primer: hENT1 3' – CACACAATTGCCCGGAACAGGAAGGAG) were used to amplify the extracted cDNA in a Perkin-Elmer 480 Thermal Cycler using the following conditions: 2 min at 94°C; 15 s at 94°C, 30 s at 55°C, 1.5 min/kb at 68°C (for 35 cycles); 7 min at 68°C. PCR amplified DNA samples were then resolved on a 1.0% agarose gel and visualized under UV light. Bands that were found at the corresponding the hENT1 cDNA size (1377 kb) were isolated and purified using the PureLink™ Quick Gel Extraction Kit. Purified PCR products were then sequenced as before.

3.5 Transient transfections:

PK15-NTD cells were transfected with empty-p3xFLAG (empty control), wild-type hENT1-p3xFLAG, and mutants hENT1-C416A, hENT1-439A, or EL5-mutants-p3xFLAG (16 individual mutants) using Lipofectamine LTX® following the manufacturer's instruction (Invitrogen, Burlington, ON). Briefly, 18.75 µg plasmid DNA was incubated with 3.75 ml Opti-MEM® media, 18.75 µl Plus reagent, and 46.87 µl of Lipofectamine LTX® for 30 min. After 30 min, the DNA-Lipofectamine complex was slowly added to near (90%) confluent cells grown in T75 flasks void of antibiotics and incubated for at least 24 hrs before their utilization.

3.6 Crude Cell Membrane Preparations:

PK15-NTDs expressing hENT1-p3xFLAG or hENT1-mutants-p3xFLAG were harvested from T175 flasks by 0.05% Trypsin/0.53 mM EDTA. Cells pellets were then resuspended in 5 mM sodium phosphate buffer containing a mammalian protease inhibitor cocktail (Calbiochem, Billerica, MA) for 30 min on ice. Cells were then sonicated using a Sonic Dismembrator model 150 for 30 s and then centrifuged at 3,000× *g* for 30 min at 4°C to pellet nuclei and whole cells. The supernatant containing the crude cell membranes were then centrifuged for 1 hr at 30,000 × *g* at 4°C to pellet the membranes. The remaining membrane pellet was then resuspended in 5 mM sodium phosphate buffer and protease inhibitor cocktail mix and protein content was determined by the Bradford colormetric assay. Resuspended crude membranes were either used immediately for subsequent assays or frozen at -80°C to be used at a later date.

3.7 Treatment with MTS reagents:

PK15-NTD cells expressing hENT1-p3xFLAG or hENT1-mutants-p3xFLAG were harvested from culture flasks using 0.05% Trypsin/0.53 mM EDTA, diluted with media containing 10% (v/v) BGS, collected by centrifugation at 6,000x*g*, and washed twice with phosphate-buffered saline (PBS; 137 mM NaCl, 6.3 mM Na₂HPO₄, 2.7 mM KCl, 1.5 mM KH₂PO₄, 0.5 mM MgCl₂ • 6H₂O, 0.9 mM CaCl₂ • 2H₂O, pH 7.4, 22°C). Cell pellets were then suspended in PBS for [³H]NBMPR binding assays or sodium-free N-methyl-D-glucamine (NMG) buffer (pH 7.25, containing 140 mM NMG, 5 mM KCl, 4.2 mM KHCO₃, 0.36 mM K₂HPO₄, 0.44 mM KH₂PO₄, 10 mM HEPES, 0.5 mM MgCl₂, and 1.3 mM CaCl₂) for [³H]2-chloroadenosine uptake assays. Cell suspensions were incubated with 0.1% dimethylsulfoxide (DMSO, control) or MTS reagents dissolved in DMSO. Cell suspensions were then washed three times with PBS or NMG, depending on the assay type, by centrifugation to remove un-reacted MTS reagents. A concentration versus time course analysis was performed with each MTS reagent to optimize the concentration and incubation period needed for a maximal distinguishable effect. In some experiments, 10 nM NBMPR or 1 mM adenosine was included in the MTS treatment protocol to assess the ability of these ENT1 ligands to protect the cells from MTS modification.

3.8 [³H]NBMMPR binding assay:

PK15-NTD cells expressing empty-p3xFLAG, hENT1-p3xFLAG or hENT1-mutants-p3xFLAG (~75,000 cells per assay) were suspended in PBS and incubated with [³H]NBMMPR for 45 min at room temperature (~22°C). Cells were collected on Whatman Binder-Free Glass Microfiber Filters: Type 934-AH using a 24-port Brandel cell harvester, washed twice with Tris buffer (10 mM Tris, pH 7.4, 4°C) and analyzed for ³H content using standard liquid scintillation counting techniques. Specifically bound [³H]NBMMPR was defined as total binding minus cell-associated [³H]NBMMPR in the presence of 10 μM nitrobenzylthioguanosine riboside (NBTGR) (nonspecific binding). Nonlinear regression was used to fit hyperbolic curves (GraphPad Prism 4.03) of specific [³H]NBMMPR binding against the free concentration of [³H]NBMMPR, in order to determine K_d and B_{max} values. Curves were fitted using one-site specific binding based on the equation $Y = B_{max} * X / (K_d + X)$, where Y= specific binding and X= concentration of radioligand.

3.9 5'-S-[2-(1-[(fluorescein-5-yl) thioureido] hexanoamido) ethyl]-6-N (2-nitrobenzyl) -5'-thio adenosine (FTH-SAENTA) Inhibition Assay:

PK15-NTD cells transfected with hENT1-p3xFLAG, C416A-p3xFLAG, C439A-p3xFLAG or EL5-mutants-p3xFLAG were incubated with 5 nM [³H]NBMMPR for 40 min in the presence and absence of 100 nM FTH-SAENTA (membrane impermeable) or 10 μM NBTGR (non-specific binding) and then processed as described above for the [³H]NBMMPR binding assays. FTH-SAENTA would displace only the extracellular binding sites of [³H]NBMMPR as the large fluorescein tag prevents access to intracellular pools [143, 182]. Data was calculated as the total amount of NBTGR-sensitive [³H]NBMMPR binding inhibited by FTH-SAENTA which represented the percentage of sites expressed at the membrane.

3.10 [³H]2-chloroadenosine uptake assay:

Uptake was initiated by the addition of suspended cells (~750,000 cells per assay) in NMG buffer to [³H]2-chloroadenosine layered over 200 μl of silicon/mineral oil (21:4 vol/vol) in 1.5-ml microcentrifuge tubes. Parallel assays were conducted in the absence (total uptake) and presence (non-transporter-mediated uptake) of 5 μM NBMMPR/dipyridamole to determine the ENT1-mediated uptake of substrate in each

condition. Initial rates of uptake were determined from time-courses of cellular uptake of [³H]2-chloroadenosine and calculated an incubation time of 5 s for measuring transport studies [157]. After the defined incubation time of 5 s, uptake was terminated by centrifugation for 10 s (~12,000 × g). Aqueous substrate and oil layers were removed by aspiration, and pelleted cells were digested in 1 M NaOH overnight (12–16 h). A sample of the digest was removed and analyzed for ³H content using standard liquid scintillation counting techniques. Uptake data are presented as pmol/μl of intracellular volume after correction for the amount of extracellular ³H in the cell pellet. Total volume was determined by incubating cells with ³H₂O for 3 min and processed as above. Extracellular water space was estimated by extrapolation of the linear time course of nonmediated uptake to zero time. To determine K_m, curves were fitted using the Michaelis-Menten equation: $Y = V_{\max} * X / (K_m + X)$, where Y= rate of mediated uptake and X= substrate concentration.

3.11 Inhibition studies:

PK15-NTD cells transfected with hENT1-p3xFLAG or the hENT1-mutant-p3xFLAG were incubated with 0.5 nM [³H]NBMPR for 40 min in the presence and absence of a range of concentrations of test inhibitor, and then processed as described above for the [³H]NBMPR binding assays. IC₅₀ values were determined as the concentration of inhibitor that produced a 50% decrease in the specific binding of [³H]NBMPR. For inhibition of uptake, cells were incubated with 10 μM [³H]2-chloroadenosine in the presence and absence of a range of concentrations of test inhibitor layered over 200 μl of silicon/mineral oil (21:4 vol/vol) in 1.5-ml microcentrifuge tubes. Assays were processed as described above for the [³H]2-chloroadenosine uptake assays. K_i values were derived from IC₅₀ values based on the equation of Cheng and Prusoff [183] using the K_d for [³H]NBMPR binding or the K_m for [³H]2-chloroadenosine uptake determined under the same conditions. Cheng-Prusoff equation: $K_i = IC_{50} / (1 + [L] / K_d)$, where [L]= concentration of free radioligand used and K_d= dissociation constant of the radioligand for the receptor. Data were fitted using the one-site sigmoid dose-response with variable slope model (GraphPad Prism 4.03), using the following equation:

$Y = \text{Bottom} + (\text{Top} - \text{Bottom}) / (1 + 10^{((\text{Log}IC50 - X) * \text{HillSlope}))}$, where $Y =$ % total binding and $X =$ logarithm concentration of the inhibitor. Top and bottom are the maximal and minimal limits constrained to 100% and 0% of total site-specific binding, respectively.

3.12 Cell Surface Biotinylation:

The biotinylation and isolation of cell surface proteins for Western blot analysis was performed as per manufacturer's instructions (Thermo Scientific, Rockford, IL, USA). In brief, untransfected and transiently transfected wild-type hENT1 and C416A PK15-NTD cells were grown in four T75 flasks, washed with cold PBS and incubated for 30 min with cold membrane-impermeable Sulfo-NHS-SS-Biotin on a rocking platform at 4°C. The cells were harvested and washed with Tris-Buffered Saline (TBS) with subsequent centrifugation at 500 × g for 3 min. Cell pellets were lysed, sonicated, and vortexed periodically on ice for 30 min. Cell lysate was spun at 10,000 × g for 2 min at 4°C after which the supernatant was added to the column of NeutrAvidin Agarose and incubated for 60 min at 20°C with end-over-end mixing using a rotator. The column was then washed and cell surface protein was eluted from the column using end-over-end mixing for 60 min incubation with SDS-PAGE and DTT sample buffer. The eluted protein samples were then used for Western blot analysis.

3.13 Western Blot Analysis:

Cell surface expression levels of wild-type hENT1-p3xFLAG and C416A-p3xFLAG were estimated by western blot analysis where biotinylated samples were loaded into 12% polyacrylamide gels (1.5 M Tris pH 8.8, 0.1% sodium dodecyl sulfate (SDS), bis-acrylamide, 0.05% ammonium persulfate (APS), 0.05% TEMED) and run in the Mini-PROTEAN® Tetra Cell electrophoresis system for ~1 hr at 120 V. Following electrophoresis, gels were transferred to polyvinylidene fluoride (PVDF) membranes using a Trans-Blot® SD Semi-Dry Electrophoretic Transfer Cell at 440 mA, 20 V limit for 45 min. Membranes were blocked for 1 hr at room temperature with 5% skim milk-TBST buffer (0.5 mM Tris, 13.8 mM NaCl, 2.7 mM KCl, 0.05% Tween-20), and then incubated overnight at 4°C with primary monoclonal mouse anti-FLAG Ab (1:2,500 in 5% skim milk-

TBST). Membranes were washed with TBST and incubated for 1 hr at room temperature with secondary goat anti-mouse HRP conjugated antibody (1:25,000 in 5% skim milk-TBST), and then washed further with TBST. Membranes were incubated for 1 min with LumiGLO chemiluminescent reagent and then imaged using the Molecular Imager®VersaDoc™ 5000 MP System (Bio-Rad Laboratories, Hercules, CA). Na⁺/K⁺-ATPase was used as a cell surface loading control after membranes were stripped with mild Stripping Buffer (200 mM glycine, 1% Tween-20, and 0.1% SDS; pH 2.2). Following this, membranes were washed twice with PBS and TBST before being blocked for 1 hr with 5% skim milk. The membranes were incubated overnight at 4°C with primary mouse antibody to Na⁺/K⁺-ATPase (1:2,500 in 5% skim milk/TBST). After three washes with TBST, membranes were incubated for 1 hour at room temperature with secondary goat anti-mouse HRP conjugated antibody (1:25,000 in 5% skim milk/TBST). After a final three washes, the membranes were visualized as above.

3.14 Data analysis and statistics:

Data are presented as means ± SEM with hyperbolic curves fitted using Graphpad Prism 5.0 software. Where appropriate, statistical analysis was performed using a One-way ANOVA (Dunnett's), or a paired student's t test with p<0.05.

Chapter 4: Results

Many attempts have been made to determine the role of cysteines in nucleoside transport function; however results from those studies have been inconsistent. Within the murine system, NEM and pCMBS treatments have indicated the involvement of two cysteines in ENT1 function [157, 174]. In our own lab, the membrane permeable thiol modifying compound NEM significantly inhibited binding of the selective probe NBMPR at low concentrations, while at high concentrations enhanced binding. Additionally, the negatively charged membrane impermeable reagent pCMBS inhibited NBMPR binding when allowed access to the intracellular side. This suggested that there are two cysteine residues involved in the two distinct effects. To extend these previous studies, experiments were carried out with a different set of sulfhydryl-reactive MTS reagents of different sizes and charges to probe the locations of cysteines. These reagents possess enhanced sensitivity and reaction rates against cysteine residues in comparison to NEM and pCMBS. Changes in hENT1 functionality were assessed by measuring binding of the prototypical inhibitor [³H]NBMPR and the transport kinetics of the substrate [³H]2-chloroadenosine.

4.1 Validation that hENT1-p3XFlag functions in PK15-NTD cells:

Initial studies confirmed that the PK15-NTD cells transfected with empty-vector were devoid of nucleoside transport activity and did not bind [³H]NBMPR (Vector only from Figure 4.1A). After stable transfection of wild-type hENT1-p3xFLAG, PK15-hENT1 cells specifically bound [³H]NBMPR with a K_d of 0.4 ± 0.02 nM to a maximum of $3.6 \pm 0.2 \times 10^5$ ENT1 sites/cell (Figure 4.1A). Membranes prepared from the PK15-hENT1 transfectants had an affinity for [³H]NBMPR of 0.1 ± 0.02 nM and bound 1.2 ± 0.1 pmol/mg protein (Figure 4.1B). PK15 cells transfected with hENT1 cDNA accumulated [³H]2-chloroadenosine via a NBMPR-sensitive transport process with a V_{max} of 9.5 ± 0.8 pmol/ μ l/s and K_m of 71 ± 8 μ M (Figure 4.1C). Fundamentally, PK15-hENT1 cells bound NBMPR with high affinity (nM) and transported 2-chloroadenosine with high affinity (μ M). These characteristics are consistent with a fully functional ENT1-type transporter,

and are similar to previous reports of hENT1 constructs expressed in this cell model [181] indicating that the N-terminus FLAG epitope did not significantly affect transporter functionality.

4.1.1 Inhibitor profile for PK15-hENT1 cells

To determine if there were any compound specific differences and sensitivities for the coronary vasodilators in transfected hENT1-FLAG-tagged constructs, the PK15-hENT1 cells were incubated with increasing concentrations of competitive inhibitors to determine their ability to alter [³H]NBMPR binding or [³H]2-chloroadenosine uptake. The coronary vasodilators: Dipyridamole, dilazep, and draflazine inhibited the binding of [³H]NBMPR with K_i values of 22 ± 8 , 1.9 ± 0.4 , and 3.3 ± 0.7 nM, respectively (Figure 4.2A). Additionally, dipyridamole, dilazep, NBMPR, and NBTGR inhibited [³H]2-chloroadenosine influx with K_i values of 111 ± 35 , 10.4 ± 1.7 , 2.0 ± 1.0 , and 8.6 ± 1.9 nM, respectively (Figure 4.2B). These values reflect the inhibitor's capacity to effectively block the permeation site as previously seen in other studies [98, 133, 157, 184]. Draflazine, dipyridamole, and dilazep are competitive inhibitors of the binding of NBMPR and substrate uptake in a variety of experimental models indicating that the expression vector and FLAG-tag did not alter the hENT1 binding site for these inhibitors and verified the mammalian cell model [86, 171, 185].

4.1.2 DTT treatment had no effect on PK15-hENT1 cells

In the analysis of the amino acid sequence of hENT1, there were five potential disulfide bridges that were identified using a network predictor site, *DiANNA 1.1 web server*, utilizing all of the ten endogenous cysteines highlighted in Figure 2.1. In this model, the potential bridges would link [C87-C378]; [C193-C222]; [C213-C333], [C297-C414], and [C416-C439]. To determine the presence and importance of these potential disulfide bridges, PK15-hENT1 cells and cell membranes were treated with dithiothreitol (DTT) and assessed for [³H]NBMPR binding. Dithiothreitol treatment (2 mM, 10 min, room

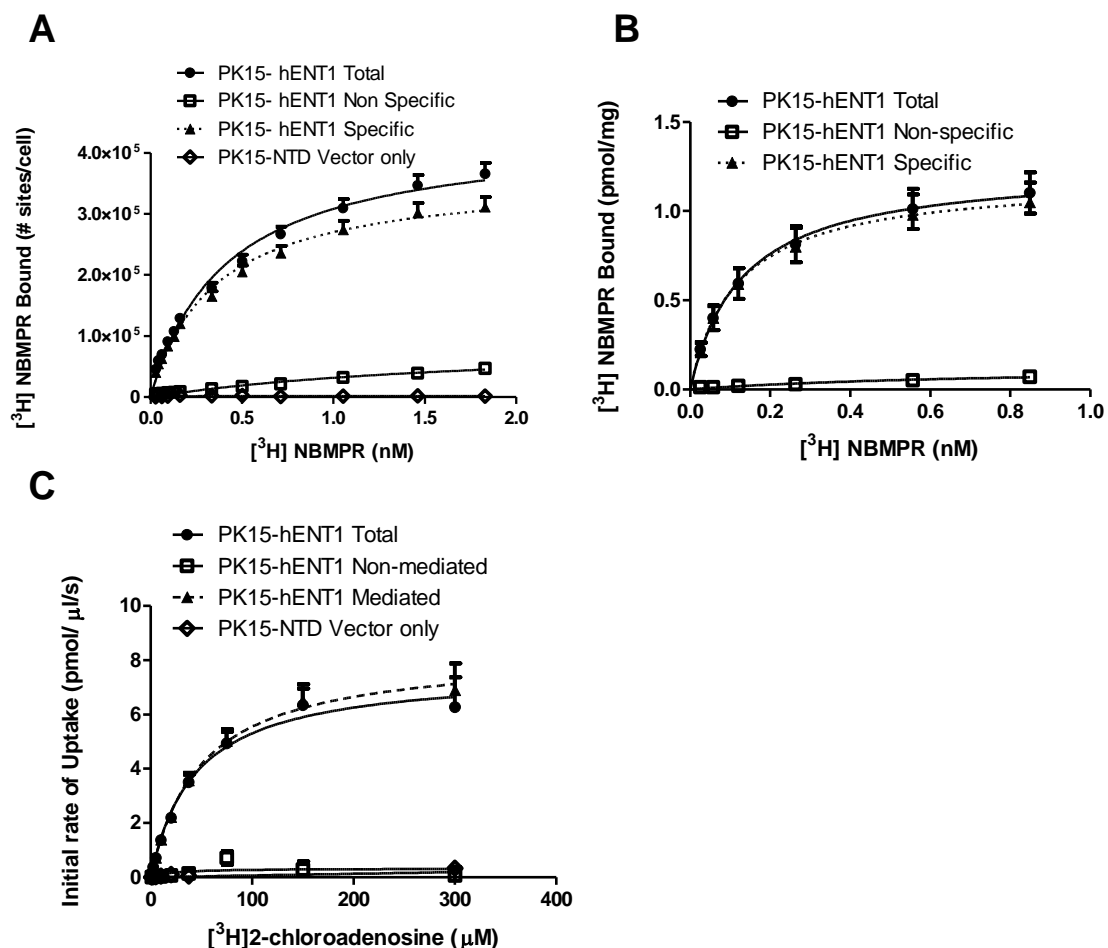
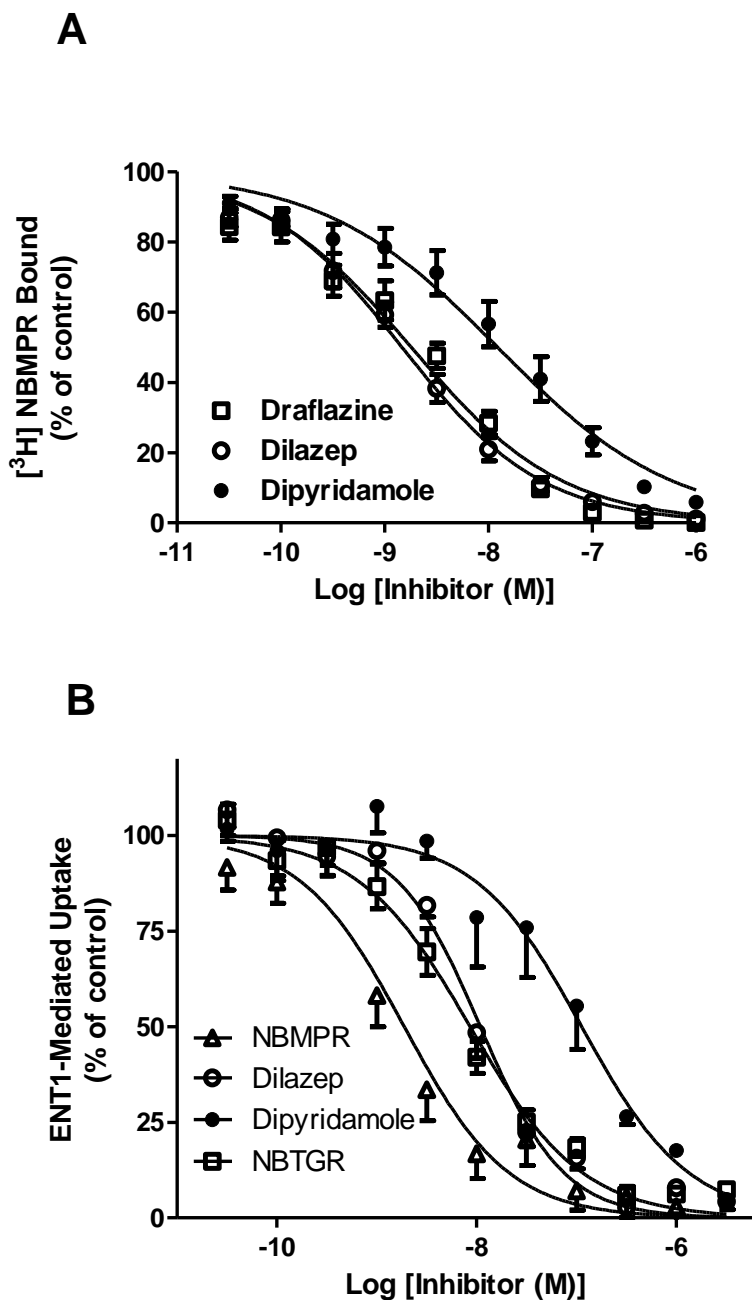


Figure 4.1. Characterization of PK15-hENT1. $[^3\text{H}]$ NBMPR binding of PK15-hENT1 cells (**Panel A**), PK15-hENT1 membranes (**Panel B**) and $[^3\text{H}]$ 2-chloroadenosine uptake of PK15-hENT1 cells (**Panel C**). Specific binding of PK15-hENT1 or PK15-NTD cells was determined by total bound minus non-specific bound where cells or membranes were incubated with a range of concentrations of $[^3\text{H}]$ NBMPR in the presence (nonspecific binding) and absence of 10 μM NBTGR (total binding). Each point represents the mean \pm SEM from at least 11 experiments done in duplicate. Nonlinear regression analysis was used to fit hyperbolic curves to the site-specific binding of $[^3\text{H}]$ NBMPR plotted against the free $[^3\text{H}]$ NBMPR concentration at steady-state. (**Panel C**) Concentration-dependent uptake of $[^3\text{H}]$ 2-chloroadenosine to PK15-hENT1 or PK15-NTD cells incubated with a range of concentrations of $[^3\text{H}]$ 2-chloroadenosine for 5 seconds in the presence or absence of 10 μM dipyrindamole/NBTGR. Each point represents the mean \pm SEM of the cellular accumulation of $[^3\text{H}]$ 2-chloroadenosine from at least ten independent experiments conducted in duplicate.



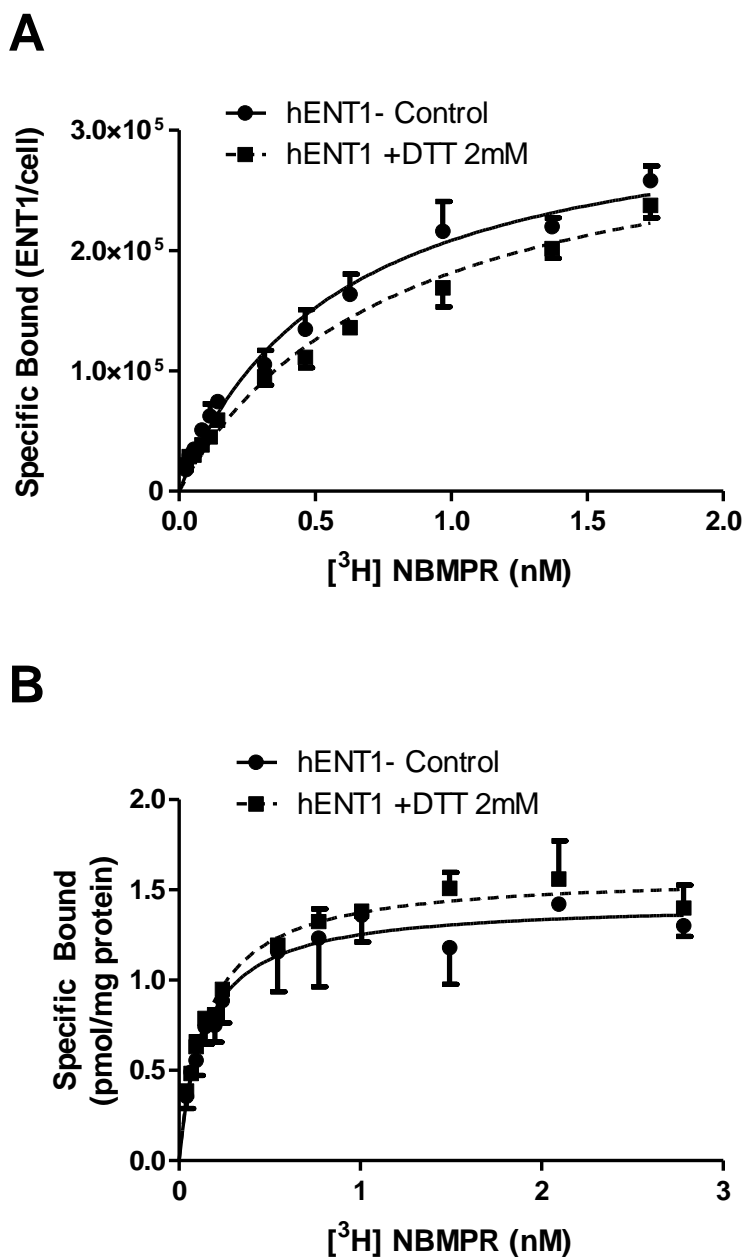


Figure 4.3. Effect of DTT on PK15-hENT1 activity. Effect of 2mM DTT treatment to $[^3\text{H}]$ NBMPR binding of PK15-hENT1 cells (**Panel A**) and PK15-hENT1 membranes (**Panel B**). Cells or membranes were treated with 2 mM DTT for 10 min at room temperature and then incubated with a range of concentrations of $[^3\text{H}]$ NBMPR (abscissa) in the presence (nonspecific binding) and absence of 10 μM NBTGR (total binding). Each point represents the mean \pm SEM from at least four experiments done in duplicate. Nonlinear regression analysis was used to fit hyperbolic curves to the site-specific binding of $[^3\text{H}]$ NBMPR plotted against the free $[^3\text{H}]$ NBMPR concentration at steady-state.

temperature) of the PK15-hENT1 cells and membranes had no effect on the binding of [³H]NBMPR (Figure 4.3A and 4.3B), suggesting that the potential sulfhydryl bonds between cysteine residues were not contributing to protein structure of importance to NBMPR binding. Alternatively, this suggested that all ten cysteines possessed free sulfhydryl groups that were potentially available to react with the MTS reagents.

4.2 Optimization of MTS reagents

To define an optimal incubation period, MTS reagents were initially used at a concentration taken from the literature, MTSET 1 mM, MTSES 10 mM, and MMTS 5 mM [162]. These were then incubated with PK15-hENT1 cells for various times (1-15 min) and analyzed for [³H]NBMPR binding. A 10 min incubation period revealed significant decreases in B_{max} at MTSET 1.0 mM and an increase in B_{max} at MMTS 5 mM with no further increases or decreases observed at 15 minutes (Figures 4.4A, 4.4B, 4.4C). This incubation period was subsequently used while varying the concentrations of MTS reagents and functional characterization of hENT1. Optimal concentrations of MTS reagents were determined to be 1 mM MMTS, 5 mM MTSES, 5 mM MTSET where their DMSO-treated control produced no effect, indicating that the vehicle was not contributing to the observed effects.

4.3 Effects of MTS reagents on hENT1 function and ligand binding:

As mentioned previously the MTS reagents: MTSES, MMTS, MTSET (Figure 1.12) were used in this study due to their selectivity to cysteines as well as their reactivity in mild conditions. Because they come in a variety of charges, sizes, and lipophilicity they are able to better probe the location of cysteines and provide information about their environment. These MTS reagents tested the surface accessibility of cysteines by covalent modification at thiol side chains which may cause a change in transporter function and hence further elucidate the contributions of cysteines to hENT1 structure and function.

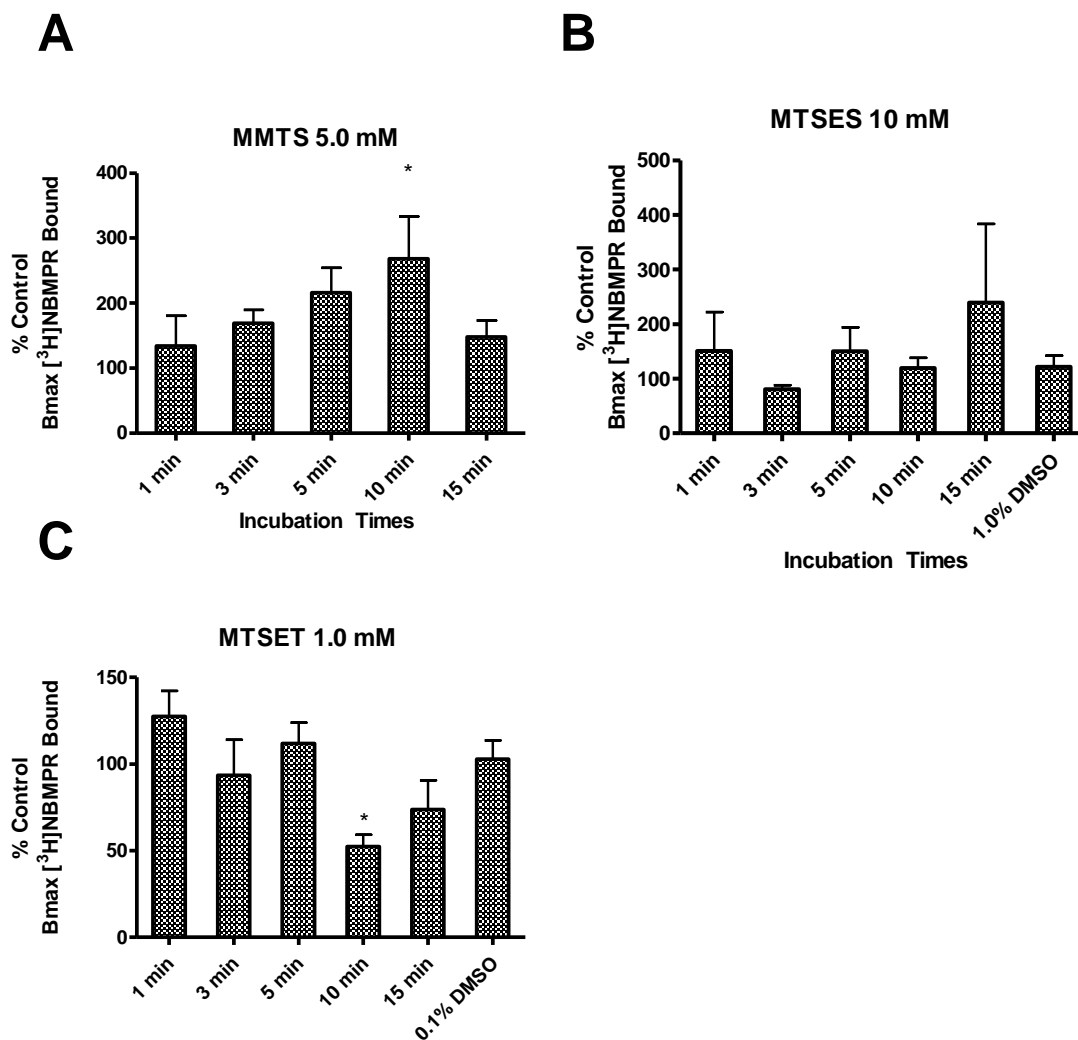


Figure 4.4. Varying incubation times with MTS reagents to PK15-hENT1 cells. Cells were treated with (**Panel A**) 5 mM MMTS, (**Panel B**) 10 mM MTSES, (**Panel C**) 1 mM MTSET for incubation periods of 1 min to 15 min and then assessed for [³H]NBMPR binding. B_{max} were calculated. Nonlinear regression analysis was used to fit hyperbolic curves to the site-specific binding of [³H]NBMPR plotted against the free [³H]NBMPR concentration at steady-state. Each bar represents the mean \pm SEM from at least four experiments done in duplicate. * Indicates a significant change in B_{max} from the MTS reagent at that time point compared to the B_{max} from DMSO-treated PK15-hENT1 cells ($P < 0.05$ one-way ANOVA : Dunnett's post-test).

4.3.1 Effects of MMTS on NBMPR Binding: the NBMPR binding site is sensitive to neutral thiol modification

MMTS, which like NEM is a neutral membrane-permeable reagent, caused a significant $62 \pm 11\%$ increase in the number of NBMPR binding sites in intact cells with no change in binding affinity (Figure 4.5A). However, in isolated membranes prepared from these cells, MMTS inhibited binding by about 30% (Figure 4.5B). To investigate further the difference in MMTS effect on intact cells (enhancement) versus membranes (inhibition), intact cells were treated with MMTS (or DMSO as control) and then used to prepare isolated membranes for analysis of [^3H]NBMPR binding. The membranes derived from cells treated with MMTS had significantly lower binding ($B_{\text{max}} = 1.7 \pm 0.2$ pmol/mg) than did membranes prepared from cells treated with DMSO alone (controls, $B_{\text{max}} = 2.2 \pm 0.4$ pmol/mg) (Figure 4.6A). Similarly, the binding of [^3H]NBMPR to broken cell preparations (no separation of membrane components) was also decreased by treatment with MMTS (Figure 4.6B). In addition, to determine whether transmembrane ion gradients played a role in these divergent effects of MMTS, cells were treated with MMTS in either PBS (pH 7.4), NMG (pH 7.25), or 50 mM Tris-HCl of varying pH (6.0, 7.2, or 8.2). There were no differences in the results obtained when using the PBS, NMG, and Tris-HCl (pH 7.2–7.4) incubation conditions. However, incubating cells with MMTS in 50 mM Tris at pH 8.2 eliminated completely the ability of MMTS to enhance the binding of [^3H]NBMPR (Figure 4.7A, 4.7B, 4.7C). Finally, the competitive inhibition of [^3H]NBMPR by dipyridamole, draflazine and dilazep was assessed for potential changes after MMTS treatment. Treatment of the neutral thiol reagent had no effect on the ability of dipyridamole, dilazep or draflazine to inhibit the binding of [^3H]NBMPR to wild-type hENT1 (Figure 4.8).

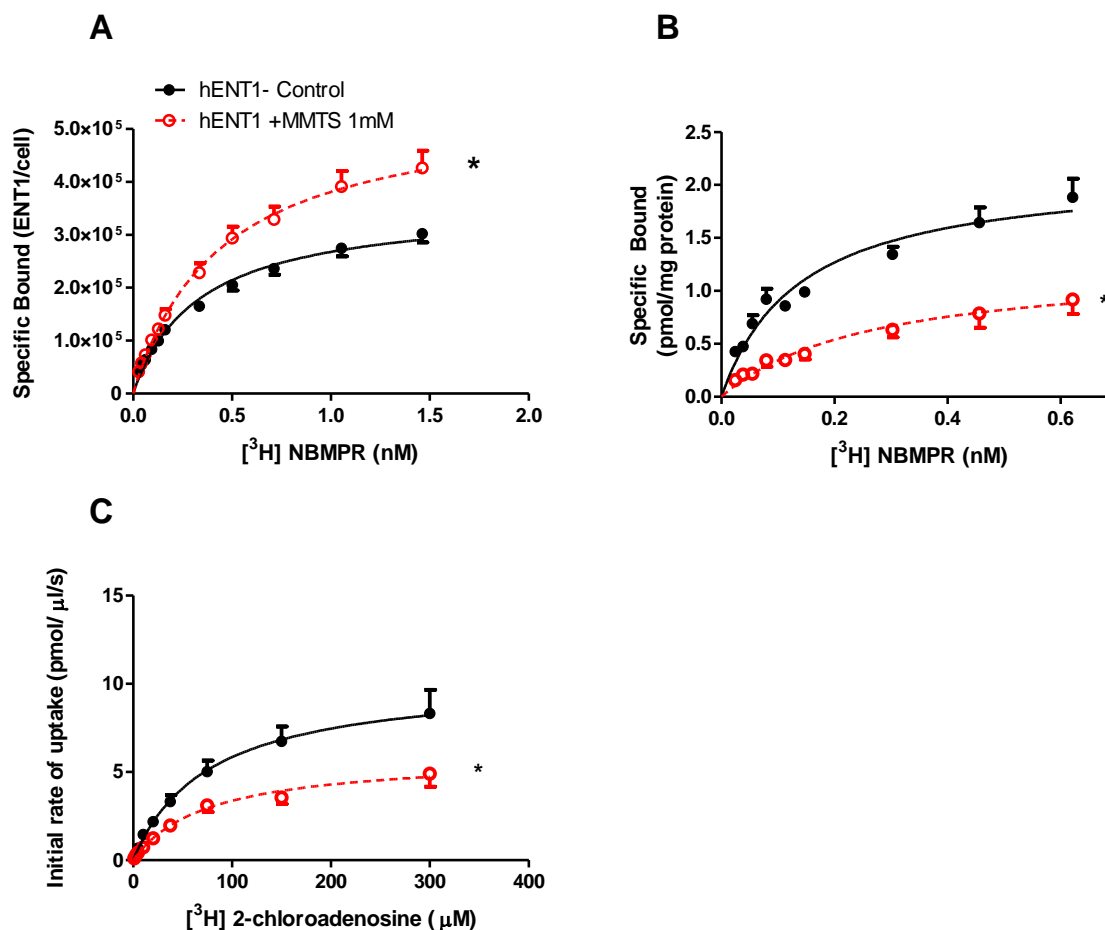


Figure 4.5. Treatment of hENT1 with MMTS. Effects of MMTS on [³H]NBMPR binding by PK15-hENT1 cells (**Panel A**), cell membranes (**Panel B**) and on [³H]2-chloroadenosine uptake by PK15-hENT1 cells (**Panel C**). Cells or membranes were incubated with either 1 mM MMTS or 0.1% DMSO (Control) for 10 min, washed thrice, and then incubated with a range of concentrations of [³H]NBMPR (abscissa) in the presence and absence of 10 μM NBTGR to define total and nonspecific binding or then assessed for their capacity to accumulate [³H]2-chloroadenosine (5 s incubation) in the presence and absence of 5 μM NBTGR/dipyridamole. Each point represents the mean ± SEM from at least 5 experiments done in duplicate. * Significant difference from control B_{\max} for NBMPR binding studies and control V_{\max} for uptake studies (Student's t test for paired samples, $P < 0.05$)

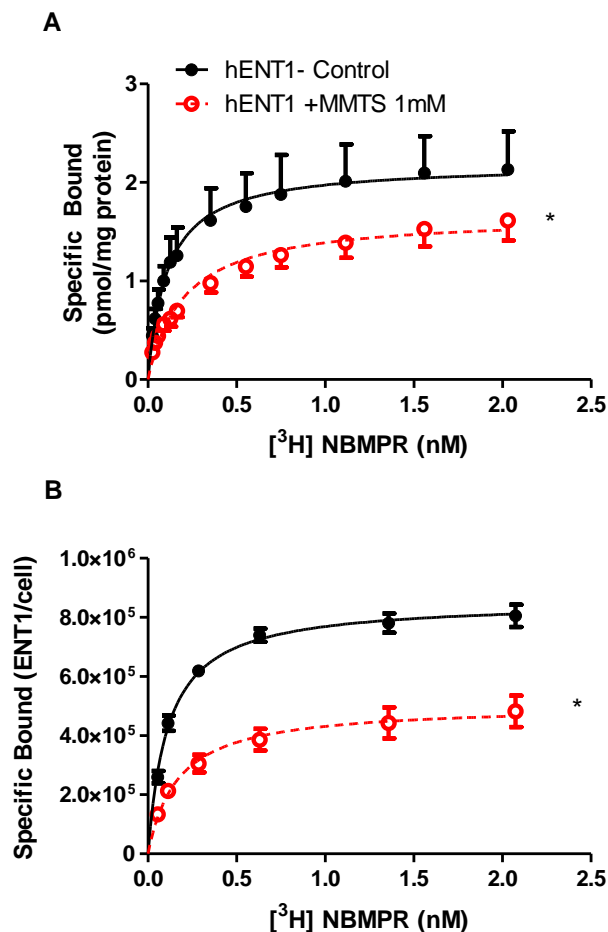


Figure 4.6. Effects of isolating membranes to the treatment of hENT1 with MMTS. Specific binding of [³H]NBMPR to PK15-hENT1 cell membranes isolated from cells pre-treated with MMTS (**Panel A**) and from cells that were treated with MMTS and then broken open (**Panel B**). PK15-hENT1 cells were incubated with (○) and without MMTS (●), washed, and then membranes prepared. Isolated cell membranes were incubated with a range of concentrations of [³H]NBMPR (abscissa) in the presence (nonspecific binding) and absence of 10 μM NBTGR (total binding). Specific binding was determined by total bound minus non-specific bound. Each point represents the mean ± SEM from at least four independent experiments done in duplicate. * Significant difference from control B_{max} (Student's t test for paired samples, $P < 0.05$).

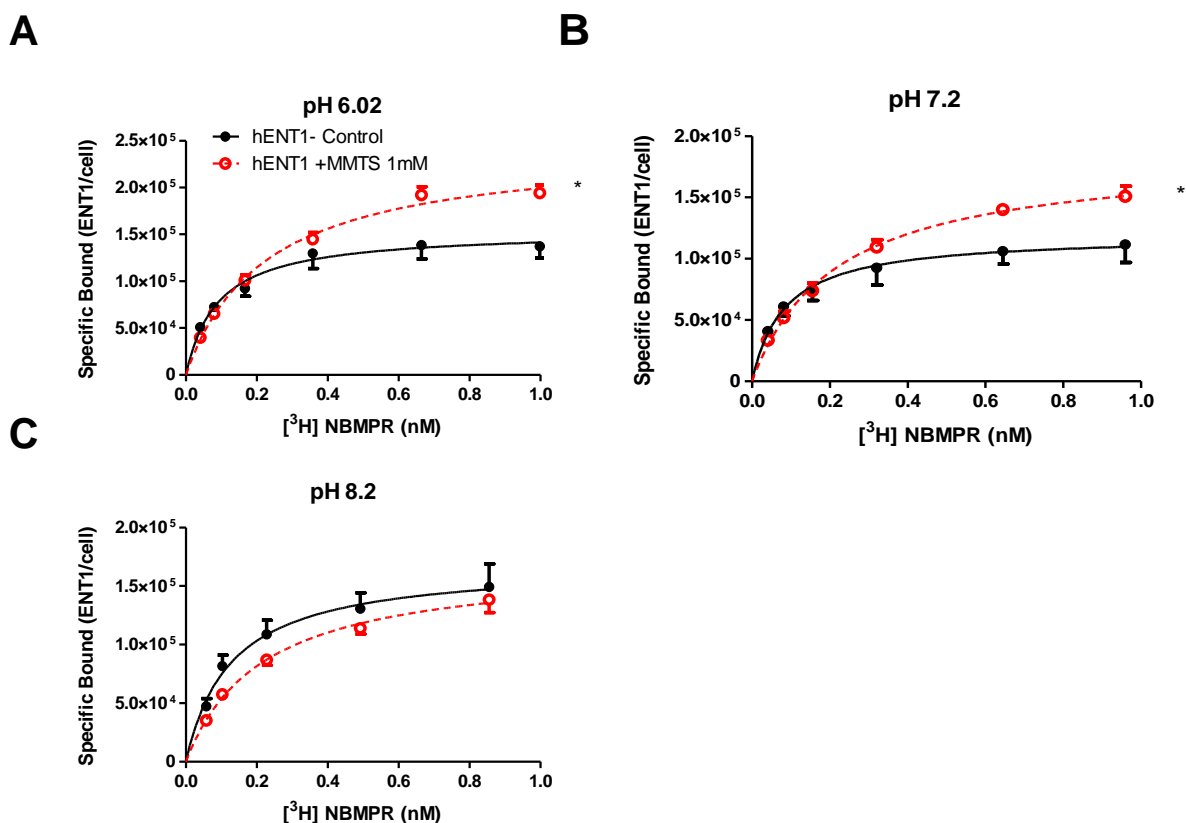


Figure 4.7. MMTS effects are dependent on pH. Effect of pH on the capacity of MMTS to modify [³H]NBMPR binding to cells transfected with wild-type hENT1. Intact cells were treated with 0.1% DMSO (controls, closed symbols/ solid lines) or 1 mM MMTS (open symbols/ dashed lines) in 50 mM TRIS at pH 6.0 (**Panel A**), pH 7.2 (**Panel B**), or pH 8.2 (**Panel C**) for 10 min at room temperature, washed extensively with PBS (pH 7.4), and then exposed to a range of concentrations of [³H]NBMPR in the presence and absence of 10 μ M NBTGR to define the amount of site-specific binding of this ligand in each cell (ENT1/cell, left ordinate). Each point is the mean \pm SEM from at least 4 experiments conducted in duplicate. * Indicates a significant effect of MMTS relative to control B_{max} (Students *t*-test for paired samples, $P < 0.05$).

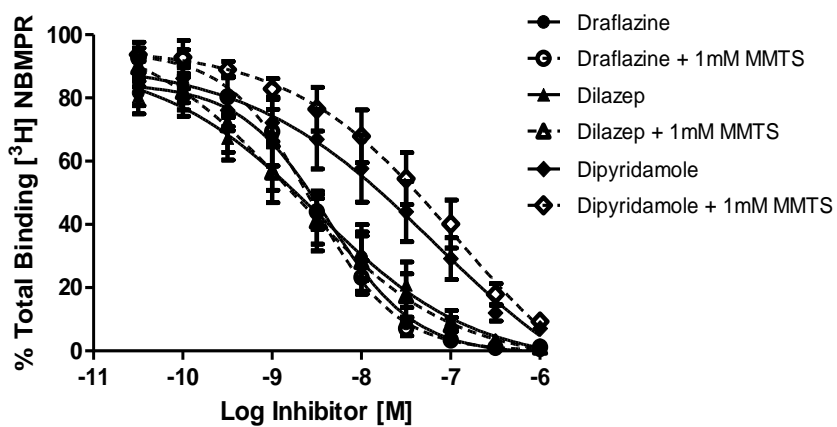


Figure 4.8. Effects of MMTS treatment of hENT1 on inhibitor binding. Inhibition of $[^3\text{H}]$ NBMPR binding by a range of concentrations of inhibitors on cells that were pretreated with either 0.1% DMSO (solid lines, closed symbols) or 1 mM MMTS (dashed lines, open symbols). Each point is the mean \pm SEM from at least four experiments.

4.3.1.1 Effect of pH on PK15-hENT1 activity

Given that MMTS effects were abolished when treatment took place in basic pH medium, we considered the fundamental effects of pH on hENT1 function. To compare the effect of pH on PK15-hENT1 activity, we utilized 50 mM Tris at pH 6.2, 7.2, and 8.2 for our incubation media due to its buffering range at that pH. Cells expressing recombinant wildtype hENT1 cells were harvested, washed in the described buffer and incubated with a range of [³H]NBMPR concentrations to determine site-specific binding. Specific binding of [³H]NBMPR in pH 6.2 and 7.2 yielded near identical B_{max} values of $3.9 \pm 0.7 \times 10^5$ ENT1 sites/cell and $3.5 \pm 0.6 \times 10^5$ ENT1 sites/cells, respectively. However, specific binding of [³H]NBMPR in pH 8.2 showed an increased B_{max} of $6.3 \pm 0.8 \times 10^5$ ENT1 sites/cell or a 45% increase compared to pH 7.2 (Figure 4.9A). Affinities for all three pH were not significantly different, pH 6.2 K_d = 0.1 ± 0.02 nM, pH 7.2 K_d = 0.1 ± 0.01 nM, and pH 8.2 K_d = 0.1 ± 0.003 nM. To determine if the change in B_{max} at pH 8.2 could be due to the loss of K⁺ and/or Cl⁻ ion gradients (our experiments were repeated using NMG buffer at pH 7.4 and 8.2 and found a similar results where incubation in NMG at pH 8.2 caused an increase in B_{max} by $52 \pm 20\%$ compared to NMG at pH 7.2 (Figure 4.9B). Additionally, affinities for [³H]NBMPR were not significantly different; pH 7.4 K_d = 0.14 ± 0.02 nM, pH 8.4 K_d = 0.18 ± 0.04 nM. To determine if the increase seen in [³H]NBMPR B_{max} represented an increase in functional hENT1 transporters at the membrane, [³H]2-chloroadenosine uptake assays were performed with NMG buffer at pH 7.4 and pH 8.4. Initial rates of uptake for wildtype hENT1 were unaffected by the change in pH (Figure 4.9C); pH 7.4 V_{max} = 6.5 ± 1.2 pmol/μl/s versus pH 8.4 V_{max} = 6.6 ± 1.5 pmol/μl/s.

4.3.2 Effects of MMTS on 2-chloroadenosine uptake: substrate transport by hENT1 is sensitive to neutral thiol modification

MMTS inhibited the NBMPR-sensitive uptake of [³H]2-chloroadenosine by PK15-hENT1

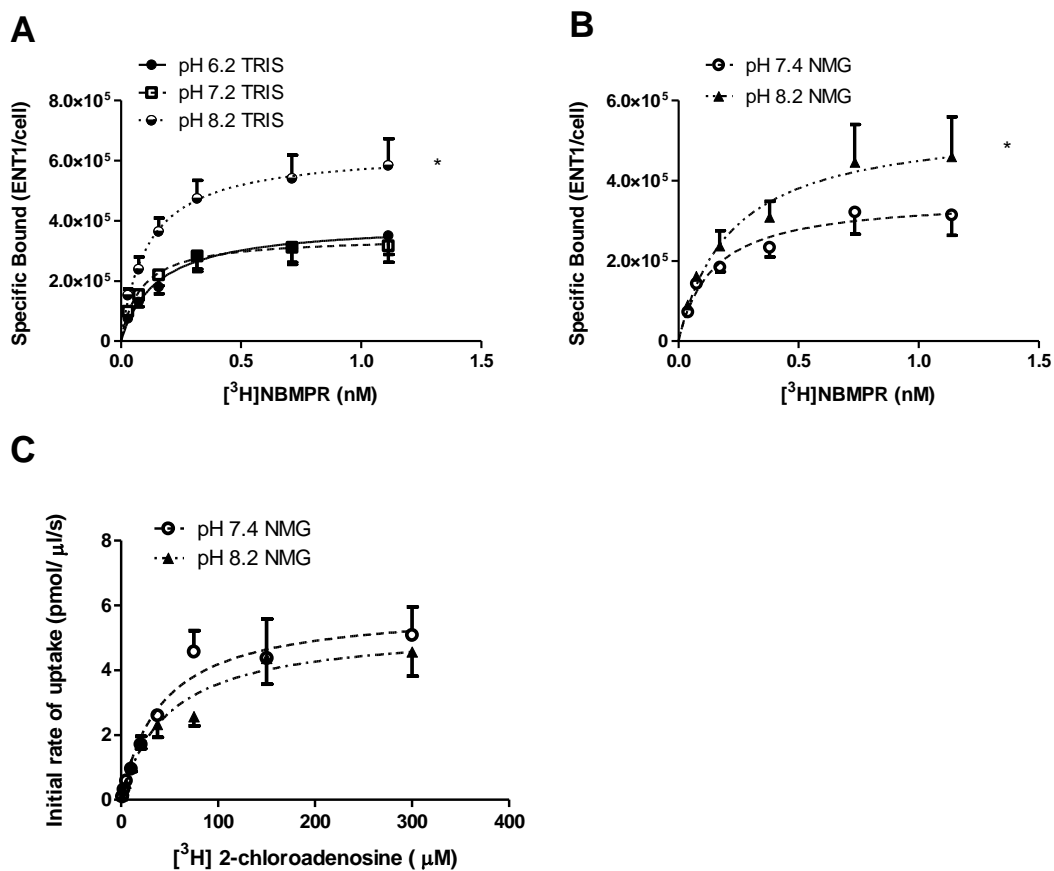


Figure 4.9. NBMPR binding to hENT1 is sensitive to pH. Effect of pH on [³H]NBMPR binding of cells transfected with wild-type hENT1 incubated with Tris (**Panel A**) or NMG (**Panel B**) and the effect of pH on [³H]2-chloroadenosine uptake (**Panel C**). Intact cells were incubated in 50 mM Tris at pH 6.2, pH 7.2, or pH 8.2 (**Panel A**) or in NMG at pH 7.4 or pH 8.2 (**Panel B**) and then exposed to a range of concentrations of [³H]NBMPR in the presence and absence of 10 μM NBTGR to define the amount of site-specific binding of this ligand in each cell. **Panel C** shows intact cells incubated in NMG at pH 7.4 or pH 8.2 and then assessed for [³H]2-chloroadenosine mediated uptake using a 5 s incubation time in the presence and absence of 5 μM NBTGR/dipyridamole to define the transporter-mediated uptake component. Each point is the mean ± SEM from at least 4 experiments conducted in duplicate. * Indicates a significant effect of pH 8.2 relative to pH 7.2 B_{max} (Students *t*-test for paired samples, P < 0.05).

cells (by 36 %) (Figure 4.5C), and led to a significant decrease in the ability of dipyrindamole ($K_i = 413 \pm 124$ nM), NBMPR ($K_i = 5.8 \pm 1.0$ nM) and dilazep ($K_i = 16 \pm 2$ nM) to inhibit [3 H]2-chloroadenosine uptake (Figure 4.10A). On the other hand, the ability of substrates such as adenosine and inosine to inhibit [3 H]2-chloroadenosine uptake was unaffected by MMTS treatment (Figure 4.10B).

4.3.3 Protection of hENT1 from the effects of MMTS

To determine if the effects of MMTS could be blocked with either inhibitor or substrate, PK15-hENT1 cells were treated with MMTS in the presence of unlabelled NBMPR or adenosine. Given that the inhibitor binding site is predicted to overlap the substrate translocation site but with a different set of binding determinants, both the prototypical inhibitor (NBMPR) and substrate (adenosine) were used in these protection studies at concentrations that were above their calculated affinities to the transporter. Co-incubation of cells with MMTS and either adenosine (1 mM) or NBMPR (10 nM) produced a similar enhancement of [3 H]NBMPR binding in intact cells as did MMTS alone (Figure 4.11A, 4.11B).

4.3.4 Effects of MTSES on NBMPR binding and on 2-chloroadenosine uptake: the NBMPR binding pocket is sensitive to negatively charged thiol modification of cytoplasmic cysteines.

The negatively charged reagent pCMBS in previous studies produced either no effect on intact cells or a much smaller effect compared to NEM on ENT1 function in different cell models and conditions. We assessed the effects of the negatively charged reagent, MTSES, on PK15-hENT1 cells. The negatively charged membrane-impermeable thiol modifier MTSES had no effect on [3 H]NBMPR binding in whole cells but did inhibit [3 H]NBMPR binding to isolated membranes (~60% inhibition to 0.43 ± 0.11 pmol/mg) (Figures 4.12A, 4.12B). The inability of MTSES to affect NBMPR binding of whole cells mimics previous studies in our lab by Vyas *et al.* and Robillard *et al.* where pCMBS was only able to inhibit NBMPR binding in broken cell preparations [157, 174]. In addition to

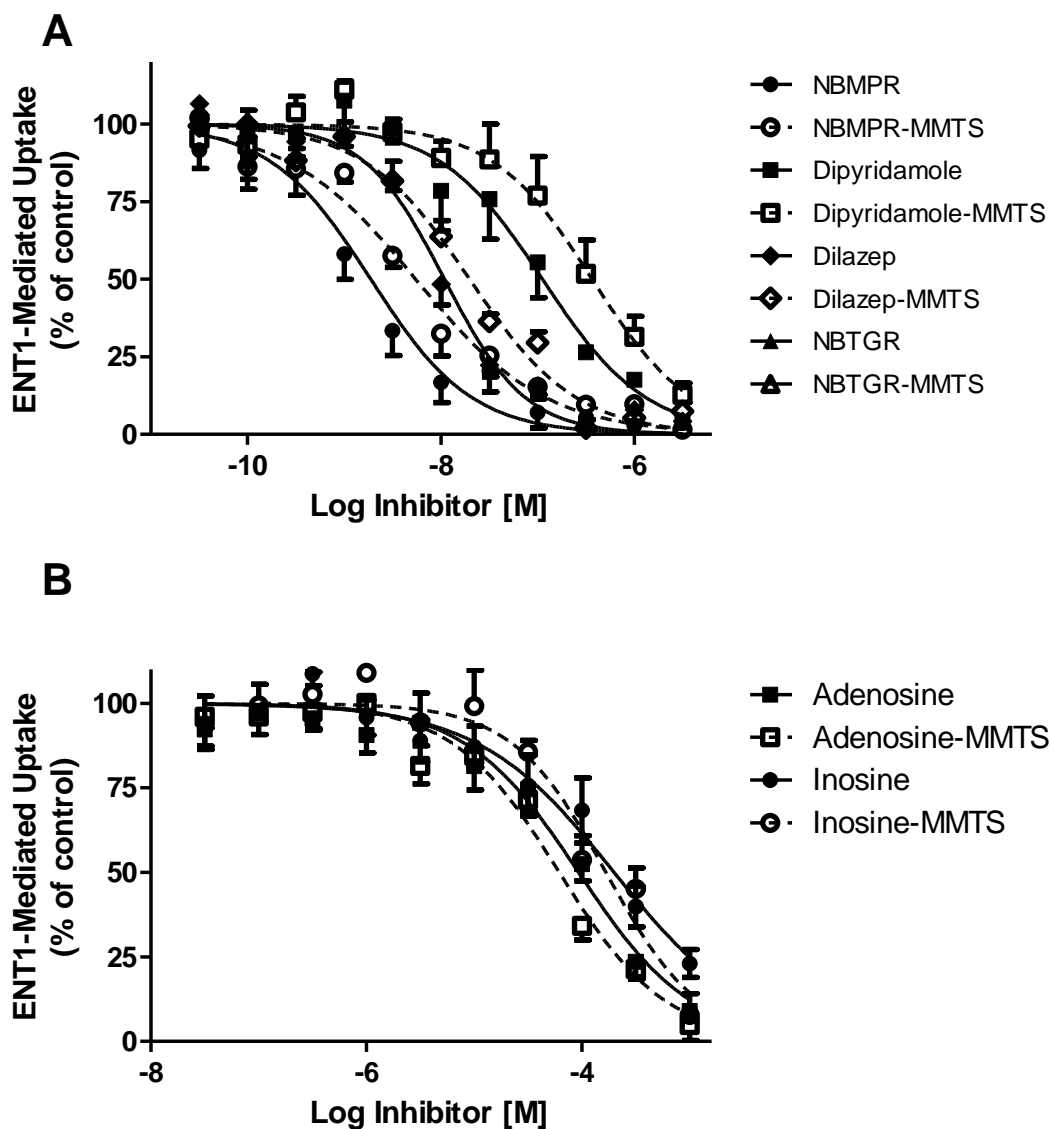


Figure 4.10. Effects of the treatment of hENT1 with MMTS on the inhibition of substrate uptake. Inhibition of [^3H]2-chloroadenosine uptake by a range of concentrations of inhibitors (**Panel A**) and of substrates (**Panel B**) by cells that have been pretreated with either 0.1% DMSO (solid lines, closed symbols) or 1 mM MMTS (dashed lines, open symbols). Each point is the mean \pm SEM from at least four experiments.

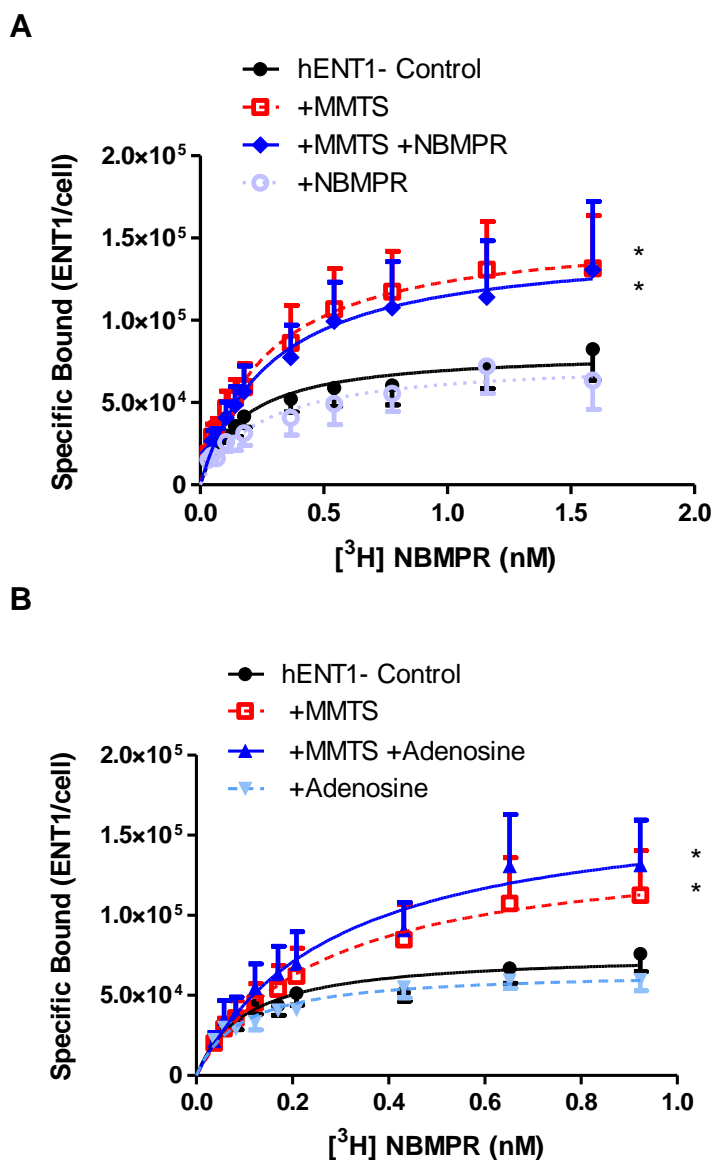


Figure 4.11. NBMPR and adenosine are unable to protect against MMTS effects. Effect of MMTS on NBMPR binding to cells by co-incubation with 10 nM NBMPR (**Panel A**) and 1 mM adenosine (**Panel B**). PK15-hENT1 cells were incubated for 10 min at room temperature with 0.1% DMSO (control), 10 nM NBMPR (+NBMPR) or 1 mM adenosine (+adenosine), 1 mM MMTS (+MMTS) or the combination of 10 nM NBMPR/1 mM adenosine and 1 mM MMTS. After extensive washing to remove NBMPR and un-reacted MMTS, cells were exposed to a range of concentrations of ^{3}H NBMPR in the presence and absence of 10 μM NBTGR to define the site-specific binding. Each point is the mean \pm SEM from at least five experiments conducted in duplicate. * Indicates there was a significant difference between the MMTS, NBMPR/MMTS or adenosine/MMTS treated cells compared with their respective experimental control B_{max} (Students *t*-test for paired samples, $P < 0.05$).

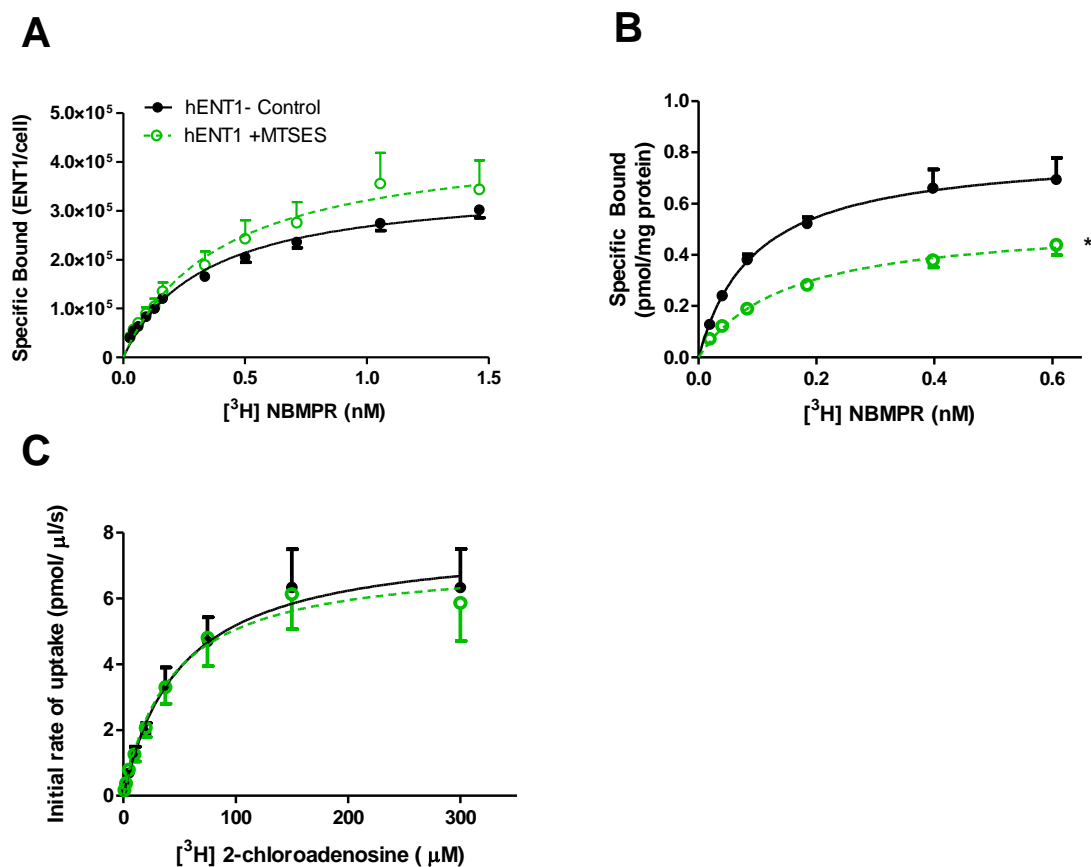


Figure 4.12. Effect of MTSES on hENT1. Effects of MTSES on [³H]NBMPR binding of PK15-hENT1 cells (**Panel A**), cell membranes (**Panel B**) and on [³H]2-chloroadenosine uptake by PK15-hENT1 cells (**Panel C**). Cells or membranes were incubated with either 5 mM MTSES or 0.5% DMSO (Control) for 10 min, washed thrice, and then incubated with a range of concentrations of [³H]NBMPR (abscissa) in the presence and absence of 10 μM NBTGR to define total and nonspecific binding (**Panel A and B**) or cells were assessed for their capacity to accumulate [³H]2-chloroadenosine (5 s incubation) in the presence and absence of 5 μM NBTGR/dipyridamole (**Panel C**). Each point represents the mean ± SEM from at least five experiments. * Significant difference from control B_{max} (Student's t test for paired samples, *P* < 0.05).

having no effect in whole cell NBMPR binding, MTSES treatment of PK15-hENT1 cells had no effect on [³H]2-chloroadenosine uptake (Figure 4.12C).

4.3.5 Effects of MTSET on NBMPR binding and 2-chloroadenosine uptake: the NBMPR binding pocket and substrate translocation site are sensitive to a thiol modifier with a positive charge

Previous studies on ENT1-thiol modification have limited their thiol reagents to ones of neutral or negative charge. Our study widened the scope of cysteine accessibility by using a positively charged sulfhydryl reagent, MTSET. Though MTSET and MTSES are similar in size, they differ in charge and therefore may provide additional information on hENT1 structure as any differences in effects between them may be attributable to the charge difference. Treatment of PK15-hENT1 cells with the membrane-impermeable MTSET produced a slight but significant decrease (13 %) in [³H]NBMPR binding in intact cells (Figure 4.13A). This same treatment also decreased binding to isolated membranes (by about 60% to 0.42 ± 0.18 pmol/mg) (Figure 4.13B). When testing the sensitivity of hENT1 transport mechanism to the thiol modification by a positively charged reagent, MTSET increased the V_{max} of [³H]2-chloroadenosine uptake by 45 % with no change in K_m (Figure 4.13C).

4.4 Summary of MTS effects

In all cases, the effects on [³H]NBMPR binding and [³H]2-chloroadenosine uptake reflected a change in maximum (B_{max} , V_{max}) rather than a change in affinity (K_d , K_m) for the ligand. As summarized in Table 4.1, the neutral membrane permeable MMTS caused significant effects in both binding B_{max} and uptake V_{max} . The negatively charged membrane impermeable reagent MTSES produced no changes in whole cell hENT1 functionality. The positively charged membrane impermeable reagent MTSET caused a decrease in binding B_{max} and an enhanced uptake V_{max} . All three MTS reagents produced a significant decrease in NBMPR binding in broken cell membrane preparations. This

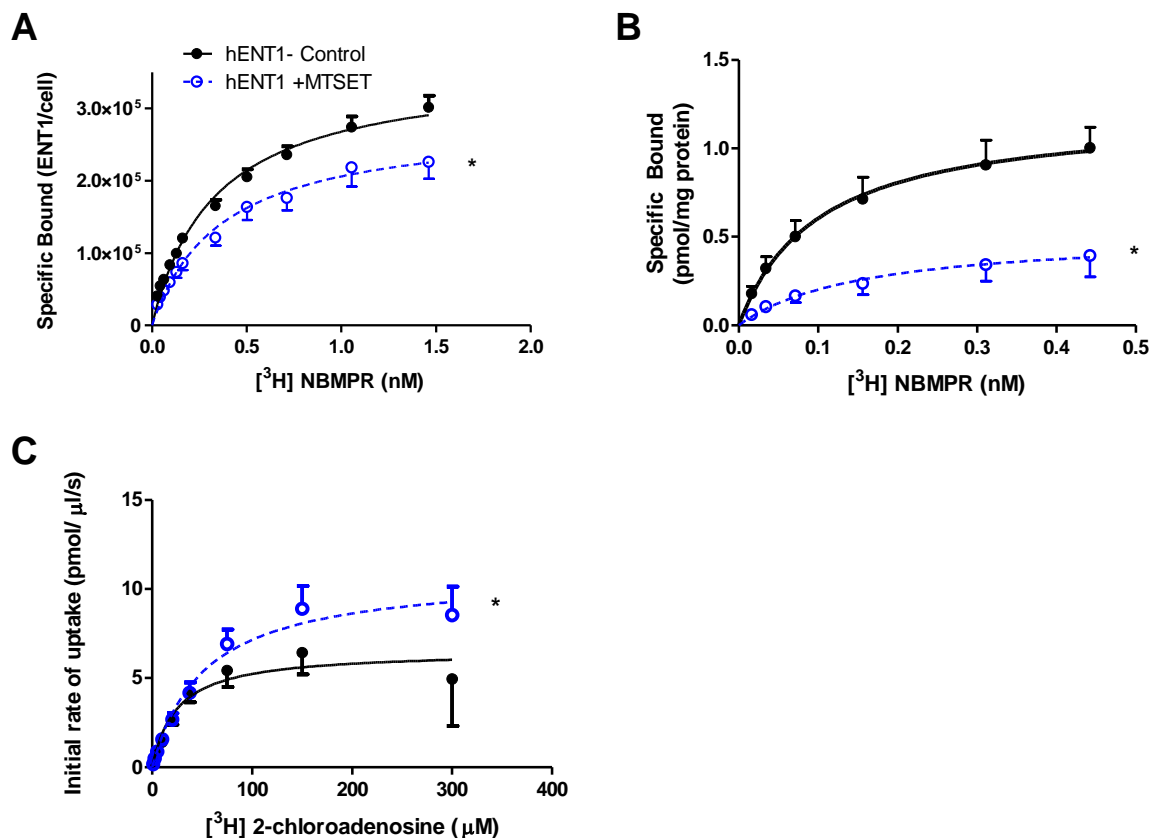


Figure 4.13. Effect of MTSET on hENT1. Effects of MTSET on [³H]NBMPR binding by PK15-hENT1 cells (**Panel A**), cell membranes (**Panel B**) and on [³H]2-chloroadenosine uptake by PK15-hENT1 cells (**Panel C**). Cells or membranes were incubated with either 5 mM MTSET or 0.5% DMSO (Control) for 10 min, washed thrice, and then incubated with a range of concentrations of [³H]NBMPR (abscissa) in the presence and absence of 10 μM NBTGR to define total and nonspecific binding (**Panel A and B**) or assessed for their capacity to accumulate [³H]2-chloroadenosine (5 s incubation) in the presence and absence of 5 μM NBTGR/dipyridamole (**Panel C**). Each point represents the mean ± SEM from at least 5 experiments done in duplicate. * Significant difference from control B_{max} for NBMPR binding studies and control V_{max} for uptake studies (Student's t test for paired samples, *P* < 0.05)

suggests there is a hENT1 cysteine being modified by the positively charged reagent MTSET that could not be accessed by the negatively charged reagent MTSES in whole cells. In addition to this predicted-extracellular cysteine, there is also a second cysteine that is being modified by the membrane permeable reagent MMTS to cause an increase in NBMPR binding located within a lipophilic environment. Lastly, there is a cysteine located cytoplasmically that is contributing to NBMPR binding. This is yet another cysteine given that modification of this cytoplasmic cysteine with all three MTS reagents results in a decrease in NBMPR binding. These results support our first and second hypotheses where we hypothesized that there were two separate cysteines located in two separate environments that when modified would affect hENT1 function; one of these cysteines was predicted to be in a hydrophobic environment, and the second cysteine was predicted to be in a cytoplasmic location.

4.5 Mutation of 10 endogenous cysteines

The preceding studies indicated the importance of cysteine residues to hENT1 function. Therefore to determine which cysteines were involved in the effects observed with MTS reagents (Table 4.1), we systematically mutated each cysteine to serine (a modest change in reactive side chain and size) and assessed mutant function. Additionally, the cysteine to serine mutants were tested for their sensitivity to MTS reagents and examined to see if they contributed to those effects in wild-type hENT1. The intent of this approach was to determine the cysteine responsible for the MTSET effects. Subsequently, the residue could be removed to construct an extracellular cysteine-less mutant unresponsive to MTSET to create a template for future cysteine mutagenesis studies in mapping the extracellular binding domain of NBMPR.

Table 4.1. Summary of the effects of MTS reagents on [³H]NBMPR binding (B_{max}) and [³H]2-chloroadenosine (V_{max}) by cells and cell membranes transfected with hENT1. Data shown are the percent change mean \pm SEM from at least four independent experiments.

MTS Reagent	[³ H]NBMPR binding of intact cells (B_{max})	[³ H]NBMPR binding of cell membrane (% control B_{max})	[³ H]2-chloroadenosine uptake (% control V_{max})
MMTS	62 \pm 11% increase in B_{max}	43 \pm 5% decrease in B_{max}	36 \pm 16% decrease in V_{max}
MTSET	13 \pm 4% decrease in B_{max}	71 \pm 10% decrease in B_{max}	45 \pm 24% increase in V_{max}
MTSES	No effect	29 \pm 12% decrease in B_{max}	No effect

4.5.1 Mutation of C87 to serine

hENT1-C87S cells bound [³H]NBMPR with a K_d of 0.3 ± 0.06 nM which is not significantly different from that obtained for wild-type hENT1 (Figure 4.14A, Table 4.2). Likewise, membranes prepared from these cells had a K_d of 0.2 ± 0.04 nM which is similar to that determined for wild-type hENT1 membranes (Figure 4.14B). However, the K_m for [³H]2-chloroadenosine uptake (27 ± 3 μ M) was significantly lower than that seen for wild-type hENT1 (71 ± 8 μ M) (Figure 4.14C, Table 4.2). The B_{max} of [³H]NBMPR binding and the V_{max} of [³H]2-chloroadenosine uptake by hENT1-C87S cells were $1.4 \pm 0.1 \times 10^5$ ENT1 sites/cell and 6.5 ± 0.4 pmol/ μ l/s (Figure 4.14A, 4.14C), respectively, giving a V_{max}/B_{max} ratio of $4.6 \pm 0.5 \times 10^{-5}$ pmol/ENT1/s which is significantly greater than the V_{max}/B_{max} ratio of for the wild-type hENT1 (calculated from all control data sets).

4.5.1.1 C87S MTS treatment

As seen for the wild-type hENT1, MMTS treatment increased the B_{max} of [³H]NBMPR binding to hENT1-C87S by $49 \pm 12\%$, and decreased the V_{max} of [³H]2-chloroadenosine influx by $20 \pm 14\%$ with no significant change in K_d (Figure 4.15A, 4.15C). Neither MTSES nor MTSET had any effect on [³H]NBMPR binding to intact hENT1-C87S transfected cells (Figure 4.16A, 4.16C). However, as in wild-type hENT1, MTSET enhanced ($51 \pm 24\%$) the V_{max} of [³H]2-chloroadenosine uptake by hENT1-C87S and MTSES had no effect (Figure 4.16B, 4.16D). In isolated membranes MMTS decreased the B_{max} of [³H]NBMPR binding (from 0.7 ± 0.05 to 0.3 ± 0.01 pmol/mg), with no significant change in K_d (Figure 4.15B).

4.5.2 Mutation of C193 to serine

hENT1-C193S cells bound [³H]NBMPR with a K_d of 0.2 ± 0.03 nM to a maximum of $2.5 \pm 0.3 \times 10^5$ ENT1 sites/cell (Figure 4.17A, Table 4.2). Membranes prepared from these cells had a K_d of 0.1 ± 0.02 nM and a [³H]NBMPR B_{max} of 17 ± 2 pmol/mg protein (Figure 4.17B). The K_m and V_{max} for [³H]2-chloroadenosine uptake were 39 ± 5 μ M and 5.1 ± 0.6 pmol/ μ l/s (Figure 4.17C, Table 4.2), respectively, resulting in a V_{max}/B_{max} ratio of 2.0 ± 0.3 pmol/ENT1/s which is similar to that seen in for the wild-type hENT1.

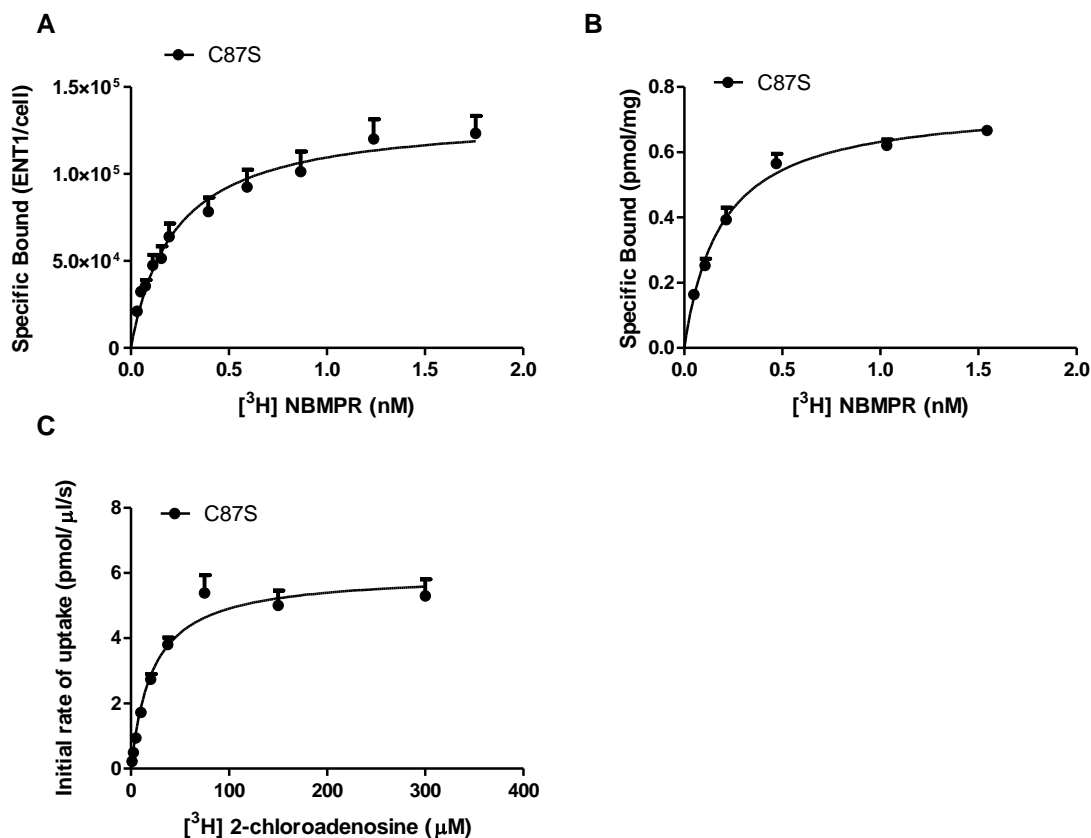


Figure 4.14. Characterization of PK15-C87S. $[^3\text{H}]$ NBMPR binding of PK15-C87S cells (**Panel A**) and PK15-C87S membranes (**Panel B**) and $[^3\text{H}]$ 2-chloroadenosine uptake of PK15-C87S cells (**Panel C**). For **panels A and B**, cells and membranes were incubated with a range of concentrations of $[^3\text{H}]$ NBMPR (abscissa) in the presence (nonspecific binding) and absence of 10 μM NBTGR (total binding). Specific binding was determined by total bound minus non-specific bound. Each point represents the mean \pm SEM from at least four experiments done in duplicate. For **panel C**, cells were incubated with a range of concentrations of $[^3\text{H}]$ 2-chloroadenosine for 5 s in the presence (Non-mediated) or absence (Total uptake) of 5 μM dipyridamole/NBTGR. Transporter-mediated uptake (Mediated) was calculated as the difference between the total and non-mediated uptake components. Each point represents the mean \pm SEM of the cellular accumulation of $[^3\text{H}]$ 2-chloroadenosine from at least four independent experiments conducted in duplicate.

Table 4.2. Summary of effects of cysteine mutations on the binding of [³H]NBMPR to PK15-hENT1 cells and the uptake of [³H]2-chloroadenosine by PK15-hENT1 cells. Data shown are the means \pm SEM from at least four independent experiments. * Significant difference from wildtype hENT1 affinities ($P < 0.05$ one-way ANOVA : Dunnett's post-test). n/d indicates that values were not determined

	NBMPR Binding		2-chloroadenosine Uptake	
	B _{max} (# ENT1 sites/cell) $\times 10^5$	K _d (nM)	V _{max} (pmol/ μ l/s)	K _m (μ M)
PK15-NTD	n/d	n/d	n/d	n/d
PK15- hENT1	3.6 \pm 0.20	0.38 \pm 0.02	9.5 \pm 0.75	71 \pm 7.7
PK15-C87S	1.4 \pm 0.12	0.30 \pm 0.06	6.5 \pm 0.40	27 \pm 2.5*
PK15-C193S	2.5 \pm 0.30	0.24 \pm 0.03	5.1 \pm 0.56	39 \pm 4.7*
PK15-C213S	2.8 \pm 0.62	0.45 \pm 0.10	22 \pm 2.8	77 \pm 10
PK15-C222S	2.0 \pm 0.16	0.29 \pm 0.04	9.3 \pm 1.3	63 \pm 11
PK15-C297S	1.3 \pm 0.25	0.30 \pm 0.04	5.7 \pm 0.68	61 \pm 13
PK15-C333S	4.3 \pm 0.40	0.37 \pm 0.06	6.7 \pm 0.75	39 \pm 5.0*
PK15-C378S	4.7 \pm 0.35	0.39 \pm 0.03	11 \pm 1.0	57 \pm 6.3
PK15-C414S	2.1 \pm 0.23	0.45 \pm 0.05	6.3 \pm 0.42	35 \pm 5.0*
PK15-C416A	4.6 \pm 2.3	0.10 \pm 0.02	n/d	n/d
PK15-C439A	8.6 \pm 1.4	0.50 \pm 0.10	8.4 \pm 0.80	165 \pm 32

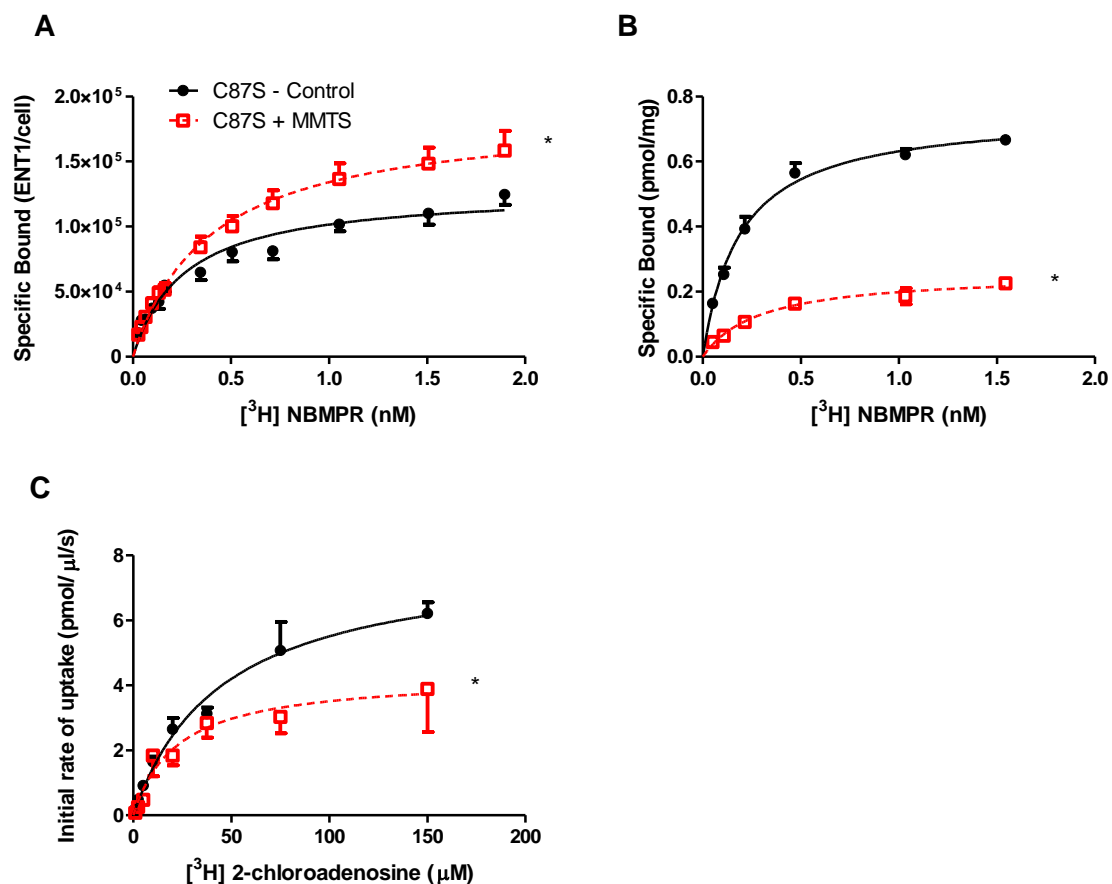


Figure 4.15. Effect of MMTS treatment on C87S activity. Effects of MMTS on [³H]NBMPR binding of PK15-C87S cells (**Panel A**), cell membranes (**Panel B**) and on [³H]2-chloroadenosine uptake by PK15-C87S cells (**Panel C**). Cells or cell membranes were incubated with either 1 mM MMTS or 0.1% DMSO (Control) for 10 min, washed extensively, and then incubated with a range of concentrations of [³H]NBMPR in the presence and absence of 10 μM NBTGR to define total and nonspecific binding (**Panel A and B**). **Panel C** describes the concentration-dependent uptake of [³H]2-chloroadenosine of cells treated for 10 min with 1 mM MMTS or 0.1% DMSO (Control) and washed three times. Cells were incubated with a range of concentrations of [³H]2-chloroadenosine for 5 s in the presence (Non-mediated) or absence (Total uptake) of 5 μM dipyridamole/NBTGR. Each point represents the mean ± SEM of the cellular accumulation of [³H]2-chloroadenosine from at least four independent experiments conducted in duplicate. * Significant difference from control B_{max} for NBMPR binding studies and control V_{max} for uptake studies (Student's t test for paired samples, *P* < 0.05)

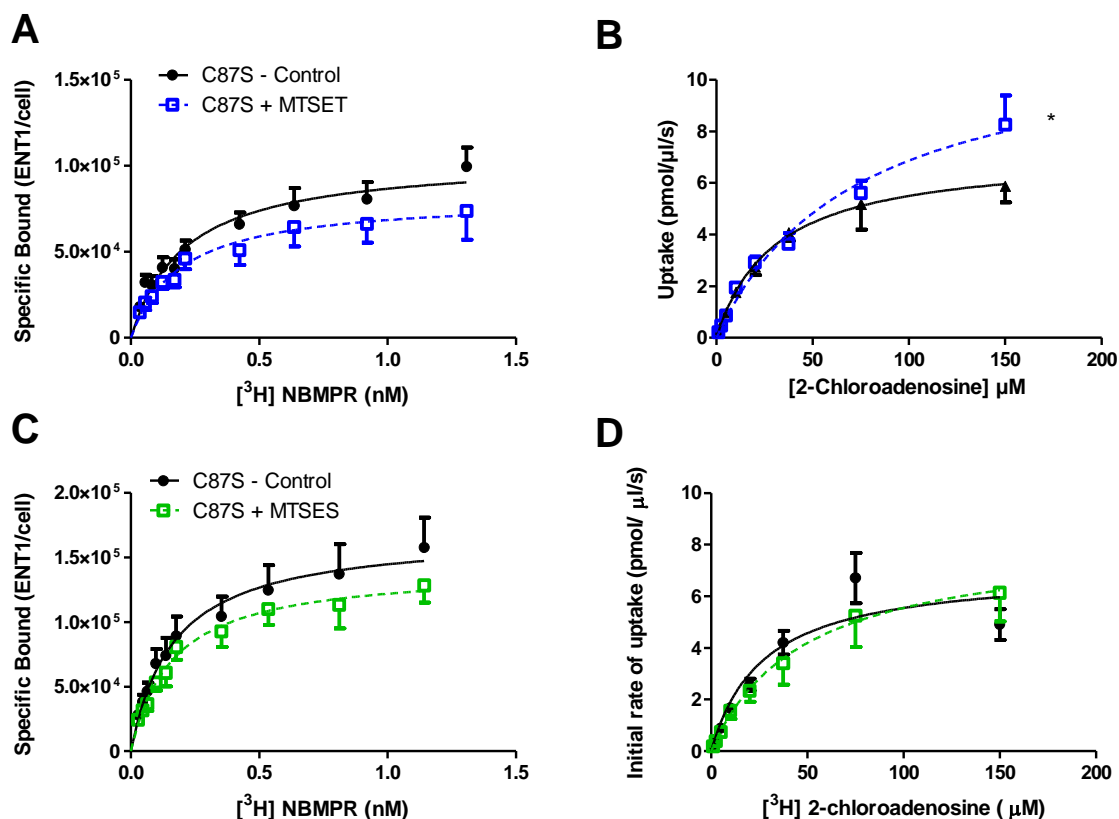


Figure 4.16. Treatment of C87S with MTSET and MTSES. Effects of MTSET (Panel A and B) and MTSES (Panel C and D) on $[^3\text{H}]$ NBMPR binding and on $[^3\text{H}]$ 2-chloroadenosine uptake by hENT1-C87S expressed in PK15-NTD cells. For Panel A and C, cells were incubated with either 5 mM MTSET (Panel A), or 5 mM MTSES (Panel C) for 10 min, washed extensively, and then incubated with a range of concentrations of $[^3\text{H}]$ NBMPR in the presence and absence of 10 μM NBTGR to define total and nonspecific binding. Each point represents the mean \pm SEM from at least 5 experiments done in duplicate. For Panel B and D, cells were incubated with either 5 mM MTSET (Panel B) or 5 mM MTSES (Panel D) for 10 min, washed extensively, and then incubated with a range of concentrations of $[^3\text{H}]$ 2-chloroadenosine for 5 s in the presence (Non-mediated) or absence (Total uptake) of 5 μM dipyridamole/NBTGR. Each point represents the mean \pm SEM of the cellular accumulation of $[^3\text{H}]$ 2-chloroadenosine from at least four independent experiments conducted in duplicate. * Significant difference from control B_{max} for NBMPR binding studies and control V_{max} for uptake studies (Student's t test for paired samples, $P < 0.05$)

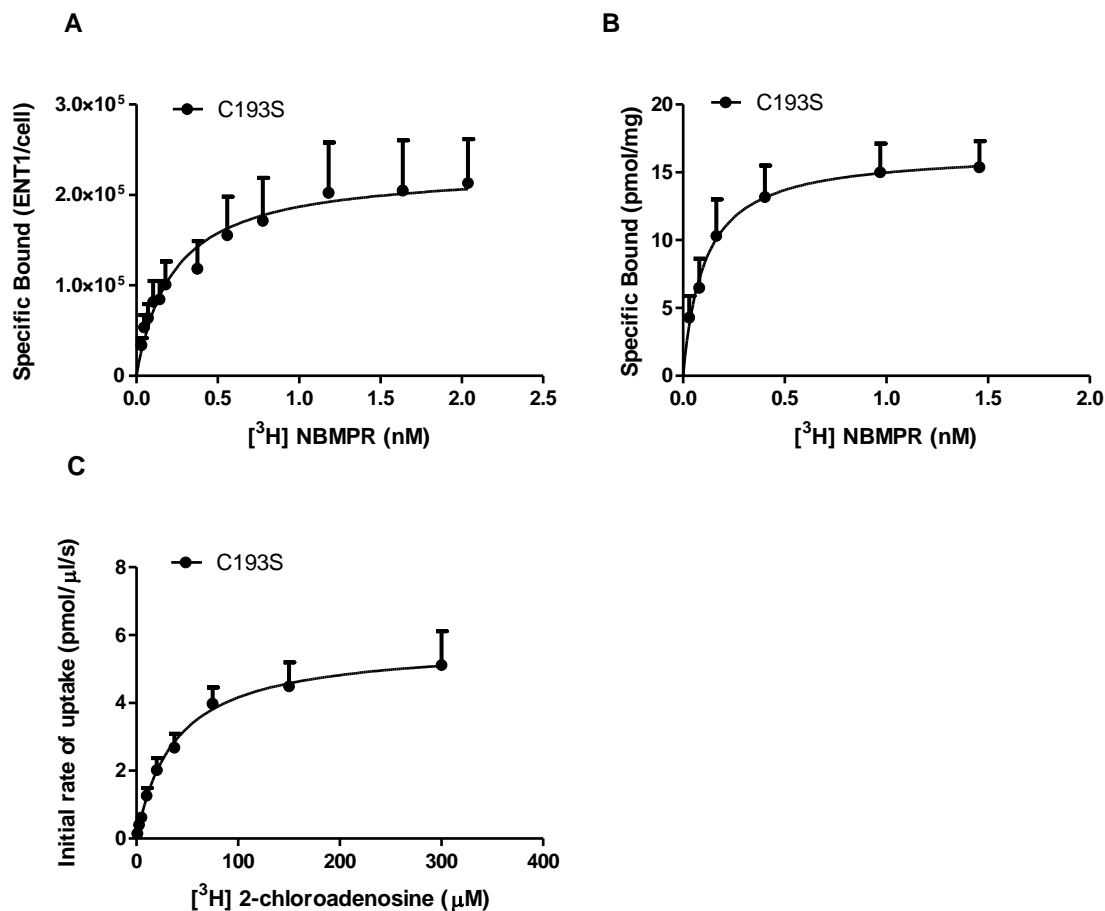


Figure 4.17. Characterization of PK15-C193S. [³H]NBMPR binding of PK15-C1963S cells (**Panel A**) and PK15-C193S membranes (**Panel B**) and [³H]2-chloroadenosine uptake of PK15-C193S cells (**Panel C**). For **panels A and B**, cells and membranes were incubated with a range of concentrations of [³H]NBMPR (abscissa) in the presence (nonspecific binding) and absence of 10 μM NBTGR (total binding). Specific binding was determined by total bound minus non-specific bound. Each point represents the mean ± SEM from at least four experiments done in duplicate. For **panel C**, cells were incubated with a range of concentrations of [³H]2-chloroadenosine for 5 s in the presence (Non-mediated) or absence (Total uptake) of 5 μM dipyridamole/NBTGR. Transporter-mediated uptake (Mediated) was calculated as the difference between the total and non-mediated uptake components. Each point represents the mean ± SEM of the cellular accumulation of [³H]2-chloroadenosine from at least four independent experiments conducted in duplicate.

4.5.2.1 Effects of MTS treatment on the function of C193S

MMTS treatment more than doubled ($106 \pm 28\%$ increase) the number of [^3H]NBMPR binding sites in hENT1-C193S cells relative to wild-type hENT1 (Figure 4.18A), and this effect was significantly greater than that observed for any of the other hENT1 mutants tested in this study. Also, unlike that observed for the wild-type hENT1 and other mutants, MMTS did not affect the rate of [^3H]2-chloroadenosine uptake in the C193S cells (Figure 4.18B). Likewise, the membrane-impermeable reagents (MTSET and MTSES) had no effect on either [^3H]NBMPR binding or [^3H]2-chloroadenosine uptake in these cells (Figure 4.19A, 4.19B).

4.5.3 Mutation of C213 to serine

hENT1-C213S cells bound [^3H]NBMPR with a K_d of 0.4 ± 0.1 nM to a maximum of $2.8 \pm 0.6 \times 10^5$ ENT1 sites/cell (Figure 4.20A, Table 4.2). Membranes prepared from these cells had a K_d of 0.2 ± 0.02 nM and a [^3H]NBMPR B_{max} of 0.7 ± 0.03 pmol/mg protein (Figure 4.20B). The K_m and V_{max} for [^3H]2-chloroadenosine uptake were 77 ± 10 μM and 22 ± 3 pmol/ $\mu\text{l/s}$ (Figure 4.20C, Table 4.2), respectively, resulting in a $V_{\text{max}}/B_{\text{max}}$ ratio of 7.9 ± 2.0 pmol/ENT1/s which is significantly greater than that of wild-type hENT1. The cells transfected with hENT1-C213S appeared to increase in their transport and binding capacity with time. In this way they were distinct from the other hENT1-mutants tested, which remained relatively consistent in their binding and transport capacity throughout the study.

4.5.3.1 C213S MTS treatments

The effects of the MTS reagents were comparable to that seen for the wild-type hENT1 cells. MMTS treatment induced a $56 \pm 20\%$ increase in [^3H]NBMPR binding B_{max} and a $40 \pm 7\%$ decrease in the V_{max} of [^3H]2-chloroadenosine uptake (Figure 4.21A, 4.21B). MTSET inhibited [^3H]NBMPR binding by a significant $18 \pm 12\%$, but had no effect of [^3H]2-chloroadenosine uptake (Figure 4.22A, 4.22B), which makes this mutant similar to C193S in that regard. MTSES had no effect on either [^3H]NBMPR binding or [^3H]2-

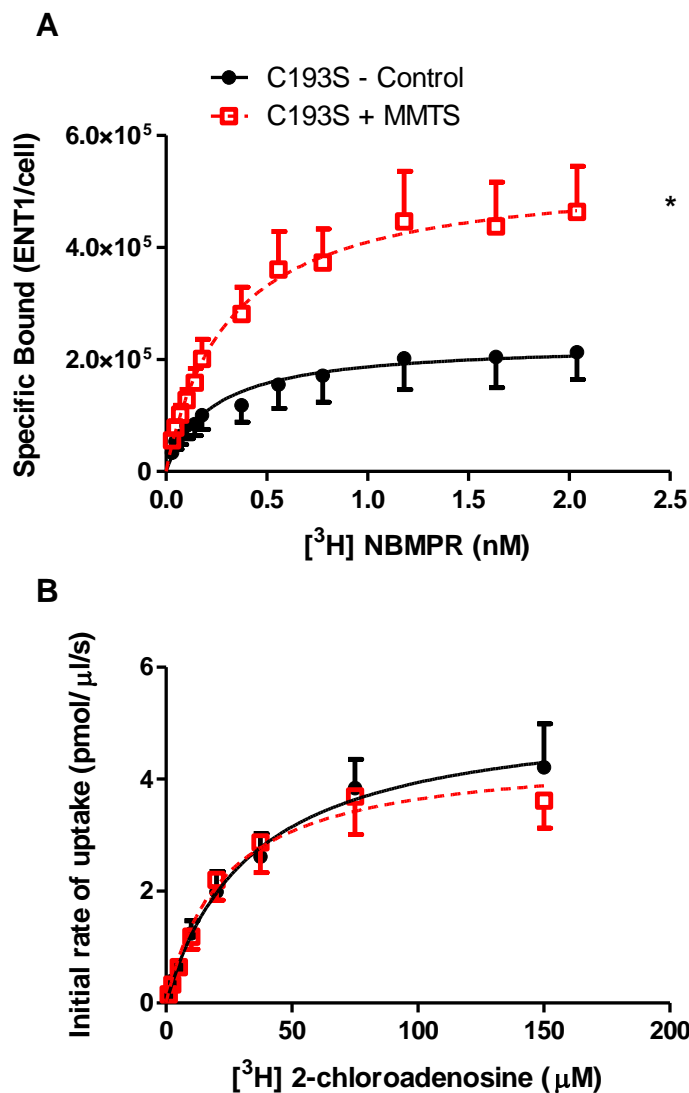


Figure 4.18. Effects of MMTS treatment on C193S activity. Effects of MMTS on [³H]NBMPR binding (**Panel A**) and [³H]2-chloroadenosine (**Panel B**) uptake by hENT1-C193S expressed in PK15-NTD cells. Cells were incubated with either 1 mM MMTS or 0.1% DMSO (Control) for 10 min, washed extensively, and then incubated with a range of concentrations of [³H]NBMPR in the presence and absence of 10 μM NBTGR to define total and nonspecific binding. **Panel B** describes the concentration-dependent uptake of [³H]2-chloroadenosine of cells treated for 10 min with 1 mM MMTS or 0.1% DMSO (Control) and washed three times. Cells were incubated with a range of concentrations of [³H]2-chloroadenosine for 5 s in the presence (Non-mediated) or absence (Total uptake) of 5 μM dipyrindamole/NBTGR. Each point represents the mean ± SEM of the cellular accumulation of [³H]2-chloroadenosine from at least four independent experiments conducted in duplicate. * Significant difference from control B_{max} (Student's t test for paired samples, *P* < 0.05).

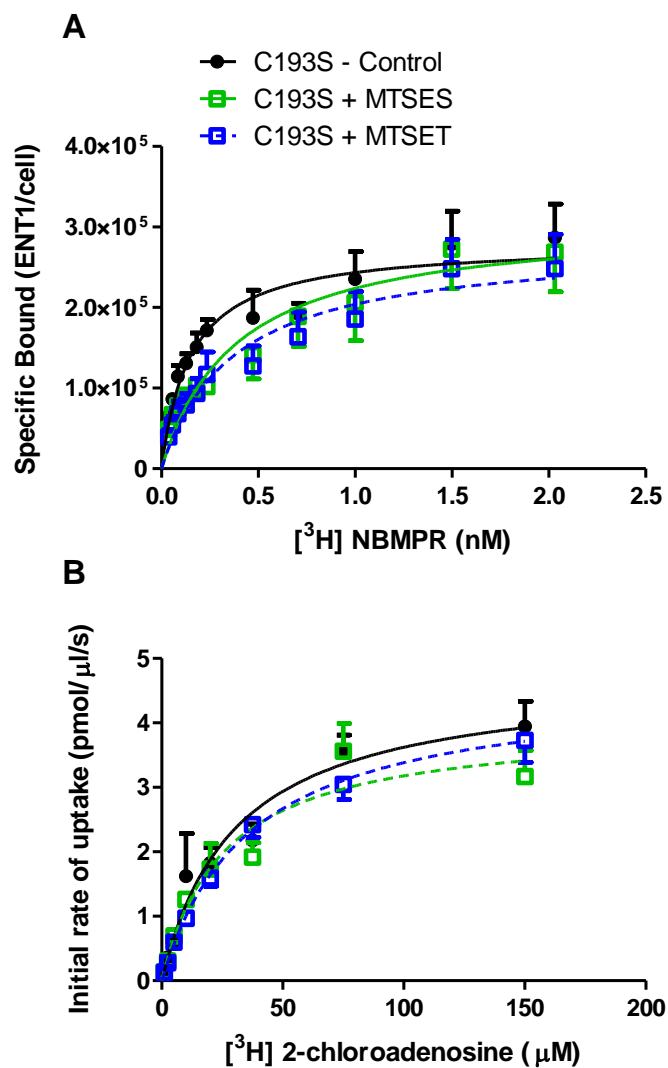


Figure 4.19. Treatment of C193S with MTSET and MTSES. Effects of MTSET and MTSES on [³H]NBMPR binding (**Panel A**) and [³H]2-chloroadenosine (**Panel B**) uptake by hENT1-C193S expressed in PK15-NTD cells. Cells were incubated with either 5 mM MTSET (blue squares), or 5 mM MTSES (green squares) for 10 min, washed extensively, and then incubated with a range of concentrations of [³H]NBMPR in the presence and absence of 10 μM NBTGR to define total and nonspecific binding. **Panel B** describes the concentration-dependent uptake of [³H]2-chloroadenosine of cells treated for 10 min with either 5 mM MTSET or 5 mM MTSES and washed three times. Cells were then incubated with a range of concentrations of [³H]2-chloroadenosine for 5 s in the presence (Non-mediated) or absence (Total uptake) of 5 μM dipyridamole/NBTGR. Each point represents the mean ± SEM of the cellular accumulation of [³H]2-chloroadenosine from at least five independent experiments conducted in duplicate.

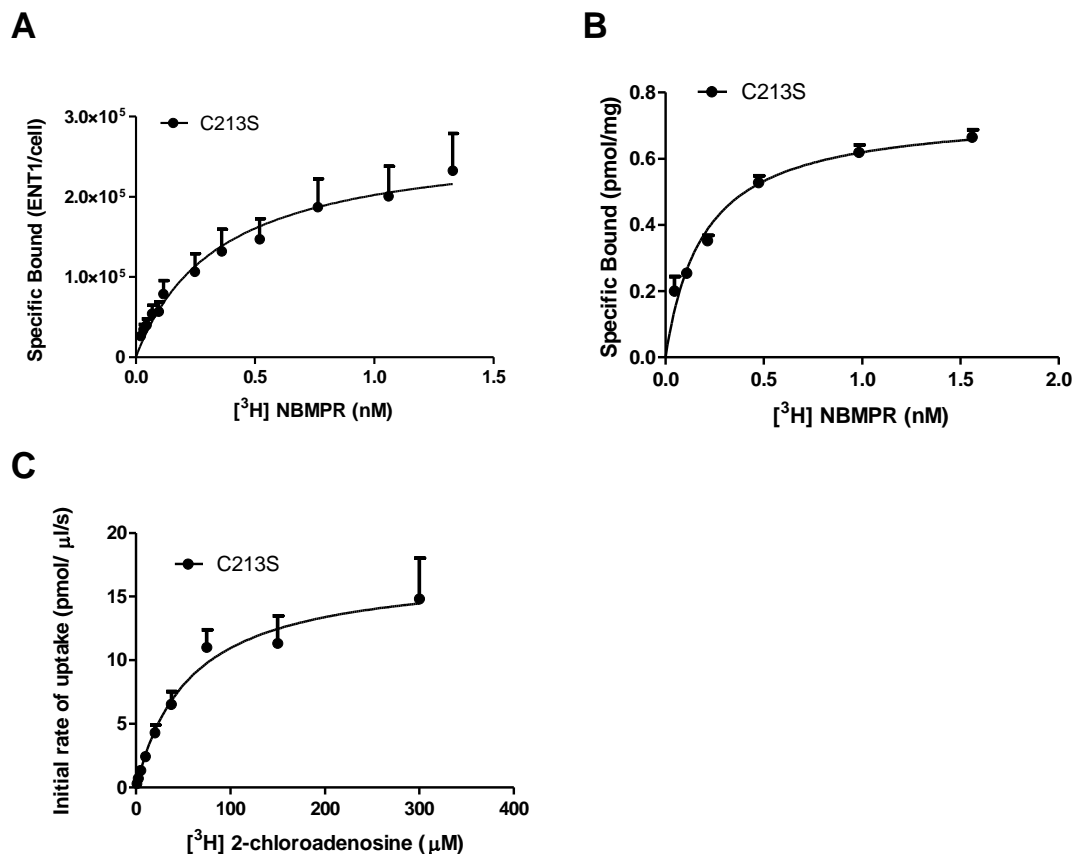


Figure 4.20. Characterization of PK15-C213S. [³H]NBMPR binding of PK15-C213S cells (**Panel A**) and PK15-C213S membranes (**Panel B**) and [³H]2-chloroadenosine uptake of PK15-C213S cells (**Panel C**). For **panels A and B**, cells and membranes were incubated with a range of concentrations of [³H]NBMPR (abscissa) in the presence (nonspecific binding) and absence of 10 μM NBTGR (total binding). Specific binding was determined by total bound minus non-specific bound. Each point represents the mean ± SEM from at least four experiments done in duplicate. For **panel C**, cells were incubated with a range of concentrations of [³H]2-chloroadenosine for 5 s in the presence (Non-mediated) or absence (Total uptake) of 5 μM dipyridamole/NBTGR. Transporter-mediated uptake (Mediated) was calculated as the difference between the total and non-mediated uptake components. Each point represents the mean ± SEM of the cellular accumulation of [³H]2-chloroadenosine from at least four independent experiments conducted in duplicate.

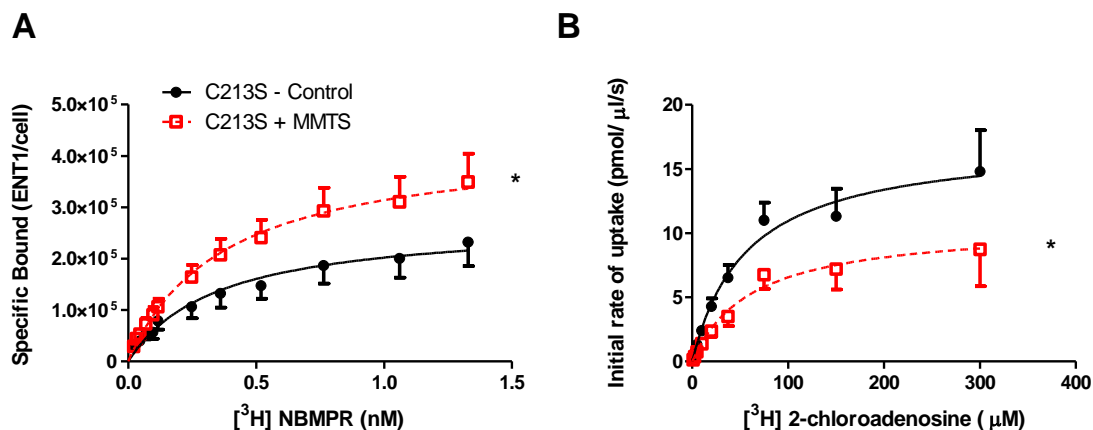


Figure 4.21. Treatment of C213S with MMTS. Effects of MMTS on [³H]NBMPR binding (**Panel A**) and [³H]2-chloroadenosine (**Panel B**) uptake by hENT1-C213S expressed in PK15-NTD cells. Cells were incubated with either 1 mM MMTS or 0.1% DMSO (Control) for 10 min, washed extensively, and then incubated with a range of concentrations of [³H]NBMPR in the presence and absence of 10 μM NBTGR to define total and nonspecific binding. Specific binding was calculated as the difference between the total and nonspecific binding components. Each point represents the mean ± SEM from at least 5 experiments done in duplicate. **Panel B** describes the concentration-dependent uptake of [³H]2-chloroadenosine of cells treated for 10 min with 1 mM MMTS or 0.1% DMSO (Control) and washed three times. Cells were incubated with a range of concentrations of [³H]2-chloroadenosine for 5 s in the presence (Non-mediated) or absence (Total uptake) of 5 μM dipyridamole/NBTGR. Transporter-mediated uptake (Mediated) was calculated as the difference between the total and non-mediated uptake components. Each point represents the mean ± SEM of the cellular accumulation of [³H]2-chloroadenosine from at least four independent experiments conducted in duplicate. * Significant difference from control B_{max} for NBMPR binding studies and control V_{max} for uptake studies (Student's t test for paired samples, $P < 0.05$)

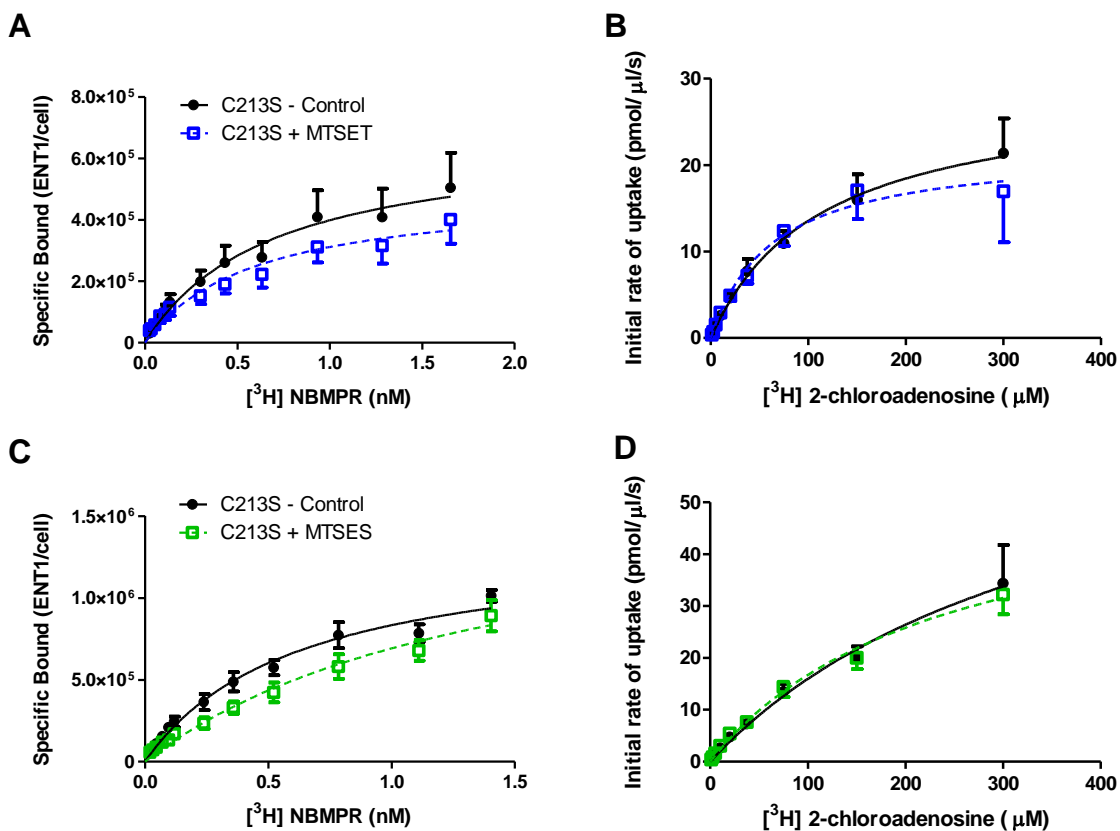


Figure 4.22. Treatment of C213S with MTSET and MTSES. Effects of MTSET (Panel A and B) and MTSES (Panel C and D) on [³H]NBMPR binding and on [³H]2-chloroadenosine uptake of hENT1-C213S expressed in PK15-NTD cells. For Panel A and C, cells were incubated with either 5 mM MTSET (Panel A), or 5 mM MTSES (Panel C) for 10 min, washed extensively, and then incubated with a range of concentrations of [³H]NBMPR in the presence and absence of 10 μM NBTGR to define total and nonspecific binding. Each point represents the mean ± SEM from at least 5 experiments done in duplicate. For Panel B and D, cells were incubated with either 5 mM MTSET (Panel B) or 5 mM MTSES (Panel D) for 10 min, washed extensively, and then incubated with a range of concentrations of [³H]2-chloroadenosine for 5 s in the presence (Non-mediated) or absence (Total uptake) of 5 μM dipyridamole/NBTGR. Transporter-mediated uptake (Mediated) was calculated as the difference between the total and non-mediated uptake components. Each point represents the mean ± SEM of the cellular accumulation of [³H]2-chloroadenosine from at least four independent experiments conducted in duplicate.

chloroadenosine uptake in the C213S mutants (Figure 4.22C, 4.22D).

4.5.4 Mutation of C222 to serine

hENT1-C222S cells bound [³H]NBMPR with a K_d of 0.3 ± 0.04 nM to a maximum of $2.0 \pm 0.2 \times 10^5$ ENT1 sites/cell (Figure 4.23A, Table 4.2). Membranes prepared from these cells had a K_d of 0.08 ± 0.01 nM and a [³H]NBMPR B_{max} of 0.5 ± 0.05 pmol/mg protein (Figure 4.23B). The K_m and V_{max} for [³H]2-chloroadenosine uptake were 63 ± 11 μ M and 9.3 ± 1.3 pmol/ μ l/s (Figure 4.23C, Table 4.2), respectively, resulting in a V_{max}/B_{max} ratio of 4.7 ± 0.8 pmol/ENT1/s, which is significantly greater than that of wild-type hENT1.

4.5.4.1 C222S MTS treatments

MMTS treatment had no significant effect on [³H]NBMPR binding to hENT1-C222S in intact cells (Figure 4.24A), making this the only mutant studied that did not respond to MMTS with an increase in [³H]NBMPR binding. MTSES had no effect on NBMPR binding however MTSET induced a slight inhibition of [³H]NBMPR binding, similar to that seen in the hENT1 wild-type cells and the C213S mutants (Figure 4.25A). The C222S cells were also similar to the C87S and C213S mutants and the hENT1 wild-type cells in that MMTS caused a significant decrease ($53 \pm 21\%$) in the maximal rate of [³H]2-chloroadenosine uptake (Figure 4.24B). Neither MTSET nor MTSES affected [³H]2-chloroadenosine uptake by the hENT1-C222S cells (Figure 4.25B). The hENT1-C222S mutant was also the only one of those studied that did not show a significant decrease in [³H]NBMPR binding B_{max} in isolated cell membranes treated with MMTS. Additionally, when C222S intact cells were treated with MMTS (or DMSO as control) and then used to prepare isolated membranes for analysis of [³H]NBMPR binding, the membranes derived from cells treated with MMTS had B_{max} that were not significantly different than those membranes prepared from cells treated with DMSO alone (Figure 4.26A, 4.26B). MMTS did however, appear to decrease the affinity of [³H]NBMPR for its binding sites in the C222S cells relative to wild-type hENT1 (K_d of 0.2 ± 0.03 and 0.08 ± 0.01 nM in C222S and hENT1 wild-type, respectively). MTSET treatment, on the other hand, almost

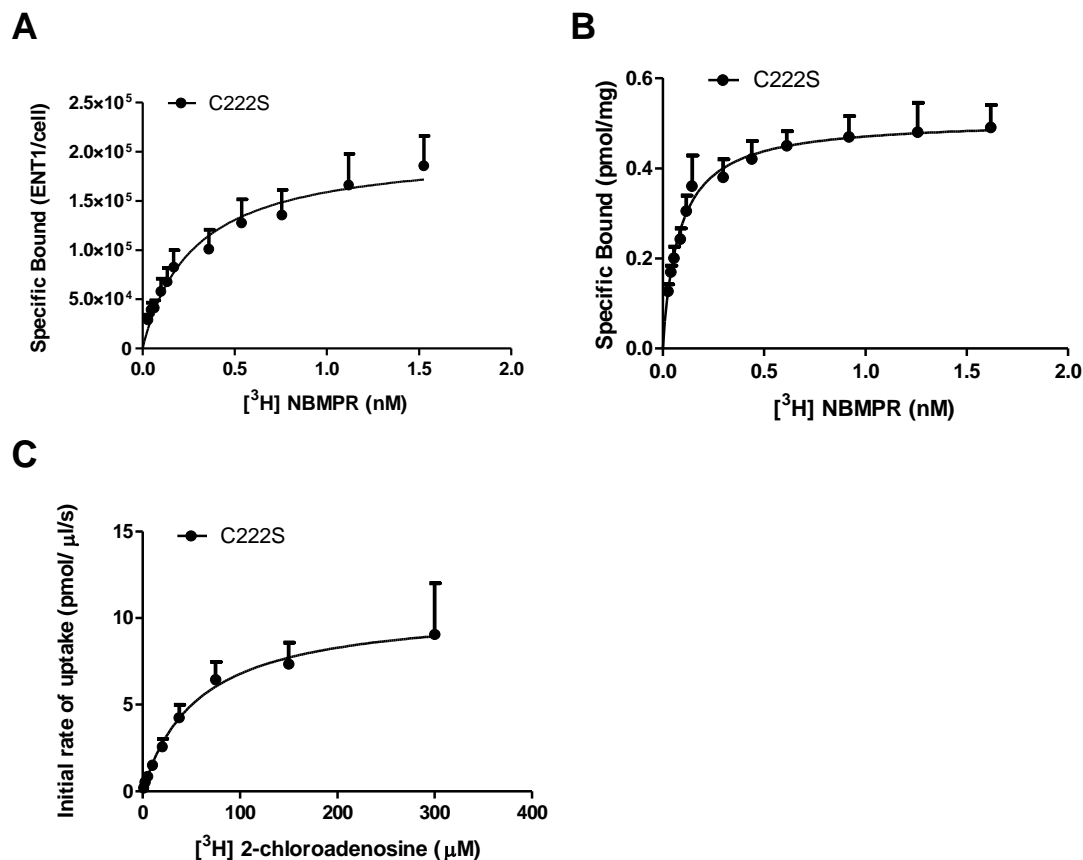


Figure 4.23. Characterization of PK15-C222S. $[^3\text{H}]$ NBMPR binding of PK15-C222S cells (**Panel A**) and PK15-C222S membranes (**Panel B**) and $[^3\text{H}]$ 2-chloroadenosine uptake of PK15-C222S cells (**Panel C**). For **panels A and B**, cells and membranes were incubated with a range of concentrations of $[^3\text{H}]$ NBMPR (abscissa) in the presence (nonspecific binding) and absence of 10 μM NBTGR (total binding). Specific binding was determined by total bound minus non-specific bound. Each point represents the mean \pm SEM from at least four experiments done in duplicate. For **panel C**, cells were incubated with a range of concentrations of $[^3\text{H}]$ 2-chloroadenosine for 5 s in the presence (Non-mediated) or absence (Total uptake) of 5 μM dipyridamole/NBTGR. Transporter-mediated uptake (Mediated) was calculated as the difference between the total and non-mediated uptake components. Each point represents the mean \pm SEM of the cellular accumulation of $[^3\text{H}]$ 2-chloroadenosine from at least four independent experiments conducted in duplicate.

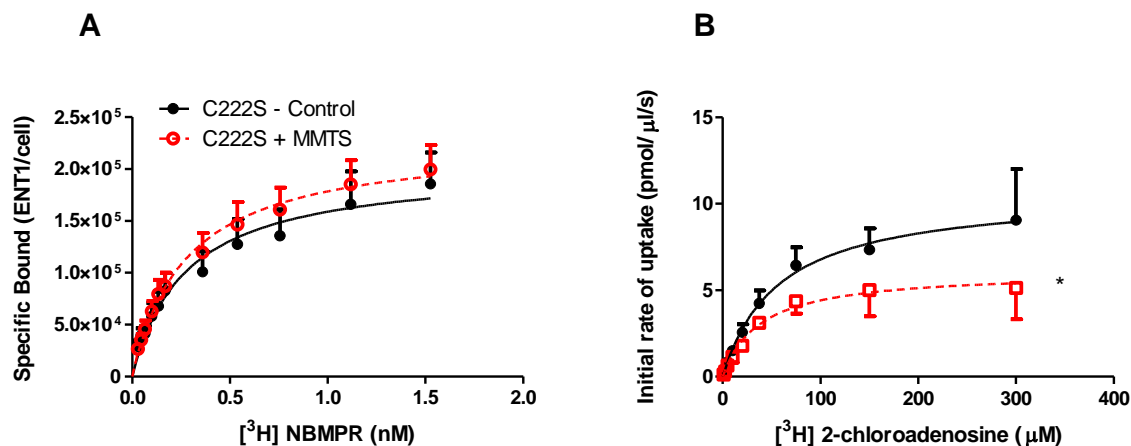


Figure 4.24. Treatment of C222S with MMTS: NBMPR binding to C222S is insensitive to MMTS. Effects of MMTS on $[^3\text{H}]$ NBMPR binding (**Panel A**) and $[^3\text{H}]$ 2-chloroadenosine (**Panel B**) uptake by hENT1-C222S expressed in PK15-NTD cells. Cells were incubated with either 1 mM MMTS or 0.1% DMSO (Control) for 10 min, washed extensively, and then incubated with a range of concentrations of $[^3\text{H}]$ NBMPR in the presence and absence of 10 μM NBTGR to define total and nonspecific binding. Specific binding was calculated as the difference between the total and nonspecific binding components. Each point represents the mean \pm SEM from at least 5 experiments done in duplicate. **Panel B** describes the concentration-dependent uptake of $[^3\text{H}]$ 2-chloroadenosine of cells treated for 10 min with 1 mM MMTS or 0.1% DMSO (Control) and washed three times. Cells were incubated with a range of concentrations of $[^3\text{H}]$ 2-chloroadenosine for 5 s in the presence (Non-mediated) or absence (Total uptake) of 5 μM dipyridamole/NBTGR. Transporter-mediated uptake (Mediated) was calculated as the difference between the total and non-mediated uptake components. Each point represents the mean \pm SEM of the cellular accumulation of $[^3\text{H}]$ 2-chloroadenosine from at least four independent experiments conducted in duplicate. * Significant difference from control V_{max} (Student's t test for paired samples, $P < 0.05$).

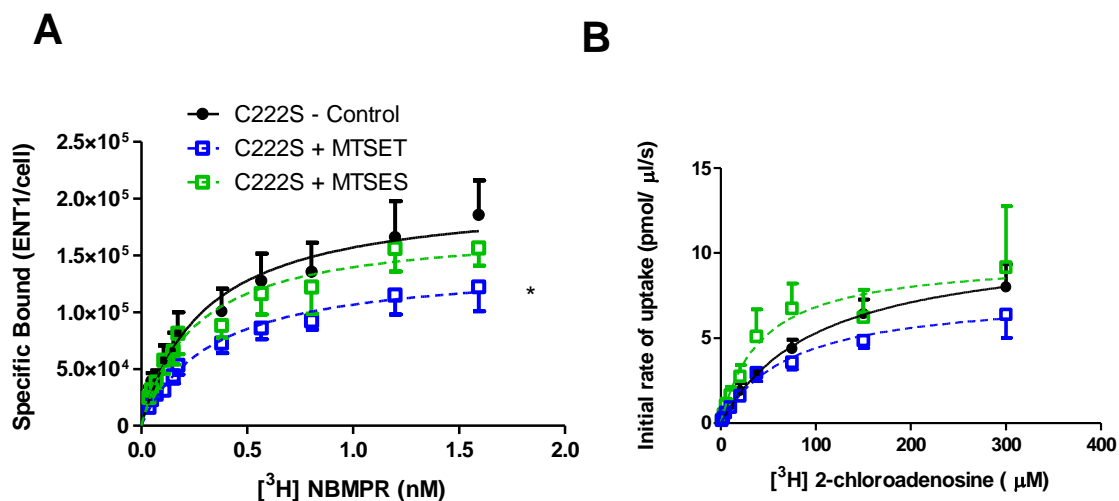


Figure 4.25. Treatment of C222S with MTSET and MTSES. Effects of MTSET and MTSES on [³H]NBMPR binding (**Panel A**) and [³H]2-chloroadenosine (**Panel B**) uptake by hENT1-C222S expressed in PK15-NTD cells. Cells were incubated with either 5 mM MTSET (blue squares), or 5 mM MTSES (green squares) for 10 min, washed extensively, and then incubated with a range of concentrations of [³H]NBMPR in the presence and absence of 10 μM NBTGR to define total and nonspecific binding. Specific binding was calculated as the difference between the total and nonspecific binding components. Each point represents the mean ± SEM from at least 5 experiments done in duplicate. **Panel B** describes the concentration-dependent uptake of [³H]2-chloroadenosine of cells treated for 10 min with either 5 mM MTSET or 5 mM MTSES and washed three times. Cells were then incubated with a range of concentrations of [³H]2-chloroadenosine for 5 s in the presence (Non-mediated) or absence (Total uptake) of 5 μM dipyridamole/NBTGR. Transporter-mediated uptake (Mediated) was calculated as the difference between the total and non-mediated uptake components. Each point represents the mean ± SEM of the cellular accumulation of [³H]2-chloroadenosine from at least four independent experiments conducted in duplicate. * Significant difference from control B_{max} (Student's t test for paired samples, *P* < 0.05).

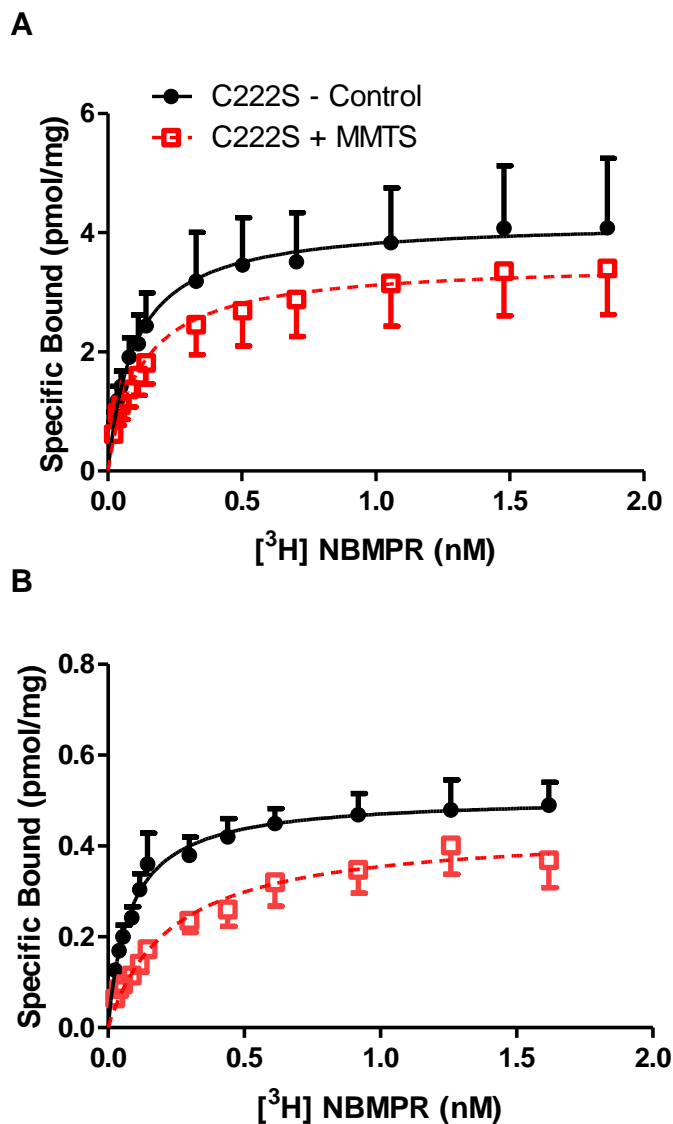


Figure 4.26. Cell membrane treatment of C222S with MMTS.

Effects of MMTS on $[^3\text{H}]$ NBMPR binding to hENT1-C222S cell membranes isolated from cells pre-treated with MMTS (**Panel A**) and hENT1-C222S cell membranes treated with MMTS (**Panel B**). PK15-C222S cells and membranes were incubated with a range of concentrations of $[^3\text{H}]$ NBMPR (abscissa) in the presence (nonspecific binding) and absence of 10 μM NBTGR (total binding). Each point represents the mean \pm SEM from at least four experiments done in duplicate. Nonlinear regression analysis was used to fit hyperbolic curves to the site-specific binding of $[^3\text{H}]$ NBMPR plotted against the free $[^3\text{H}]$ NBMPR concentration at steady-state.

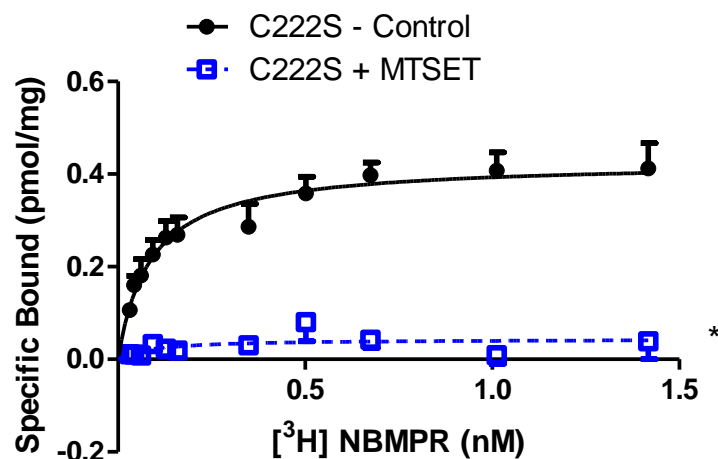


Figure 4.27. Cell membrane treatment of C222S with MTSET. Effect of MTSET on [³H]NBMPR binding by PK15-C222S cell membranes. Membranes were incubated with either 5 mM MTSET or 0.5% DMSO (Control) for 10 min, washed thrice, and then incubated with a range of concentrations of [³H]NBMPR (abscissa) in the presence and absence of 10 μM NBTGR to define total and nonspecific binding. Specific binding (ordinate) was calculated as the difference between the total and nonspecific binding components. Each point represents the mean ± SEM from at least 5 experiments done in duplicate. * Significant difference from control B_{max} (Student's t test for paired samples, $P < 0.05$).

completely eliminated [³H]NBMPR binding to the isolated membranes (0.04 ± 0.01 pmol/mg protein versus 0.4 ± 0.01 pmol/mg protein in the control cells) (Figure 4.27).

4.5.4.2 C222S pH effects

Mutation of C222 to serine abolished the effects of MMTS treatment similarly to the way alkaline pH abolished the effects of MMTS treatment in wild-type hENT1. Given that wild-type hENT1 showed enhanced binding in alkaline pH, and that MMTS is targeted to C222, we hypothesized that C222 was also involved in the pH effects seen in wild-type. PK15-C222S cells were incubated with NMG buffer at pH 7.4 and 8.4 and we found specific binding of [³H]NBMPR in pH 7.4 and 8.4 yielded near identical B_{\max} values of $4.9 \pm 0.1 \times 10^5$ ENT1 sites/cell and $5.2 \pm 0.1 \times 10^5$ ENT1 sites/cells respectively (Figure 4.28).

4.5.5 Mutation of C297 to serine:

hENT1-C297S cells bound [³H]NBMPR with a K_d of 0.3 ± 0.04 nM, which is not significantly different from that obtained in wild-type hENT1 (Figure 4.29A, Table 4.2). Membranes prepared from these cells had a K_d of 0.1 ± 0.01 nM and a [³H]NBMPR B_{\max} of 0.4 ± 0.01 pmol/mg protein (Figure 4.29B). Similarly, the K_m for [³H]2-chloroadenosine uptake was 61 ± 13 μ M for C297S-hENT1 which is not significantly different to the wild-type K_m values as previously calculated (Figure 4.29C, Table 4.2). The B_{\max} of [³H]NBMPR binding and the V_{\max} of [³H]2-chloroadenosine uptake by hENT1-C297S cells were $1.3 \pm 0.2 \times 10^5$ ENT1 sites/cell and 5.7 ± 0.6 pmol/ μ l/s, respectively, giving a V_{\max}/B_{\max} ratio of $4.5 \pm 0.9 \times 10^{-5}$ pmol/ENT1/s.

4.5.5.1 C297S MTS treatments

When treated with MMTS, hENT1-C297S showed a similar enhancement in B_{\max} of [³H]NBMPR binding by $52 \pm 4\%$ with no significant change in K_d as previously described in the wild-type (Figure 4.30A). In contrast, hENT1-C297S lost sensitivity to MMTS in relation to [³H]2-chloroadenosine uptake (Figure 4.30B). Treatment with MTSET yielded opposite results where [³H]NBMPR binding was unaffected and [³H]2-chloroadenosine

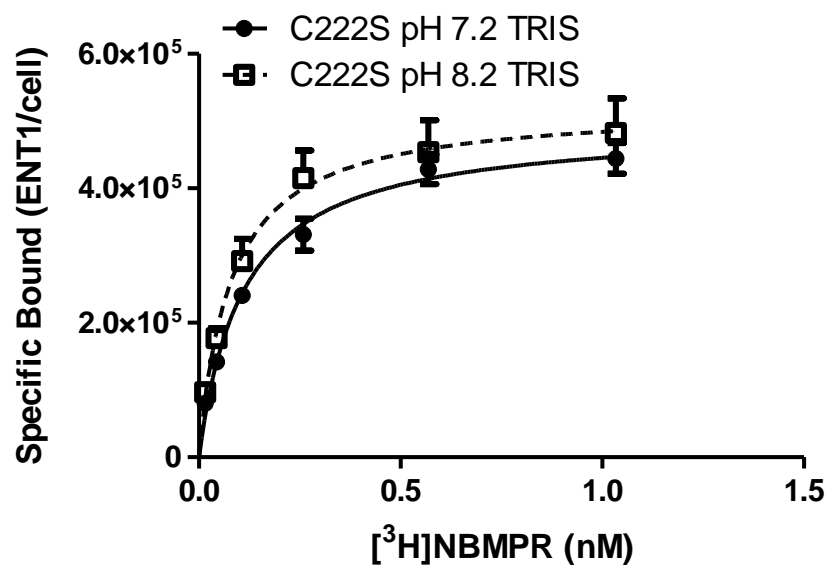


Figure 4.28. NBMPR binding to C222S is insensitive to pH. Effect of pH on [³H]NBMPR binding to PK15-C222S cells. Intact cells were incubated in NMG buffer of pH 7.2 or pH 8.2 and then exposed to a range of concentrations of [³H]NBMPR in the presence and absence of 10 μ M NBTGR to define the amount of site-specific binding of this ligand in each cell. Each point is the mean \pm SEM from at least 4 experiments conducted in duplicate.

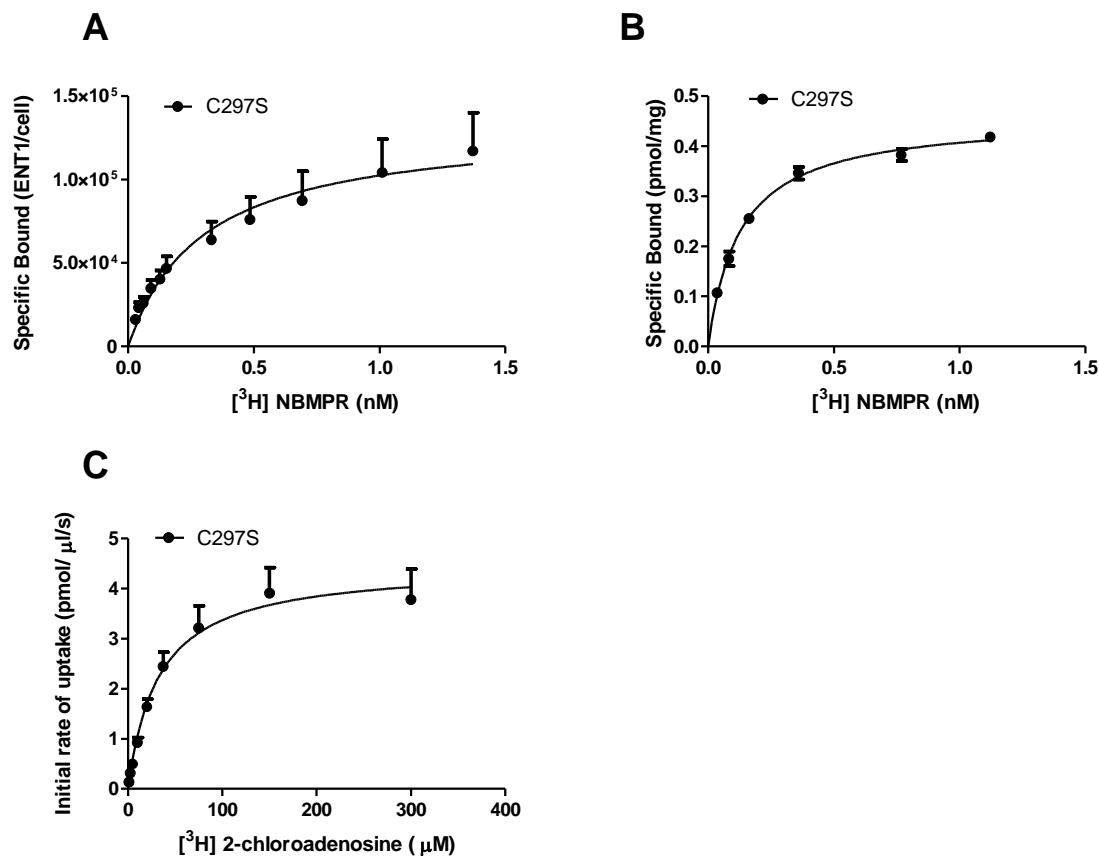


Figure 4.29. Characterization of PK15-C297S. $[^3\text{H}]$ NBMPR binding of PK15-C297S cells (**Panel A**) and PK15-C297S membranes (**Panel B**) and $[^3\text{H}]$ 2-chloroadenosine uptake of PK15-C297S cells (**Panel C**). For **panels A and B**, cells and membranes were incubated with a range of concentrations of $[^3\text{H}]$ NBMPR (abscissa) in the presence (nonspecific binding) and absence of 10 μM NBTGR (total binding). Specific binding was determined by total bound minus non-specific bound. Each point represents the mean \pm SEM from at least four experiments done in duplicate. For **panel C**, cells were incubated with a range of concentrations of $[^3\text{H}]$ 2-chloroadenosine for 5 s in the presence (Non-mediated) or absence (Total uptake) of 5 μM dipyridamole/NBTGR. Transporter-mediated uptake (Mediated) was calculated as the difference between the total and non-mediated uptake components. Each point represents the mean \pm SEM of the cellular accumulation of $[^3\text{H}]$ 2-chloroadenosine from at least four independent experiments conducted in duplicate.

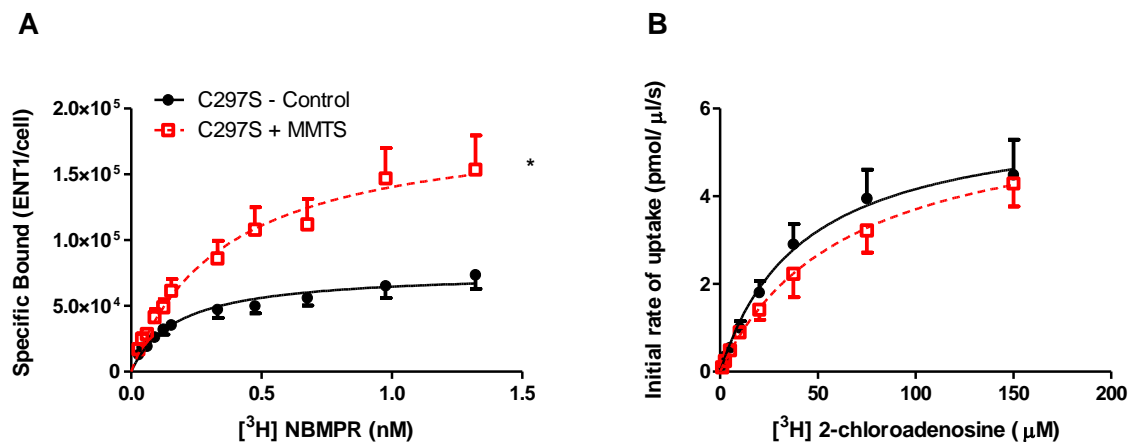


Figure 4.30. Treatment of C297S with MMTS. Effects of MMTS of [³H]NBMPR binding (**Panel A**) and [³H]2-chloroadenosine (**Panel B**) uptake by hENT1-C297S expressed in PK15-NTD cells. Cells were incubated with either 1 mM MMTS or 0.1% DMSO (Control) for 10 min, washed extensively, and then incubated with a range of concentrations of [³H]NBMPR in the presence and absence of 10 μM NBTGR to define total and nonspecific binding. Specific binding was calculated as the difference between the total and nonspecific binding components. Each point represents the mean ± SEM from at least 5 experiments done in duplicate. **Panel B** describes the concentration-dependent uptake of [³H]2-chloroadenosine of cells treated for 10 min with 1 mM MMTS or 0.1% DMSO (Control) and washed three times. Cells were incubated with a range of concentrations of [³H]2-chloroadenosine for 5 s in the presence (Non-mediated) or absence (Total uptake) of 5 μM dipyridamole/NBTGR. Transporter-mediated uptake (Mediated) was calculated as the difference between the total and non-mediated uptake components. Each point represents the mean ± SEM of the cellular accumulation of [³H]2-chloroadenosine from at least four independent experiments conducted in duplicate. * Significant difference from control B_{max} (Student's t test for paired samples, *P* < 0.05).

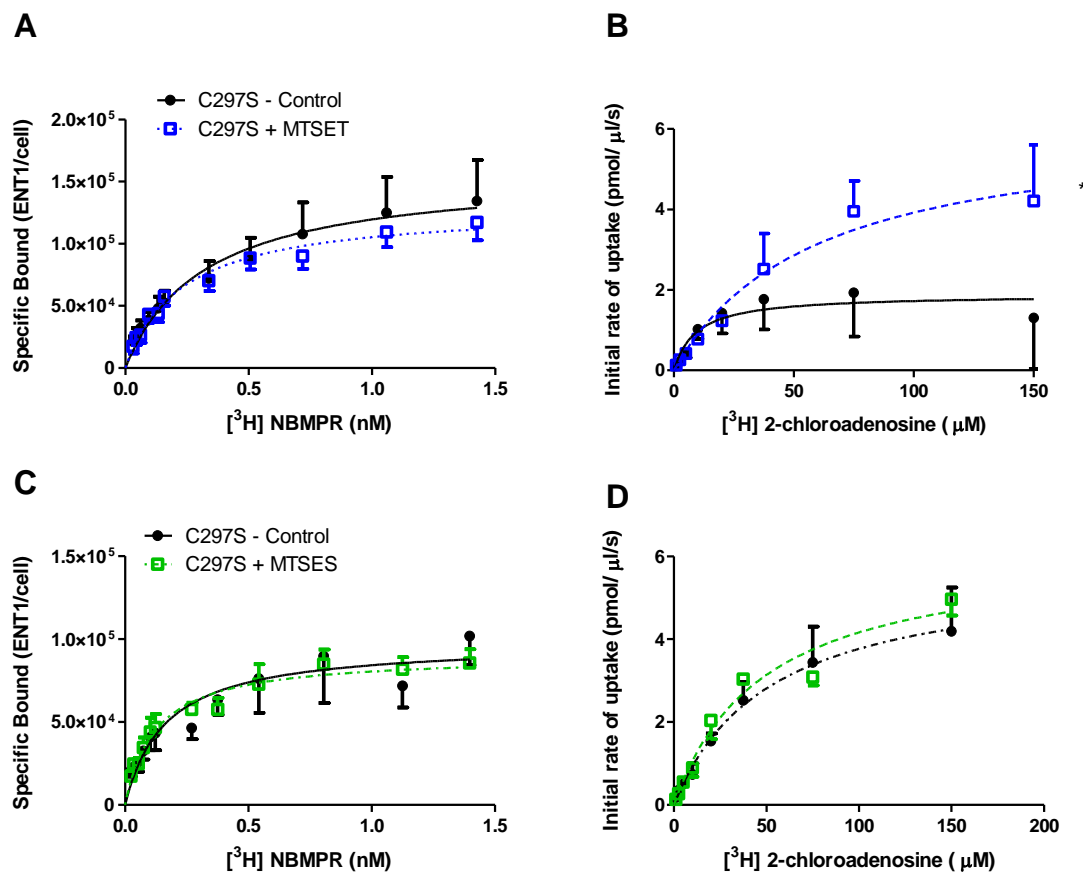


Figure 4.31. Treatment of C297S with MTSET and MTSES. Effects of MTSET (**Panel A and B**) and MTSES (**Panel C and D**) on $[^3\text{H}]$ NBMPR binding and on $[^3\text{H}]$ 2-chloroadenosine uptake of hENT1-C297S expressed in PK15-NTD cells. For **Panel A and C**, cells were incubated with either 5 mM MTSET (Panel A), or 5 mM MTSES (Panel C) for 10 min, washed extensively, and then incubated with a range of concentrations of $[^3\text{H}]$ NBMPR in the presence and absence of 10 μM NBTGR to define total and nonspecific binding. Each point represents the mean \pm SEM from at least 5 experiments done in duplicate. For **Panel B and D**, cells were incubated with either 5 mM MTSET (Panel B) or 5 mM MTSES (Panel D) for 10 min, washed extensively, and then incubated with a range of concentrations of $[^3\text{H}]$ 2-chloroadenosine for 5 s in the presence (Non-mediated) or absence (Total uptake) of 5 μM dipyridamole/NBTGR. Each point represents the mean \pm SEM of the cellular accumulation of $[^3\text{H}]$ 2-chloroadenosine from at least four independent experiments conducted in duplicate. * Significant difference from control V_{max} (Student's t test for paired samples, $P < 0.05$).

uptake V_{\max} remained sensitive to MTSET enhancement (Figure 4.31A, 4.31B). MTSES, the negatively charged impermeable reagent, had no effect on either [^3H]NBMPR or [^3H]2-chloroadenosine kinetics (Figure 4.31C, 4.31D).

4.5.6 Mutation of C333 to serine:

hENT1-C333S cells bound [^3H]NBMPR with a K_d of 0.4 ± 0.06 nM to a maximum of $4.3 \pm 0.4 \times 10^5$ ENT1 sites/cell (Figure 4.32A, Table 4.2). Membranes prepared from these cells had a K_d of 0.2 ± 0.01 nM and a [^3H]NBMPR B_{\max} of 2.4 ± 0.4 pmol/mg protein (Figure 4.32B). Transport of [^3H]2-chloroadenosine by hENT1-C333S had a K_m and V_{\max} of 39 ± 5 μM (Figure 4.32C, Table 4.2) and 6.7 ± 0.7 pmol/ $\mu\text{l/s}$, respectively. The V_{\max}/B_{\max} ratio was calculated at $1.5 \pm 0.2 \times 10^{-5}$ pmol/ENT1/s which is similar to wild-type hENT1, however the K_m of hENT1-C333S is significantly lower than wild-type indicating a greater affinity for the substrate.

4.5.6.1 C333S MTS treatments

The effect of MMTS on hENT1-C333S [^3H]NBMPR binding produced similar effects compared to wild-type as the neutral reagent caused a $77 \pm 13\%$ enhancement in B_{\max} (Figure 4.33A). In contrast, MMTS was unable to produce an effect on the [^3H]2-chloroadenosine uptake of hENT1-C333S (Figure 4.33B). Additionally, treatment with either MTSES or MTSET did not produce any effects on [^3H]2-chloroadenosine uptake or [^3H]NBMPR binding (Figure 4.34A, 4.34B).

4.5.7 Mutation of C378 to serine:

hENT1-C378S cells bound [^3H]NBMPR with a K_d of 0.4 ± 0.03 nM to a B_{\max} of $4.7 \pm 0.4 \times 10^5$ ENT1 sites/cell (Figure 4.35A, Table 4.2). Membranes prepared from these cells had a K_d of 0.1 ± 0.01 nM and a [^3H]NBMPR B_{\max} of 1.9 ± 0.12 pmol/mg protein (Figure 4.35B). The transport kinetics of [^3H]2-chloroadenosine by hENT1-C378S were calculated to have a V_{\max} of 11 ± 1.0 pmol/ $\mu\text{l/s}$ and K_m of 57 ± 6 μM (Figure 4.35C, Table 4.2). The

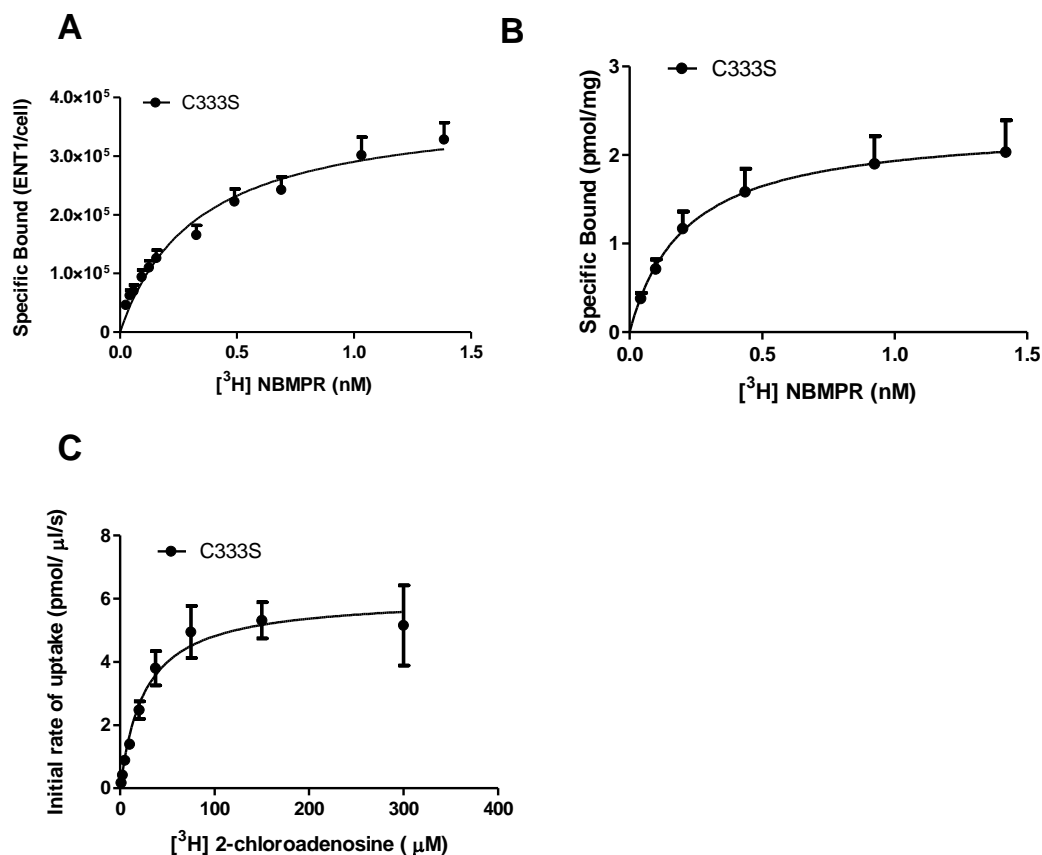


Figure 4.32. Characterization of PK15-C333S. [³H]NBMPR binding of PK15-C333S cells (**Panel A**) and PK15-C333S membranes (**Panel B**) and [³H]2-chloroadenosine uptake of PK15-C333S cells (**Panel C**). For **panels A and B**, cells and membranes were incubated with a range of concentrations of [³H]NBMPR (abscissa) in the presence (nonspecific binding) and absence of 10 μM NBTGR (total binding). Specific binding was determined by total bound minus non-specific bound. Each point represents the mean ± SEM from at least four experiments done in duplicate. For **panel C**, cells were incubated with a range of concentrations of [³H]2-chloroadenosine for 5 s in the presence (Non-mediated) or absence (Total uptake) of 5 μM dipyridamole/NBTGR. Transporter-mediated uptake (Mediated) was calculated as the difference between the total and non-mediated uptake components. Each point represents the mean ± SEM of the cellular accumulation of [³H]2-chloroadenosine from at least four independent experiments conducted in duplicate.

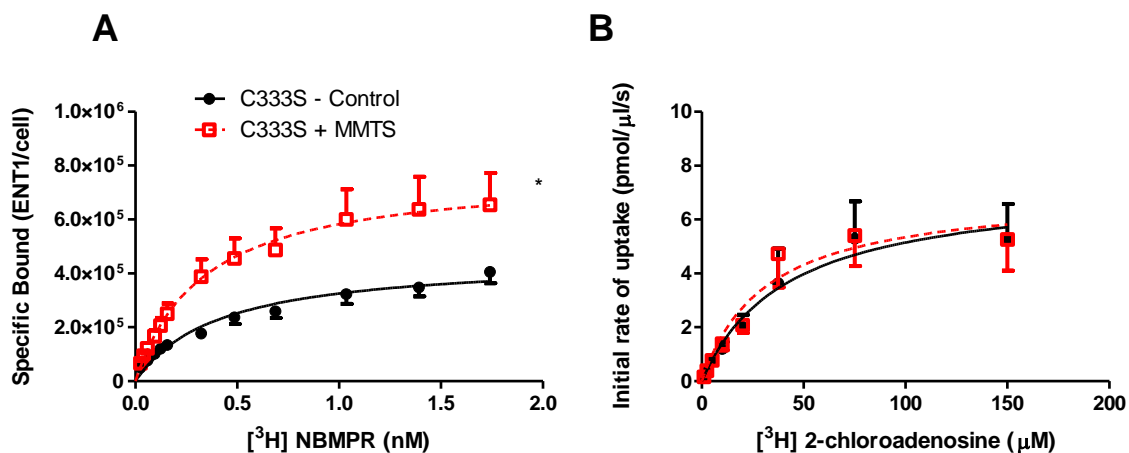


Figure 4.33. Treatment of C333S with MMTS. Effects of MMTS of $[^3\text{H}]$ NBMPR binding (**Panel A**) and $[^3\text{H}]$ 2-chloroadenosine (**Panel B**) uptake by hENT1-C333S expressed in PK15-NTD cells. Cells were incubated with either 1 mM MMTS or 0.1% DMSO (Control) for 10 min, washed extensively, and then incubated with a range of concentrations of $[^3\text{H}]$ NBMPR in the presence and absence of 10 μM NBTGR to define total and nonspecific binding. Specific binding was calculated as the difference between the total and nonspecific binding components. Each point represents the mean \pm SEM from at least 5 experiments done in duplicate. **Panel B** describes the concentration-dependent uptake of $[^3\text{H}]$ 2-chloroadenosine of cells treated for 10 min with 1 mM MMTS or 0.1% DMSO (Control) and washed three times. Cells were incubated with a range of concentrations of $[^3\text{H}]$ 2-chloroadenosine for 5 s in the presence (Non-mediated) or absence (Total uptake) of 5 μM dipyrindamole/NBTGR. Transporter-mediated uptake (Mediated) was calculated as the difference between the total and non-mediated uptake components. Each point represents the mean \pm SEM of the cellular accumulation of $[^3\text{H}]$ 2-chloroadenosine from at least four independent experiments conducted in duplicate. * Significant difference from control B_{max} (Student's t test for paired samples, $P < 0.05$).

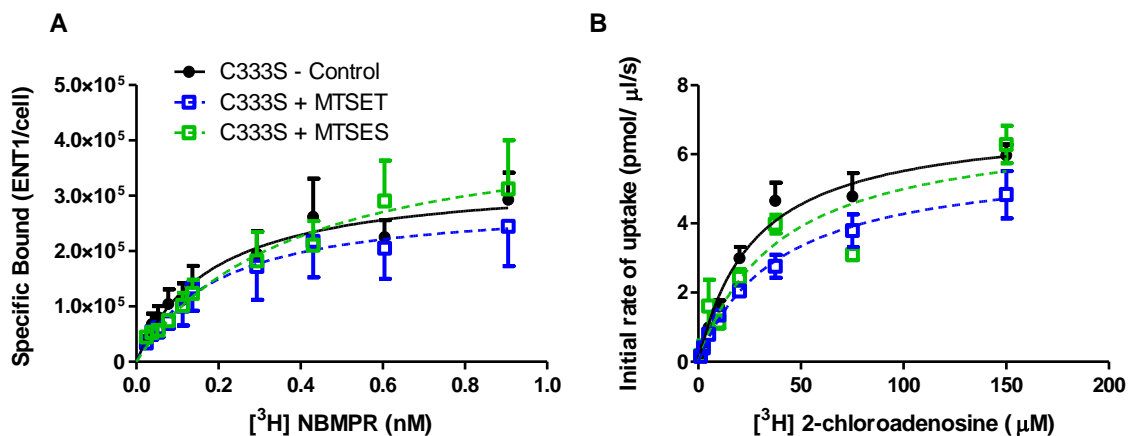


Figure 4.34. Treatment of C333S with MTSET and MTSES.

Effects of MTSET and MTSES on [³H]NBMPR binding (**Panel A**) and [³H]2-chloroadenosine (**Panel B**) uptake by hENT1-C333S expressed in PK15-NTD cells. Cells were incubated with either 5 mM MTSET (blue squares), or 5 mM MTSES (green squares) for 10 min, washed extensively, and then incubated with a range of concentrations of [³H]NBMPR in the presence and absence of 10 μM NBTGR to define total and nonspecific binding. Specific binding was calculated as the difference between the total and nonspecific binding components. Each point represents the mean ± SEM from at least 5 experiments done in duplicate. **Panel B** describes the concentration-dependent uptake of [³H]2-chloroadenosine of cells treated for 10 min with either 5 mM MTSET or 5 mM MTSES and washed three times. Cells were then incubated with a range of concentrations of [³H]2-chloroadenosine for 5 s in the presence (Non-mediated) or absence (Total uptake) of 5 μM dipyridamole/NBTGR. Transporter-mediated uptake (Mediated) was calculated as the difference between the total and non-mediated uptake components. Each point represents the mean ± SEM of the cellular accumulation of [³H]2-chloroadenosine from at least four independent experiments conducted in duplicate.

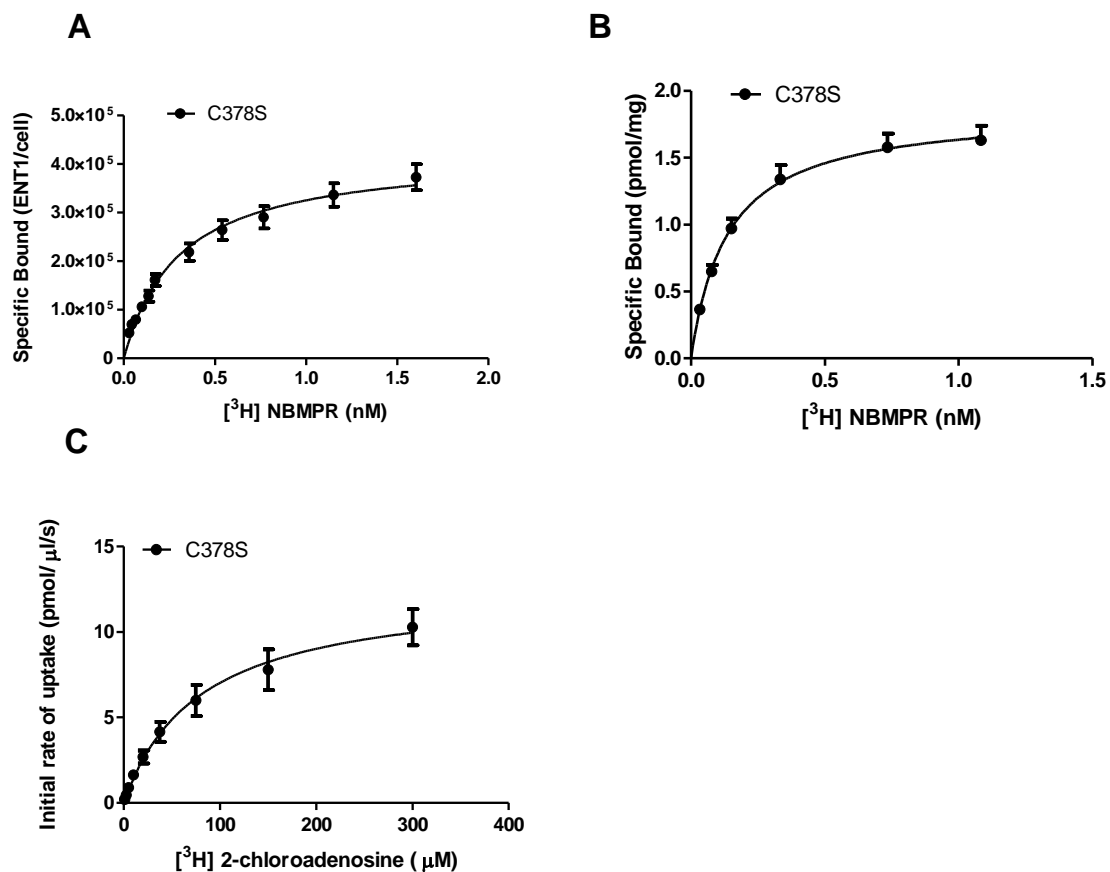


Figure 4.35. Characterization of PK15-C378S. [³H]NBMPR binding of PK15-C378S cells (**Panel A**) and PK15-C378S membranes (**Panel B**) and [³H]2-chloroadenosine uptake of PK15-C378S cells (**Panel C**). For panels A and B, cells and membranes were incubated with a range of concentrations of [³H]NBMPR (abscissa) in the presence (nonspecific binding) and absence of 10 μM NBTGR (total binding). Specific binding was determined by total bound minus non-specific bound. Each point represents the mean ± SEM from at least four experiments done in duplicate. For panel C, cells were incubated with a range of concentrations of [³H]2-chloroadenosine for 5 s in the presence (Non-mediated) or absence (Total uptake) of 5 μM dipyridamole/NBTGR. Transporter-mediated uptake (Mediated) was calculated as the difference between the total and non-mediated uptake components. Each point represents the mean ± SEM of the cellular accumulation of [³H]2-chloroadenosine from at least four independent experiments conducted in duplicate.

V_{\max}/B_{\max} ratio was determined to be $2.3 \pm 0.2 \times 10^{-5}$ pmol/ENT1/s which is similar to wild-type hENT1.

4.5.7.1 C378S MTS Treatments

After treatment with MMTS, hENT1-C378S [^3H]NBMPR B_{\max} increased by $49 \pm 14\%$ and decreased [^3H]2-chloroadenosine V_{\max} by $40 \pm 12\%$ (Figure 4.36A, 4.36B) adhering to wild-type trends seen with MMTS treatment. MTSET and MTSES treatment had no effect on either [^3H]NBMPR binding or [^3H]2-chloroadenosine transport similar to that seen in the hENT1-C333S mutant (Figure 4.37A, 4.37B).

4.5.8 Mutation of C414 to serine:

hENT1-C414S cells bound [^3H]NBMPR with a K_d of 0.4 ± 0.05 nM to a B_{\max} of $2.1 \pm 0.2 \times 10^{-5}$ ENT1 sites/cell (Figure 4.38A, Table 4.2). Membranes prepared from these cells had a K_d of 0.08 ± 0.01 nM and a [^3H]NBMPR B_{\max} of 1.5 ± 0.1 pmol/mg protein (Figure 4.38B). [^3H]2-chloroadenosine transport function remained intact as it achieved mediated uptake at a V_{\max} and K_m of 6.3 ± 0.4 pmol/ $\mu\text{l/s}$ and 35 ± 5 μM (Figure 4.38C, Table 4.2), respectively providing a V_{\max}/B_{\max} ratio of $3.0 \pm 0.3 \times 10^{-5}$ pmol/ENT1/s.

4.5.8.1 C414S MTS treatments

Treatment with MMTS increased [^3H]NBMPR B_{\max} by $98 \pm 12\%$ indicating a significant difference compared to the other cysteine mutants (Figure 4.39A). Additionally, [^3H]2-chloroadenosine V_{\max} decreased by $30 \pm 13\%$ with MMTS incubation as observed in preceding studies (Figure 4.39B). MTSES did not affect [^3H]NBMPR binding or [^3H]2-chloroadenosine transport by the hENT1-C414S cells (Figure 4.39C, 4.39D). When comparing MTSET effects of hENT1-C414S to wild-type hENT1, it was surprising to note the mutant transporter showed enhanced inhibition of [^3H]NBMPR B_{\max} by $50 \pm 9\%$ (Figure 4.40). Since MTSET effect was greater in hENT1-C414S than wild-type this suggested that the loss of the intracellularly located residue was inducing a

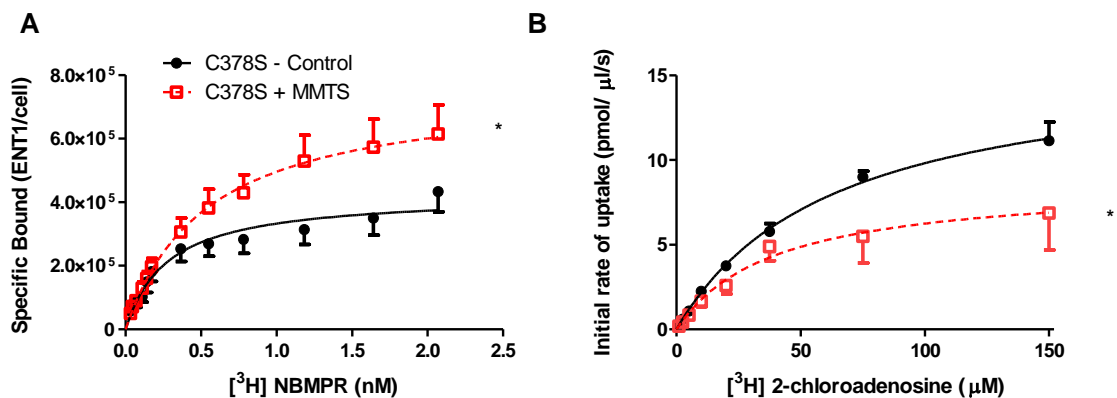


Figure 4.36. Treatment of C378S with MMTS. Effects of MMTS of [³H]NBMPR binding (**Panel A**) and [³H]2-chloroadenosine (**Panel B**) uptake by hENT1-C378S expressed in PK15-NTD cells. Cells were incubated with either 1 mM MMTS or 0.1% DMSO (Control) for 10 min, washed extensively, and then incubated with a range of concentrations of [³H]NBMPR in the presence and absence of 10 μM NBTGR to define total and nonspecific binding. Specific binding was calculated as the difference between the total and nonspecific binding components. Each point represents the mean ± SEM from at least 5 experiments done in duplicate. **Panel B** describes the concentration-dependent uptake of [³H]2-chloroadenosine of cells treated for 10 min with 1 mM MMTS or 0.1% DMSO (Control) and washed three times. Cells were incubated with a range of concentrations of [³H]2-chloroadenosine for 5 s in the presence (Non-mediated) or absence (Total uptake) of 5 μM dipyridamole/NBTGR. Transporter-mediated uptake (Mediated) was calculated as the difference between the total and non-mediated uptake components. Each point represents the mean ± SEM of the cellular accumulation of [³H]2-chloroadenosine from at least four independent experiments conducted in duplicate. * Significant difference from control B_{max} for NBMPR binding studies and control V_{max} for uptake studies (Student's t test for paired samples, $P < 0.05$)

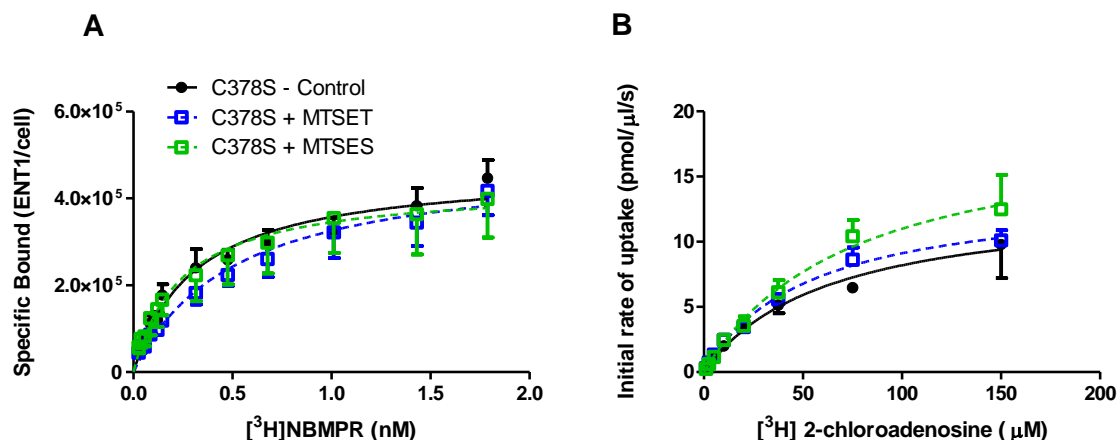


Figure 4.37. Treatment of C378S with MTSET and MTSES: NBMPR binding to C378S is insensitive to MTSET. Effects of MTSET and MTSES on [³H]NBMPR binding (**Panel A**) and [³H]2-chloroadenosine (**Panel B**) uptake by hENT1-C378S expressed in PK15-NTD cells. Cells were incubated with either 5 mM MTSET (blue squares), or 5 mM MTSES (green squares) for 10 min, washed extensively, and then incubated with a range of concentrations of [³H]NBMPR in the presence and absence of 10 μM NBTGR to define total and nonspecific binding. Specific binding was calculated as the difference between the total and nonspecific binding components. Each point represents the mean ± SEM from at least 5 experiments done in duplicate. **Panel B** describes the concentration-dependent uptake of [³H]2-chloroadenosine of cells treated for 10 min with either 5 mM MTSET or 5 mM MTSES and washed three times. Cells were then incubated with a range of concentrations of [³H]2-chloroadenosine for 5 s in the presence (Non-mediated) or absence (Total uptake) of 5 μM dipyrindamole/NBTGR. Transporter-mediated uptake (Mediated) was calculated as the difference between the total and non-mediated uptake components. Each point represents the mean ± SEM of the cellular accumulation of [³H]2-chloroadenosine from at least four independent experiments conducted in duplicate.

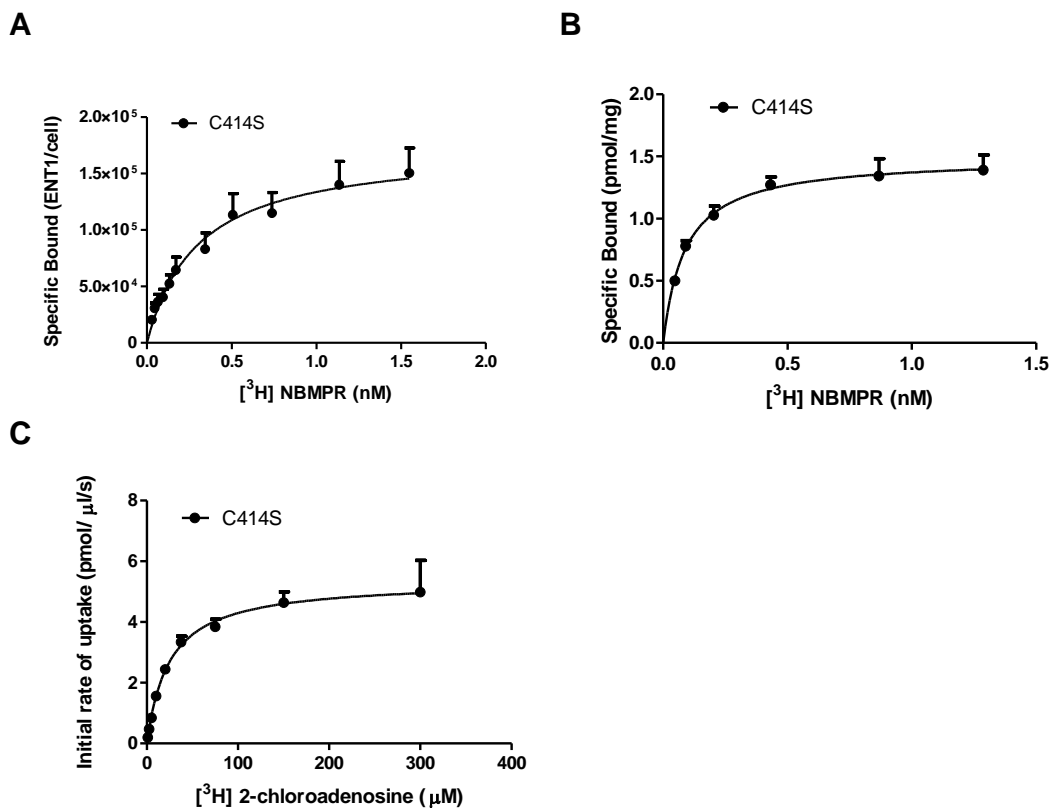


Figure 4.38. Characterization of PK15-C414S. [³H]NBMPR binding of PK15-C414S cells (**Panel A**) and PK15-C414S membranes (**Panel B**) and [³H]2-chloroadenosine uptake of PK15-C414S cells (**Panel C**). For **panels A and B**, cells and membranes were incubated with a range of concentrations of [³H]NBMPR (abscissa) in the presence (nonspecific binding) and absence of 10 μM NBTGR (total binding). Specific binding was determined by total bound minus non-specific bound. Each point represents the mean ± SEM from at least four experiments done in duplicate. For **panel C**, cells were incubated with a range of concentrations of [³H]2-chloroadenosine for 5 s in the presence (Non-mediated) or absence (Total uptake) of 5 μM dipyridamole/NBTGR. Transporter-mediated uptake (Mediated) was calculated as the difference between the total and non-mediated uptake components. Each point represents the mean ± SEM of the cellular accumulation of [³H]2-chloroadenosine from at least four independent experiments conducted in duplicate.

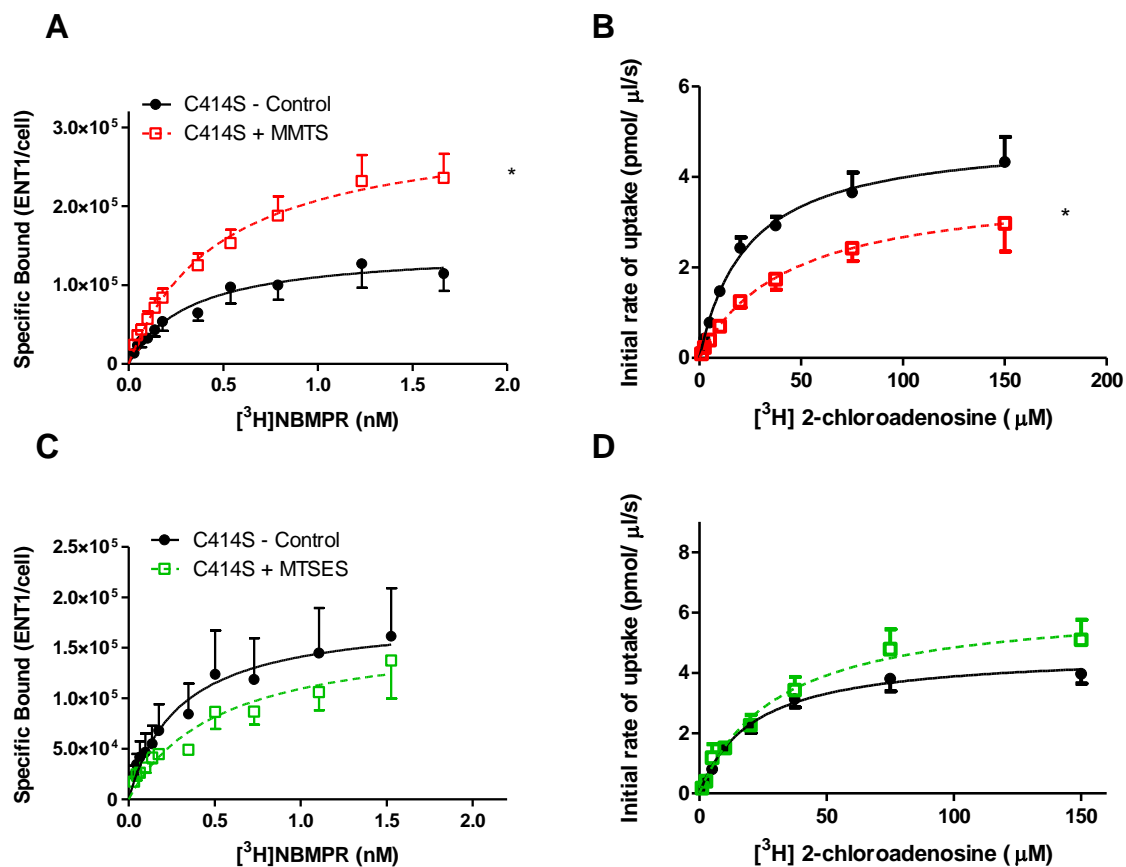


Figure 4.39. Treatment of C414S with MMTS and MTSES. Effects of MMTS (Panel A and B) and MTSES (Panel C and D) on $[^3\text{H}]$ NBMPR binding and on $[^3\text{H}]$ 2-chloroadenosine uptake of hENT1-C414S expressed in PK15-NTD cells. For Panel A and C, cells were incubated with either 1 mM MMTS (Panel A), or 5 mM MTSES (Panel C) for 10 min, washed extensively, and then incubated with a range of concentrations of $[^3\text{H}]$ NBMPR in the presence and absence of 10 μM NBTGR to define total and nonspecific binding. For Panel B and D, cells were incubated with either 1 mM MMTS (Panel B) or 5 mM MTSES (Panel D) for 10 min, washed extensively, and then incubated with a range of concentrations of $[^3\text{H}]$ 2-chloroadenosine for 5 s in the presence (Non-mediated) or absence (Total uptake) of 5 μM dipyridamole/NBTGR. Each point represents the mean \pm SEM of the cellular accumulation of $[^3\text{H}]$ 2-chloroadenosine from at least four independent experiments conducted in duplicate. * Significant difference from control B_{max} for NBMPR binding studies and control V_{max} for uptake studies (Student's t test for paired samples, $P < 0.05$)

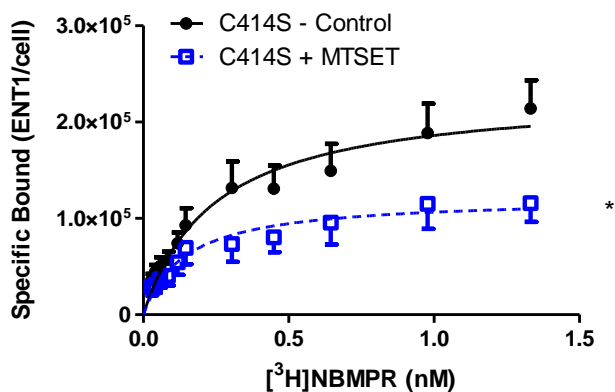


Figure 4.40. Treatment of C414S with MTSET: enhanced inhibition of NBMPR binding. Effects of MTSET on [³H]NBMPR binding by hENT1-C414S expressed in PK15-NTD cells. Cells were incubated with 5 mM MTSET (blue squares) or 0.5% DMSO (black circles) for 10 min, washed extensively, and then incubated with a range of concentrations of [³H]NBMPR in the presence and absence of 10 μM NBTGR to define total and nonspecific binding. Specific binding was calculated as the difference between the total and nonspecific binding components. Each point represents the mean ± SEM from at least 5 experiments done in duplicate. * Significant difference from control B_{max} (Student's t test for paired samples, *P* < 0.05).

conformational change allowing greater access to the MTSET-sensitive cysteine to cause inhibition of [³H]NBMPR.

4.5.8.2 Mutation of C378 and C414 to serines:

The significant decrease seen in [³H]NBMPR B_{\max} by $50 \pm 9\%$ from MTSET treatment on C414S mutant (Figure 4.40) indicated the presence of a second cysteine residue being modified. Given that removal of C378 eliminated MTSET sensitivity (Figure 4.37A) and is predicted to lie extracellularly (Figure 2.1), we proposed that C378 was the cysteine being accessed for hydrophilic thiol modification. To test this idea, a double mutant, C378S - C414S was created on the wild-type hENT1 template and its activity and sensitivity to MTS reagents determined. Double mutant hENT1-C378S-414S expressing cells bound [³H]NBMPR with a K_d of 0.22 ± 0.03 nM to a B_{\max} of $4.6 \pm 0.6 \times 10^{-5}$ ENT1 sites/cell (Figure 4.41A, Table 4.2). hENT1-C378S-414S transported [³H]2-chloroadenosine at a V_{\max} and K_m of 21 ± 5 pmol/ μ l/s and 87 ± 18 μ M (Figure 4.41B, Table 4.2), respectively providing a V_{\max}/B_{\max} ratio of $4.5 \pm 1.1 \times 10^{-5}$ pmol/ENT1/s.

4.5.8.2.1 C378-414S MTS treatments:

After treatment with MMTS, [³H]NBMPR B_{\max} increased by $65 \pm 15\%$ and [³H]2-chloroadenosine V_{\max} showed a drastic decrease of $69 \pm 8\%$ (Figure 4.42A, 4.42B). However, treatment with MTSET had no effect on either [³H]NBMPR binding or [³H]2-chloroadenosine uptake (Figure 4.43A, 4.43B) emphasizing the role of C378 in MTSET actions on wild-type hENT1. MTSES treatment also had no effect on [³H]NBMPR binding or [³H]2-chloroadenosine uptake (Figure 4.42C, 4.42D).

4.5.9 Mutation of C416 and C439 to serines and alanines:

Cells stably transfected with the C416S and C439S mutant constructs did not produce measurable level of hENT1 protein function, as determined by lack of 2-chloroadenosine uptake, NBMPR binding and immunoblotting, even though mRNA for the mutant hENT1 was clearly identified in these cells. The next approach in identifying the importance of

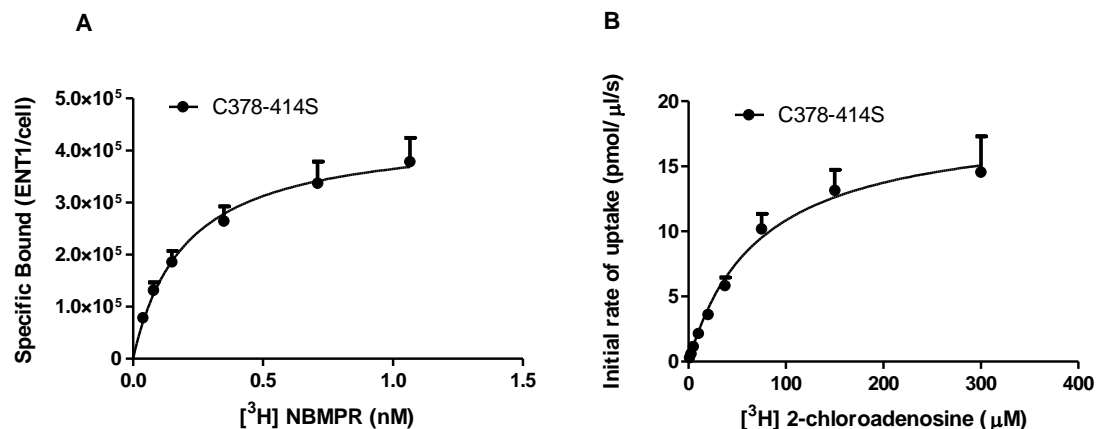


Figure 4.41. Characterization of PK15-C378-C414S. [³H]NBMPR binding (**Panel A**) and [³H]2-chloroadenosine uptake (**Panel B**) of PK15-C378-414S cells. Cells were incubated with a range of concentrations of [³H]NBMPR (abscissa) in the presence (nonspecific binding) and absence of 10 μM NBTGR (total binding). Specific binding was determined by total bound minus non-specific bound. Each point represents the mean ± SEM from at least four experiments done in duplicate. **Panel B** shows the [³H]2-chloroadenosine uptake of PK15-C378-414S cells that were incubated with a range of concentrations of [³H]2-chloroadenosine for 5 s in the presence (Non-mediated) or absence (Total uptake) of 5 μM dipyridamole/NBTGR. Transporter-mediated uptake (Mediated) was calculated as the difference between the total and non-mediated uptake components. Each point represents the mean ± SEM of the cellular accumulation of [³H]2-chloroadenosine from at least four independent experiments conducted in duplicate.

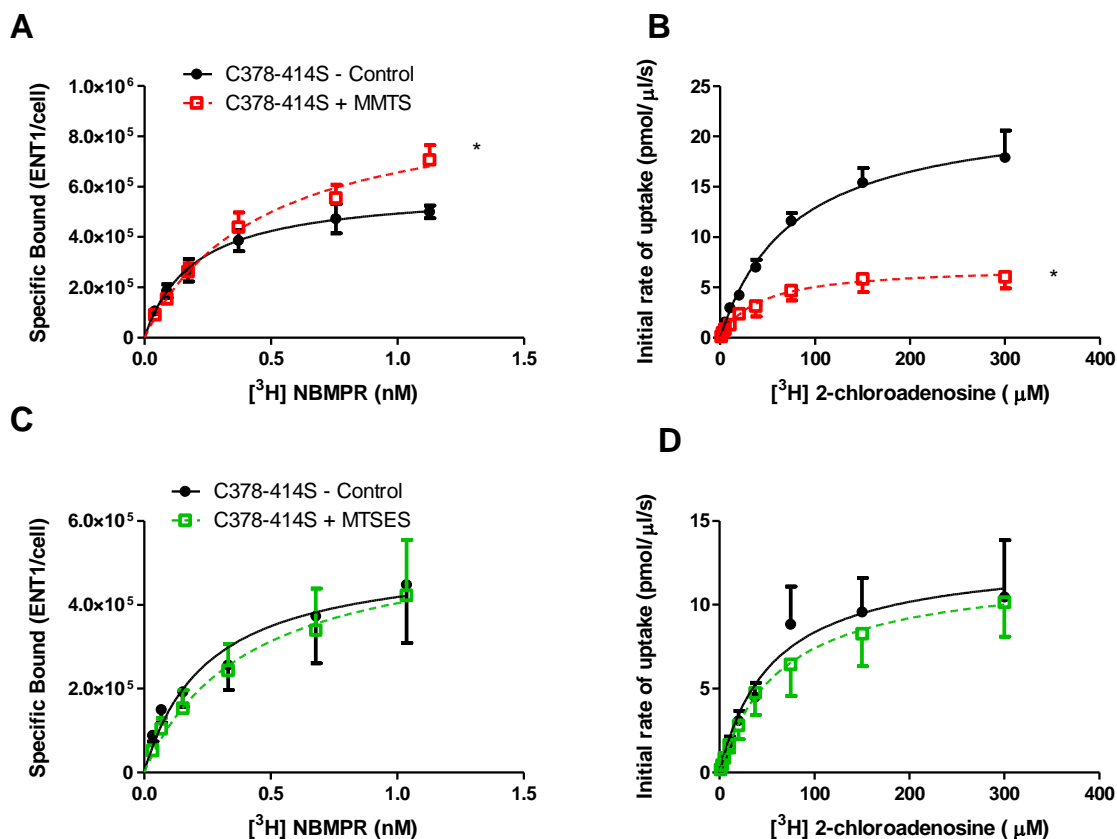


Figure 4.42. Treatment of C378-414S with MMTS and MTSES. Effects of MMTS (**Panel A and B**) and MTSES (**Panel C and D**) on [³H]NBMPR binding and on [³H]2-chloroadenosine uptake of hENT1-C378-414S expressed in PK15-NTD cells. For **Panel A and C**, cells were incubated with either 1 mM MMTS (**Panel A**), or 5 mM MTSES (**Panel C**) for 10 min, washed extensively, and then incubated with a range of concentrations of [³H]NBMPR in the presence and absence of 10 μM NBTGR to define total and nonspecific binding. For **Panel B and D**, cells were incubated with either 1 mM MMTS (**Panel B**) or 5 mM MTSES (**Panel D**) for 10 min, washed extensively, and then incubated with a range of concentrations of [³H]2-chloroadenosine for 5 s in the presence (Non-mediated) or absence (Total uptake) of 5 μM dipyridamole/NBTGR. Each point represents the mean ± SEM of the cellular accumulation of [³H]2-chloroadenosine from at least four independent experiments conducted in duplicate. * Significant difference from control B_{max} for NBMPR binding studies and control V_{max} for uptake studies (Student's t test for paired samples, *P* < 0.05)

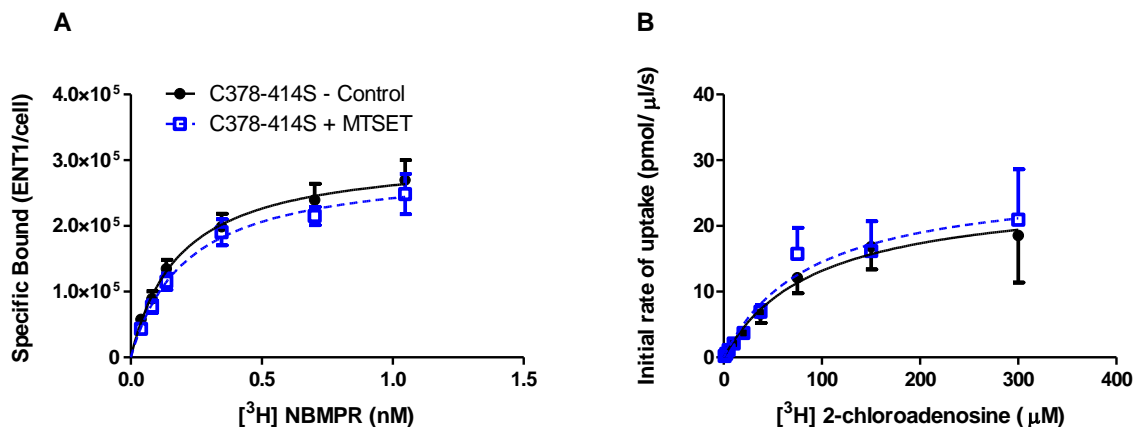


Figure 4.43. Treatment of C378-414S with MTSET: NBMPR binding to C378-414S is insensitive to MTSET. Effects of MTSET of [³H]NBMPR binding (**Panel A**) and [³H]2-chloroadenosine (**Panel B**) uptake by hENT1-C378-414S expressed in PK15-NTD cells. Cells were incubated with either 5 mM MTSET or 0.5% DMSO (Control) for 10 min, washed extensively, and then incubated with a range of concentrations of [³H]NBMPR in the presence and absence of 10 μM NBTGR to define total and nonspecific binding. Specific binding was calculated as the difference between the total and nonspecific binding components. Each point represents the mean ± SEM from at least 5 experiments done in duplicate. **Panel B** describes the concentration-dependent uptake of [³H]2-chloroadenosine of cells treated for 10 min with 5 mM MTSET or 0.5% DMSO (Control) and washed three times. Cells were incubated with a range of concentrations of [³H]2-chloroadenosine for 5 s in the presence (Non-mediated) or absence (Total uptake) of 5 μM dipyrindamole/NBTGR. Transporter-mediated uptake (Mediated) was calculated as the difference between the total and non-mediated uptake components. Each point represents the mean ± SEM of the cellular accumulation of [³H]2-chloroadenosine from at least four independent experiments conducted in duplicate.

C416 and C439 was to employ an alternate mutation to alanine (C416A, C439A); however, these mutants were also not expressed in PK15-NTD cells.

4.5.9.1 Inhibition of palmitoylation

We tested the idea that the cytoplasmically located C416 could be a target for cysteine specific palmitoylation and therefore removal of this residue may lead to improper protein targeting at the membrane and loss of transporter expression. However treatment of wild-type hENT1 cells with 100 μ M 2-Bromohexadecanoic acid (2-Br), a known blocker of palmitoylation, for 24 and 48 hrs in serum-free media lead to no changes in [3 H]NBMPR binding and [3 H]2-chloroadenosine uptake (Figure 4.44A, 4.44B). These results indicated that hENT1 expression and function is unaffected by the palmitoylation blockade by 2-Br.

4.5.9.2 Transient transfection of C416A and C439A

The two remaining cysteine mutants, PK15-C416A and PK15-C439A were analyzed through transient transfection methods. Transient transfection of empty-p3xFLAG vector showed no quantifiable binding of [3 H]NBMPR while transfection of C416A showed specific binding with a K_d of 0.1 ± 0.02 nM and B_{max} of $4.6 \pm 2.3 \times 10^5$ ENT1 sites/cell similar to wild-type (Figure 4.45A, Table 4.2). C439A bound [3 H]NBMPR with a K_d of 0.5 ± 0.1 nM and B_{max} of $8.6 \pm 1.4 \times 10^5$ ENT1 sites/cell (Figure 4.45B, Table 4.2) and transported [3 H]2-chloroadenosine with a V_{max} of 8.4 ± 0.8 pmol/ μ l/s and K_m of 165 ± 32 μ M (Figure 4.45C, Table 4.2). However, C416A showed no transport of [3 H]2-chloroadenosine (Figure 4.45C) indicating a crucial role of C416 in hENT1 function in this mammalian expression model.

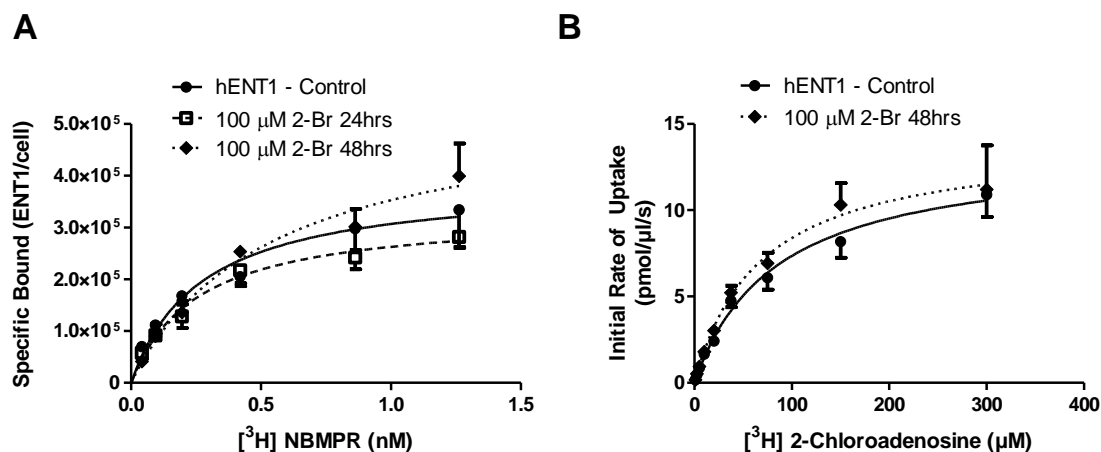


Figure 4.44. Treatment of PK15-hENT1 with 2-bromohexadecanoic acid (2-Br). Effects of 100 μM 2-Br treatment for 24 and 48 hrs on $[^3\text{H}]$ NBMPR binding (**Panel A**) and $[^3\text{H}]$ 2-chloroadenosine uptake (**Panel B**) by wild-type hENT1 expressed in PK15-NTD cells. Transfected cells were incubated and grown in serum-free media treated with 100 μM 2-Br., a palmitoylation inhibitor or Control (DMSO) for 24 or 48 hrs. Cells were harvested, washed and subjected to either $[^3\text{H}]$ NBMPR binding (Panel A) or $[^3\text{H}]$ 2-chloroadenosine uptake (Panel B) assays. Each point represents the mean \pm SEM from at least four independent experiments conducted in duplicate.

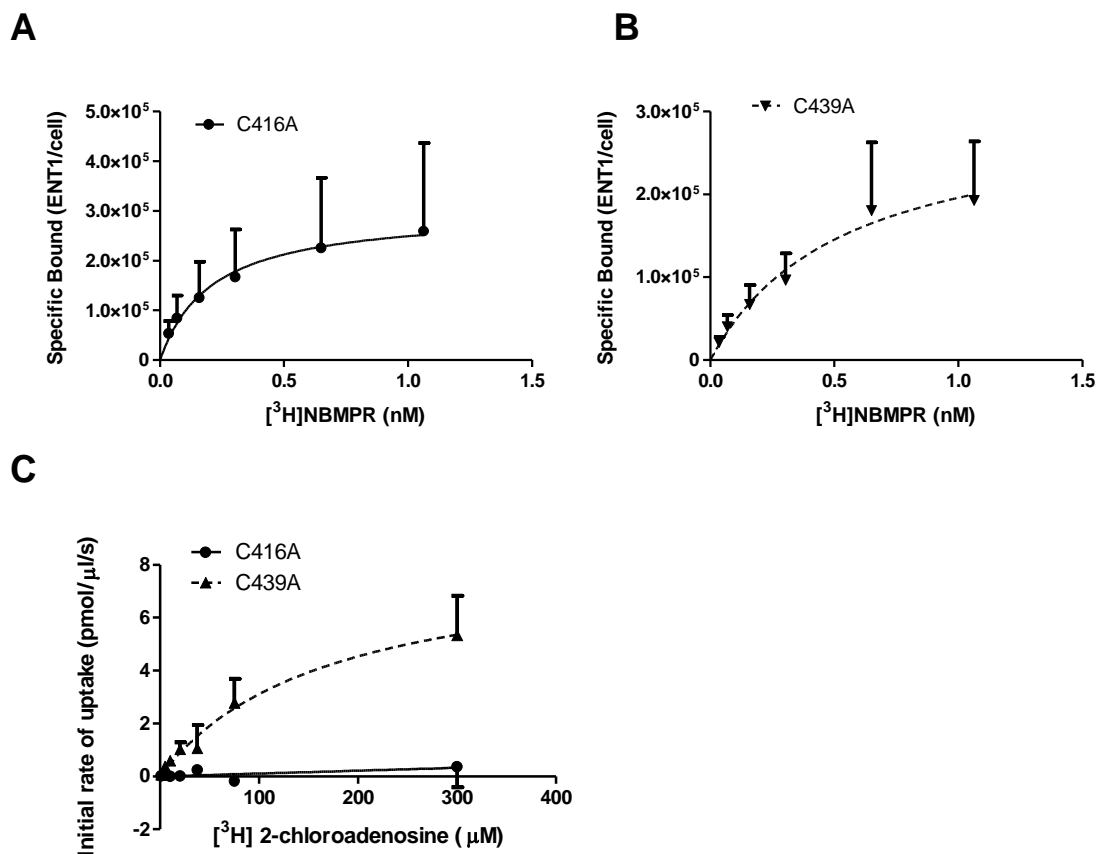


Figure 4.45. Characteristics of PK15-C416A and PK15-C439A: PK15-416A does not transport 2-chloroadenosine. $[^3\text{H}]$ NBMPR binding of PK15-C416A (**Panel A**), PK15-C439A (**Panel B**) cells and $[^3\text{H}]$ 2-chloroadenosine uptake of PK15-C416A and PK15-C439A cells (**Panel C**). Cells were incubated with a range of concentrations of $[^3\text{H}]$ NBMPR in the absence (total binding) and presence (nonspecific binding) of 10 μM NBTGR. Specific binding was calculated as the difference between the total and nonspecific binding components. Each point represents the mean \pm SEM from at least five experiments done in duplicate. **Panel C** shows the $[^3\text{H}]$ 2-chloroadenosine uptake of PK15-C416A and PK15-C439A cells that were incubated with a range of concentrations of $[^3\text{H}]$ 2-chloroadenosine for 5 s in the presence (Non-mediated) or absence (Total uptake) of 5 μM dipyridamole/NBTGR. Transporter-mediated uptake (Mediated) was calculated as the difference between the total and non-mediated uptake components. Each point represents the mean \pm SEM of the cellular accumulation of $[^3\text{H}]$ 2-chloroadenosine from at least four independent experiments conducted in duplicate.

4.5.9.3 Plasma membrane expression with biotinylation and FTH-SAENTA

Cell surface biotinylation analysis and SDS-Page Western blotting analysis were utilized to determine C416A expression at the cell membrane (Figure 4.46A). Expression of C416A-hENT1 was probed with anti-FLAG Ab, with Na⁺/K⁺-ATPase used as a plasma membrane marker. Furthermore, 79 ± 6.7% of the specific binding of NBMPR to cells expressing C416A could be inhibited by the membrane-impermeable FTH-SAENTA, indicating that the majority of the hENT1-C416A protein was processed to the plasma membrane. Similar levels of FTH-SAENTA mediated inhibition at the membrane of plasma membrane hENT1 protein was found for cells expressing the wild-type hENT1 (85 ± 1.4%) and C439A (80 ± 4.4%) (Figure 4.46B). These results indicate that mutation of C416A caused a loss in transport capability (either loss of substrate binding affinity and/or translocation function) rather than a loss of transporter expression at the plasma membrane.

4.5.9.4 Competitive inhibition of [³H]NBMPR binding by 2-chloroadenosine

To test whether the loss of transport function of C416A was due to a loss of substrate binding affinity and/or translocation mechanism, we performed inhibitor assays using 2-chloroadenosine as a competitive blocker of [³H]NBMPR binding. Given that the substrate translocation site and the NBMPR binding site are essentially overlapping, the ability of the substrate to effectively and competitively remove NBMPR from its site indicates its affinity for the transporter (essentially $K_i = K_m$). Unlabelled 2-chloroadenosine was able to inhibit the binding of [³H]NBMPR with similar affinity in both the hENT1-WT and hENT1-C416A transfectants (Figure 4.47). Given that the ability of a substrate to inhibit the binding of [³H]NBMPR generally reflects its affinity as a hENT1 substrate, this finding suggests that the loss of [³H]2-chloroadenosine transport by hENT1-C416A was not due to a decline in transporter substrate affinity. Therefore, the C416A mutant may be compromised in terms of its substrate translocation mechanism.

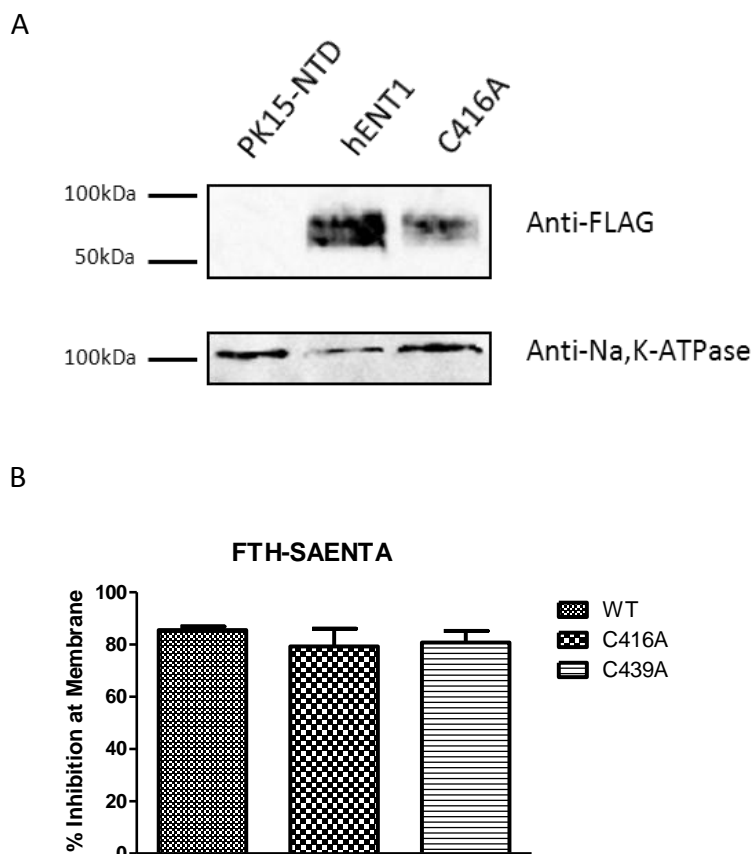


Figure 4.46. Analysis of the plasma membrane expression of PK15-hENT1 and PK15-C416A via biotinylation and FTH-SAENTA competition assays. Panel A shows the expression of C416A at the plasma membrane. Immunoblot analysis of cell surface biotinylated samples obtained from untransfected PK15-NTD cells or those transfected with hENT1 or C416A. Expression of hENT1 and C416A mutant was determined with mouse anti-FLAG antibodies (1:2,500) (Top panel). Blots were stripped and probed with anti-Na⁺, K⁺-ATPase antibody (1:2,500) (Bottom panel). **Panel B** shows the quantification of cell-surface hENT1 by competitive inhibition assay of NBMPR and FTH-SAENTA. Cells transfected with hENT1, C416A, or C439A were incubated with 5 nM [³H]NBMPR for 45 min in the absence or presence of either 100 nM FTH-SAENTA or 1 mM NBTGR. Cell surface binding was calculated from Total binding (absence of inhibitors) subtracted from the non-specific binding (1 mM NBTGR) and intracellular binding (FTH-SAENTA). Each bar represents the mean ± SEM of three independent experiments.

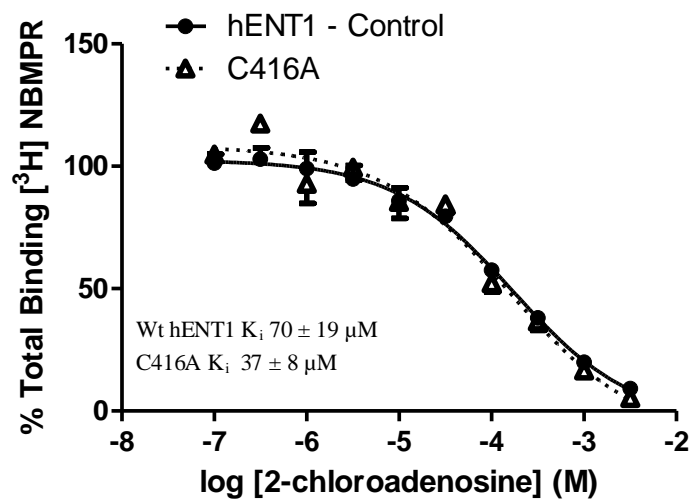


Figure 4.47. 2-chloroadenosine can effectively block NBMPR binding to C416A. Inhibition of $[^3\text{H}]$ NBMPR binding to PK15-hENT1 and PK15-C416A with a range of concentrations of 2-chloroadenosine. Data are shown as percent of control binding where control is determined as specific binding of 0.5 nM $[^3\text{H}]$ NBMPR in the absence of substrate. Each point represents the mean \pm SEM of at least three experiments done in duplicate.

4.5.9.5 C416A and C439A MTS treatments

The effects of these mutations on the sensitivity of hENT1 to MTSET and MTSES were then assessed in isolated membranes prepared from cells transiently transfected with C416A or C439A. Both cysteine mutants retained [³H]NBMPR binding activity (C416A $B_{\max} = 2.2 \pm 0.4$ pmol/mg, $K_d = 0.08 \pm 0.008$ nM; C439A $B_{\max} = 2.4 \pm 0.2$ pmol/mg, $K_d = 0.3 \pm 0.06$ nM) (Figure 4.48A, Table 4.3) similar to that seen for wild-type hENT1. MTSES and MTSET inhibited [³H]NBMPR binding to the C439A mutant, similar to that seen for the wild-type hENT1 (Figure 4.48B, 4.48C, Table 4.3). However, MTSES did not inhibit [³H]NBMPR binding in the C416A mutant (Figure 4.49, Table 4.3). Additionally, the effects of MTSET and MMTS were also diminished in the C416A mutant. These data suggest that C416 is involved in the binding of NBMPR. However, co-treatment of membranes expressing the wild-type hENT1 with MTSES and non-radiolabelled NBMPR (10 nM) or the hENT1 substrate adenosine (10 mM) did not prevent the inhibitory effects of MTSET on [³H]NBMPR binding (Figure 4.50A, 4.50B).

4.6 Summary of Cysteine Mutants

For the single cysteine mutants, neither the loss of the residue nor introduction of a serine in that position altered hENT1 ability to bind NBMPR (Table 4.2). Surprisingly, the importance of C416 was identified as a critical residue for protein expression together with C439 (TM11), given that both of these mutants showed no measurable activity or expression in our stable cell lines. Additionally, mutation of C416 to alanine caused a loss of 2-chloroadenosine transport mechanism while the ability to recognize the substrate and inhibitor NBMPR was retained. Additionally, mutation of Cys222 in TM 6 eliminated the effect of MMTS on NBMPR binding (Figure 4.24A). We therefore have addressed the first hypothesis in identifying the cysteine targeted by neutral thiol modification to cause a change in hENT1 function. MTSET inhibition of [³H]NBMPR binding is abolished in C378 (Figure 4.37A) and is even more pronounced in the C414S mutant (Figure 4.40). Given that C378 is the only cysteine predicted to lie in the extracellular space, we postulated that removal of the downstream intracellular located C414 may cause a conformational

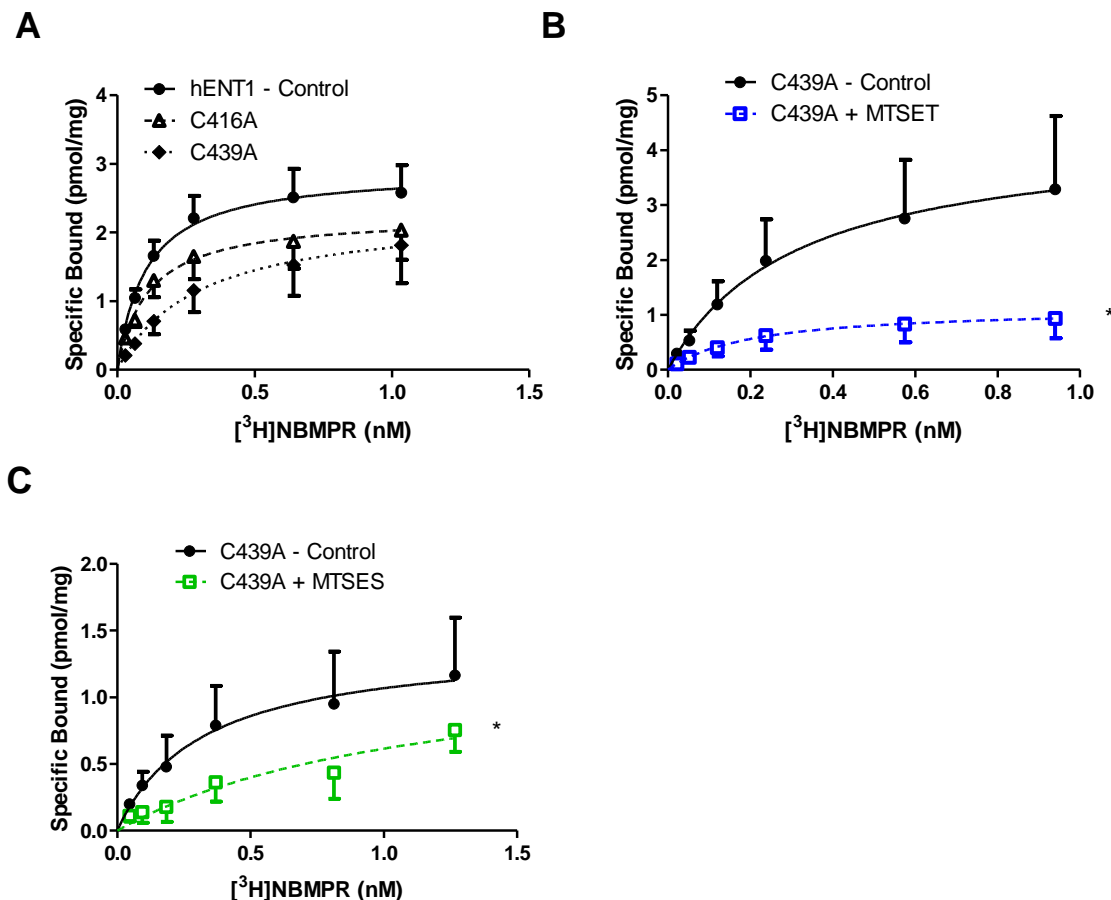


Figure 4.48. Cell membrane treatment of C439A with MTSET and MTSES. [³H]NBMPR binding by PK15-hENT1, PK15-C416A, and PK15-C439A cell membranes (**Panel A**) and the effects of MTSET (**Panel B**) and MTSES (**Panel C**) on [³H]NBMPR binding by hENT1-C439A cell membranes. Membranes were incubated with a range of concentrations of [³H]NBMPR in the absence (total binding) and presence (nonspecific binding) of 10 μ M NBTGR. Each point represents the mean \pm SEM from at least five experiments done in duplicate. For **Panel B and C**, membranes were incubated with either 5 mM MTSET (blue squares), or 5 mM MTSES (green squares) for 10 min, washed extensively, and then incubated with a range of concentrations of [³H]NBMPR in the presence and absence of 10 μ M NBTGR to define total and nonspecific binding. Each point represents the mean \pm SEM from at least 5 experiments done in duplicate. * Significant difference from control B_{max} (Student's t test for paired samples, $P < 0.05$).

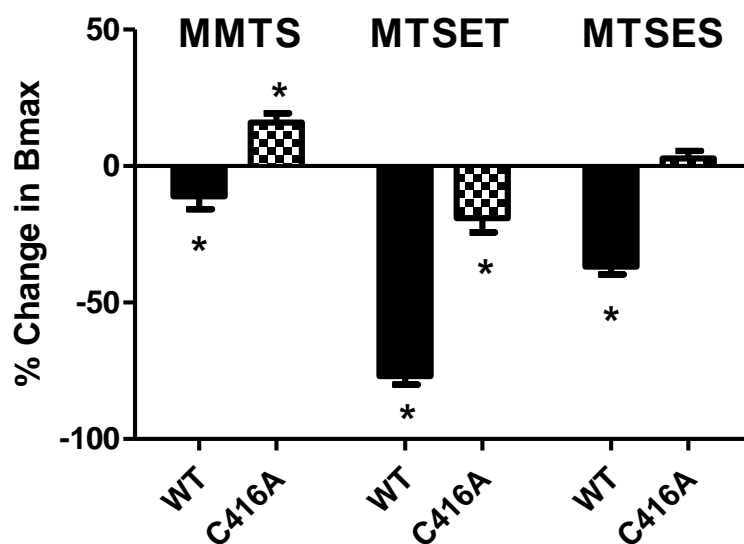


Figure 4.49. Treatment of C416A with MMTS, MTSET, MTSES: NBMPR binding to C416A is insensitive to MTS reagents. Effects of MMTS, MTSET, and MTSES on [³H]NBMPR binding by hENT1-C416A expressed in PK15-NTD cell membranes. Membranes were incubated with either 1 mM MMTS, 5 mM MTSET, or 5 mM MTSES for 10 min, washed extensively, and then incubated with a range of concentrations of [³H]NBMPR in the presence and absence of 10 μM NBTGR to define total and nonspecific binding. B_{max} were calculated from nonlinear regression analysis was used to fit hyperbolic curves to the site-specific binding of [³H]NBMPR plotted against the free [³H]NBMPR concentration at steady-state. Each bar represents the mean ± SEM from at least four experiments done in duplicate. * Significant difference from their respective untreated control B_{max} (Student's t test for paired samples, *P* < 0.05).

Table 4.3. Effects of MTS reagents on [³H]NBMPR binding (B_{max}) by cell membranes transfected with hENT1 and with C416A or C439A cysteine mutants. Membranes were prepared from cells 24 hr following transfection with the indicated hENT1 construct. The isolated membranes were then assessed for their level of site-specific [³H]NBMPR binding as described for Fig. 4.48. Values shown are the means \pm SEM from at least three independent experiments conducted in duplicate. * Significant difference from control (Student's t test for paired samples, $P < 0.05$).

		[³H]NBMPR Binding	
		B_{max} (pmol/mg)	
Cell Line	MTS Reagent	Control	Treated
hENT1-WT	MMTS	1.24 \pm 0.34	1.03 \pm 0.17
	MTSET	3.15 \pm 0.94	0.78 \pm 0.28*
	MTSES	3.19 \pm 1.51	1.92 \pm 0.85*
C416A	MMTS	1.23 \pm 0.19	1.42 \pm 0.29
	MTSET	2.73 \pm 1.17	2.30 \pm 1.14
	MTSES	2.33 \pm 0.97	2.34 \pm 0.97
C439A	MMTS	0.99 \pm 0.23	0.78 \pm 0.08
	MTSET	4.29 \pm 1.78	1.13 \pm 0.42*
	MTSES	1.57 \pm 0.61	0.71 \pm 0.25*

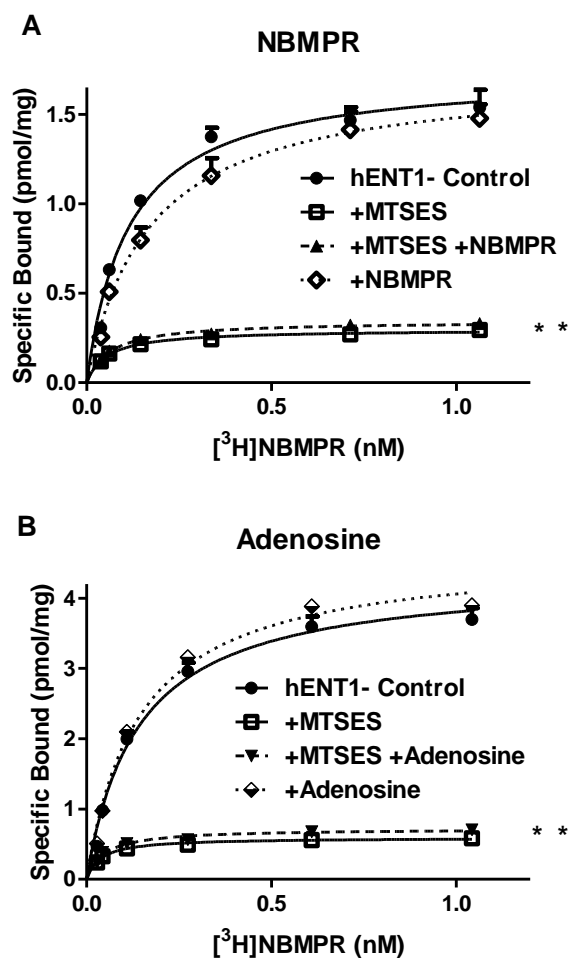


Figure 4.50. NBMPR and adenosine are unable to protect against MTSES effects in membranes. Crude membranes isolated from PK15-NTD cells transfected with hENT1 were incubated for 10 min at room temperature with 0.5% DMSO (control), 10 nM NBMPR (**Panel A**) or 1 mM adenosine (**Panel B**), 5 mM MTSES, or the combination of 10 nM NBMPR and 5 mM MTSES or 1 mM adenosine and 5 mM MTSES. After extensive washing to remove NBMPR/adenosine and unreacted MTSES, membranes were exposed to a range of concentrations of [³H]NBMPR in the presence and absence of 10 μ M NBTGR to define the site-specific binding. Each point is the mean \pm SEM from at least four experiments conducted in duplicate. * Significant difference from control B_{\max} (Student's t test for paired samples, $P < 0.05$).

change in the protein to increase accessibility to C378. Therefore, we performed a double mutation of C378S and C414S and tested MTSET inhibition of NBMPR binding. Removal of C378 in addition to C414 eliminated the [³H]NBMPR binding inhibition seen in both wild-type and C414S mutant (Figure 4.43A). This provided more evidence that C378 was the extracellularly located residue interacting with MTSET to inhibit binding. Additionally, this result suggested a structural cooperation between the two residues in two different domains (TM9 and intracellular loop 5) in forming the NBMPR binding pocket. Lastly, in cell membrane preparations, mutation of C416 to serine abolished the inhibitory effects of MTSES on NBMPR binding seen in wildtype hENT1 (Figure 4.49). This identified C416 as the intracellular residue responsible for negatively charged thiol modification indirectly involved in the NBMPR binding structure and supported the second hypothesis of this study. Given that neither 10 nM NBMPR nor 10 mM adenosine were able to protect against MTSES effects (Figure 4.50A, 4.50B), we infer that C416 does not directly interact with the ligand but may induce an indirect conformational change in structure.

4.7 SCAM analysis of Extracellular loop 5

The preceding data in section 4.5 revealed a role for the C-terminus of hENT1 in NBMPR binding and substrate uptake. These data suggest a functional interaction between C378 (TM9) and C414 (IL5), C416 as a critical amino acid involved in hENT1 functionality also located in IL5, and C378 as the target residue for MTSET inhibition of NBMPR binding. Therefore, it is of interest to determine how this C-terminal region of hENT1 interacts functionally and structurally with the TM3-6 region that has been defined previously as the part of hENT1 critical to transporter function and ligand binding [134]. As thus, or third hypothesis in Chapter 2 was that residues in extracellular loop 5 are involved in the extracellular binding pocket of hENT1. To determine their roles in hENT1 functionality, we used the MTSET-insensitive C378S mutant transporter as the background template, and the 16 residues of EL5 sequentially replaced with cysteines and then tested for their ability to bind NBMPR and transport 2-chloroadenosine in transiently transfected PK15

cells. Each mutant was also assessed for MTSET accessibility to determine whether they could be located for thiol modification.

4.7.1 Assessment of [³H]NBMPR binding for EL5 mutants

The 16 EL5-cysteine mutants were individually assessed for their ability to bind NBMPR in whole cells. Figure 4.51A showing [³H]NBMPR binding to PK15-N379C in cells is a representation of the nature of the analysis performed on the other 15 EL5 mutants. All of the 16 mutants were able to bind NBMPR with high affinity (Figure 4.51B) indicating that neither loss of these residues nor the introduction of cysteine at that position abrogated the NBMPR binding site in a critical manner.

4.7.2 Assessment of [³H]2-chloroadenosine uptake for EL5 mutants

The 16 EL5-cysteine mutants were also individually assessed for their ability to transport [³H]2-chloroadenosine. Figure 4.52A showing [³H]2-chloroadenosine uptake of PK15-I380C into cells is a representation of the nature of the analysis performed on the other 15 EL5 mutants. Our results indicate that eleven of the EL5-cysteine mutants were able to transport [³H]2-chloroadenosine however, N379C, F390C, E391C, H392C, and D393C showed no measurable uptake of [³H]2-chloroadenosine (Figure 4.52B).

4.7.2.1 Expression of N379C, F390C, E391C, H392C, and D393C at the membrane

To determine whether the loss of function from the five EL5-cysteine mutants was due to a loss of expression at the plasma membrane, we performed FTH-SAENTA inhibition assays. Extracellular binding sites for NBMPR were calculated from transfected cells incubated with and without FTH-SAENTA which is membrane impermeable and hence will block the binding of NBMPR at extracellular sites. N379C, F390C, E391C, H392C, and D393C all showed high levels of hENT1 expression at the plasma membrane at approximately the same levels as seen with wild-type hENT1 (Figure 4.53).

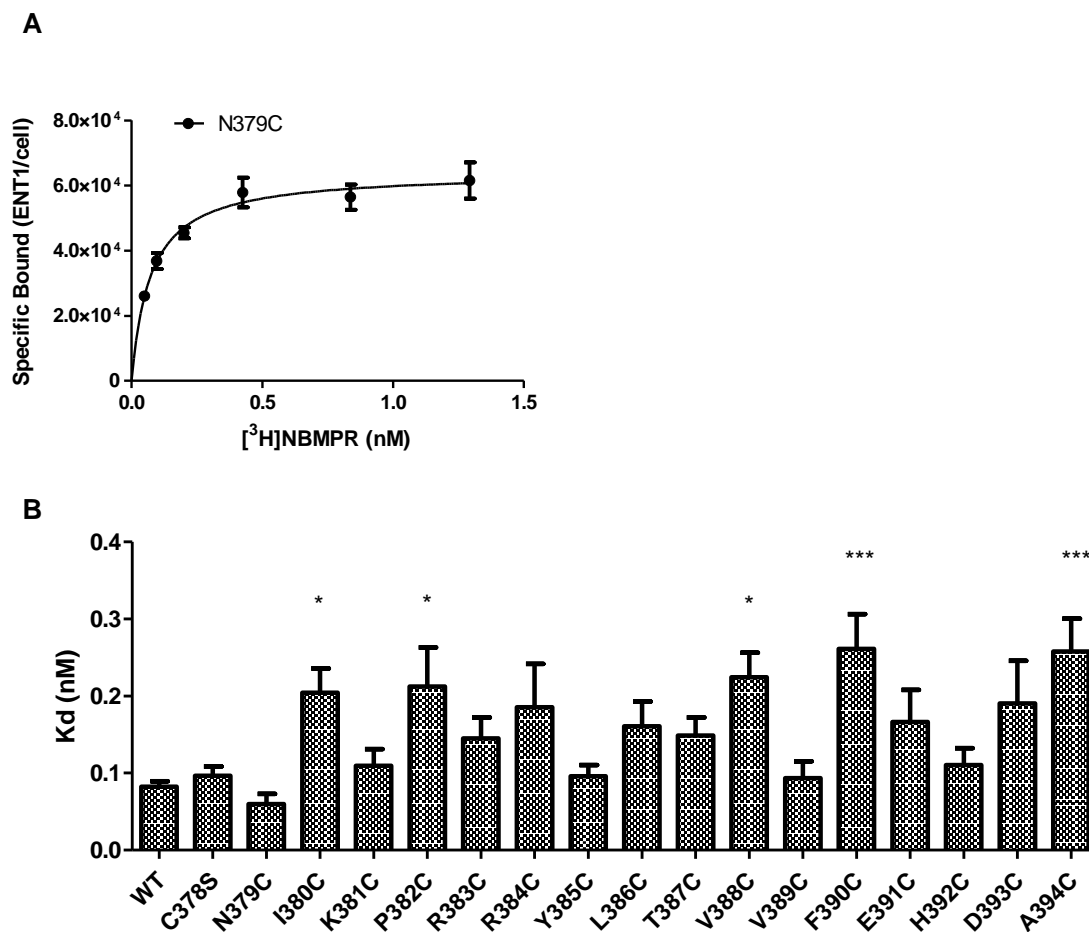


Figure 4.51. EL5 mutants bind NBMPR with high affinities. Binding affinities of $[^3\text{H}]$ NBMPR to wild-type hENT1, hENT1-C378S, and hENT1-extracellular loop 5 cysteine mutants. Binding affinities were determined from nonlinear regression analysis used to fit hyperbolic curves to the site-specific binding of $[^3\text{H}]$ NBMPR plotted against the free $[^3\text{H}]$ NBMPR concentration at steady-state (example of the analysis shown in **Panel A**). **Panel B** depicts the binding affinities (K_d) shown in nM; solid bars represent the mean \pm SEM from at least six experiments done in duplicate. * Indicates a significant difference from WT affinity ($P < 0.05$ one-way ANOVA : Dunnett's post-test) *** Indicates a significant difference from WT affinity ($P < 0.001$ one way ANOVA: Dunnett's post-test)

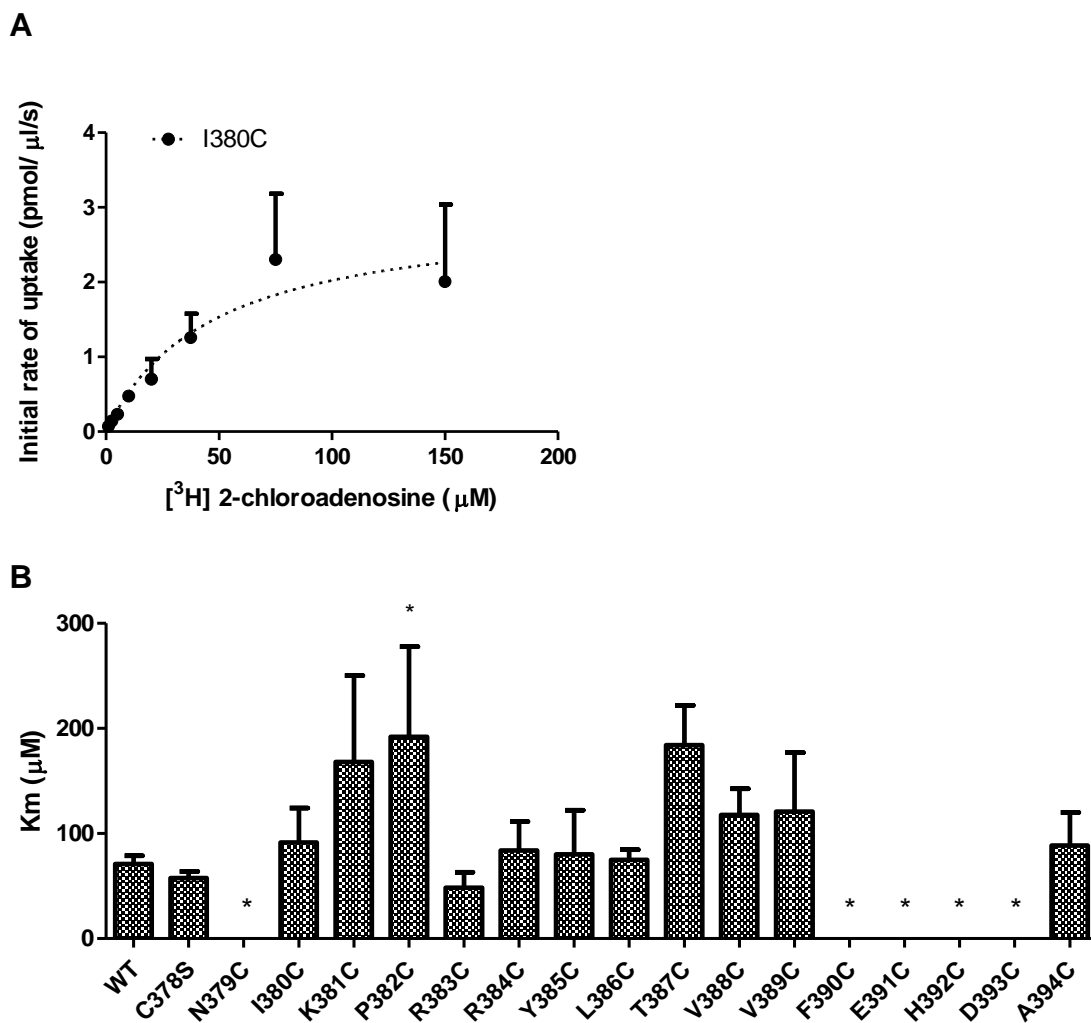


Figure 4.52. N379C, F390C, E391C, H392C, and D393C show no measurable uptake of $[^3\text{H}]$ 2-chloroadenosine. Transport affinities of $[^3\text{H}]$ 2-chloroadenosine to wild-type hENT1, hENT1-C378S, and hENT1-extracellular loop 5 cysteine mutants. Transport affinities were determined from non-linear regression analysis of Michaelis-Menten fitted uptake, calculated as the difference between the total and non-mediated uptake components (example of the analysis shown in **Panel A**). **Panel B** depicts the substrate affinity shown in μM ; solid bars represents the mean \pm SEM from at least three experiments done in duplicate. * Indicates a significant difference from WT affinity ($P < 0.05$ one-way ANOVA : Dunnett's post-test) where five EL5 mutants showed no transport of $[^3\text{H}]$ 2-chloroadenosine.

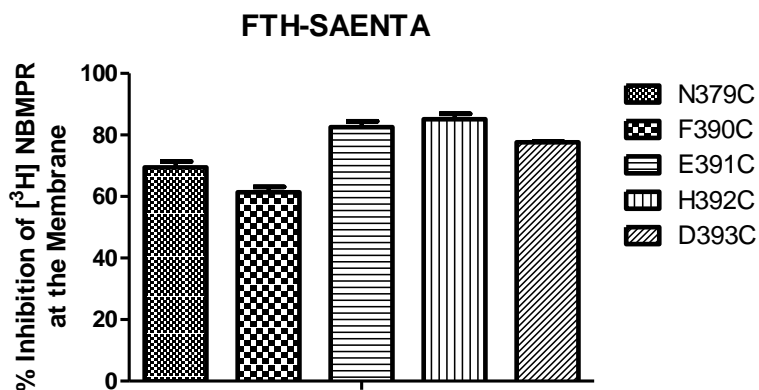


Figure 4.53. Quantification of cell-surface hENT1 by competitive inhibition assay of NBMPR and FTH-SAENTA of N379C, F390C, E391C, H392C, or D393C. Cells transfected with N379C, F390C, E391C, H392C, or D393C were incubated with 5 nM [³H]NBMPR for 45 min in the absence or presence of either 100 nM FTH-SAENTA or 1 mM NBTGR. Cell surface binding was calculated from Total binding (absence of inhibitors) subtracted from the non-specific binding (1 mM NBTGR) and intracellular binding (FTH-SAENTA). Each bar represents the mean \pm SEM of three independent experiments.

4.7.2.2 Competitive inhibition with 2-chloroadenosine

To determine whether the loss of [³H]2-chloroadenosine transport was due to a loss of transport mechanism or a loss of substrate affinity for the transporter, we performed competitive inhibition assays using non-labeled 2-chloroadenosine as our competitive inhibitor. 2-chloroadenosine was able to inhibit the binding of [³H]NBMPR with similar affinity to the N379C, F390C, E391C, H392C, and D393C mutants (Figure 4.54). This suggests that the loss of [³H]2-chloroadenosine transport by these five mutants was not due to a loss of substrate recognition of the transporter but rather to the disruption of the translocation mechanism.

4.7.3 Effects of MTSET on extracellular loop five mutants

To determine if amino acids in EL5 when mutated to cysteine were sensitive to MTSET modification, PK15-EL5 mutants were treated with 5 mM MTSET and tested for [³H]NBMPR binding as depicted in Figure 4.55A using the N379C mutant as an example of how the analyses were performed. Treatment of MTSET caused an inhibition of NBMPR binding in all EL5-cysteine mutants except for V389C. Inhibition of binding ranged from 10-50% decreases in B_{max} (Figure 4.55B).

4.7.3.1 Protection against the effects of MTSET on extracellular loop five mutants with NBMPR

To determine whether residues in EL5 that were sensitive to MTSET could be protected from thiol modification, cells were co-incubated with NBMPR and MTSET. Figure 4.56A showing [³H]NBMPR binding to PK15-I380C after co-incubation with NBMPR and MTSET is a representation of the protection experiments performed on the rest of the EL5 mutants. Our results indicated that co-incubation with NBMPR blocked MTSET inhibitory effects on N379C (Figure 4.56B). This indicated that NBMPR may have direct contact or be in very close vicinity with N379C where its binding can block MTSET modification.

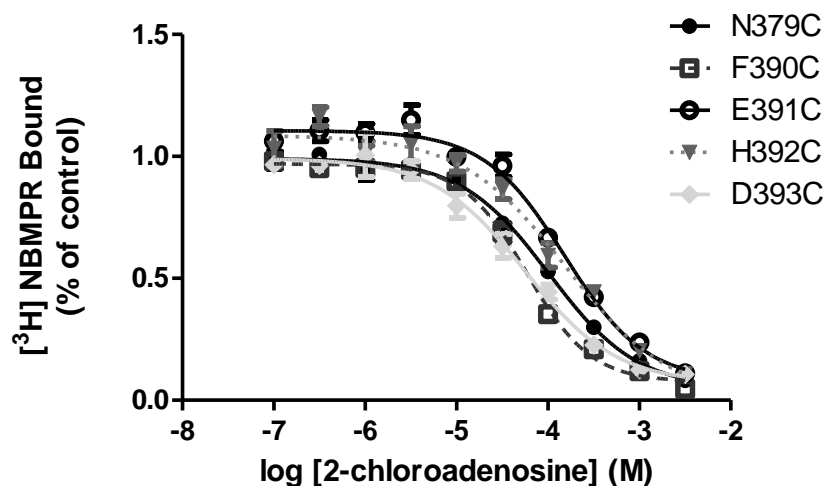


Figure 4.54. 2-chloroadenosine can effectively block NBMPR binding to N379C, F390C, E391C, H392C, or D393C. Inhibition of $[^3\text{H}]$ NBMPR binding to PK15-N379C, PK15-F390C, PK15-E391C, PK15-H392C, and PK15-D393C with a range of concentrations of 2-chloroadenosine. Data are shown as percent of control binding where control is determined as specific binding of 0.5 nM $[^3\text{H}]$ NBMPR in the absence of substrate. Each point represents the mean \pm SEM of at least three experiments done in duplicate.

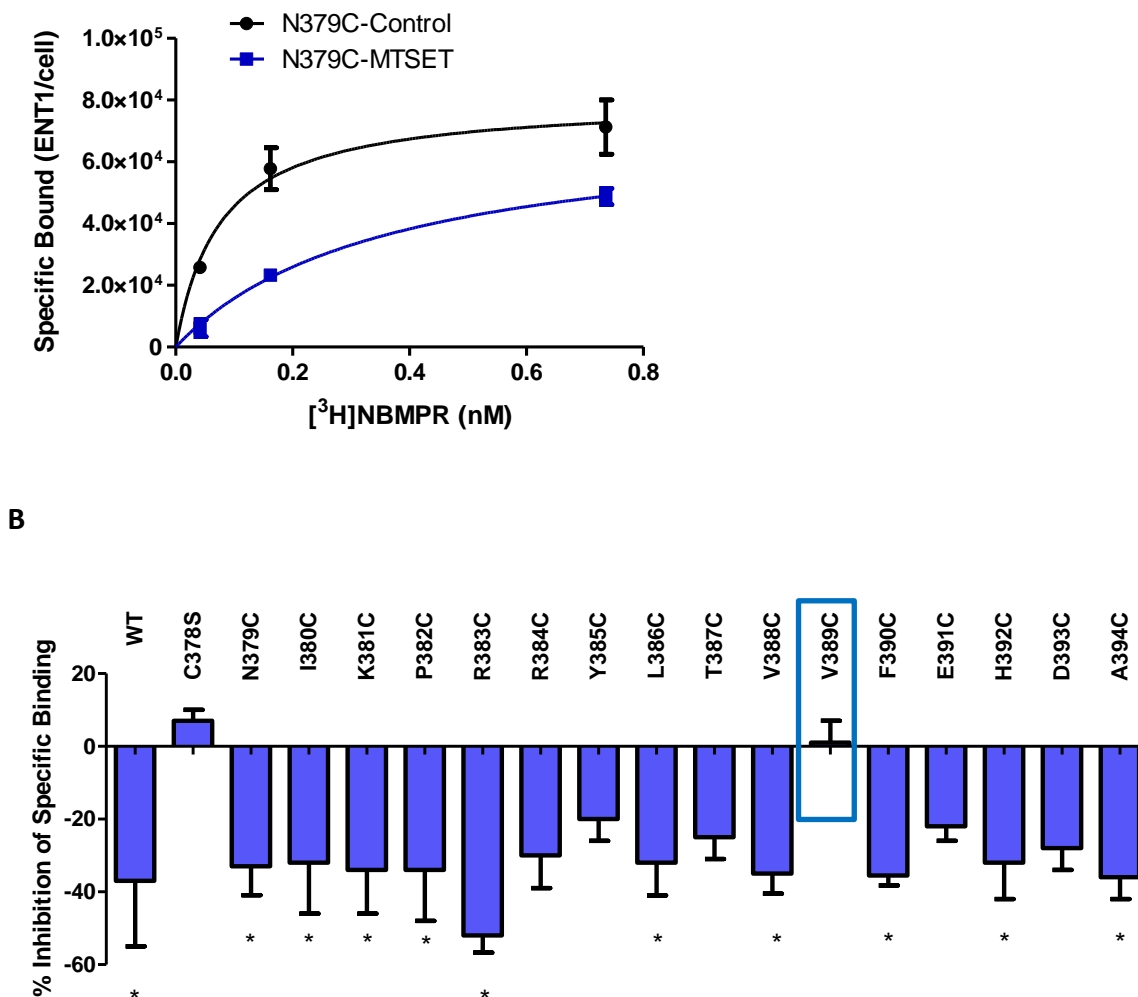
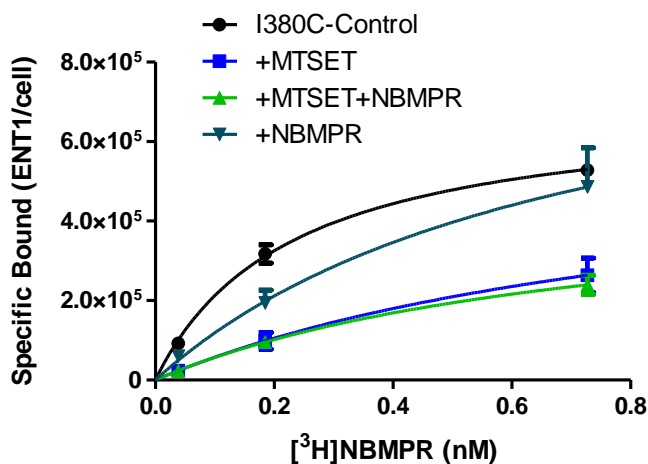


Figure 4.55. NBMPR binding of all EL5 mutants except V389C are sensitive to MTSET. Effects of MTSET on $[^3\text{H}]$ NBMPR binding by hENT1-mutants expressed in PK15-NTD cells. Cells were treated with 5 mM MTSET for 10 min, washed extensively, and then assessed for $[^3\text{H}]$ NBMPR as mentioned in methods. B_{max} were calculated from nonlinear regression analysis was used to fit hyperbolic curves to the site-specific binding of $[^3\text{H}]$ NBMPR plotted against the free $[^3\text{H}]$ NBMPR concentration at steady-state as depicted in **Panel A**. **Panel B** depicts the inhibition of specific binding of $[^3\text{H}]$ NBMPR to PK15-hENT1 and EL5 mutants calculated from their respective controls (DMSO treated); solid bars represents the mean \pm SEM from at least three experiments done in duplicate. The blue box indicates the residue insensitive to MTSET inhibition of NBMPR binding. * Significant difference from each mutants respective control B_{max} (Student's t test for paired samples, $P < 0.05$).

A



B

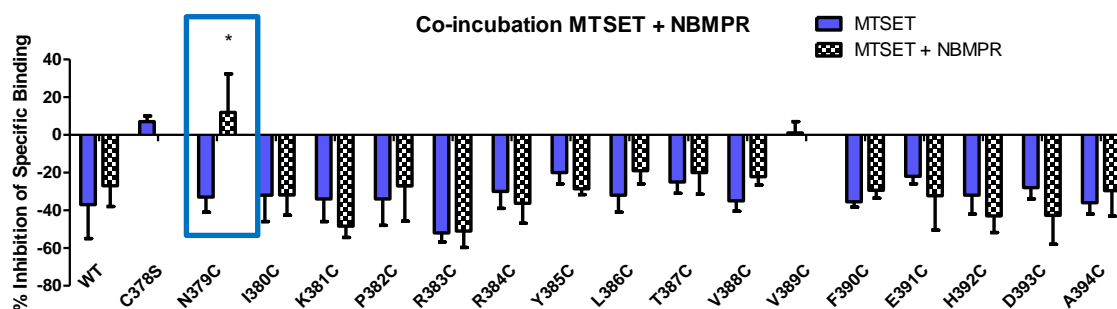


Figure 4.56. NBMPR is able to protect N379C against MTSET effects in cells. Co-incubation of MTSET with 10 nM NBMPR. PK15-hENT1 cells transfected with wild-type hENT1 or cysteine mutants were incubated for 10 min at room temperature with 0.5% DMSO (control), 10 nM NBMPR (+NBMPR), 5 mM MTSET (+MTSET) or the combination of 5 mM MTSET+ 10 nM NBMPR. After extensive washing to remove NBMPR and unreacted MTSET, cells were exposed to a range of concentrations of [³H]NBMPR in the presence and absence of 10 μM NBTGR to define the site-specific binding as shown in **Panel A** for the I380C mutant. **Panel B** depicts the inhibition of specific binding of [³H]NBMPR to PK15-hENT1 and EL5 mutants calculated from their respective controls (DMSO treated); solid bars represents the mean ± SEM from at least three experiments done in duplicate. Blue box indicated where NBMPR was able to protect against MTSET effects. * Significant difference from MTSET treated inhibition of NBMPR binding B_{max} (Student's t test for paired samples, $P < 0.05$).

4.7.3.2 Protection against the effects of MTSET on extracellular loop five mutants with adenosine

To determine if modified cysteines in EL5 could also become protected by a substrate, cells were co-incubated with adenosine and MTSET and then tested for changes in [³H]NBMPR binding. Figure 4.57A showing [³H]NBMPR binding to PK15-N379C after co-incubation with adenosine and MTSET is a representation of the protection experiments performed on the rest of the EL5 mutants. In this manner, the separate binding determinants could be distinguished for substrates and inhibitors. Co-incubation of adenosine blocked MTSET inhibitory effects on R384C, Y385C, L386C (Figure 4.57B). These residues are predicted to be in the middle of the extracellular loop and could therefore have direct contact with adenosine to prevent that large positively charged reagent to react.

4.8 Summary of EL5 mutants

For the 16 individual cysteine mutations in EL5, all 16 mutants retained the ability to bind NBMPR with high affinity. This indicated that none of the amino acids in EL5 are critical for NBMPR to bind. However, five of the 16 mutants lost the ability to transport 2-chloroadenosine (N379C, F390C, E391C, H392C, and D393C). This loss of transport was attributed to a complication in the transport mechanism as the mutant transporters were expressed at the membrane and retained the ability of 2-chloroadenosine to inhibit NBMPR binding. Finally, it was found that all residues except for V389C were sensitive to MTSET inhibition of binding indicating that modification at those sites impacted NBMPR binding. NBMPR co-incubation protected N379C indicating that it may be in close proximate location to the inhibitor recognition site. Additionally, adenosine co-incubation protected R384C, Y385C, and L386C indicating their possible involvement in adenosine interactions with the transporter.

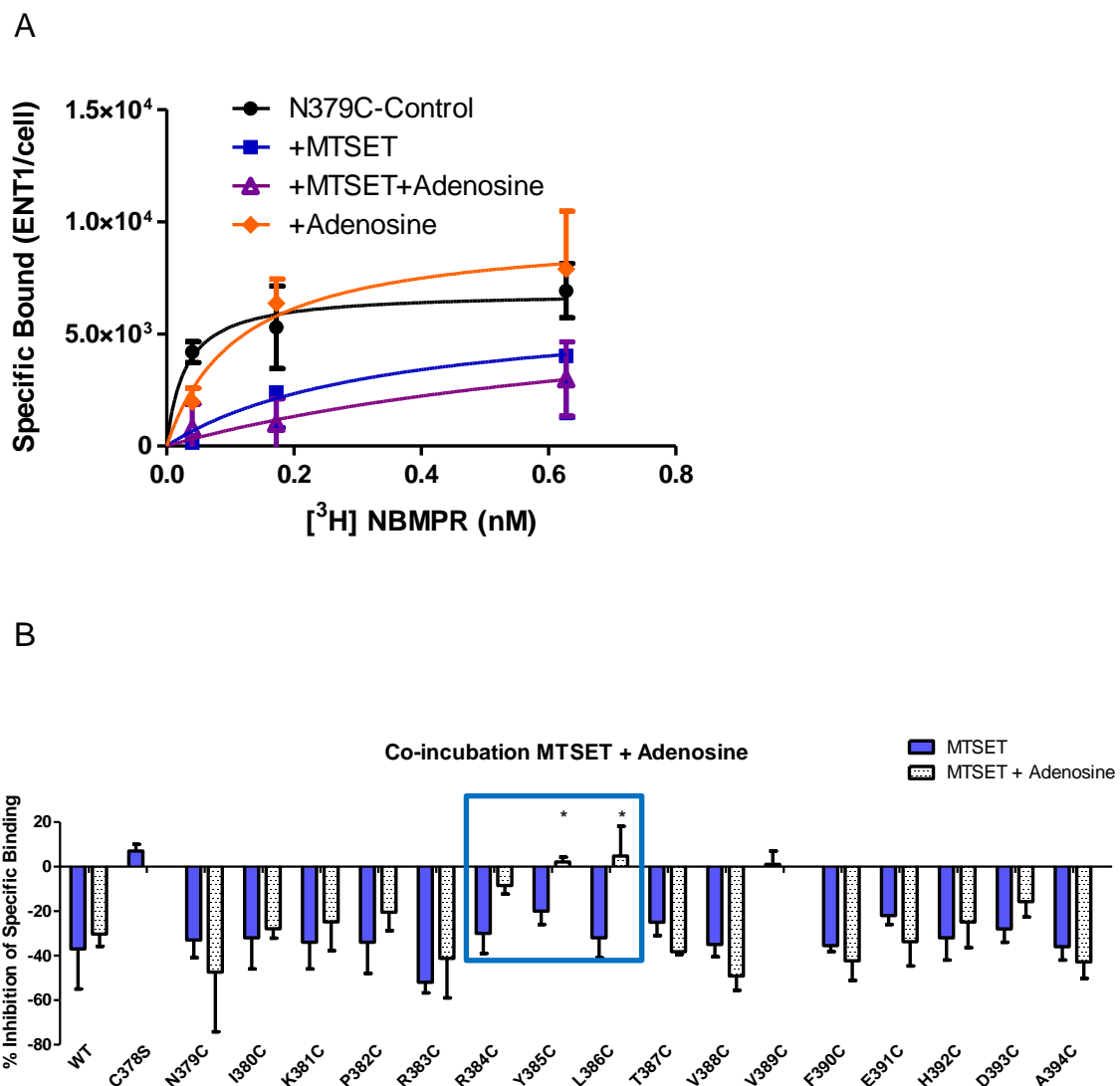


Figure 4.57. Adenosine protects R384C, Y385C, and L386C against MTSET effects in cells. Co-incubation of MTSET with 1 mM adenosine. PK15-hENT1 cells transfected with wild-type hENT1 or cysteine mutants were incubated for 10 min at room temperature with 0.5% DMSO (control), 1 mM adenosine, 5 mM MTSET, or the combination of 5 mM MTSET + 1 mM adenosine. After extensive washing to remove adenosine and un-reacted MTSET, cells were exposed to a range of concentrations of $[^3\text{H}]$ NBMPR in the presence and absence of 10 μM NBTGR to define the site-specific binding as depicted in **Panel A** with the N379C mutant. **Panel B** depicts the inhibition of specific binding of $[^3\text{H}]$ NBMPR to PK15-hENT1 and EL5 mutants calculated from their respective controls (DMSO treated); solid bars represents the mean \pm SEM from at least three experiments done in duplicate. Blue box indicated where adenosine was able to protect against MTSET effects. * Significant difference from MTSET treated inhibition of NBMPR binding B_{max} (Student's t test for paired samples, $P < 0.05$).

Chapter 5: Discussion

In mammalian cells, nucleoside and nucleoside analogue transport processes are mediated through two major protein families termed CNTs and ENTs [42, 51]. A major contributor to these transport processes is the hENT1 subtype which is selectively inhibited by NBMPR at nanomolar concentrations and by coronary vasodilators with high affinities [114-117]. Functionally, TM 3 to 6 have been observed to be necessary for inhibitor binding [134, 135]. This region of TM3-6 is also predicted to be the site where substrates are recognized for transport. Results from human and rat chimeric studies where mutants missing TM3-6 were unable to bind NBMPR or transport uridine. In this manner, the NBMPR binding site and the substrate translocation pathway are suggested to overlap since NBMPR is able to competitively inhibit substrate transport [86, 133, 136]. Conversely, increasing concentrations of substrates competitively inhibit NBMPR binding to hENT1. This indicates that the functional substrate binding site of hENT1 and the site to which NBMPR binds are within the same region.

The coronary vasodilators, which act as ENT1 inhibitors, were also found to inhibit both NBMPR binding and nucleoside transport in a competitive manner and the region of TM3-6 is again indicated in their sensitivities [82, 179, 186]. However, mutagenesis studies on hENT1 involving TM1 and TM11 (outside of the TM3-6 domains) have indicated the possibility that these TM domains are relatively proximal to each other [100, 187]. Mutagenesis of Leu442 in TM11 altered sensitivities to NBMPR and dipyridamole when Met33 in TM1 was first mutated to isoleucine. This suggested that regions outside of TM3-6 also play essential structural and functional roles for hENT1. However, information on how hENT1 folds into the membrane as well as the important functional features of hENT1 is still unknown. Understanding how the TM domains and loops are arranged will allow for the development of effective isoform-specific inhibitors and generation of selective cytotoxic nucleoside analogues targeted for hENT1. The current inhibitors of nucleoside transport, except for NBMPR, are not selective for the ENT1 subtype and may inhibit several subfamilies of nucleoside transporters, which may

not be favorable for targeted therapies. The same is true for the cytotoxic nucleoside analogues, as they are able to use multiple families of nucleoside transporters to produce their effects which could be unfavorable for host cell preservation [188]. Therefore, the physiological and pharmacological properties of these agents are dependent on their specificity and selectivity to nucleoside transporters. Due to the unavailability of 3-D crystal structures of hENT1, structure function studies on hENT1 rely heavily on mutagenesis approaches.

Prior to this thesis, it was suggested that cysteines may play an important role for ENT1 function since treatment with thiol modifying reagents such as pCMBS and NEM altered NBMPR binding and substrate translocation [157, 171, 172, 174]. However, the location and contribution of these residues remained unknown. This study explored the hENT1 permeant site by targeting cysteine residues and the region of the C-terminus to better understand the specific functional determinants involved in transporter activity. Since hENT1 is an integral membrane protein and not readily isolated for biophysical analysis, the relationships between various regions of the protein have not yet been delineated. An approach commonly used for such intransigent proteins, is cysteine scanning mutagenesis to assess the aqueous accessibility of various regions of the protein given that cysteines can be targeted for chemical modification with a wide variety of sulfhydryl modifying reagents. The use of this technique has been applied to several integral membrane proteins such as P-glycoprotein (Pgp) and glucose transporter (Glut1) to reveal information on protein topology and ligand binding domains [168, 189-191]. For example, cysteine scanning mutagenesis of the Glut1 transporter found predicted exofacial residues of TM 7 to be accessible to the external aqueous environment and provided support for the placement of TM7 in the glucose permeation pathway. However, this approach requires a clear understanding of the roles of endogenous cysteines in transporter function, which has been addressed in this study. Additionally, although it is known that TM3-6 are critical for hENT1 transporter function, it is also important to determine if and how other regions contribute to the binding pocket as recent evidence points toward the involvement of these flanking

domains of hENT1. We targeted the region of EL5 and found it to be indirectly involved in the NBMPR binding pocket as well having singular residues critical in substrate translocation.

5.1 Wild-type hENT1 is sensitive to neutral and positively charged thiol modification

To initially assess the involvement of cysteine residues in hENT1 function, we used the sulfhydryl modifiers MMTS, MTSET, and MTSES (Figure 1.12) to probe with free accessible thiols and determine their relative location and purpose. The reaction of MTS reagents to free sulfhydryls is via a nucleophilic attack of the thiolate anion (RS^-) to the disulfide bond ($-\text{S}-\text{S}-$) of the MTS reagent resulting in the formation of a mixed disulfide. The present study supports previous work from our lab where the neutral and therefore membrane permeable sulfhydryl reagent MMTS, like NEM, caused an increase in NBMPR B_{max} of hENT1 in whole cells (Figure 4.5A) [174]. In contrast with what was observed with NEM, this same treatment caused a decrease in the maximal rate of uptake of [^3H]2-chloroadenosine (Figure 4.5C). This finding is contrary to general dogma in the field that changes in NBMPR binding site numbers reflect changes in ENT1-mediated transport capacity [86]. Under many conditions, it has been shown that NBMPR binding sites are proportional to V_{max} values for nucleoside uptake in erythrocytes suggesting that the presence of NBMPR-binding sites can be used as a measure of functional ENT1 transporters [192]. However, our study demonstrates that this assumption should be confirmed before further analyses are taken. While such striking conflicting results have not been reported previously, there have been reports where changes in nucleoside uptake did not correlate with the changes in the amount of transporter present at the cell membrane. Our data imply that the ‘increased’ NBMPR binding sites induced by MMTS treatment are not actually functional transporters at the plasma membrane [71]. This suggests that not all hENT1 exhibiting high-affinity [^3H]NBMPR binding are necessarily functional transporters, and may reflect different hENT1 subpopulations within the cell as previously described [67, 193-195]. One possibility is that MMTS treatment may have caused an increase in NBMPR binding sites

found within membranes of intracellular organelles. It has been shown that expression of hENT1 has been found in nuclear membranes, endoplasmic reticulum, and mitochondria suggesting that there is a mix of subpopulations of hENT1. These transporters have also been shown to be functionally active at those sites, suggesting that they play a role in the transport of nucleosides between the cytosol and lumen of these organelles.

In times of high growth and energy consumption, it is possible that the increased presence of these transporters is needed to fuel these processes. Additionally, nucleoside analogues, which exhibit clinical mitochondrial toxicity, have been correlated to nucleoside transporter expression at mitochondrial membranes [196-198]. In one case, the overexpression of hENT1 in MDCK cells resulted in enhanced mitochondrial toxicity of the hepatitis B uridine analog Fialuridine (FIAU)[97]. According to this reasoning, the separate effects of MMTS on hENT1 function may be due to its modification of transporters found in two separate membrane populations. The difference between MMTS treatments in whole cells versus membranes from cells pretreated with MMTS may also be explained in this way. A reduction in the number of binding sites was observed in membrane preparations of cells pre-treated with MMTS (Figure 4.6A), indicating the loss of intracellular compartments (such as nuclei and mitochondria) by differential centrifugation may be involved in the loss of the B_{\max} enhancement. It may be possible that MMTS is modifying those transporters in whole cell experiments to cause an increase in B_{\max} and this hENT1 population is lost during cell membrane preparations. Furthermore, incubating cells with MMTS in 50 mM Tris at a pH of 8.2 eliminated the ability of MMTS to enhance the binding of [3 H]NBMPR (Figure 4.7C). This indicated that basic pH either increased hydrolysis of the thiol modifier destroying the active reagent or caused de-protonation of the protein causing thiol moieties to become unreactive. To test this hypothesis, we compared the effects of varying pH on [3 H]NBMPR binding and [3 H]2-chloroadenosine uptake by hENT1. Our results found that buffers of basic pH (both Tris and NMG) enhanced [3 H]NBMPR B_{\max} by approximately 50% compared to [3 H]NBMPR binding in pH 7.4 indicating that the

transporter was sensitive to enhanced pH and hydrogen ion concentrations (Figure 4.9A, 4.9B). The result that pH altered NBMPR binding and not substrate transport (Figure 4.9C) indicates that the increase in binding sites may not reflect functional transporters at the plasma membrane but may be due to exposing previously hidden binding sites.

In addition to the MMTS enhancement of NBMPR binding in whole cells, we observed a decrease in NBMPR binding with MTSET, the positively charged reagent (Figure 4.13A). Prior to this study, sulfhydryl reagents used to probe ENT1 have included those that were neutral (NEM) or negatively charged (pCMBS) [157, 172, 174, 199, 200]. As mentioned previously, pCMBS had no effect on ENT1 in intact cells in the same way that the negatively charged MTSES had no effect in the present study (Figure 4.12A, 4.12C). However, positively charged MTSET appeared able to access and modify a cysteine in intact cells which caused changes in both [³H]NBMPR binding and [³H]2-chloroadenosine uptake. This indicates that there is a cysteine that can be accessed by MTSET located in a hydrophilic region or extracellularly that has an impact on the permeation site or pathway. Either blocking of a cysteine thiol or the introduction of a large positively charged alkyl group caused a change in transporter conformation to alter the number of NBMPR binding sites as well as substrate uptake velocity. An increase in V_{max} with MTSET treatment may result from an increase in mobility of the transporter due to increased plasticity (Figure 4.13C). Transporter plasticity has been shown to have an impact on substrate translocation rates in hENT2 as mutational analysis at residue isoleucine 33 to methionine was found to have increased V_{max} values for purine nucleosides [187]. Additionally, mutation of methionine 89 to cysteine and phenylalanine 334 to tyrosine of hENT1 both increase V_{max} relative to wild-type hENT1, indicating that they possessed increased rates of catalytic turnover [138, 143]. In our case, it is possible that MTSET modifies a cysteine in a manner that causes a minor distortion at the NBMPR binding site, while making the substrate binding site more transport active. These findings suggest that there are two separate cysteines involved in hENT1 ligand conformation; one located in a region that is accessible only to MMTS and another in an extracellular, possibly negatively charged region accessible to MTSET.

Given that C378 is the only cysteine predicted to lie at the extracellular face of the transporter shown in Figure 2.1 (and potentially close to negatively charged residues E391 and D393 on the opposite end of extracellular loop 5), it was predicted as being the target residue for the membrane impermeable reagent MTSET (Figure 5.1). The present study also highlighted again the contribution of intracellular cytoplasmic cysteines to the transport/binding competence of hENT1. Treatment with MMTS, MTSES, and MTSET all caused a significant decrease in NBMPR binding B_{max} in broken cell preparations (Figure 4.5B, 4.12B, 4.13B) showing that modification of intracellular cysteines produces an impact on NBMPR binding, known to be located on the exofacial surface. As previously mentioned, the negatively charged reagent pCMBS has been shown in multiple models to modify intracellularly located cysteine(s) to cause a decrease in NBMPR binding to ENT1. Given that C414 and C416 are predicted to be located on the 5th intracellular loop of hENT1, it is suggested that they are the possible targets of this type of modification.

5.2 Assessment of single cysteine to serine mutants

To determine which of any of the ten cysteines in hENT1 were important for its function and which are implicated in MTS mediated effects, site-directed mutagenesis was used to replace cysteine residues with serines or alanines. We found the transport and binding activities of the C87S, C193S, C213S, C222S, C297S, C333S, C378S, and C414S mutants to be comparable to that of wild-type hENT1. This indicated that none of these residues are crucial for substrate binding or protein expression. Though there were some significant differences in the affinity of [³H]NBMPR and [³H]2-chloroadenosine for the various mutants, these relatively minor differences in affinity (under 2-fold in most cases) likely reflect subtle shifts in the overall structure of the inhibitor/substrate binding domains due to minor disruptions of the hydrogen bonding network maintaining tertiary structure. Specifically, C87S, C193S, C222S and C297S each had a slightly higher affinity for [³H]NBMPR relative to the wild-type ENT1. Additionally, C87S and C193S had a significantly higher affinity for [³H]2-chloroadenosine in the cellular uptake transport assays, as did C333S and C414S. This indicated that mutation of these residues into

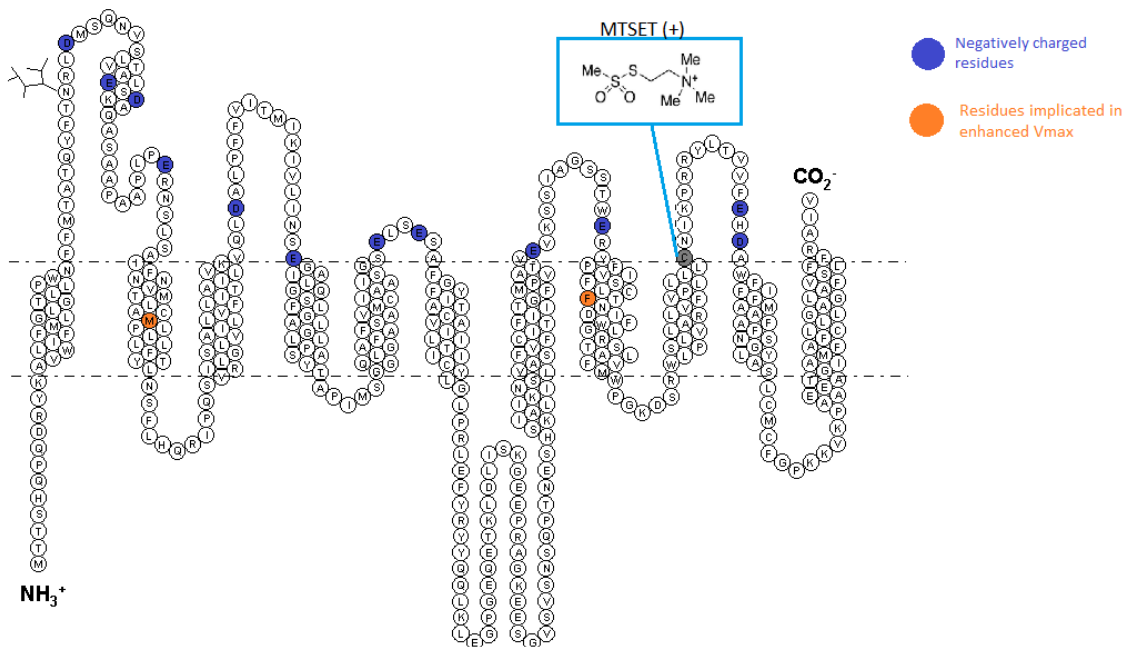


Figure 5.1 Predicted topology of hENT1 with C378 highlighted in grey as the target residue for positively charged thiol modification with MTSET (+). Negatively charged amino acids found in predicted extracellular regions are highlighted in blue and suggested to be in close vicinity to C378. Residues highlighted with orange are residues that have been implicated in enhanced V_{max} of substrate transport similar to the effect of MTSET on hENT1 [^3H]2-chloroadenosine uptake in cells.

serines could have produced a change in the conformation of hENT1 for increased substrate affinity.

However, mutation of C416 or C439 to either a serine or alanine was not tolerated in our stable mammalian cell model where there was no ENT1 expression observed either via NBMPR binding or Western blotting. These results suggest important roles for C416 located in the 5th intracellular loop and C439 located in TM11 in the proper post-transcriptional processing of the hENT1 protein. These results differ from previous studies with mENT1 Δ 11, the functional mENT1 splice variant that is truncated after TM8, where loss of the last three TM helices and associated loops did not alter its expression or basic functionality [157]. Additionally, our results diverges from those of previous studies on the ENT parasitic homologs in *Plasmodium falciparum* ENT1 (PfENT1) and *Leishmania donovani* ENT (*LdNT1.1*) [201, 202] where expression and function of cysteine-less versions of ENT1 have been described. This difference could reflect species differences in ENT1 structure/processing, or the different heterologous expression models used. A recent study has also demonstrated the activity of a cysteine-less version of hENT1 (hENT1C-) in which all 10 endogenous cysteine residues were mutated to serine [203]. However, this study utilized an enhanced expression vector pGEMHE in *Xenopus* oocytes to characterize hENT1C-, where as in our model we have utilized a mammalian expression system that may differ in cellular environment by potentially employing more complex posttranslational modifications. Since cysteines can be palmitoylated and contribute to protein trafficking and membrane tethering, we tested the hypothesis that C416 and C439 were targets for this post-translational modification. Though C416 was predicted to be palmitoylated (CSS-Palm 3.0), our study determined that the palmitoylation inhibitor 2-Br had no effect on hENT1 function (Figure 4.44) suggesting that C416 was not acting as a palmitoylation site. At closer inspection, the location of C439 was noted to be adjacent to the conserved GxxxG motif. The GxxxG motif often associates in helix-helix interactions specifically as a dimerization arrangement [204-206]. It is possible that mutation of C439 abrogates this motif and interrupts interactions that could be essential for protein folding and assembly.

Unpublished work from our lab by Cunningham, F. *et al.*, has validated the importance of this motif. Mutation of G445 to leucine in hENT1 was not tolerated and could not be expressed despite transfection of the cells being confirmed by mRNA extraction and subsequent DNA sequencing, similarly to that observed here for C416S and C439A mutants. Additionally, it is noted that the pig kidney epithelial cells used for expression of human ENT1 may have modified cellular characteristics due to earlier methods on selecting for nucleoside transporter deficiency.

Furthermore, an endoplasmic reticulum retention signal (KKVK) is found between C416 and C439 (three amino acids downstream of C416) which could also explain their ineffectual expression. This motif is used as a quality control signal within the cell to determine whether proteins are destined for degradation, secretion, or expression [207, 208]. The proximity of these residues to the motif raises the possibility that displacement or adjustment of the signal sequence may result in altered sorting and trafficking of mutant proteins and therefore impacting their expression in our stable mammalian cell models. However, transient expression of these constructs did result in the expression of hENT1 protein as defined by immunoblotting and NBMPR binding. This suggested that chronic expression of these mutant proteins was deleterious to cell function and that they were degraded via the cellular unfolded-protein response mechanisms.

5.2.1 Mutation of C416 to alanine alters the transport mechanism

With expression in transient transfection models, we assessed the ability of C416A and C439A to bind [³H]NBMPR and transport [³H]2-chloroadenosine (Figure 4.45A, 4.45B). We found C439 to bind NBMPR with relatively high affinity and transport [³H]2-chloroadenosine as well (Figure 4.45C). Surprisingly the C416A mutant bound [³H]NBMPR with high affinity, but was unable to transport [³H]2-chloroadenosine (Figure 4.45C). This suggested that the loss of C416 or introduction of alanine at that position produced two separate effects at the inhibitor site and the substrate site. To determine whether this change in transport competence was due to a loss of hENT1 expression at

the plasma membrane, as NBMPR can bind to intracellular hENT1 sites in other cell compartment membranes. C416A expression levels were measured at the plasma membrane by cell surface biotinylation and FTH-SAENTA competition assays (Figure 4.46A, 4.45B) but no difference between wild-type hENT1 and C416A and C439A was detected suggesting that C416A was found at the plasma membrane but was not transporting.

To determine whether this loss of function was due to loss of recognition for the substrate or due to loss of the transport mechanism, it was determined that 2-chloroadenosine inhibited the binding of [³H]NBMPR both the hENT1-WT and hENT1-C416A transfectants with similar affinity (Figure 4.47). This indicates that 2-chloroadenosine can still interact with hENT1-C416A with high affinity but is not able to activate the transport mechanism. Given that the ability of a substrate to inhibit [³H]NBMPR binding generally reflects its affinity as a hENT1 substrate, this finding suggests that the loss of [³H]2-chloroadenosine transport by hENT1-C416A was not due to a decline in transporter substrate affinity. Therefore, the C416A mutant may be compromised in terms of its substrate translocation mechanism. A similar effect has been observed for mutations at glycine 179 in TM5 where substitutions with amino acids with large side chains such as leucine or valine eliminated transporter activity but had no effect on membrane expression [139]. Once again, if using the *ab initio* model, the endofacial ends of TM10 and TM5 are located are in close proximity to one another and more importantly are positioned in a “V” shape within the membrane (Figure 5.2). Given that C416 is close to the cytoplasmic end of TM10, it is possible that mutation at this site alters the positioning of TM10 thereby shifting the hydrophilic space between TM5 and 10 and abolishing transport.

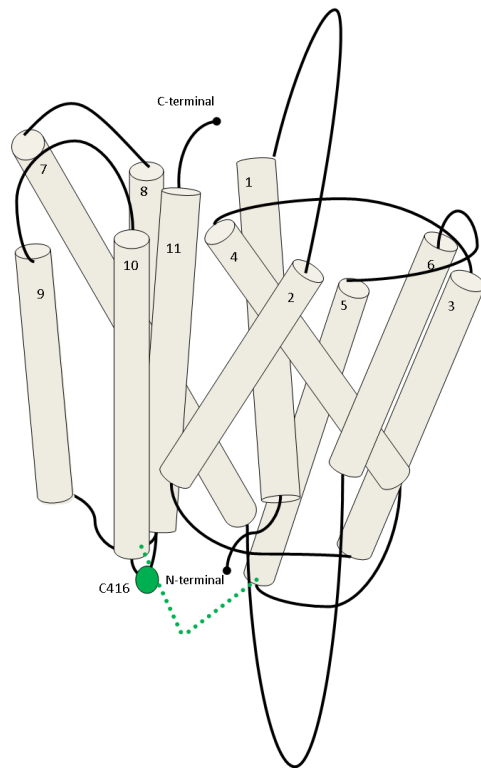
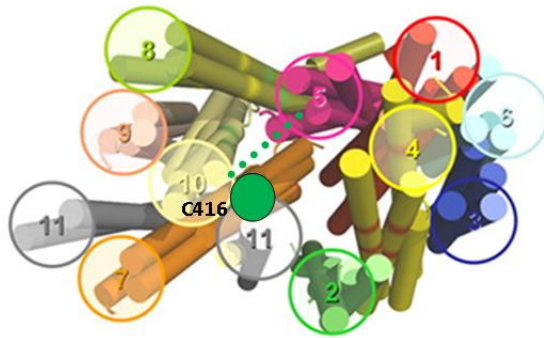
A**B**

Figure 5.2. Simulated topologies of hENT1 based on the *ab initio* model of LdNT1.1. **Panel A** shows a side view of the generated figure of hENT1 with numbered transmembrane helices based on the models described by Valdes *et al.*, 2009. [156] shown in **Panel B**. Cys416 is shown in the green circle off the predicted site of intracellular loop 5. Dashed green lines illustrate the potential interaction between TM5 and TM10.

5.2.2 Cysteine 222 is responsible for MMTS effects

When the functional mutants were treated with MTS and then subjected to NBMPR binding analysis, we found that mutation of the conserved cysteine at position 222 (C222) in TM 6 to serine resulted in the loss of MMTS sensitivity (Figure 4.24A). This suggested that C222 is responsible for the enhancement of activity observed after MMTS treatment of wild-type hENT1. For further validation, C222S was exposed to MMTS and then membranes were isolated and NBMPR binding assays were performed. Interestingly, C222S did not display the same decrease in NBMPR binding sites in the membranes under these conditions as it did with experiments using the wild-type hENT1 cells (Figure 4.26A, 4.26B). As neither of the other charged thiol reagents (MTSET and MTSES) enhanced NBMPR binding, it indicates that they were not able to access and modify C222 because of its location. Since MMTS is a neutral membrane permeable reagent and enhances NBMPR binding by targeting C222, it is reasonable to conclude that C222 is located in a hydrophobic region and validates our first hypothesis in which there is a cysteine in a hydrophobic domain that can be modified to alter hENT1 function. In support of this conclusion, it is worth noting that C222 is adjacent to hydrophobic amino acids like isoleucine and leucine which can be critical for membrane insertions and anchoring (Figure 5.3). For MMTS to modify C222, it is possible that loss of the thiol functional group increases lipophilicity at the end of TM6 to free previously hidden binding sites within the cell. However, when MMTS was applied directly to broken cell preparations of C222S, the number of NBMPR binding sites still declined similar to that observed using wild-type hENT1 cell membranes, indicating that C222S was not responsible for the reduction in NBMPR binding under these conditions.

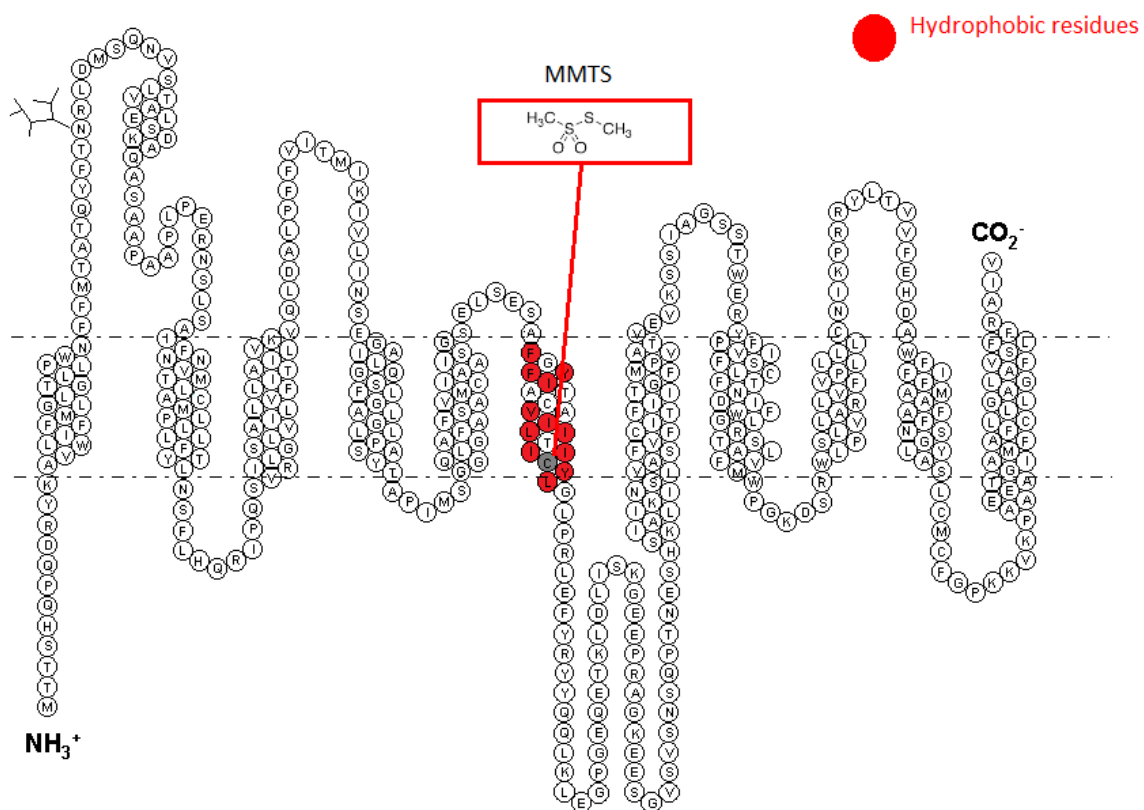


Figure 5.3 Predicted topology of hENT1 with C222 highlighted in grey as the target residue for neutral thiol modification with MMTS. Hydrophobic amino acids of transmembrane 6 are highlighted in red and suggested to be in close vicinity to C222.

Therefore, it is suggested that MMTS has a dual effect on NBMPR binding to hENT1 involving at least two distinct cysteine residues. In intact cells, MMTS both enhances NBMPR binding via modification of the intra-membrane C222, and inhibits NBMPR binding via modification of another cysteine residue cytoplasmically located, most likely C416. The enhancement of NBMPR binding via C222 is lost upon cell lysis and subsequent differential centrifugation to prepare the membranes, leaving only the inhibitory component. This suggests that the enhancing effect of MMTS relies on other intracellular components, or it involves ENT1 proteins in intracellular compartments that are lost during the membrane preparation. The effect of MMTS could not be reversed by co-incubation of the cells with adenosine or NBMPR. Hence C222 that MMTS is interacting with is either not directly part of the binding domain or MMTS can still gain access to this residue in spite of the proximity of these agents. Furthermore, mutation of C222 to serine was also able to abolish the effect that basic pH had on [³H]NBMPR binding (Figure 4.28). This suggested that C222 was responsible for causing an increase in [³H]NBMPR binding when cells were incubated in basic pH. It may be possible that C222 becomes deprotonated in basic pH and that this change in reactivity of the residue causes [³H]NBMPR to bind to more intracellular sites. Given that both MMTS and basic pH increased B_{max} , and both effects were abolished with mutation of C222, it is proposed that the reactivity of this residue plays an important role in stabilizing the transporter to the NBMPR conformation.

Additionally, C222S retained MMTS-inhibition of [³H]2-chloroadenosine V_{max} (Figure 4.24B) indicating that the residue was not the cysteine responsible for the inhibition of substrate uptake. This suggests that C222 is not a shared residue between the NBMPR binding site and the substrate translocation pathway and this in turn implies a physical distinction between the NBMPR binding site from the substrate translocation site. It is important to note that NBMPR has been shown to be a competitive inhibitor of nucleoside transport in various models [179, 209], and nucleoside substrates are competitive inhibitors of NBMPR binding [90, 210]. Therefore, there is clearly an overlap

in the NBMPR and substrate binding sites of hENT1. Cysteine 222 appears either to be in the distinctive NBMPR binding region, or is affecting NBMPR binding to that region via MMTS-induced conformational changes. When looking for the cysteines involved in the V_{\max} enhancement effect with MMTS, we found mutation of C193 (TM5), C297 (TM7), or C333 (TM8) to serine led to a significant reduction of the MMTS effect on [^3H]2-chloroadenosine uptake. This study could not narrow down the search for the implicated cysteine or cysteines. This could be in part due to MMTS acting with all three cysteines or that these cysteines act in combination to produce those effects. These results suggest that a distinct cysteine, or sets of cysteines, is involved in the effect of the MTS reagents on substrate transport versus NBMPR binding.

5.2.3 Cysteine 378 is responsible for MTSET effects

When determining which cysteine was involved in MTSET effects, the function of C193S, C213S, C297S, C333S, and C378S was observed to be insensitive to MTSET. Surprisingly, mutation of C414 to serine produced an even greater inhibition in [^3H]NBMPR binding with MTSET treatment (Figure 4.40). Given that MTSET is a large membrane-impermeable positively charged reagent and that C193, C213, C297 and C333 are located within TM regions (Figure 2.1), it was suggested that they were not involved in MTSET effects but rather mutation of these residues could have altered transporter conformation to bury C378 making its side chain inaccessible to MTSET. C378 is a conserved residue that is predicted to be positioned at the interface of TM9 and the extracellular loop indicating that it has a higher probability of interacting with a charged reagent. Additionally, mutation of the intracellular C414 seemed to produce an enhanced accessibility to the targeted residue. The region between C378 and C414 includes EL5 and TM10, therefore it is possible that TM10 plays an important structural and/or functional link between these two residues.

To test this idea, a stably expressed functional double mutant of C378 and C414 to serines was produced and tested for MTSET sensitivity. The double mutant (C378S-

C414S) was insensitive to MTSET inhibition of NBMPR binding as previously observed for the C378S mutant which indicated that C378 is likely the targeted residue (Figure 4.43A). The structural and/or functional cooperation between C378 and C414 is a novel finding as residues in the cytoplasmic domain are not known to show influences on the extracellular binding domain. However, a recent finding by Yao *et al.* (2011) indicated low amounts of nucleobase transport by wild-type hENT1 in an enhanced expression vector pGEMHE and suggested that C414 was responsible for this nucleobase activity. It must also be noted, that we have not found any evidence for nucleobase (hypoxanthine) transport by recombinant hENT1 expressed in the PK15-NTD at concentrations of nucleobases below 400 μ M (unpublished data). Thus, the nucleobase transport observed by hENT1 by Yao *et al.* may reflect the expression model used, or higher concentrations of nucleobases than employed in previous studies are required to measure observable transporter-mediated uptake. Therefore, we have found C378 to possibly be in a region that is of anionic character so that, when modified with a positively charged reagent, it inhibits binding of NBMPR. Since MTSET cannot cross the membrane, this inhibition of NBMPR binding is therefore restricted to those sites found at the plasma membrane supporting the conclusion that C378 resides in a hydrophilic or extracellular environment. When reviewing the 2-D topology of hENT1, it is noted that there are negative charges located near the membrane boundaries in EL4 and EL5 (E391, D393) indicating that they may form a pocket of negatively charged environment near the membrane that C378 may lie within (Figure 5.1). In this way, if EL4 and EL5 are relative close, the adjoining TMs may also lie in close proximity and possibly TM7 and TM10 may also be neighbors. Once again, when assessing the *ab initio* model of LdNT1.1 (Figure 1.11), the exofacial ends of TM7 and TM10 are shown to be adjacent with one another and may contribute to the NBMPR binding domain (Figure 5.4).

The mENT1 Δ 11 variant that had lost the ability to covalently bind NBMPR, has already indicated the importance of TM9-11 and EL5 in the NBMPR covalent attachment. The results of the present study provide more evidence on this area of the

transporter and indicate that C378 (located at the TM9 and EL5 interface) may be adjacent to important determinants of NBMPR binding. Additionally, this study found that residue C414 in intracellular loop 5 can be an important contributor to extracellular regions of hENT1. Since C414 mutation to serine enhances the ability of MTSET inhibition at C378, this suggests that modification at cytoplasmic portions of the transporter impacts the extracellular side. As previously described, mutation of C416 (close to C414) in IL5 abrogated the translocation function, our results in this section further validates the role of intracellular residues in impacting transporter function. This suggests that the cytoplasmic ends of TM10 and 11 are conformationally linked to TM3-6 which has already been shown to partially form the active site of hENT1.

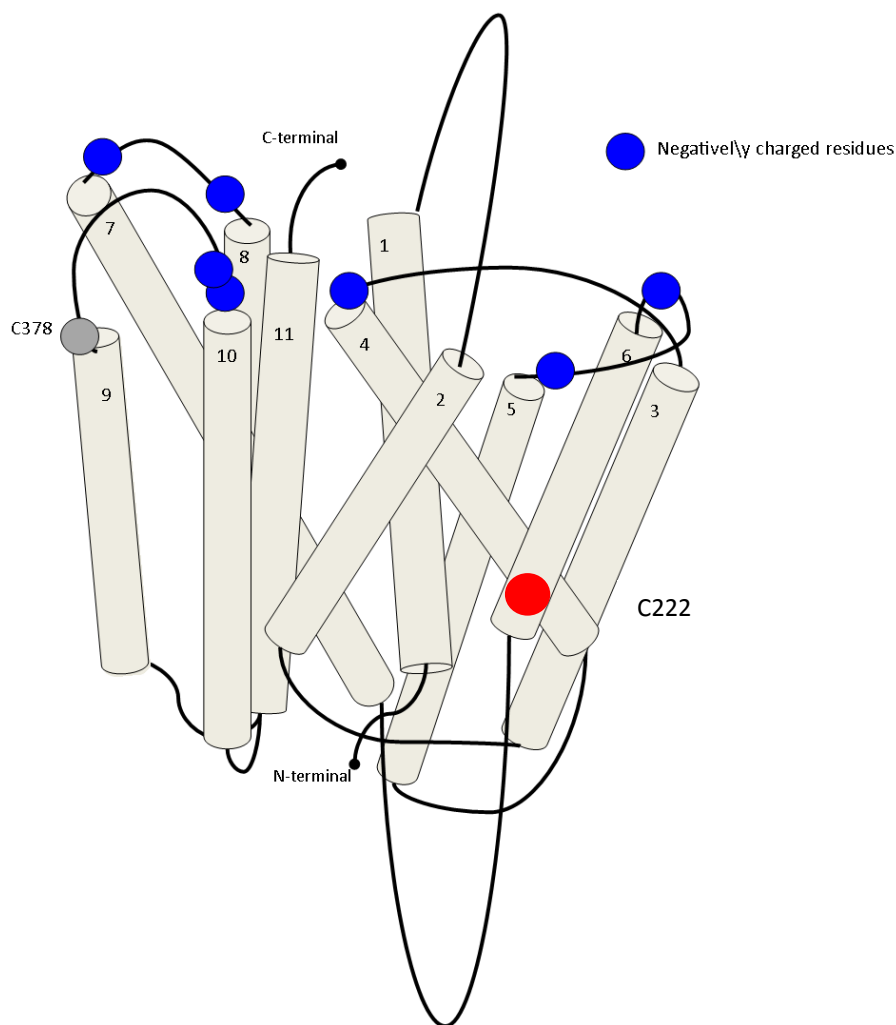


Figure 5.4. Simulated topology of hENT1 based on the *ab initio* model of LdNT1.1. highlighting extracellular negatively charged amino acids. Cys378 is shown in the grey circle at the TM9 interface, Cys 222 shown in the red circle, blue circles indicate relative positions of negatively charged amino acids. Representation of the side view of the LdNT1.1 model described by Valdes *et al.*, 2009. [156]

5.2.4 Cysteine 416 is responsible for MTSES effects in membrane preparations

Cysteine mutants treated with MTSES in whole cells produced no effects in either [^3H]NBMPR binding or [^3H]2-chloroadenosine uptake as previously seen with wild-type hENT1. This validated that effects observed in broken cell preparations are due to the contribution of intracellularly located cysteines. When membrane preparations enriched for cysteine mutants (C87S, C193S, C213S, C222S, C297S, C333S, C414S, and C439A) were subjected to MTSES treatment, significant inhibition of NBMPR binding was observed. The single cysteine mutant that was unaffected by MTSES treatment was C416A (Figure 4.49). Thus, MTSES and MMTS treatment did not decrease [^3H]NBMPR binding in the C416A mutant and the effect of MTSET was significantly less relative to wild-type hENT1. This indicates that C416 is in a cytoplasmic location, which supports the 2-D topology model of hENT1 and substantiates the second hypothesis in this thesis where it was proposed that there is a cytoplasmic-located cysteine that when modified causes a change in hENT1 function. The conserved residues, C416 was also found to be the targeted residue in IL5 for thiol modification that is involved in the NBMPR binding pocket. In effect, since neither adenosine nor NBMPR alone could protect against these effects (Figure 4.50A, 4.50B), it is suggested that there is no direct interaction and hence C416 most likely does not line the permeation pathway nor lie in the inhibitor binding site. The alternating access mechanism proposed in Chapter 1 of this thesis suggests that ENT1 has an extracellular and intracellular site that can alternate between the two conformations depending on whether a substrate is bound.

It is also suggested that the extracellular site can bind NBMPR and other inhibitors to lock it in that conformation. Therefore, it is possible that the location of IL5 is not directly part of the ligand binding site but that interaction with C416 with MTS reagents may lock hENT1 in an inwardly faced conformation. The modification may be the result of either introduction of a charged/uncharged alkyl group or loss of the hydrogen bonding interactions of sulfhydryl groups. Given that C416 has already been implicated in 2-chloroadenosine uptake mechanism but is still able to bind NBMPR with

high affinity, it was proposed that C416 has an important function in the orientation of TM helix 10 and 11 to TM 3-6, which is the previously recognized ligand binding domain. It is possible that the packing of TMs helices around the solvent-accessible permeant and inhibitor binding site requires the aid of C416. The recently published *ab initio* model of the LdNT1.1, highlighted the structure to have one inner bundle of TM helices (1, 2, 4, 5, 7, 8, 10, 11) encompassing a hydrophilic cavity and the remaining TMs (3, 6, and 9) encircling the inner bundle [156]. Following this model, the results of the present study indicate that the cytoplasmic link between TM10 and 11 (where C416 is located) may actually not be central to ligand translocation or recognition but instead may have a conformational role in keeping the TM helices stable for substrate interaction. Therefore, it is possible that modification at C416 with MTS reagents may alter the angle or rotation of these transmembrane domains causing the effects seen in NBMPR binding (Figure 5.2).

5.3 Role of residues in EL5

With the results from the preceding studies highlighting the roles of TM9-11 and IL5 in the structure and function of hENT1, examination was extended into the role of EL5. This region of hENT1 has not been clearly defined in its function; however, evidence from studies of CeENT1 revealed that an Ala and Thr in TM 1 and 11, respectively, impaired uridine and adenosine transport and that L442 of hENT1 was involved in permeant selectivity [100]. Recent studies have also identified Phe334, Asn338, (TM8) and Leu442 (TM11) of ENT1 as contributing to interactions with coronary vasodilators [100, 143]. Additionally, there is a multitude of evidence that extracellular loops can contribute in the function of integral membrane proteins. For example, studies on the Na⁺/H⁺ exchanger 1 (NHE1) have found that its extracellular loop 2 (EL2) is implicated in substrate and inhibitor sensitivities. Residues Pro153, Pro154 and Phe155 all found in EL2 were critical for NHE1 activity [211]. Furthermore, the Cys-loop family of ligand-gated ion channels have implicated extracellular residues to undergo conformational changes that are critical in function [212-215]. There is also evidence of transporters

such as hOCT2 that show the contribution of extracellular loops in protein folding, membrane expression, and oligomeric assembly [216]. In our study, mutation of each residue in EL5 to cysteine produced no change in the ability of hENT1 to bind [³H]NBMPR. This indicated that none of the residues in EL5 are crucial points of contact for NBMPR binding or that the cysteine introduced into that location retained the ability to recognize [³H]NBMPR and perform the same hydrogen bonding capabilities or retained the same flexibilities.

5.3.1 N379C, F390C, E391C, H392C, and D393C are critical in transporter function

When assessing EL5 mutants in their ability to transport [³H]2-chloroadenosine; N379C, F390C, E391C, H392C, and D393C showed no uptake of the substrate (Figure 4.53). It is important to note that N379, F390, H392, and D393 are conserved residues between mammalian homologs of ENT1. To determine whether the loss of transport in these five mutants was due to a loss of transporter expression at the membrane, FTH-SAENTA inhibition assays were performed. In this manner, only the transporters expressed at the plasma membrane would be inhibited by the membrane-impermeable analogue. The results obtained showed all five non-functional mutants to have significant expression at the plasma membrane, indicating that the loss of transport function was most likely due to a change in substrate affinity or to a change in transport mechanism as previously observed for the C416A mutant. To test these ideas, competitive inhibition assays were performed using 2-chloroadenosine as the inhibitor against [³H]NBMPR binding. For all five non-functional mutants, 2-chloroadenosine was able to inhibit NBMPR binding with similar affinities (Figure 4.54) indicating that the substrate recognition site was still intact and 2-chloroadenosine remained a competitive inhibitor but the mechanism for transport was impaired. Given that the four residues are found in succession on one side of the loop (F390C, E391C, H392C, and D393C), it is possible that these residues are crucial in constructing part of the substrate translocation site. Additionally, E391 and D393 are both predicted to be negatively charged at physiological pH, and are able to form ionic bonds with positively charged amino acids or form ion dipole interactions

with water. Removal of these strong ionic bonding partners in this region could cause this drastic impact seen in hENT1 functionality. It is interesting to note that mutation of the positively charged residues (K381, R383, and R384) to Cys in EL5 had no effect on [³H]2-chloroadenosine uptake, suggesting that the negative charges of EL5 possess a greater role in transporter function. Furthermore the asparagine residue (N379) can also function as a chain crosslinker or in hydrogen bonding to water at the protein surface. Since asparagines are often found in protein bends it is possible that abrogation of this bend at the TM9 interface repositions the TM helix in a manner that reshapes the translocation pathway. It has already been shown that C³-OH and C⁵-OH groups of the sugar moieties of nucleoside analogues form strong interactions with hENT1 suggesting a role for hydrogen bonding between the transporter and ligand. Therefore the availability of these bonding partners via functional side chains of amino acids can have a drastic impact on hENT1 function. The previously mentioned *ab initio* model of the LdNT1.1 with one inner bundle of TM helices (1, 2, 4, 5, 7, 8, 10, 11) forming the hydrophilic pore and the remaining TMs (3, 6, and 9) surrounding the inner bundle suggests that the extracellular loop would link the inner bundle to the outer bundle [156]. Results of this study when combined with this model, suggests that the residues that are implicated in substrate uptake are located closer to the extracellular end of TM10 which is predicted to form part of the hydrophilic pore.

5.3.2 MTSET effects on EL5 mutants

When testing the accessibility of the mutated residues in EL5 to MTSET, it was observed that all mutants except for V389C to have some measurable inhibition of NBMPR binding with MTSET treatment (Figure 4.55). Given that the majority of the EL5 residues can become modified with MTSET indicates that EL5, although not directly involved in NBMPR binding, is nevertheless close enough to the pocket to disrupt it when bulky positively charged alkyl groups are attached. The maximal amount of inhibition was seen at ~50% at R383C, indicating that it may be the closest residue to the hydrophilic binding pocket and significantly block NBMPR binding when modified with a positively charged

reagent. The observation that V389C was not sensitive to MTSET is surprising given that adjacent residues are able to be sufficiently modified to inhibit binding. There may be two reasons for this effect, one is that V389C is not accessible for modification or that modification at this site does not impact NBMPR binding. However, MTSET inhibition at 15 out of the 16 EL5 mutants does support the extracellular location of this loop, supporting the 2-D topology model of hENT1. Co-incubation of NBMPR with MTSET was able to protect N379 from thiol modification indicating that the inhibitor NBMPR was able to block the reaction at that site. Co-incubation of adenosine with MTSET produced a separate set of amino acids that were protected from MTSET inhibition of binding: R384C, Y385C, and L386C. Not surprisingly, these three residues are all found in sequence within the middle or apex of EL5 which would have the greatest accessibility to ligands. These results indicate that adenosine may bind in close vicinity or in direct contact to these residues to prevent MTSET to attain access.

5.4 General conclusions

Human ENT1 is known to be the major facilitator of bi-directional nucleoside flux and uptake of anti-cancer and anti-viral analogues. Based upon data from previous glycosylation and hydropathy studies, hENT1 is predicted to have an intracellular N-terminus, extracellular C-terminus and 11 transmembrane domains. Human ENT1 is thought to function as a simple carrier, where there is one exofacial site for nucleoside or inhibitor interactions and an endofacial site for nucleoside flux. However, one of the key issues related to the function of ENT transporters is the location and structure of the permeation site. Previous studies using NEM and pCMBS have identified the importance of cysteines in ENT1 function. In this thesis, we have found the neutral membrane-permeable reagent MMTS to produce an enhancement of intracellular binding sites for the prototypical probe NBMPR. This effect was due to modification of C222 found in TM 6 indicating that it was located in a hydrophobic environment. C222 was also found to be responsible for the enhanced NBMPR binding of hENT1 in basic pH suggesting that de-protonation of C222 causes the formation of new intracellular binding sites.

Additionally, these studies are the first to show that a positively charged reagent, MTSET, can inhibit NBMPR binding in intact cells, which indicated that there was a cysteine residue accessible to the extracellular space. The cysteine responsible appears to be C378 indicating that it is in an aqueous negatively charged environment close to the inhibitor binding pocket. The predicted topology of hENT1 puts C378 near the extracellular end of TM9; therefore results are consistent with this model and show it is likely the single Cys residue accessible to positively charged modification. The association of C378 and C414 has indicated the structural and/or functional linkage between TM9 and IL5 where intracellular modifications can have a drastic impact on the extracellular side of hENT1. Conjointly, the role of C416 has been made apparent and is the first study to show the contribution of IL5 residues in the functionality of hENT1. This study establishes C416 as the cytoplasmically located cysteine that modifies the extracellular binding site and is susceptible to thiol modification by charged thiol reagents in membranes. C416 is also implicated in the permeation site or pathway of 2-chloroadenosine and has a central role in the substrate translocation mechanism. Lastly, a functional role for EL5 has been revealed which has never been examined previously. Mutational analysis found N379, F390, E391, H392, and D393 to have crucial functions for the hENT1 translocation machinery. Furthermore, MTSET treatment of EL5 mutants inhibited binding of NBMPR to hENT1, thereby suggesting that EL5 is in close proximity to the inhibitor recognition site. Finding that there are two separate sets of residues that can be protected from MTSET by using NBMPR or adenosine also indicated that the two ligands interact with hENT1 at separate orientations and determinants. In this manner, new regions of hENT1 have been identified that were previously not known to contribute to its function. This is the first study to describe the importance of extracellular loops in ENT1 function and will provide a basis for future targeting studies on hENT1 structure-function.

Chapter 6: References

1. Cerecedo, L.R., *Studies on the physiology of Pyrimidines*. J Biol Chem, 1927. **75**: p. 661–670.
2. Paterson, A.R. and S.H. Zbarsky, *In vitro synthesis of purines by rat intestinal mucosa*. Biochim Biophys Acta, 1955. **18**(3): p. 441-2.
3. Eltzschig, H.K., et al., *Coordinated adenine nucleotide phosphohydrolysis and nucleoside signaling in posthypoxic endothelium: role of ectonucleotidases and adenosine A2B receptors*. J Exp Med, 2003. **198**(5): p. 783-96.
4. Kukulski, F., et al., *Comparative hydrolysis of P2 receptor agonists by NTPDases 1, 2, 3 and 8*. Purinergic Signal, 2005. **1**(2): p. 193-204.
5. Robson, S.C., J. Seigny, and H. Zimmermann, *The E-NTPDase family of ectonucleotidases: Structure function relationships and pathophysiological significance*. Purinergic Signal, 2006. **2**(2): p. 409-30.
6. Synnestvedt, K., et al., *Ecto-5'-nucleotidase (CD73) regulation by hypoxia-inducible factor-1 mediates permeability changes in intestinal epithelia*. J Clin Invest, 2002. **110**(7): p. 993-1002.
7. Thompson, L.F., et al., *Crucial role for ecto-5'-nucleotidase (CD73) in vascular leakage during hypoxia*. J Exp Med, 2004. **200**(11): p. 1395-405.
8. Haddy, F.J., *Physiology and pharmacology of the coronary circulation and myocardium, particularly in relation to coronary artery disease*. Am J Med, 1969. **47**(2): p. 274-86.
9. Fredholm, B.B., *Adenosine, an endogenous distress signal, modulates tissue damage and repair*. Cell Death Differ, 2007. **14**(7): p. 1315-23.
10. Burnstock, G., *Purinergic signalling--an overview*. Novartis Found Symp, 2006. **276**: p. 26-48; discussion 48-57, 275-81.
11. Olah, M.E. and G.L. Stiles, *The role of receptor structure in determining adenosine receptor activity*. Pharmacol Ther, 2000. **85**(2): p. 55-75.
12. Burnstock, G., *Potential therapeutic targets in the rapidly expanding field of purinergic signalling*. Clin Med, 2002. **2**(1): p. 45-53.
13. Burnstock, G. and M. Williams, *P2 purinergic receptors: modulation of cell function and therapeutic potential*. J Pharmacol Exp Ther, 2000. **295**(3): p. 862-9.
14. Borowiec, A., et al., *Adenosine as a metabolic regulator of tissue function: production of adenosine by cytoplasmic 5'-nucleotidases*. Acta Biochim Pol, 2006. **53**(2): p. 269-78.
15. Heinonen, I., et al., *Role of adenosine in regulating the heterogeneity of skeletal muscle blood flow during exercise in humans*. J Appl Physiol, 2007. **103**(6): p. 2042-8.
16. Just, A. and W.J. Arendshorst, *A novel mechanism of renal blood flow autoregulation and the autoregulatory role of A1 adenosine receptors in mice*. Am J Physiol Renal Physiol, 2007. **293**(5): p. F1489-500.
17. Ackley, M.A., et al., *Control of glutamatergic neurotransmission in the rat spinal dorsal horn by the nucleoside transporter ENT1*. J Physiol, 2003. **548**(Pt 2): p. 507-17.
18. Umemiya, M. and A.J. Berger, *Activation of adenosine A1 and A2 receptors differentially modulates calcium channels and glycinergic synaptic transmission in rat brainstem*. Neuron, 1994. **13**(6): p. 1439-46.
19. Greene, R.W., *Adenosine: front and center in linking nutrition and metabolism to neuronal activity*. J Clin Invest, 2011. **121**(7): p. 2548-50.
20. Belardinelli, L., et al., *The A2A adenosine receptor mediates coronary vasodilation*. J Pharmacol Exp Ther, 1998. **284**(3): p. 1066-73.
21. Walko, C.M. and C. Lindley, *Capecitabine: a review*. Clin Ther, 2005. **27**(1): p. 23-44.

22. Mini, E., et al., *Cellular pharmacology of gemcitabine*. Ann Oncol, 2006. **17 Suppl 5**: p. v7-12.
23. Reigner, B., K. Blesch, and E. Weidekamm, *Clinical pharmacokinetics of capecitabine*. Clin Pharmacokinet, 2001. **40(2)**: p. 85-104.
24. Lyons, J., et al., *Decitabine: development of a DNA methyltransferase inhibitor for hematological malignancies*. Curr Opin Investig Drugs, 2003. **4(12)**: p. 1442-50.
25. Cheson, B.D., *New antimetabolites in the treatment of human malignancies*. Semin Oncol, 1992. **19(6)**: p. 695-706.
26. Robak, T., et al., *Purine nucleoside analogues for the treatment of hematological malignancies: pharmacology and clinical applications*. Curr Cancer Drug Targets, 2005. **5(6)**: p. 421-44.
27. Sigal, D.S. and A. Saven, *Cladribine in indolent non-Hodgkin's lymphoma*. Expert Rev Anticancer Ther, 2008. **8(4)**: p. 535-45.
28. Hillmen, P., *Future prospects for fludarabine-containing regimens in the treatment of hematological cancers*. Hematol J, 2004. **5 Suppl 1**: p. S76-86.
29. Dmitrovsky, E., M. Markman, and P.A. Marks, *Clinical use of differentiating agents in cancer therapy*. Cancer Chemother Biol Response Modif, 1990. **11**: p. 303-20.
30. Tripathy, D., *Overview: gemcitabine as single-agent therapy for advanced breast cancer*. Clin Breast Cancer, 2002. **3 Suppl 1**: p. 8-11.
31. Eckel, F., G. Schneider, and R.M. Schmid, *Pancreatic cancer: a review of recent advances*. Expert Opin Investig Drugs, 2006. **15(11)**: p. 1395-410.
32. Sehouli, J., *Review of gemcitabine-based combinations for platinum-resistant ovarian cancer*. Int J Gynecol Cancer, 2005. **15 Suppl 1**: p. 23-30.
33. Toschi, L., et al., *Role of gemcitabine in cancer therapy*. Future Oncol, 2005. **1(1)**: p. 7-17.
34. Mini, E., et al., *Biochemical modulation of fluoropyrimidines by antifolates and folates in an in vitro model of human leukemia*. J Chemother, 1990. **2 Suppl 1**: p. 17-27.
35. Johnston, P.G. and S. Kaye, *Capecitabine: a novel agent for the treatment of solid tumors*. Anticancer Drugs, 2001. **12(8)**: p. 639-46.
36. Rosales, J. and L.A. Leong, *Chemotherapy for metastatic colorectal cancer*. J Natl Compr Canc Netw, 2005. **3(4)**: p. 525-9.
37. Todnem, K., et al., *[Fluorinated pyrimidines in oral treatment of advanced colorectal cancer]*. Tidsskr Nor Laegeforen, 2000. **120(23)**: p. 2781-5.
38. Murray, A.W., *The biological significance of purine salvage*. Annu Rev Biochem, 1971. **40**: p. 811-26.
39. de Koning, H.P., D.J. Bridges, and R.J. Burchmore, *Purine and pyrimidine transport in pathogenic protozoa: from biology to therapy*. FEMS Microbiol Rev, 2005. **29(5)**: p. 987-1020.
40. Baldwin, S.A., et al., *Nucleoside transport as a potential target for chemotherapy in malaria*. Curr Pharm Des, 2007. **13(6)**: p. 569-80.
41. Cass, C.E., J.D. Young, and S.A. Baldwin, *Recent advances in the molecular biology of nucleoside transporters of mammalian cells*. Biochem Cell Biol, 1998. **76(5)**: p. 761-70.
42. Cass, C.E., et al., *Nucleoside transporters of mammalian cells*. Pharm Biotechnol, 1999. **12**: p. 313-52.
43. Baldwin, S.A., et al., *Nucleoside transporters: molecular biology and implications for therapeutic development*. Mol Med Today, 1999. **5(5)**: p. 216-24.
44. Hamilton, S.R., et al., *Subcellular distribution and membrane topology of the mammalian concentrative Na⁺-nucleoside cotransporter rCNT1*. J Biol Chem, 2001. **276(30)**: p. 27981-8.

45. Lai, Y., A.H. Bakken, and J.D. Unadkat, *Simultaneous expression of hCNT1-CFP and hENT1-YFP in Madin-Darby canine kidney cells. Localization and vectorial transport studies.* J Biol Chem, 2002. **277**(40): p. 37711-7.
46. Damaraju, S., et al., *Identification and functional characterization of variants in human concentrative nucleoside transporter 3, hCNT3 (SLC28A3), arising from single nucleotide polymorphisms in coding regions of the hCNT3 gene.* Pharmacogenet Genomics, 2005. **15**(3): p. 173-82.
47. Damaraju, V.L., et al., *Localization of broadly selective equilibrative and concentrative nucleoside transporters, hENT1 and hCNT3, in human kidney.* Am J Physiol Renal Physiol, 2007. **293**(1): p. F200-11.
48. Gray, J.H., R.P. Owen, and K.M. Giacomini, *The concentrative nucleoside transporter family, SLC28.* Pflugers Arch, 2004. **447**(5): p. 728-34.
49. Baldwin, S.A., et al., *The equilibrative nucleoside transporter family, SLC29.* Pflugers Arch, 2004. **447**(5): p. 735-43.
50. Hyde, R.J., et al., *The ENT family of eukaryote nucleoside and nucleobase transporters: recent advances in the investigation of structure/function relationships and the identification of novel isoforms.* Mol Membr Biol, 2001. **18**(1): p. 53-63.
51. Griffith, D.A. and S.M. Jarvis, *Nucleoside and nucleobase transport systems of mammalian cells.* Biochim Biophys Acta, 1996. **1286**(3): p. 153-81.
52. Baldwin, S.A., et al., *Functional characterization of novel human and mouse equilibrative nucleoside transporters (hENT3 and mENT3) located in intracellular membranes.* J Biol Chem, 2005. **280**(16): p. 15880-7.
53. Sandoval, I.V., et al., *Distinct reading of different structural determinants modulates the dileucine-mediated transport steps of the lysosomal membrane protein LIMP2 and the insulin-sensitive glucose transporter GLUT4.* J Biol Chem, 2000. **275**(51): p. 39874-85.
54. Barnes, K., et al., *Distribution and functional characterization of equilibrative nucleoside transporter-4, a novel cardiac adenosine transporter activated at acidic pH.* Circ Res, 2006. **99**(5): p. 510-9.
55. Rose, J.B., et al., *Equilibrative nucleoside transporter 1 plays an essential role in cardioprotection.* Am J Physiol Heart Circ Physiol, 2010. **298**(3): p. H771-7.
56. Zhang, D., et al., *Expression of human equilibrative nucleoside transporter 1 in mouse neurons regulates adenosine levels in physiological and hypoxic-ischemic conditions.* J Neurochem, 2011. **118**(1): p. 4-11.
57. Grenz, A., et al., *Equilibrative nucleoside transporter 1 (ENT1) regulates postischemic blood flow during acute kidney injury in mice.* J Clin Invest, 2012. **122**(2): p. 693-710.
58. Rose, J.B., et al., *Absence of equilibrative nucleoside transporter 1 in ENT1 knockout mice leads to altered nucleoside levels following hypoxic challenge.* Life Sci, 2011. **89**(17-18): p. 621-30.
59. Endres, C.J., et al., *The role of nucleoside transporters in the erythrocyte disposition and oral absorption of ribavirin in the wild-type and equilibrative nucleoside transporter 1-/- mice.* J Pharmacol Exp Ther, 2009. **331**(1): p. 287-96.
60. Choi, D.S., et al., *The type 1 equilibrative nucleoside transporter regulates ethanol intoxication and preference.* Nat Neurosci, 2004. **7**(8): p. 855-61.
61. Chen, J., et al., *The type 1 equilibrative nucleoside transporter regulates anxiety-like behavior in mice.* Genes Brain Behav, 2007. **6**(8): p. 776-83.
62. Bone, D.B., et al., *Nucleoside/nucleobase transport and metabolism by microvascular endothelial cells isolated from ENT1-/- mice.* Am J Physiol Heart Circ Physiol, 2010. **299**(3): p. H847-56.

63. Pressacco, J., et al., *Effects of thymidylate synthase inhibition on thymidine kinase activity and nucleoside transporter expression*. *Cancer Res*, 1995. **55**(7): p. 1505-8.
64. Pressacco, J., et al., *Modulation of the equilibrative nucleoside transporter by inhibitors of DNA synthesis*. *Br J Cancer*, 1995. **72**(4): p. 939-42.
65. Cass, C.E., et al., *Fluctuations in nucleoside uptake and binding of the inhibitor of nucleoside transport, nitrobenzylthioinosine, during the replication cycle of HeLa cells*. *Cancer Res*, 1979. **39**(4): p. 1245-52.
66. Meckling-Gill, K.A., L. Guilbert, and C.E. Cass, *CSF-1 stimulates nucleoside transport in S1 macrophages*. *J Cell Physiol*, 1993. **155**(3): p. 530-8.
67. Coe, I., et al., *PKC regulation of the human equilibrative nucleoside transporter, hENT1*. *FEBS Lett*, 2002. **517**(1-3): p. 201-5.
68. Sen, R.P., E.G. Delicado, and M.T. Miras-Portugal, *Effect of forskolin and cyclic AMP analog on adenosine transport in cultured chromaffin cells*. *Neurochem Int*, 1990. **17**(4): p. 523-8.
69. Sen, R.P., et al., *Effect of P2Y agonists on adenosine transport in cultured chromaffin cells*. *J Neurochem*, 1993. **60**(2): p. 613-9.
70. Delicado, E.G., R.P. Sen, and M.T. Miras-Portugal, *Effects of phorbol esters and secretagogues on nitrobenzylthioinosine binding to nucleoside transporters and nucleoside uptake in cultured chromaffin cells*. *Biochem J*, 1991. **279** (Pt 3): p. 651-5.
71. Reyes, G., et al., *Characterization of mammalian equilibrative nucleoside transporters (ENTs) by mass spectrometry*. *Protein Expr Purif*, 2010. **73**(1): p. 1-9.
72. Litchfield, D.W. and B. Luscher, *Casein kinase II in signal transduction and cell cycle regulation*. *Mol Cell Biochem*, 1993. **127-128**: p. 187-99.
73. Canton, D.A. and D.W. Litchfield, *The shape of things to come: an emerging role for protein kinase CK2 in the regulation of cell morphology and the cytoskeleton*. *Cell Signal*, 2006. **18**(3): p. 267-75.
74. Stolk, M., et al., *Subtype-specific regulation of equilibrative nucleoside transporters by protein kinase CK2*. *Biochem J*, 2005. **386**(Pt 2): p. 281-9.
75. Bone, D.B., et al., *Differential regulation of mouse equilibrative nucleoside transporter 1 (mENT1) splice variants by protein kinase CK2*. *Mol Membr Biol*, 2007. **24**(4): p. 294-303.
76. Abdulla, P. and I.R. Coe, *Characterization and functional analysis of the promoter for the human equilibrative nucleoside transporter gene, hENT1*. *Nucleosides Nucleotides Nucleic Acids*, 2007. **26**(1): p. 99-110.
77. Vasquez, G., et al., *Role of adenosine transport in gestational diabetes-induced L-arginine transport and nitric oxide synthesis in human umbilical vein endothelium*. *J Physiol*, 2004. **560**(Pt 1): p. 111-22.
78. Aguayo, C., et al., *Equilibrative nucleoside transporter 2 is expressed in human umbilical vein endothelium, but is not involved in the inhibition of adenosine transport induced by hyperglycaemia*. *Placenta*, 2005. **26**(8-9): p. 641-53.
79. Puebla, C., et al., *High D-glucose reduces SLC29A1 promoter activity and adenosine transport involving specific protein 1 in human umbilical vein endothelium*. *J Cell Physiol*, 2008. **215**(3): p. 645-56.
80. Archer, R.G., V. Pitelka, and J.R. Hammond, *Nucleoside transporter subtype expression and function in rat skeletal muscle microvascular endothelial cells*. *Br J Pharmacol*, 2004. **143**(1): p. 202-14.
81. Eltzschig, H.K., et al., *HIF-1-dependent repression of equilibrative nucleoside transporter (ENT) in hypoxia*. *J Exp Med*, 2005. **202**(11): p. 1493-505.

82. Yao, S.Y., et al., *Molecular cloning and functional characterization of nitrobenzylthioinosine (NBMPR)-sensitive (es) and NBMPR-insensitive (ei) equilibrative nucleoside transporter proteins (rENT1 and rENT2) from rat tissues.* J Biol Chem, 1997. **272**(45): p. 28423-30.
83. Li, C.C. and J. Hochstadt, *Transport mechanisms in isolated plasma membranes. Nucleoside processing by membrane vesicles from mouse fibroblast cells grown in defined medium.* J Biol Chem, 1976. **251**(4): p. 1175-80.
84. Barker, P.H. and A.S. Clanachan, *Inhibition of adenosine accumulation into guinea pig ventricle by benzodiazepines.* Eur J Pharmacol, 1982. **78**(2): p. 241-4.
85. Jarvis, S.M. and J.D. Young, *Nucleoside translocation in sheep reticulocytes and fetal erythrocytes: a proposed model for the nucleoside transporter.* J Physiol, 1982. **324**: p. 47-66.
86. Jarvis, S.M., D. McBride, and J.D. Young, *Erythrocyte nucleoside transport: asymmetrical binding of nitrobenzylthioinosine to nucleoside permeation sites.* J Physiol, 1982. **324**: p. 31-46.
87. Wohlhueter, R.M., W.E. Brown, and P.G. Plagemann, *Kinetic and thermodynamic studies on nitrobenzylthioinosine binding to the nucleoside transporter of Chinese hamster ovary cells.* Biochim Biophys Acta, 1983. **731**(2): p. 168-76.
88. AP, I.J., et al., *Radioligand binding studies on the nucleoside transport protein.* Adv Exp Med Biol, 1991. **309A**: p. 411-4.
89. Handa, M., et al., *Cloning of a novel isoform of the mouse NBMPR-sensitive equilibrative nucleoside transporter (ENT1) lacking a putative phosphorylation site.* Gene, 2001. **262**(1-2): p. 301-7.
90. Griffiths, M., et al., *Cloning of a human nucleoside transporter implicated in the cellular uptake of adenosine and chemotherapeutic drugs.* Nat Med, 1997. **3**(1): p. 89-93.
91. Wu, S.K., et al., *Fine tuning of rabbit equilibrative nucleoside transporter activity by an alternatively spliced variant.* J Drug Target, 2005. **13**(8-9): p. 521-33.
92. Vickers, M.F., et al., *Uridine recognition motifs of human equilibrative nucleoside transporters 1 and 2 produced in Saccharomyces cerevisiae.* Nucleosides Nucleotides Nucleic Acids, 2004. **23**(1-2): p. 361-73.
93. Zhang, J., et al., *The role of nucleoside transporters in cancer chemotherapy with nucleoside drugs.* Cancer Metastasis Rev, 2007. **26**(1): p. 85-110.
94. Jennings, L.L., et al., *Distinct regional distribution of human equilibrative nucleoside transporter proteins 1 and 2 (hENT1 and hENT2) in the central nervous system.* Neuropharmacology, 2001. **40**(5): p. 722-31.
95. Musa, H., et al., *Immunocytochemical demonstration of the equilibrative nucleoside transporter rENT1 in rat sinoatrial node.* J Histochem Cytochem, 2002. **50**(3): p. 305-9.
96. Mani, R.S., et al., *Demonstration of equilibrative nucleoside transporters (hENT1 and hENT2) in nuclear envelopes of cultured human choriocarcinoma (BeWo) cells by functional reconstitution in proteoliposomes.* J Biol Chem, 1998. **273**(46): p. 30818-25.
97. Lai, Y., C.M. Tse, and J.D. Unadkat, *Mitochondrial expression of the human equilibrative nucleoside transporter 1 (hENT1) results in enhanced mitochondrial toxicity of antiviral drugs.* J Biol Chem, 2004. **279**(6): p. 4490-7.
98. Young, J.D., et al., *Human equilibrative nucleoside transporter (ENT) family of nucleoside and nucleobase transporter proteins.* Xenobiotica, 2008. **38**(7-8): p. 995-1021.
99. Appleford, P.J., et al., *Functional redundancy of two nucleoside transporters of the ENT family (CeENT1, CeENT2) required for development of Caenorhabditis elegans.* Mol Membr Biol, 2004. **21**(4): p. 247-59.

100. Visser, F., et al., *Identification and mutational analysis of amino acid residues involved in dipyridamole interactions with human and Caenorhabditis elegans equilibrative nucleoside transporters*. J Biol Chem, 2005. **280**(12): p. 11025-34.
101. Carter, N.S., et al., *Isolation and functional characterization of the PfNT1 nucleoside transporter gene from Plasmodium falciparum*. J Biol Chem, 2000. **275**(14): p. 10683-91.
102. Parker, M.D., et al., *Identification of a nucleoside/nucleobase transporter from Plasmodium falciparum, a novel target for anti-malarial chemotherapy*. Biochem J, 2000. **349**(Pt 1): p. 67-75.
103. Aronow, B., et al., *Two high affinity nucleoside transporters in Leishmania donovani*. Mol Biochem Parasitol, 1987. **22**(1): p. 29-37.
104. Landfear, S.M., *Molecular genetics of nucleoside transporters in Leishmania and African trypanosomes*. Biochem Pharmacol, 2001. **62**(2): p. 149-55.
105. Downie, M.J., et al., *PfNT2, a permease of the equilibrative nucleoside transporter family in the endoplasmic reticulum of Plasmodium falciparum*. J Biol Chem, 2010. **285**(27): p. 20827-33.
106. Vodnala, M., et al., *Adenosine kinase mediates high affinity adenosine salvage in Trypanosoma brucei*. J Biol Chem, 2008. **283**(9): p. 5380-8.
107. de Koning, H.P. and S.M. Jarvis, *Adenosine transporters in bloodstream forms of Trypanosoma brucei brucei: substrate recognition motifs and affinity for trypanocidal drugs*. Mol Pharmacol, 1999. **56**(6): p. 1162-70.
108. de Koning, H.P., et al., *Differential regulation of nucleoside and nucleobase transporters in Crithidia fasciculata and Trypanosoma brucei brucei*. Mol Biochem Parasitol, 2000. **106**(1): p. 93-107.
109. Stein, A., et al., *Equilibrative nucleoside transporter family members from Leishmania donovani are electrogenic proton symporters*. J Biol Chem, 2003. **278**(37): p. 35127-34.
110. Arastu-Kapur, S., et al., *Functional analysis of an inosine-guanosine transporter from Leishmania donovani. The role of conserved residues, aspartate 389 and arginine 393*. J Biol Chem, 2003. **278**(35): p. 33327-33.
111. Liu, W., et al., *Functional characterization of nucleoside transporter gene replacements in Leishmania donovani*. Mol Biochem Parasitol, 2006. **150**(2): p. 300-7.
112. Acimovic, Y. and I.R. Coe, *Molecular evolution of the equilibrative nucleoside transporter family: identification of novel family members in prokaryotes and eukaryotes*. Mol Biol Evol, 2002. **19**(12): p. 2199-210.
113. Shryock, J.C. and L. Belardinelli, *Adenosine and adenosine receptors in the cardiovascular system: biochemistry, physiology, and pharmacology*. Am J Cardiol, 1997. **79**(12A): p. 2-10.
114. Chang-Chun, C., et al., *Nucleoside transport inhibition mediates lidoflazine-induced cardioprotection during intermittent aortic crossclamping*. J Thorac Cardiovasc Surg, 1992. **104**(6): p. 1602-9.
115. Masuda, M., et al., *Effect of nucleoside transport inhibition on adenosine and hypoxanthine accumulation in the ischemic human myocardium*. Arch Int Pharmacodyn Ther, 1993. **322**: p. 45-54.
116. Parkinson, F.E., et al., *Effects of nitrobenzylthioinosine on neuronal injury, adenosine levels, and adenosine receptor activity in rat forebrain ischemia*. J Neurochem, 2000. **75**(2): p. 795-802.
117. Van Belle, H., *Myocardial protection by nucleoside transport inhibition*. Transplant Proc, 1995. **27**(5): p. 2804-5.

118. Chaudary, N., et al., *Transport characteristics of HL-1 cells: a new model for the study of adenosine physiology in cardiomyocytes*. *Biochem Cell Biol*, 2002. **80**(5): p. 655-65.
119. Dennis, D.M., et al., *Modulation of atrioventricular nodal function by metabolic and allosteric regulators of endogenous adenosine in guinea pig heart*. *Circulation*, 1996. **94**(10): p. 2551-9.
120. Baxter, G.F., *Role of adenosine in delayed preconditioning of myocardium*. *Cardiovasc Res*, 2002. **55**(3): p. 483-94.
121. Mubagwa, K. and W. Flameng, *Adenosine, adenosine receptors and myocardial protection: an updated overview*. *Cardiovasc Res*, 2001. **52**(1): p. 25-39.
122. Wright, A.M., W.P. Gati, and A.R. Paterson, *Enhancement of retention and cytotoxicity of 2-chlorodeoxyadenosine in cultured human leukemic lymphoblasts by nitrobenzylthioinosine, an inhibitor of equilibrative nucleoside transport*. *Leukemia*, 2000. **14**(1): p. 52-60.
123. Clarke, M.L., et al., *The role of membrane transporters in cellular resistance to anticancer nucleoside drugs*. *Cancer Treat Res*, 2002. **112**: p. 27-47.
124. Damaraju, V.L., et al., *Nucleoside anticancer drugs: the role of nucleoside transporters in resistance to cancer chemotherapy*. *Oncogene*, 2003. **22**(47): p. 7524-36.
125. King, K.M., et al., *A comparison of the transportability, and its role in cytotoxicity, of clofarabine, cladribine, and fludarabine by recombinant human nucleoside transporters produced in three model expression systems*. *Mol Pharmacol*, 2006. **69**(1): p. 346-53.
126. Hubeek, I., et al., *The human equilibrative nucleoside transporter 1 mediates in vitro cytarabine sensitivity in childhood acute myeloid leukaemia*. *Br J Cancer*, 2005. **93**(12): p. 1388-94.
127. Spratlin, J., et al., *The absence of human equilibrative nucleoside transporter 1 is associated with reduced survival in patients with gemcitabine-treated pancreas adenocarcinoma*. *Clin Cancer Res*, 2004. **10**(20): p. 6956-61.
128. Takagaki, K., et al., *Gene-expression profiling reveals down-regulation of equilibrative nucleoside transporter 1 (ENT1) in Ara-C-resistant CCRF-CEM-derived cells*. *J Biochem*, 2004. **136**(5): p. 733-40.
129. Seve, P. and C. Dumontet, *Chemoresistance in non-small cell lung cancer*. *Curr Med Chem Anticancer Agents*, 2005. **5**(1): p. 73-88.
130. Borbath, I., et al., *Human equilibrative nucleoside transporter 1 (hENT1) expression is a potential predictive tool for response to gemcitabine in patients with advanced cholangiocarcinoma*. *Eur J Cancer*, 2012. **48**(7): p. 990-6.
131. Zlatopolskiy, B.D., et al., *Towards to hENT1-nucleoside transporter selective imaging agents. Synthesis and in vitro evaluation of the radiolabeled SAENTA analogues*. *Bioorg Med Chem Lett*, 2009. **19**(17): p. 5151-4.
132. Sundaram, M., et al., *Topology of a human equilibrative, nitrobenzylthioinosine (NBMPR)-sensitive nucleoside transporter (hENT1) implicated in the cellular uptake of adenosine and anti-cancer drugs*. *J Biol Chem*, 2001. **276**(48): p. 45270-5.
133. Vickers, M.F., et al., *Functional production and reconstitution of the human equilibrative nucleoside transporter (hENT1) in *Saccharomyces cerevisiae*. Interaction of inhibitors of nucleoside transport with recombinant hENT1 and a glycosylation-defective derivative (hENT1/N48Q)*. *Biochem J*, 1999. **339** (Pt 1): p. 21-32.
134. Sundaram, M., et al., *Chimeric constructs between human and rat equilibrative nucleoside transporters (hENT1 and rENT1) reveal hENT1 structural domains interacting with coronary vasoactive drugs*. *J Biol Chem*, 1998. **273**(34): p. 21519-25.

135. Sundaram, M., et al., *Equilibrative nucleoside transporters: mapping regions of interaction for the substrate analogue nitrobenzylthioinosine (NBMPR) using rat chimeric proteins*. *Biochemistry*, 2001. **40**(27): p. 8146-51.
136. Young, J.D., et al., *Photoaffinity labeling of the human erythrocyte nucleoside transporter by N6-(p-Azidobenzyl)adenosine and nitrobenzylthioinosine. Evidence that the transporter is a band 4.5 polypeptide*. *J Biol Chem*, 1983. **258**(4): p. 2202-8.
137. SenGupta, D.J. and J.D. Unadkat, *Glycine 154 of the equilibrative nucleoside transporter, hENT1, is important for nucleoside transport and for conferring sensitivity to the inhibitors nitrobenzylthioinosine, dipyridamole, and dilazep*. *Biochem Pharmacol*, 2004. **67**(3): p. 453-8.
138. Endres, C.J. and J.D. Unadkat, *Residues Met89 and Ser160 in the human equilibrative nucleoside transporter 1 affect its affinity for adenosine, guanosine, S6-(4-nitrobenzyl)-mercaptapurine riboside, and dipyridamole*. *Mol Pharmacol*, 2005. **67**(3): p. 837-44.
139. SenGupta, D.J., et al., *A single glycine mutation in the equilibrative nucleoside transporter gene, hENT1, alters nucleoside transport activity and sensitivity to nitrobenzylthioinosine*. *Biochemistry*, 2002. **41**(5): p. 1512-9.
140. Spyropoulos, I.C., et al., *TMRPres2D: high quality visual representation of transmembrane protein models*. *Bioinformatics*, 2004. **20**(17): p. 3258-60.
141. Endres, C.J., D.J. Sengupta, and J.D. Unadkat, *Mutation of leucine-92 selectively reduces the apparent affinity of inosine, guanosine, NBMPR [S6-(4-nitrobenzyl)-mercaptapurine riboside] and dilazep for the human equilibrative nucleoside transporter, hENT1*. *Biochem J*, 2004. **380**(Pt 1): p. 131-7.
142. Paproski, R.J., et al., *Mutation of Trp29 of human equilibrative nucleoside transporter 1 alters affinity for coronary vasodilator drugs and nucleoside selectivity*. *Biochem J*, 2008. **414**(2): p. 291-300.
143. Visser, F., et al., *Residues 334 and 338 in transmembrane segment 8 of human equilibrative nucleoside transporter 1 are important determinants of inhibitor sensitivity, protein folding, and catalytic turnover*. *J Biol Chem*, 2007. **282**(19): p. 14148-57.
144. Paul, B., M.F. Chen, and A.R. Paterson, *Inhibitors of nucleoside transport. A structure-activity study using human erythrocytes*. *J Med Chem*, 1975. **18**(10): p. 968-73.
145. Paterson, A.R., S.R. Naik, and C.E. Cass, *Inhibition of uridine uptake in HeLa cells by nitrobenzylthioinosine and related compounds*. *Mol Pharmacol*, 1977. **13**(6): p. 1014-23.
146. Gupte, A. and J.K. Buolamwini, *Novel C2-purine position analogs of nitrobenzylmercaptapurine riboside as human equilibrative nucleoside transporter 1 inhibitors*. *Bioorg Med Chem*, 2007. **15**(24): p. 7726-37.
147. Vickers, M.F., et al., *Comparison of the interaction of uridine, cytidine, and other pyrimidine nucleoside analogues with recombinant human equilibrative nucleoside transporter 2 (hENT2) produced in Saccharomyces cerevisiae*. *Biochem Cell Biol*, 2002. **80**(5): p. 639-44.
148. Chang, C., et al., *Molecular requirements of the human nucleoside transporters hCNT1, hCNT2, and hENT1*. *Mol Pharmacol*, 2004. **65**(3): p. 558-70.
149. Zhu, Z. and J.K. Buolamwini, *Constrained NBMPR analogue synthesis, pharmacophore mapping and 3D-QSAR modeling of equilibrative nucleoside transporter 1 (ENT1) inhibitory activity*. *Bioorg Med Chem*, 2008. **16**(7): p. 3848-65.
150. Gupte, A. and J.K. Buolamwini, *CoMFA and CoMSIA 3D-QSAR studies on S(6)-(4-nitrobenzyl)mercaptapurine riboside (NBMPR) analogs as inhibitors of human equilibrative nucleoside transporter 1 (hENT1)*. *Bioorg Med Chem Lett*, 2009. **19**(2): p. 314-8.

151. Pao, S.S., I.T. Paulsen, and M.H. Saier, Jr., *Major facilitator superfamily*. *Microbiol Mol Biol Rev*, 1998. **62**(1): p. 1-34.
152. DeFelice, L.J., *Transporter structure and mechanism*. *Trends Neurosci*, 2004. **27**(6): p. 352-9.
153. Agbanyo, F.R., C.E. Cass, and A.R. Paterson, *External location of sites on pig erythrocyte membranes that bind nitrobenzylthioinosine*. *Mol Pharmacol*, 1988. **33**(3): p. 332-7.
154. Abramson, J., et al., *Structure and mechanism of the lactose permease of Escherichia coli*. *Science*, 2003. **301**(5633): p. 610-5.
155. Huang, Y., et al., *Structure and mechanism of the glycerol-3-phosphate transporter from Escherichia coli*. *Science*, 2003. **301**(5633): p. 616-20.
156. Valdes, R., et al., *An ab Initio structural model of a nucleoside permease predicts functionally important residues*. *J Biol Chem*, 2009. **284**(28): p. 19067-76.
157. Robillard, K.R., et al., *Characterization of mENT1Delta11, a novel alternative splice variant of the mouse equilibrative nucleoside transporter 1*. *Mol Pharmacol*, 2008. **74**(1): p. 264-73.
158. Yao, S.Y., et al., *Identification of Cys140 in helix 4 as an exofacial cysteine residue within the substrate-translocation channel of rat equilibrative nitrobenzylthioinosine (NBMPR)-insensitive nucleoside transporter rENT2*. *Biochem J*, 2001. **353**(Pt 2): p. 387-93.
159. Mindell, J.A., et al., *Reaction of diphtheria toxin channels with sulfhydryl-specific reagents: observation of chemical reactions at the single molecule level*. *Proc Natl Acad Sci U S A*, 1994. **91**(12): p. 5272-6.
160. Kenyon, G.L. and T.W. Bruice, *Novel sulfhydryl reagents*. *Methods Enzymol*, 1977. **47**: p. 407-30.
161. Karlin, A. and M.H. Akabas, *Substituted-cysteine accessibility method*. *Methods Enzymol*, 1998. **293**: p. 123-45.
162. Akabas, M.H., et al., *Acetylcholine receptor channel structure probed in cysteine-substitution mutants*. *Science*, 1992. **258**(5080): p. 307-10.
163. Xu, W.Y., et al., *Use of cysteine replacements and chemical modification to alter XIP, the autoinhibitory region of the Na-Ca exchanger. Inhibition of the activated plasma membrane Ca pump*. *Ann N Y Acad Sci*, 1996. **779**: p. 286-7.
164. Sucic, S. and L.J. Bryan-Lluka, *Roles of transmembrane domain 2 and the first intracellular loop in human noradrenaline transporter function: pharmacological and SCAM analysis*. *J Neurochem*, 2005. **94**(6): p. 1620-30.
165. Eduljee, C., et al., *SCAM analysis reveals a discrete region of the pore turret that modulates slow inactivation in Kv1.5*. *Am J Physiol Cell Physiol*, 2007. **292**(3): p. C1041-52.
166. Matulef, K., G.E. Flynn, and W.N. Zagotta, *Molecular rearrangements in the ligand-binding domain of cyclic nucleotide-gated channels*. *Neuron*, 1999. **24**(2): p. 443-52.
167. Zhu, Q. and J.R. Casey, *Topology of transmembrane proteins by scanning cysteine accessibility mutagenesis methodology*. *Methods*, 2007. **41**(4): p. 439-50.
168. Mueckler, M. and C. Makepeace, *Model of the exofacial substrate-binding site and helical folding of the human Glut1 glucose transporter based on scanning mutagenesis*. *Biochemistry*, 2009. **48**(25): p. 5934-42.
169. Slotboom, D.J., W.N. Konings, and J.S. Lolkema, *Cysteine-scanning mutagenesis reveals a highly amphipathic, pore-lining membrane-spanning helix in the glutamate transporter GltT*. *J Biol Chem*, 2001. **276**(14): p. 10775-81.
170. Lee, B.L., et al., *Structural and functional analysis of transmembrane XI of the NHE1 isoform of the Na⁺/H⁺ exchanger*. *J Biol Chem*, 2009. **284**(17): p. 11546-56.

171. Jarvis, S.M. and J.D. Young, *Nucleoside transport in rat erythrocytes: two components with differences in sensitivity to inhibition by nitrobenzylthioinosine and p-chloromercuriphenyl sulfonate*. J Membr Biol, 1986. **93**(1): p. 1-10.
172. Lee, C.W., L.B. Goh, and Y. Tu, *Sensitivity to inhibition by N-ethylmaleimide: a property of nitrobenzylthioinosine-sensitive equilibrative nucleoside transporter of murine myeloma cells*. Biochim Biophys Acta, 1995. **1268**(2): p. 200-8.
173. Deziel, M.R., C.Y. Jung, and A. Rothstein, *The topology of the major band 4.5 protein component of the human erythrocyte membrane: characterization of reactive cysteine residues*. Biochim Biophys Acta, 1985. **819**(1): p. 83-92.
174. Vyas, S., B. Ahmadi, and J.R. Hammond, *Complex effects of sulfhydryl reagents on ligand interactions with nucleoside transporters: evidence for multiple populations of ENT1 transporters with differential sensitivities to N-ethylmaleimide*. Arch Biochem Biophys, 2002. **403**(1): p. 92-102.
175. Kong, W., K. Engel, and J. Wang, *Mammalian nucleoside transporters*. Curr Drug Metab, 2004. **5**(1): p. 63-84.
176. Gati, W.P., et al., *Sensitivity of acute leukemia cells to cytarabine is a correlate of cellular es nucleoside transporter site content measured by flow cytometry with SAENTA-fluorescein*. Blood, 1997. **90**(1): p. 346-53.
177. Mackey, J.R., et al., *Immunohistochemical variation of human equilibrative nucleoside transporter 1 protein in primary breast cancers*. Clin Cancer Res, 2002. **8**(1): p. 110-6.
178. Paterson, A.R. and J.M. Oliver, *Nucleoside transport. II. Inhibition by p-nitrobenzylthioguanosine and related compounds*. Can J Biochem, 1971. **49**(2): p. 271-4.
179. Young, J.D. and S.M. Jarvis, *Nucleoside transport in animal cells*. Biosci Rep, 1983. **3**(4): p. 309-22.
180. Shi, M.M., et al., *Nucleoside transport. Photoaffinity labelling of high-affinity nitrobenzylthioinosine binding sites in rat and guinea pig lung*. Biochem Biophys Res Commun, 1984. **118**(2): p. 594-600.
181. Ward, J.L., et al., *Kinetic and pharmacological properties of cloned human equilibrative nucleoside transporters, ENT1 and ENT2, stably expressed in nucleoside transporter-deficient PK15 cells. Ent2 exhibits a low affinity for guanosine and cytidine but a high affinity for inosine*. J Biol Chem, 2000. **275**(12): p. 8375-81.
182. Paproski, R.J., et al., *The role of human nucleoside transporters in uptake of 3'-deoxy-3'-fluorothymidine*. Mol Pharmacol, 2008. **74**(5): p. 1372-80.
183. Cheng, Y. and W.H. Prusoff, *Relationship between the inhibition constant (K1) and the concentration of inhibitor which causes 50 per cent inhibition (I50) of an enzymatic reaction*. Biochem Pharmacol, 1973. **22**(23): p. 3099-108.
184. Hammond, J.R., *Interaction of a series of draflazine analogues with equilibrative nucleoside transporters: species differences and transporter subtype selectivity*. Naunyn Schmiedebergs Arch Pharmacol, 2000. **361**(4): p. 373-82.
185. Griffith, D.A., A.R. Conant, and S.M. Jarvis, *Differential inhibition of nucleoside transport systems in mammalian cells by a new series of compounds related to lidoflazine and mioflazine*. Biochem Pharmacol, 1990. **40**(10): p. 2297-303.
186. Jarvis, S.M., *Nitrobenzylthioinosine-sensitive nucleoside transport system: mechanism of inhibition by dipyridamole*. Mol Pharmacol, 1986. **30**(6): p. 659-65.
187. Visser, F., et al., *Mutation of residue 33 of human equilibrative nucleoside transporters 1 and 2 alters sensitivity to inhibition of transport by dilazep and dipyridamole*. J Biol Chem, 2002. **277**(1): p. 395-401.

188. Galmarini, C.M., J.R. Mackey, and C. Dumontet, *Nucleoside analogues: mechanisms of drug resistance and reversal strategies*. Leukemia, 2001. **15**(6): p. 875-90.
189. Mueckler, M. and C. Makepeace, *Cysteine-scanning mutagenesis and substituted cysteine accessibility analysis of transmembrane segment 4 of the Glut1 glucose transporter*. J Biol Chem, 2005. **280**(47): p. 39562-8.
190. Loo, T.W. and D.M. Clarke, *Identification of residues in the drug-binding domain of human P-glycoprotein. Analysis of transmembrane segment 11 by cysteine-scanning mutagenesis and inhibition by dibromobimane*. J Biol Chem, 1999. **274**(50): p. 35388-92.
191. Loo, T.W. and D.M. Clarke, *Determining the structure and mechanism of the human multidrug resistance P-glycoprotein using cysteine-scanning mutagenesis and thiol-modification techniques*. Biochim Biophys Acta, 1999. **1461**(2): p. 315-25.
192. Jarvis, S.M., et al., *Species differences in nucleoside transport. A study of uridine transport and nitrobenzylthioinosine binding by mammalian erythrocytes*. Biochem J, 1982. **208**(1): p. 83-8.
193. Liang, L. and R.M. Johnstone, *Evidence for an internal pool of nucleoside transporters in mammalian reticulocytes*. Biochim Biophys Acta, 1992. **1106**(1): p. 189-96.
194. Boumah, C.E., et al., *Functional expression of the nitrobenzylthioinosine-sensitive nucleoside transporter of human choriocarcinoma (BeWo) cells in isolated oocytes of Xenopus laevis*. Biochem J, 1994. **299** (Pt 3): p. 769-73.
195. Boumah, C.E., D.L. Hogue, and C.E. Cass, *Expression of high levels of nitrobenzylthioinosine-sensitive nucleoside transport in cultured human choriocarcinoma (BeWo) cells*. Biochem J, 1992. **288** (Pt 3): p. 987-96.
196. Barile, M., et al., *3'-Azido-3'-deoxythymidine uptake into isolated rat liver mitochondria and impairment of ADP/ATP translocator*. Biochem Pharmacol, 1997. **53**(7): p. 913-20.
197. Camins, A., et al., *Characterization of nitrobenzylthioinosine binding sites in the mitochondrial fraction of rat testis*. Life Sci, 1996. **58**(9): p. 753-9.
198. Jimenez, A., et al., *Further characterization of an adenosine transport system in the mitochondrial fraction of rat testis*. Eur J Pharmacol, 2000. **398**(1): p. 31-9.
199. Dahlig-Harley, E., et al., *Binding of nitrobenzylthioinosine to high-affinity sites on the nucleoside-transport mechanism of HeLa cells*. Biochem J, 1981. **200**(2): p. 295-305.
200. Tse, C.M., J.S. Wu, and J.D. Young, *Evidence for the asymmetrical binding of p-chloromercuriphenyl sulphonate to the human erythrocyte nucleoside transporter*. Biochim Biophys Acta, 1985. **818**(3): p. 316-24.
201. Riegelhaupt, P.M., I.J. Frame, and M.H. Akabas, *Transmembrane segment 11 appears to line the purine permeation pathway of the Plasmodium falciparum equilibrative nucleoside transporter 1 (PfENT1)*. J Biol Chem, 2010. **285**(22): p. 17001-10.
202. Valdes, R., et al., *Transmembrane domain 5 of the LdNT1.1 nucleoside transporter is an amphipathic helix that forms part of the nucleoside translocation pathway*. Biochemistry, 2004. **43**(21): p. 6793-802.
203. Yao, S.Y., et al., *Nucleobase transport by human equilibrative nucleoside transporter 1 (hENT1)*. J Biol Chem, 2011. **286**(37): p. 32552-62.
204. Furthmayr, H. and V.T. Marchesi, *Subunit structure of human erythrocyte glycophorin A*. Biochemistry, 1976. **15**(5): p. 1137-44.
205. McClain, M.S., et al., *Essential role of a GXXXG motif for membrane channel formation by Helicobacter pylori vacuolating toxin*. J Biol Chem, 2003. **278**(14): p. 12101-8.
206. Russ, W.P. and D.M. Engelman, *The GxxxG motif: a framework for transmembrane helix-helix association*. J Mol Biol, 2000. **296**(3): p. 911-9.

207. Cosson, P. and F. Letourneur, *Coatomer interaction with di-lysine endoplasmic reticulum retention motifs*. Science, 1994. **263**(5153): p. 1629-31.
208. Teasdale, R.D. and M.R. Jackson, *Signal-mediated sorting of membrane proteins between the endoplasmic reticulum and the golgi apparatus*. Annu Rev Cell Dev Biol, 1996. **12**: p. 27-54.
209. Plagemann, P.G., R.M. Wohlhueter, and C. Woffendin, *Nucleoside and nucleobase transport in animal cells*. Biochim Biophys Acta, 1988. **947**(3): p. 405-43.
210. Kwong, F.Y., et al., *Mammalian nitrobenzylthioinosine-sensitive nucleoside transport proteins. Immunological evidence that transporters differing in size and inhibitor specificity share sequence homology*. J Biol Chem, 1992. **267**(30): p. 21954-60.
211. Lee, B.L., et al., *Structural and functional analysis of extracellular loop 2 of the Na(+)/H(+) exchanger*. Biochim Biophys Acta, 2009. **1788**(12): p. 2481-8.
212. Cederholm, J.M., et al., *Conformational changes in extracellular loop 2 associated with signal transduction in the glycine receptor*. J Neurochem, 2010. **115**(5): p. 1245-55.
213. Thompson, A.J., H.A. Lester, and S.C. Lummis, *The structural basis of function in Cys-loop receptors*. Q Rev Biophys, 2010. **43**(4): p. 449-99.
214. Sigel, E., A. Buhr, and R. Baur, *Role of the conserved lysine residue in the middle of the predicted extracellular loop between M2 and M3 in the GABA(A) receptor*. J Neurochem, 1999. **73**(4): p. 1758-64.
215. Cederholm, J.M., P.R. Schofield, and T.M. Lewis, *Gating mechanisms in Cys-loop receptors*. Eur Biophys J, 2009. **39**(1): p. 37-49.
216. Pelis, R.M., et al., *Functional Significance of Conserved Cysteines in the Human Organic Cation Transporter 2*. Am J Physiol Renal Physiol, 2012.

Appendices

July 10, 2012

Jamie Park
The University of Western Ontario
Dept. of Physiology and Pharmacology
Medical Sciences Bldg., Rm 216
London, ON N6A 5C1
Canada



Dear Jamie Park:

This is to grant you permission to include the following article in your thesis entitled "Human Nucleoside Transporter Subtype 1: Structure - Function Analysis Using Cysteine Mutagenesis and Thiol Modifying Techniques" for The University of Western Ontario:

Jamie S. Park, Scott J. Hughes, Frances K. M. Cunningham, and James R. Hammond, Identification of Cysteines Involved in the Effects of Methanethiosulfonate Reagents on Human Equilibrative Nucleoside Transporter 1, *Mol Pharmacol* October 2011 80:735-746

On the first page of each copy of this article, please add the following:

Reprinted with permission of the American Society for Pharmacology and Experimental Therapeutics. All rights reserved.

In addition, the original copyright line published with the paper must be shown on the copies included with your thesis.

Sincerely yours,

August 17, 2012

Jamie Park
Physiology and Pharmacology
The University of Western Ontario
Medical Sciences Building, Room 216
London, ON N6A 5C1
Canada



Dear Jamie Park:

This is to grant you permission to include the following article in your thesis entitled "Human Equilibrative Nucleoside Transporter Subtype 1: Structure-Function Analysis Using Cysteine Mutagenesis and Thiol Modifying Techniques" for The University of Western Ontario:

Jamie S. Park and James R. Hammond, Cysteine Residues in the TM9-TM11 Region of the Human Equilibrative Nucleoside Transporter Subtype 1 Play an Important Role in Inhibitor Binding and Translocation Function, *Mol Pharmacol* mol.112.079616; published ahead of print July 26, 2012, doi:10.1124/mol.112.079616

On the first page of each copy of this article, please add the following:

Reprinted with permission of the American Society for Pharmacology and Experimental Therapeutics. All rights reserved.

In addition, the original copyright line published with the paper must be shown on the copies included with your thesis.

Sincerely yours,

OXFORD UNIVERSITY PRESS LICENSE
 TERMS AND CONDITIONS
 Jul 10, 2012

This is a License Agreement between Jamie Park ("You") and Oxford University Press ("Oxford University Press") provided by Copyright Clearance Center ("CCC"). The license consists of your order details, the terms and conditions provided by Oxford University Press, and the payment terms and conditions.

All payments must be made in full to CCC. For payment instructions, please see information listed at the bottom of this form.

License Number	2944840409063
License date	Jul 09, 2012
Licensed publisher	content Oxford University Press
Licensed publication	content Molecular Biology and Evolution
Licensed title	content Molecular Evolution of the Equilibrative Nucleoside Transporter Family: Identification of Novel Family Members in Prokaryotes and Eukaryotes:
Licensed author	content Yugo Acimovic, Imogen R. Coe
Licensed date	content 12/01/2002
Type of Use	Thesis/Dissertation
Institution name	
Title of your work	Human Nucleoside Transporter Subtype 1: Structure - Function Analysis Using Cysteine Mutagenesis and Thiol Modifying Techniques
Publisher of your work	n/a
Expected publication date	Aug 2012
Permissions cost	0.00 USD
Value added tax	0.00 USD
Total	0.00 USD
Total	0.00 USD

ELSEVIER
TERMS AND CONDITIONS
Jul 10, 2012

LICENSE

This is a License Agreement between Jamie Park ("You") and Elsevier ("Elsevier") provided by Copyright Clearance Center ("CCC"). The license consists of your order details, the terms and conditions provided by Elsevier, and the payment terms and conditions.

All payments must be made in full to CCC. For payment instructions, please see information listed at the bottom of this form.

Supplier	Elsevier The Boulevard, Langford Kidlington, Oxford, OX5 1GB, UK	Limited Lane
Registered Company Number	1982084	
Customer name	Jamie Park	
Customer address	Dept. of Physiology and Pharmacology London, ON N6A 5C1	
License number	2942070400293	
License date	Jul 04, 2012	
Licensed content publisher	Elsevier	
Licensed content publication	Bioorganic & Medicinal Chemistry	
Licensed content title	Constrained NBMPR analogue synthesis, pharmacophore mapping and 3D-QSAR modeling of equilibrative nucleoside transporter 1 (ENT1) inhibitory activity	
Licensed content author	Zhengxiang Zhu, John K. Buolamwini	
Licensed content date	1 April 2008	
Licensed content volume number	16	
Licensed content issue number	7	
Number of pages	18	
Start Page	3848	
End Page	3865	
Type of Use	reuse in a thesis/dissertation	
Portion	figures/tables/illustrations	
Number of figures/tables/illustrations	of 1	
Format	both print and electronic	
Are you the author of this Elsevier article?	No	

Will you be translating?	No
Order reference number	
Title of your thesis/dissertation	Human Nucleoside Transporter Subtype 1: Structure - Function Analysis Using Cysteine Mutagenesis and Thiol Modifying Techniques
Expected completion date	Aug 2012
Estimated size (number of pages)	300
Elsevier VAT number	GB 494 6272 12
Permissions price	0.00 USD
VAT/Local Sales Tax	0.0 USD / 0.0 GBP
Total	0.00 USD

THE JOURNAL OF BIOLOGICAL CHEMISTRY

Copyright Permission Policy

These guidelines apply to the reuse of articles, figures, charts and photos in the *Journal of Biological Chemistry*, *Molecular & Cellular Proteomics* and the *Journal of Lipid Research*.

For authors reusing their own material:

Authors need **NOT** contact the journal to obtain rights to reuse their own material. They are automatically granted permission to do the following:

- Reuse the article in print collections of their own writing.
 - Present a work orally in its entirety.
 - Use an article in a thesis and/or dissertation.
 - Reproduce an article for use in the author's courses. (If the author is employed by an academic institution, that institution also may reproduce the article for teaching purposes.)
 - Reuse a figure, photo and/or table in future commercial and noncommercial works.
 - Post a copy of the paper in PDF that you submitted via BenchPress.
- Only authors who published their papers under the "Author's Choice" option may post the final edited PDFs created by the publisher to their own/departamental/university Web sites.
 - All authors may link to the journal site containing the final edited PDFs created by the publisher.

Please note that authors must include the following citation when using material that appeared in an ASBMB journal:

"This research was originally published in Journal Name. Author(s). Title. *Journal Name*. Year; Vol:pp-pp. © the American Society for Biochemistry and Molecular Biology."

For other parties using material for noncommercial use:

Other parties are welcome to copy, distribute, transmit and adapt the work — at no cost and without permission — for noncommercial use as long as they attribute the work to the original source using the citation above.

Examples of noncommercial use include:

- Reproducing a figure for educational purposes, such as schoolwork or lecture presentations, with attribution.
- Appending a reprinted article to a Ph.D. dissertation, with attribution.

Curriculum Vitae

Jamie Park

Education

Ph.D. in Pharmacology and Toxicology 2007-2012
 Schulich School of Medicine and Dentistry
 The University of Western Ontario

B.M.Sc. Honors Bachelor of Medical Sciences 2002-2007
 Schulich School of Medicine and Dentistry
 The University of Western Ontario

Scholarships and Awards

NSERC Postgraduate Scholarship Doctoral Award 2007-2012
 Natural Sciences and Engineering Research Council of Canada
 (NSERC PGS D)

Ontario Graduate Scholarship 2009-2010
 Ontario Ministry of Training, Colleges and Universities
 (OGS) (Declined)

Western Graduate Research Scholarship 2007-2012
 The University of Western Ontario
 (WGRS)

Schulich Scholarship for Medical Research 2007-2011
 Schulich School of Medicine and Dentistry
 The University of Western Ontario
 (SSMR)

CSBMCB Best poster award 2010
 The 53rd Canadian Society of Biochemistry Molecular and Cell Biology Conference
 Membrane Proteins in Health and Disease

Graduate Thesis Research Award 2010
 Department of Physiology and Pharmacology

The University of Western Ontario	
CSPT Trainee Travel Awards	2008-2010
The Canadian Society of Pharmacology and Therapeutics	
Helen Reid Award	2006-2007
The University of Western Ontario	
Dean's Honors List	2006-2007
The University of Western Ontario	
Gold Medal Award	2006-2007
The University of Western Ontario	
The University of Western Ontario	2002-2003
Entrance Scholarship	
Ontario Ministry of Training, Colleges and Universities	2002-2003
Queen Elizabeth II Aiming for the Top Scholarship	

Research and Professional Experience

Research Assistant	2007-present
Department of Physiology and Pharmacology The University of Western Ontario	
Supervisor: Dr. James R. Hammond	
Project: Human Nucleoside Transporter Subtype 1: Structure - Function Analysis Using Cysteine Mutagenesis and Thiol Modifying Techniques	
Certificate of Attendance	November 2, 2011
Pfizer Investigator Training Program: Clinical Trials Continuing Professional Development Schulich School of Medicine and Dentistry The University of Western Ontario	
Faculty of Science Research Intern	2005-2006
The University of Western Ontario Agriculture and Agri-Food Canada Southern Crop Protection and Food Research Centre : Soil Pathology	
Supervisor: Dr. Pervaiz Abbasi	
Project: Developing and evaluating microbial agents for biological control of plant pathogens	

Teaching Experience

Teaching Assistant

2007-2012

Course: Pharmacology/Toxicology 3358Y laboratory course
Department of Physiology and Pharmacology
The University of Western Ontario

Publications

Park J.S., Hammond J.R. (2012). Cysteine residues in the TM9-TM11 region of the human equilibrative nucleoside transporter subtype 1 play an important role in inhibitor binding and translocation function. *Molecular Pharmacology* Epub ahead of print July 26, 2012 as doi:10.1124/mol.112.079616.

Park J.S., Hughes S.J., Cunningham F.K.M., Hammond J.R. (2011). Identification of Cysteines Involved in the Effects of Methanethiosulfonate Reagents on Human Equilibrative Nucleoside Transporter 1. *Molecular Pharmacology*. 80(4):735-746.

Robillard K.R., Bone D.B., **Park J.S.**, Hammond J.R (2008). Characterization of mENT1 Δ 11, a novel alternative splice variant of the mouse equilibrative nucleoside transporter 1. *Molecular Pharmacology*. 74(1):264-73

Poster Presentations

Park J.S., Hammond J.R. (2012) Roles of Cysteine 378 and Cysteine 416 in Human Equilibrative Nucleoside Transporter 1 Function and Ligand Interactions. Poster presented in Toronto, Ontario, Canada June 12-15, at the annual Canadian Society of Pharmacology and Therapeutics Meeting Modern Therapeutics 2012: Advances in Physiology, Pharmacology and Pharmaceutical Sciences.

Park J.S., Hammond J.R. (2011) pH sensitive interaction of NBMPR with human equilibrative nucleoside 1 . Poster presented in Physiology and Pharmacology Research Day, Gowdey Lecture, The University of Western Ontario.

Park J.S., Hammond J.R. (2010) Modification of equilibrative nucleoside transporter 1 (ENT1) function by sulfhydryl reagents involves cysteine residues in transmembrane regions 6 and 7. Poster presented in Copenhagen, Denmark July 17-23, 2010 at the IUPHAR 16th World Congress of Basic and Clinical Pharmacology.

Park, J.S., Hammond J.R. (2010) Cysteine 222 is the target of methylmethanethiosulfonate (MMTS) modification of NBMPR binding to human

equilibrative nucleoside transporter subtype 1. Poster presented in Banff, Alberta, Canada April 15-18th at the 53rd Canadian Society of Biochemistry, Molecular and Cell Biology Conference.

Park J.S., Cunningham F., Hughes S., Frieburger L., Hammond J.R. (2009) Preliminary Analysis of Cysteine Mutants of Human Equilibrative Nucleoside Transporter 1 . Poster presented in Physiology and Pharmacology Research Day, Gowdey Lecture, The University of Western Ontario.

Park J.S., Cunningham F., Hughes S., Hammond J.R. (2009) Preliminary Analysis of Cysteine Mutants of Human Equilibrative Nucleoside Transporter 1. Oral presentation given in Saskatoon, Saskatchewan, Canada May 30 - June 2, 2009 at the Canadian Society of Pharmacology and Therapeutics Conference Innovations in Pharmacology.

Park J.S., Hammond J.R. (2008) Sulfhydryl Modifiers Have Biphasic Effects on Human Equilibrative Nucleoside Transporter 1 (hENT1) Translocation Activity and Ligand Binding. Poster presented in Physiology and Pharmacology Research Day, Stevenson Lecture, The University of Western Ontario.

Park J.S., Hammond J.R. (2008) Sulfhydryl Modifiers Have Biphasic Effects on Human Equilibrative Nucleoside Transporter 1 (hENT1) Translocation Activity and Ligand Binding. Poster presented in Quebec City, Quebec, Canada July 27 - August 1st 2008 at the International Conference: CPT 2008 Clinical Pharmacology and Therapeutics.

Professional Memberships

Student Member (CSPT)

2007-2012

The Canadian Society of Pharmacology and Therapeutics

References

Dr. James R. Hammond, Professor